NETWORK DESIGN AND OPTIMISATION IN CLOSE RANGE PHOTOGRAMMETRY

ANDREW R. MARSHALL

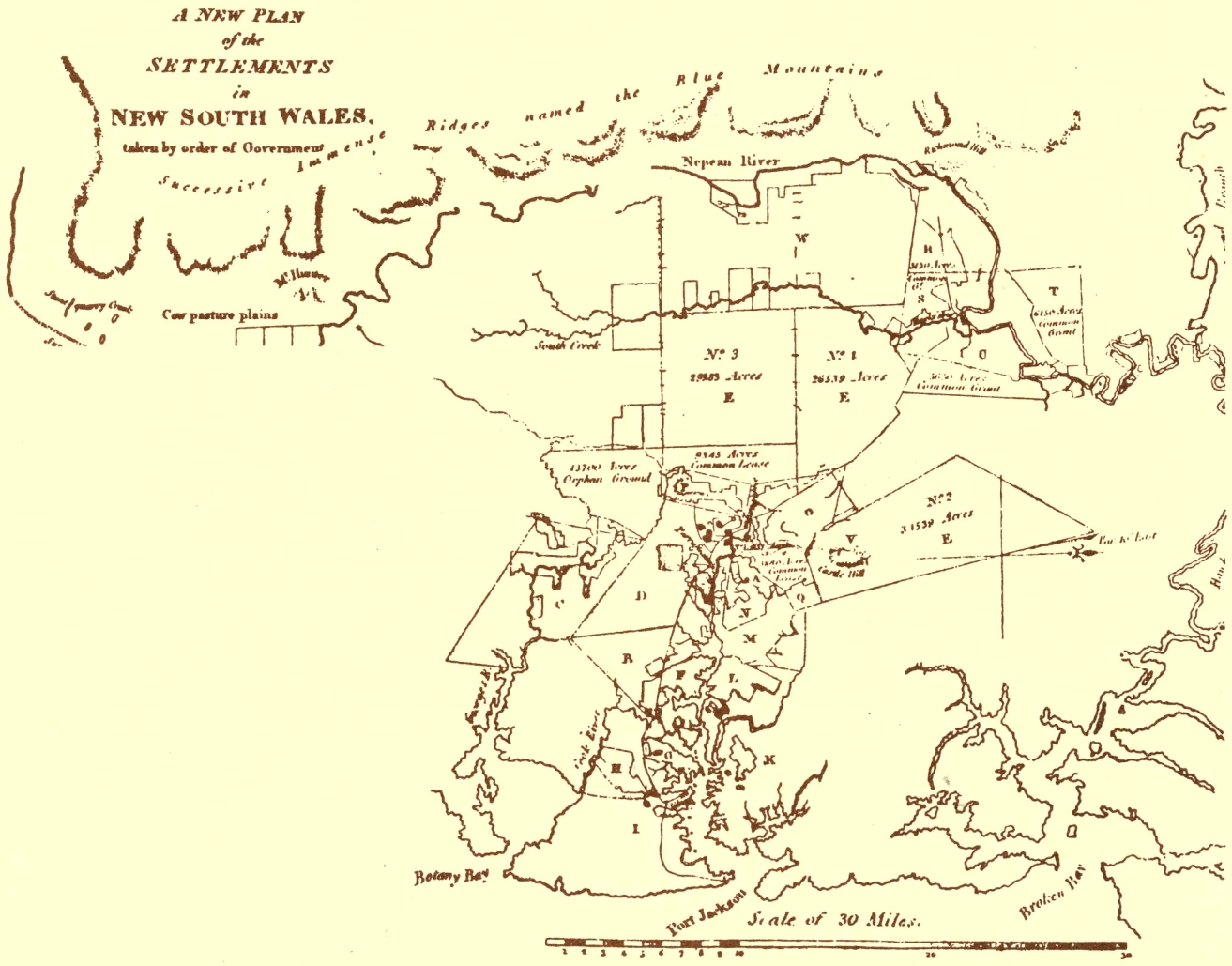

UNISURV S-36, 1989

Reports from

SCHOOL OF SURVEYING

THE UNIVERSITY OF NEW SOUTH WALES KENSINGTON, NSW AUSTRALIA 2033

UNISURV REPORT S-36, 1989

NETWORK DESIGN AND OPTIMIZATION IN CLOSE RANGE PHOTOGRAMMETRY

Andrew R. Marshall

Received: May, 1989

SCHOOL OF SURVEYING
UNIVERSITY OF NEW SOUTH WALES
P.O. BOX 1
KENSINGTON N.S.W. 2033
AUSTRALIA

National Library of Australia

Card No. and ISBN 0 85839 054 X

ABSTRACT

A thorough procedure for the design and evaluation of close range photogrammetric networks has been developed and presented. For high precision photogrammetric applications, where precisions of the order of 1:250,000 of the object diameter may be required, network design procedures form a fundamental tool for ensuring that the network to be implemented will achieve the desired precision and will be economically viable.

Detailed formulations of the principles of close range photogrammetry, applicable least squares estimation techniques and the close range photogrammetric mathematical model have been described. These formulations, which are essentially derived from first principles, aim at maintaining the continuity of theory from the least squares and photogrammetric fundamentals through to the network design principles.

Network design principles are developed with respect to the four basic network design problems.

Zero-Order Design (**ZOD**) - the datum definition problem
First-Order Design (**FOD**) - the network configuration problem
Second-Order Design (**SOD**) - the observation "weight" problem
Third-Order Design (**TOD**) - the network densification problem

Solutions to the datum problem are assessed in terms of applicable least squares solutions, which include the zero-variance computational base solution, Bayesian and ridge regression solutions and free network solutions. The network configuration problem has been evaluated with respect to the factors which influence it. The primary factors include imaging geometry and the number of camera stations. Solutions for the "weight" and densification problems are introduced and applicability of these problems in close range photogrammetric network design is evaluated.

Measures for assessing network quality are developed. These measures are essentially precision based, however those measures based upon accuracy, reliability and sensitivity criteria are also developed.

Network design for close range photogrammetry is basically achieved by iterative network simulations. Computer software, based upon interactive computer graphics and network simulation, has been developed in order to determine the effect of the various design problem solutions upon the object point precision estimates.

The network design problems are linked via a practical example. A case study of the close range photogrammetric mensuration of the Port Kembla coal loader is carried out. Typical design problems are assessed and an alternative network design proposed.

ACKNOWLEDGEMENTS

This project has been encouraged and supported by a number of people who have both directly and indirectly provided valuable assistance in the past year. I wish to thank :

Associate Professor John Trinder, who supervised the project and gave valuable assistance in the formulation and editing of this manuscript.

Mr Brian Donnelly, who provided discussion and assistance in areas of both computing and photogrammetry.

B.H.P. Engineering, for providing a scholarship for the project, and Mr Tony Burns, for his advice and assistance.

My family, for their support, and in particular my wife, Vanessa, for her encouragement and support during this period of study.

CONTENTS

1. INTRODUCTION

"Photogrammetry is the art, science and technology of obtaining reliable information about physical objects and the environment through processes of recording, measuring and interpreting photographic images and patterns of electromagnetic radiant energy and other phenomena" (Slama (ed) (1980)).

Close range photogrammetry is a specialized branch of photogrammetry which is predominantly non-topographic, terrestrial based and which involves measurement of objects with a camera to object distance of less than three hundred metres. The majority of close range photogrammetric activities satisfy the above definition, however the definition is not absolute and some photogrammetric applications, which fall under the banner of "close range", do not meet all of the above requirements.

Applications of close range photogrammetry have traditionally been in the areas of Archaeology, Architecture, Medicine, Crime and Accident Investigation, Industry and Engineering. Techniques used for aerial photogrammetry, which are well developed and understood, have been adapted to these close range photogrammetric applications. The adaptation of these techniques to close range photogrammetry, however, has not resulted in the high precisions which are required in the areas of engineering and industrial metrology and monitoring.

By contrast, analytical photogrammetric techniques based upon multi-station convergent photography have in recent times enabled the close range photogrammetrist the potential for high precision measurements and so enabled entry into the fields of industrial and engineering metrology.

The advantages of close range photogrammetry, over conventional surveying techniques, in industry and engineering are numerous. These advantages include a minimal "down" time of the object being measured, the capability of measuring hot or toxic objects and the capability of measuring moving objects. The most important advantage of close range photogrammetry is the potential to acquire the photograph in a short space of time. In industrial applications where "time means money", the object being

measured must be measured over a short space of time to avoid loss of production. With the recently developed analytical methods in close range photogrammetry, high precision of the order of 1:250,000 of the object diameter can be achieved; in some cases sub-micron precision has been reported. Close range photogrammetry therefore offers a competitive metrology method, capable of meeting the majority of precision requirements.

For high precision close range photogrammetry an adaptation of conventional aerial photogrammetric methods is not feasible. Apart form the basic foundation of both techniques upon the principles of photogrammetry, both techniques exhibit different characteristics in terms of precision requirements and image acquisition methods. These basic differences are summarized in table 1.1, which has been adapted from Granshaw (1980).

Table 1.1 The difference between aerial and close range photogrammetry

Close Range Photogrammetry	Aerial Photogrammetry
• Object may have truly spatial characteristics (large depth)	• Relief is small compared to flying height
• Precision in all three coordinates may be equally important	• Precision requirements differ for height and planimetry
• A restricted format is likely	• Entire format is usable
• Spatial nature of the object necessitates photography with varying position and orientation	• Vertical photography is used exclusively
• May be possible to target all points	• Targets only for control points, if at all
• The total number of photographs is usually small	• A large block may consist of thousands of photographs
• It is possible to determine camera parameters accurately	• Auxiliary data have only limited accuracy
• Flexible approach required due to differences from project to project	• A fairly standardized approach for all applications

The fundamental difference between aerial and close range photogrammetry relates to flexibility. In close range photogrammetry the nature of precision requirements, and the techniques to meet such requirements, vary from project to project. It is therefore necessary to evaluate

each project individually in order to formulate an overall design which can be economically implemented, but which allows recovery of position to the required degree of precision.

Close range photogrammetric network design, for high precision applications, requires no explicit justification. In these applications, especially where achievable precision is pushed to the limit, it is essential to be able to determine the most appropriate design, in terms of specified quality criteria, and whether the required precision requirements can in fact be achieved based upon the physical and practical constraints for the project.

The aim of this project is to develop the techniques for close range photogrammetric network design and therefore allow the photogrammetrist the flexibility to formulate a close range network for a specific task, which will meet specified quality criteria and which can be implemented with assurity.

For the purposes of meeting the aim of the project, most of the concepts associated with close range photogrammetric network design have been developed from first principles. This is especially evident in development of the least squares theory and application of this to network design. The reasons for this detailed development are two fold. The first reason relates to the diverse least squares notation evident in photogrammetric and least squares literature. For the purposes of understanding advanced estimation techniques, with an emphasis on photogrammetric evaluations, the theory has been developed in detail with a consistent notation and form. Developments directly pertinent to close range photogrammetric network design are therefore not plagued by ambiguity in notation and meaning of the least squares and photogrammetric theory.

The second reason for the detailed theoretical developments relates to the general lack of understanding in the general photogrammetric fraternity to the particular requirements of close range photogrammetric evaluations and the significance of such evaluations in terms of least squares theory. For example, the concepts of rank deficiency, free network adjustments, zero-variance computational base and the network design problems, to name a few, are relatively unknown in photogrammetry. Most photogrammetrists in Australia have entered the profession via the area of aerial photogrammetry and consequently such evaluation concepts need not be explicitly understood.

As close range photogrammetry becomes more accepted as a precise metrology tool it will be necessary for an understanding of photogrammetric evaluation principles, least squares evaluation techniques and the implication of these techniques upon parameter and precision estimates.

In this report Chapters 2 to 4 develop the theory of close range photogrammetric and least squares methods. Chapter 2 introduces the fundamental close range photogrammetric principles, including mathematical principles, evaluation techniques, data and image acquisition techniques and error sources. Chapter 3 develops the least squares theory in detail and covers the formulation of the least squares mathematical model through to solution methods for rank deficient systems, with an emphasis on minimally constrained solutions. Chapter 4 combines the preceding two chapters and formulates the methods for least squares estimation in close range photogrammetry. Development of the least squares observation equations is carried out in full in the appendix.

Chapters 5 to 10 develop the concepts and solution techniques for close range photogrammetric network design. Chapter 5 introduces the network design principles, including quality criteria and solution methods. The principles of the zero-order and first-order design problems are introduced. The applicability of the second-order and third-order design problems to close range photogrammetry is also covered. Chapter 6 involves the development of measures of assessing network quality. Such measures are predominantly precision based, however measures for accuracy, reliability and sensitivity are also developed. Chapter 7 describes the computer software developed to verify and illustrate many of the conclusions formulated with respect to network design. The software is an interactive computer graphics network design and simulation package. Chapters 8 and 9 develop, in detail, the solution techniques for the zero-order and first-order design problems respectively. The zero-order solutions assessed include the zero-variance computational base solution, Bayesian and ridge regression solutions and free network solutions. Examples of the applicability of the various solutions are included. First-order design is evaluated by trial and error network simulations. The factors which influence first-order design include imaging geometry and the number of camera stations. Examples to illustrate the effect of the various factors pertaining to network configuration are included. Chapter 10 is a case study of a typical close range photogrammetric mensuration problem. The

study verifies the network simulation method and addresses several of the typical problem areas in network design. The study effectively combines the various design problems into a single unit for overall assessment.

In high precision close range photogrammetry, the requirement for a priori network design is essential in order to achieve an "optimal" network in terms of network quality and economy. In this report the methods for designing "optimal" networks have been developed so that the solutions presented will both improve understanding of network design principles and will emphasize the need for network design in high precision close range photogrammetry.

2. FUNDAMENTAL PRINCIPLES OF CLOSE RANGE PHOTOGRAMMETRY

Close range photogrammetry, as defined in Chapter 1, is essentially a terrestrial based photogrammetric system with object to camera distances of less than three hundred metres. Mensuration techniques, based on close range photogrammetry, will be investigated with an emphasis on mathematical formulations, data evaluation techniques, image acquisition techniques and error sources.

2.1 Mathematical Principles

The mathematical principles of close range photogrammetry will be investigated in terms of the basic geometry of the photograph and in terms of the relationship between object and image, as defined by the collinearity condition.

2.1.1 Geometry of the Terrestrial Photograph

In photography the image formed on the photograph is a function of the perspective projection of points from the object being photographed to the photographic film. A perspective projection is one in which all points are projected onto a flat reference plane through one point which is called the perspective centre. Figure 2.1 shows the perspective projection and the relationship between object, perspective centre and the reference plane. In photography the photographic film is located in the reference plane and the optical centre of the camera lens, which is generally referred to as the front nodal point, is located at the perspective centre.

Orientation of the camera at the instant of photography is determined by two basic sets of parameters. The first set, called *interior orientation* parameters, refers to the perspective geometry of the camera.

The parameters of interior orientation are :

1. the principal distance, f .
2. the coordinates of the principal point, x_o and y_o .
3. the geometric distortion characteristics of the lens system .

Parameters of interior orientation are either determined by laboratory calibration, and held fixed in the estimation process, or treated as unknown parameters and solved for in the estimation process.

The second set of parameters, called *exterior orientation* parameters, define the geographic location of a particular camera station and the direction of the optical axis of the camera. The parameters relating to geographic location, defined in a three dimensional rectangular coordinate system, are X_L, Y_L and Z_L. The orientation parameters which define the orientation of the optical axis of the camera are given by three rotation angles. These rotation angles will be defined in section 2.1.2.2.

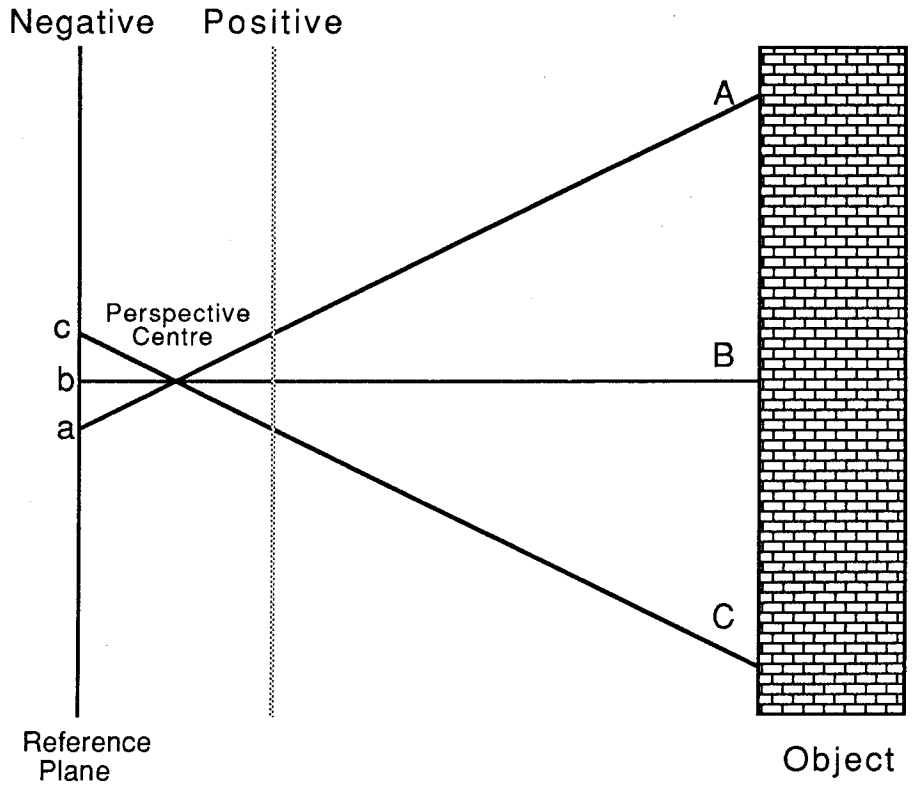

Figure 2.1 Perspective projection for a terrestrial photograph

The coordinates and coordinate systems of interest in close range photogrammetry are :

1. $\begin{pmatrix} X_i \\ Y_i \\ Z_i \end{pmatrix}$ Coordinates of object point **A.** (Object space coordinate system)

2. $\begin{pmatrix} X_L \\ Y_L \\ Z_L \end{pmatrix}$ Coordinates of perspective centre (Object space coordinate system)

3. $\begin{pmatrix} x_i \\ y_i \end{pmatrix}$ Coordinates of image point **a.** (Image space coordinate system)

4. $\begin{pmatrix} x_o \\ y_o \end{pmatrix}$ Coordinates of the principal point. (Image space coordinate system)

Figure 2.2 depicts the basic geometry of the terrestrial photograph and object and image coordinate systems.

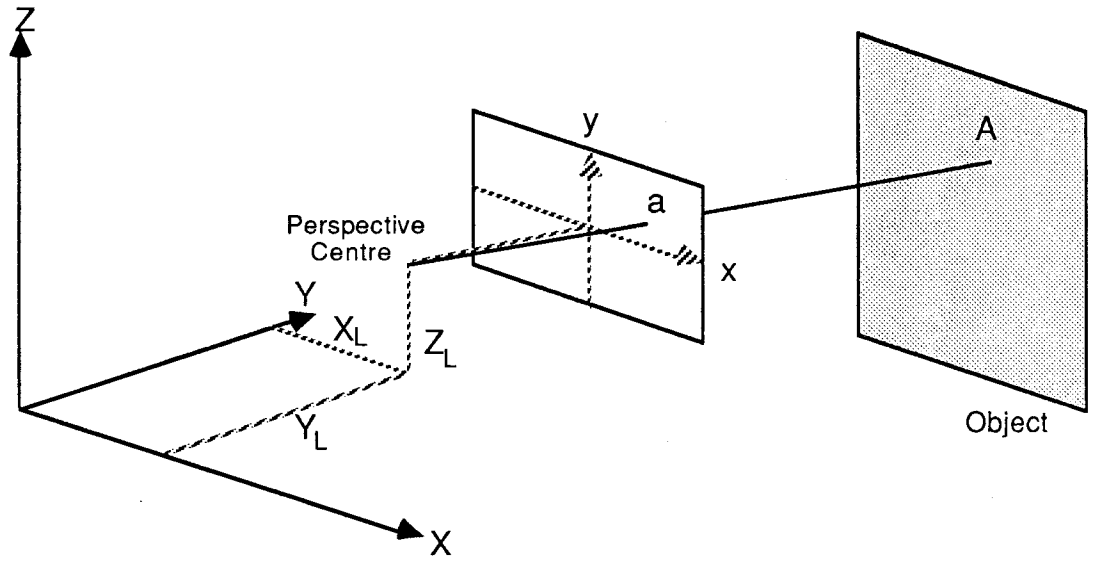

Figure 2.2 Geometry of the close range photograph

2.1.2 Mathematical Relationship between Object and Image Coordinates

2.1.2.1 Collinearity Condition

The mathematical relationship between object and image coordinates can be established by considering the collinearity condition. This condition is established at the time of photograph exposure and states that, at the instant of photography, the ray from the object point to the perspective centre and the ray from the perspective centre to the corresponding image point are collinear. The condition also applies during photogrammetric reconstruction and hence can be utilized to formulate transformation relationships between object and image coordinates. Implicit in the condition, for several object to image point rays, is a coplanarity requirement. Such a requirement means that all image points must be coplanar and hence the reference plane must be flat.

2.1.2.2 Formulation of the Collinearity Equation

Consider two vectors $\tilde{\mathbf{a}}$, the vector from the perspective centre to the image point, and $\tilde{\mathbf{A}}$, the vector from the object point to the perspective centre. The two vectors are collinear if one is a scalar multiple of the other.

$$\tilde{\mathbf{a}} = k\,\tilde{\mathbf{A}} \qquad ..(2.1)$$

where k is a scale factor relating $\tilde{\mathbf{a}}$ to $\tilde{\mathbf{A}}$

$$\tilde{\mathbf{a}} = \begin{pmatrix} x_i - x_o \\ y_i - y_o \\ -f \end{pmatrix} \qquad ..(2.2)$$

where x_i, y_i = image coordinates of point i.
x_o, y_o = image coordinates of the principal point.
f = principal distance.
and $\tilde{\mathbf{a}}$ is defined in the image space coordinate system.

$$\tilde{\mathbf{A}} = \begin{pmatrix} X_i - X_L \\ Y_i - Y_L \\ Z_i - Z_L \end{pmatrix} \qquad ..(2.3)$$

where X_i, Y_i, Z_i = object coordinates of point i.
X_L, Y_L, Z_L = object coordinates of the perspective centre.
and $\tilde{\mathbf{A}}$ is defined in the object space coordinate system.

To relate the vector $\tilde{\mathbf{A}}$ to the vector $\tilde{\mathbf{a}}$, in the same coordinate system, $\tilde{\mathbf{A}}$ must be premultiplied by a rotation matrix, denoted by **M**. This matrix defines the spatial orientation of the image space coordinate system with respect to the object space coordinate system. The rotation matrix is a 3 by 3 orthogonal matrix and is a function of the three rotation angles adopted and the sequence in which the three rotations occur. Successive rotations about fixed axes are not commutative and hence the order of rotation is important. Unless rotations are small the order in which rotations are applied will affect the magnitude of each rotation.

In a general notation the rotation matrix is of the form :

$$\mathbf{M} = \begin{pmatrix} m_{11} & m_{12} & m_{13} \\ m_{21} & m_{22} & m_{23} \\ m_{31} & m_{32} & m_{33} \end{pmatrix} \qquad ..(2.4)$$

In close range photogrammetry the rotations which are usually adopted are azimuth (α), tilt (θ) and kappa (κ) rotations, as shown in figure 2.3. These rotations are defined in the following way.

Azimuth (α)

The azimuth rotation is a rotation about the y-axis of the image coordinate system and is positive in the clockwise direction with respect to the positive y direction. For the special case where the ground coordinate system is defined with the Z-axis corresponding to the vertical and the Y-axis corresponding to the direction of true north, the azimuth is the angle measured clockwise from true north to the camera axis. In the image coordinate system the camera axis coincides with the negative z axis.

The rotation matrix, M_α, for the azimuth rotation is :

$$M_\alpha = \begin{pmatrix} \cos\alpha & -\sin\alpha & 0 \\ 0 & 0 & 1 \\ -\sin\alpha & -\cos\alpha & 0 \end{pmatrix} \qquad ..(2.5)$$

Tilt (θ)

The tilt rotation is a rotation about the x-axis of the image coordinate system and is positive in the clockwise direction with respect to the positive x direction. Hence a depression of the camera (negative z) axis will be a negative rotation and an elevation of the camera axis will be a positive rotation. For the special case described for the azimuth rotation, tilt is the angle between the horizontal plane and the camera optical axis.

The rotation matrix, M_θ, for the tilt rotation is :

$$M_\theta = \begin{pmatrix} 1 & 0 & 0 \\ 0 & \cos\theta & \sin\theta \\ 0 & -\sin\theta & \cos\theta \end{pmatrix} \qquad ..(2.6)$$

Kappa (κ)

The kappa rotation is a rotation about the z-axis of the image coordinate system and is measured positive in the clockwise direction with respect to the positive z direction.

The rotation matrix, M_κ, for the kappa rotation is :

$$M_\kappa = \begin{pmatrix} \cos\kappa & \sin\kappa & 0 \\ -\sin\kappa & \cos\kappa & 0 \\ 0 & 0 & 1 \end{pmatrix} \qquad ..(2.7)$$

An advantage of using the rotation angles azimuth, tilt and kappa is that these rotations can be easily measured to a high degree of accuracy in terrestrial applications. This facilitates the use of such measurements as constraints in any subsequent estimation or adjustment process. The application and effect of such constraints will be investigated in Chapter 5.

Derivation of the rotation matrix, **M**, is carried out by considering the subject rotations in the following order :

azimuth $\Rightarrow$ tilt $\Rightarrow$ kappa

For this sequence of rotations the rotation matrix is given by :

$$\mathbf{M} = M_\kappa M_\theta M_\alpha \qquad ..(2.8)$$

Slama (ed) (1980);Ch 2 defines the rotation matrix in the order of tilt, azimuth then kappa rotations. A disadvantage of this rotation sequence is that the tilt becomes dependent upon the azimuth. For example, a 10° tilt at zero azimuth, once rotated about 180° will become a -10° tilt. Consequently the application of this rotation sequence can be confusing, especially in cases where rotations are specified a priori and the direction of view is with respect to these pre-determined rotations, and can lead to error in formulation of the rotation matrix. Rotations in the order azimuth, tilt then kappa are not affected in the same manner.

Substitution of equations 2.5, 2.6 and 2.7 into equation 2.8 gives the following definition of the rotation matrix, **M**.

$$
\begin{aligned}
m_{11} &= \cos\kappa.\cos\alpha - \sin\kappa.\sin\theta.\sin\alpha \\
m_{12} &= -\cos\kappa.\sin\alpha - \sin\kappa.\sin\theta.\cos\alpha \\
m_{13} &= \sin\kappa.\cos\theta \\
m_{21} &= -\sin\kappa.\cos\alpha - \cos\kappa.\sin\theta.\sin\alpha \\
m_{22} &= \sin\kappa.\sin\alpha - \cos\kappa.\sin\theta.\cos\alpha \\
m_{23} &= \cos\kappa.\cos\theta \\
m_{31} &= -\cos\theta.\sin\alpha \\
m_{32} &= -\cos\theta.\cos\alpha \\
m_{33} &= -\sin\theta
\end{aligned}
\qquad ..(2.9)
$$

For the geometry of figure 2.2, where tilt and kappa rotations are zero and which is typical in many close range photogrammetric applications, the rotation matrix, **M**, reduces to the following form.

$$
\mathbf{M} = \begin{pmatrix} 1 & 0 & 0 \\ 0 & 0 & 1 \\ 0 & -1 & 0 \end{pmatrix} \qquad ..(2.10)
$$

Multiplication of equation 2.1 by **M** leads to the following equation which defines the collinearity relationship between object and image coordinates and which is termed the *collinearity equation.*

$$
\begin{pmatrix} x_i - x_o \\ y_i - y_o \\ -f \end{pmatrix} = k\,\mathbf{M} \begin{pmatrix} X_i - X_L \\ Y_i - Y_L \\ Z_i - Z_L \end{pmatrix} \qquad ..(2.11)
$$

Since the scale factor, **k**, varies for each ray from the object points to the image points, the sum of which is called the bundle of rays, and is usually unknown, it is generally eliminated from equation 2.11. This is achieved by dividing the first two equations in turn by the third equation. The collinearity equation is therefore usually written as :

$$x_i - x_o = -f\left(\frac{m_{11}(X_i - X_L) + m_{12}(Y_i - Y_L) + m_{13}(Z_i - Z_L)}{m_{31}(X_i - X_L) + m_{32}(Y_i - Y_L) + m_{33}(Z_i - Z_L)}\right) \quad ..(2.12)$$

$$y_i - y_o = -f\left(\frac{m_{21}(X_i - X_L) + m_{22}(Y_i - Y_L) + m_{23}(Z_i - Z_L)}{m_{31}(X_i - X_L) + m_{32}(Y_i - Y_L) + m_{33}(Z_i - Z_L)}\right) \quad ..(2.13)$$

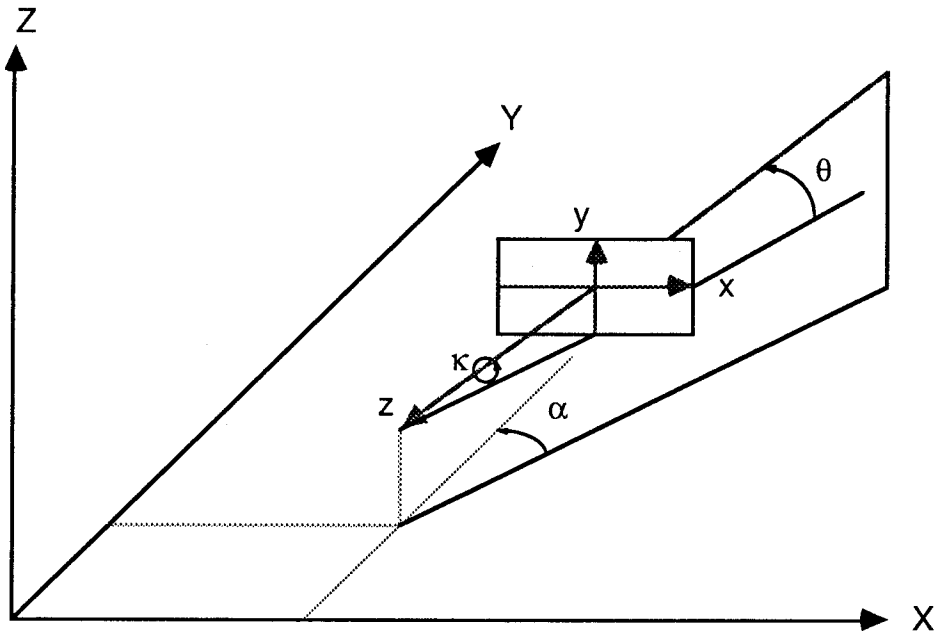

Figure 2.3 Exterior orientation by tilt, azimuth and kappa rotations.

Further descriptions of the collinearity equations is given in Moffitt and Mikhail (1980) and Slama (ed) (1980);Ch 2.

2.2 Evaluation Techniques

Photogrammetric evaluation techniques can be broadly classified into three basic groups. These include :

1. Analogue Solutions
2. Semi-Analytical Solutions
3. Analytical Solutions

Analogue evaluation techniques are defined as " .. the processes of establishing positions and elevations of points using spatial models oriented in analogue instruments" (Slama (ed) (1980);Ch 9). In other words the photographic or optical model is physically reconstructed and position is derived from it.

Limitations of analogue solutions for close range photogrammetry include requirements that "normal", or near "normal", photography is utilized. In close range photogrammetry, where the most precise imaging geometries for position determination are required and hence convergent multi-station photography is often utilized, analogue solutions are therefore not practical. Another limitation of the analogue approach is that, in general, analogue plotters do not have sufficient principal distance ranges to accommodate close range photography (Jodoin (1987). Analogue plotters such as the Wild A40 and the Zeiss Terragraph are designed specifically for terrestrial applications while plotters such as the Wild A7 and A10 Autographs are designed for either aerial or terrestrial applications. Such plotters, despite special design considerations, are still limited in allowable tilt and convergence angles. Mechanical limitations are therefore a major drawback for analogue close range photogrammetry.

Another drawback of the analogue approach relates to the limitation that a simultaneous solution can only be carried out for two photographs of the object space. This limits both the coverage of the object space and the number of object points which can be measured in the object space. Considering these limitations, along with the fact that analogue plotters are now obsolete, analogue solutions are considered unacceptable for close range applications and hence will not be developed as a viable evaluation technique.

Semi-Analytical evaluation techniques have the same basic limitations as the analogue solutions. In the semi-analytical approach optical models of the object space are reconstructed for the measurement of discrete points. The remainder of the data reduction and processing is carried out computationally. A requirement, as with the analogue case, exists for "normal" or near "normal" photography and hence many of the limitations associated with the analogue approach also apply to the semi-analytical approach. Both the analogue and semi-analytical solutions are viable evaluation techniques

for aerial photogrammetry, where photography is essentially "normal", however implementation in close range photogrammetry is neither feasible or practical. For typical close range photogrammetric applications, where convergent multi-station photography is employed, analogue and semi-analytical solutions cannot be utilized.

Analytical evaluation techniques are based on numerical or computational processes. Analytical photogrammetry can be defined as ".. the mathematical transformation between an image point in one rectangular coordinate system and the corresponding object point in another rectangular coordinate system" (Slama (ed) (1980);Ch 9).

The basic computational unit of analytical solutions is the bundle of rays which originates at the object points, passes through the image points and terminates at the exposure station. For each ray, image coordinates, xi and yi, are measured. By utilizing the collinearity equations, equations 2.12 and 2.13, the unknown parameters can be derived. In considering the bundle of rays a solution can be obtained in which all observations are simultaneously evaluated. Although several analytical approaches have been developed, eg sequential adjustments, independent model adjustments and simultaneous adjustments, analysis of the simultaneous adjustment technique will be the only process evaluated.

In the simultaneous approach the bundle of rays is considered and hence all unknown parameters are solved simultaneously. The parameters which may be solved include the parameters of exterior orientation of one or more cameras, object point coordinates, interior orientation parameters (if included in the mathematical model) and any other additional unknowns added to the system.

There are several basic simultaneous adjustment techniques. These include the *Direct Linear Transformation* and the *bundle* adjustment.

The *Direct Linear Transformation*, developed by Abdel-Aziz and Karara (1971), is a non-rigorous solution to the photogrammetric adjustment problem. The technique relies on the basic assumption that the projective, or exterior orientation, parameters can be perfectly recovered in any adjustment procedure. In other words the estimated exterior orientation parameters are

error free. Consequently, in the evaluation of object point coordinates and their precision, no account is made of the effect of the exterior orientation parameters upon the object point estimates (Brown (1980)). The Direct Linear Transformation has the advantage that it is computationally simple and efficient and solution time, for a given photogrammetric system, is quick. The solution is based on the direct transformation of image coordinates to object space coordinates, with the basic equations of the solution being :

$$x = \frac{L_1X + L_2Y + L_3Z + L_4}{L_9X + L_{10}Y + L_{11}Z + 1}$$

$$y = \frac{L_5X + L_6Y + L_7Z + L_8}{L_9X + L_{10}Y + L_{11}Z + 1} \qquad ..(2.14)$$

where x,y = image coordinates
X,Y,Z = corresponding object coordinates
L_1-L_{11} = transformation parameters

The Direct Linear Transformation approach is less accurate and less rigorous than the bundle adjustment approach, description of which will follow. However it offers quick and efficient solutions to photogrammetric adjustment problems. A major advantage of the technique is that no fiducial marks are required on the photography and it is therefore applicable to photography of non-metric cameras where there may be no fiducial marks (Marzan and Karara (1976), Jodoin (1987)). Systematic errors in the image coordinates can be resolved by adding additional parameters to equation 2.14, the process of which is covered in section 2.4.5.

The *bundle adjustment* was developed by Brown (1957) and is a mathematically rigorous solution for photogrammetric evaluations. Solution for all parameters can be undertaken by simultaneously considering the bundle of rays from all exposure stations to all object points. The solution is based on the collinearity equations, equations 2.12 and 2.13, from which a mathematical model is established and solution is via the method of estimation by least squares. The technique offers a direct solution as relative and absolute orientations of the photograph are not treated separately and hence the solution, and resulting error propagation, are mathematically rigorous.

The bundle adjustment approach, apart from being mathematically complete, offers a large amount of flexibility in the estimation process. The

photogrammetric observational network can be multi-station or a stereo-pair and convergent or normal. The estimation process can include solution for uncompensated systematic errors and can allow for the addition of auxiliary information, such as distance observations and control point observations etc.

Theoretically the bundle adjustment offers the highest accuracy of any of the adjustment processes in photogrammetry. This is due to :

1. the possibility of correcting for systematic errors in the photographic image.
2. accurate recovery of the inner orientation of each photograph.
3. accurate reconstruction of the model in the object space due to more redundancy in the solution.
4. the capability of handling more than two photographs.
5. the capability of handling convergent photography. (which is especially important for close range applications)
6. the mathematical completeness of the solution, especially with respect to the propagation of errors.

When the process was initially put into practice it was assumed that unresolved systematic errors in the image coordinates would have little or no effect upon the resulting solution. This meant that the only errors accounted for in the solution were the random observational errors in the image coordinates, which would be minimized in any least squares estimation procedure. Such an assumption, however, proved to be invalid as residual systematic errors, caused by phenomenon such as lens distortion, film unflatness, film deformations and atmospheric refraction, were found to introduce errors into the estimation process which drastically reduced achieved accuracies. The incorporation of additional parameters into the least squares solution, which model unresolved systematic errors in the image coordinates, has meant that the bundle adjustment solutions now meet theoretical accuracy expectations. Error sources and solutions for the effect of such errors is covered in section 2.4.

In this section the various evaluation techniques have been briefly assessed. In this report, estimation techniques for close range photogrammetry will be restricted to the bundle adjustment approach due to the flexibility and the mathematical completeness of the solution. The

alternative analytical solutions can be adapted if necessary or applicable, by applying similar procedures to those developed for the bundle solution. The bundle adjustment processes are covered, in detail, in Chapter 4.

2.3 Data and Image Acquisition

Data acquisition systems in close range photogrammetry can be classified into three basic groups depending on the type of data acquired and the equipment used. These systems include :

1. a camera, whether digital or analogue, for the acquisition of raw data in the form of a photograph or image.
2. a comparator or analytical plotter, for the measurement of image coordinate data from the photograph or image.
3. conventional surveying equipment, for the acquisition of auxiliary data such as control coordinates, distances, elevation differences etc.

The third group above will not be analysed as techniques for the acquisition of such data can be found in any conventional surveying text. Evaluation of photogrammetric cameras and comparators and analytical plotters, suitable for analytical photogrammetric applications, will be given.

2.3.1 Close Range Photogrammetric Cameras

Cameras, for use in close range photogrammetric applications, can be classified as either analogue or digital, depending on the form of the output, ie output in the form of an analogue photograph or a digital image. Conventionally cameras acquire analogue images, however recent advances in digital technology have facilitated the use of digital or CCD cameras for the acquisition of raw data. *Analogue cameras* can be classed as either metric or non-metric.

Metric cameras are those which have been designed and calibrated specifically for photogrammetric applications. These cameras have known and stable interior orientation and are usually of fixed focus (Moffitt and Mikhail (1980)). Metric cameras usually incorporate a low distortion lens system and in general have an image surface or reference plane which is a

true plane. Metric cameras are usually used as single units, however two cameras can be used simultaneously by mounting the two cameras at either end of a bar of definite length. Cameras of this form are called stereometric cameras and are limited to the case of "normal" photography. Slama (ed) (1980);Ch 16 and Moffitt and Mikhail (1980) give specifications of the various metric and stereometric cameras available in 1980. Table 2.1, from Slama (ed) (1980);Ch 16, lists specifications for some of the available metric cameras.

A recent advance in the design of metric cameras for close range photogrammetry has taken place in the USA by GSI, Geodetic Services Inc., USA, which has developed the CRC-1 close range camera specifically for close range photogrammetry. The CRC-1 is a large format roll film camera with applications in high precision photogrammetric evaluations. Specifications of the CRC-1 are listed in Table 2.2 (Brown (1982)).

Advantages of the CRC-1 include :

1. Large square format (230 x 230 mm).
2. incorporation of a reseau, for measurement of film unflatness and film deformations.
3. continuous focussing.

Use of the CRC-1, in close range photogrammetry, has resulted in proportional accuracies of the order 1:100,000 to 1:250,000 (Brown (1987), Fraser (1988b)) and sub-micron precision of object point coordinate estimation. Hence the CRC-1 is a major advance in camera technology for high precision photogrammetric applications. A future development in analogue camera technology is the metric camera, to be called the CRC-2, which is soon to be released by GSI. The CRC-2 will be similar to the CRC-1, but will be smaller format (130mm x 130mm), have a nominal 100mm focal length and will have a smaller physical size. These physical characteristics would indicate a reduction in achievable precision compared to the CRC-1, however it is anticipated that improved manufacturing and design techniques will facilitate comparable precision (Fraser (1989)).

Table 2.1. Specifications of single metric cameras

Manufacturer	Model	Format* of Photographic Material (cm)	Nominal Focal Length (mm)	Total Depth of Field (m)	Tilt Range of Camera Axis & Number of Intermediate Tilt Steps	Photographic Material	Comments
Galileo	Verostat	9 × 12 U	100		0→±90° (2)	glass plates or cut film	variable principal distance (in steps)
Galileo	FTG-1b	10 × 15 H	155	10→∞	0→±36° (continuous)	glass plates	variable principal distance (in steps)
Hasselblad	MK70 (Biogon lens)	6 × 6	60	0.9→∞	unlimited[4]	70mm film	Δ hand held or on tripod. variable principal distance (continuous mode) single frame exposure or sequence exposure
Hasselblad	MK70 (Planar lens)	6 × 6	100	15→∞[7]	unlimited[4]	70mm film	∇ fixed focus at ∞ (upon request fixed focus at desired distances down to 2m). Δ hand held or on tripod. motor driven; single frame exposure or sequence exposure.
Jenoptik Jena	UMK 10/1318 FP	13 × 18 UH	99	1.4→∞	−30°→+90° (7)	glass plates	Lamegon 8/100 lens with distortion <12μm for object distances ∞→3.6m.
	UMK 10/1318 NP						Lamegon 8/100 N lens with distortion <12μm for object distances 4.2→1.4m.
Jenoptik Jena	UMK 10/1318 FF	13 × 18 UH	99	1.4→∞	−30°→+90° (7)	190mm roll film & glass plates (with adapter)	Lamegon 8/100 lens with distortion <12μm for object distances ∞→3.6m.
	UMK 10/1318 NF						Lamegon 8/100 N lens with distortion <12μm for object distances 4.2→1.4m.
Jenoptik Jena	19/1318 Phototheodolite	13 × 18 H	190	25→∞	none[6]	glass plates	δ lens can be shifted vertically (+30→−45mm) in snap-in steps of 5mm.
Kelsh	K-470	10.5 × 12.7 UH	90	2→∞	none	cut film, roll film, glass plates.	image format offset from the optical axis of the lens by 13mm.
Sokkisha	MK165	12 × 16.5 U	165	10→∞	0→±30° (2)	glass plates	variable principal distance (in steps).
Wild	P32	6.5 × 9 UH	64	0.6→∞	on T1, T16 or T2: 0→±40° (continuous) on GW 1: 0→±30° (continuous)	glass plates, cut film, roll film	variable principal distance (in steps—interchangeable spacers).
Wild	P31	10.2 × 12.7 UH (4" × 5")	100	6.6→∞ (f/22) 12.4→∞ (f/5.6)	0→±30° (3) also +90°	glass plates & cut film	variable principal distance (in steps—interchangeable spacers)—wide-angle lens.
	"	"	45	1.5→∞ (f/22) 3.6→∞ (f/5.6)	"	"	Super-wide-angle lens.
	"	"	200	18→640 (f/22) 26→53 (f/5.6)	"	"	Normal-angle lens. Standard focusing 35 m; adapter rings on request; minimum distance 8m.
Zeiss (Oberkochen)	TMK-6	9 × 12 UH	60	5→∞	0→±90° (2)	glass plates	6 close-up lenses are available for object-distances of 0.5m, 0.6m, 0.75m, 1m, 1.5m, and 2.5m.
Zeiss (Oberkochen)	TMK-12	9 × 12 UH	120	20→∞	0→±90° (2)	glass	

*U/H: format Upright/Horizontal; UH: format Upright or Horizontal

Table 2.2 Specifications of the CRC-1 metric camera

GENERAL

- Large format (23 x 23 cm) roll film camera
- Standard aerial mapping film reels used (9.5 inch width, 4 inch diameter)
- Capacity approximately 140 exposures per roll (125 feet, 4 mil thick)
- Four illuminated corner fiducials

FILM PLATEN

- Film flattened by means of internal vacuum pump
- Patented reseau system incorporated into back of platen (7 x 7 array standard; 13 x 13 array optional)
- Surface flat to within ±5μm; function defining departures from flatness calibrated to within ±0.50μm.
- Platen rigidly fixed with respect to lens cone, rendering each reseau image the equivalent of a fiducial mark.

INTERCHANGEABLE LENS CONES

- 120 mm (88° x 88°)
- 155 mm (73° x 73°)
- 240 mm (51° x 51°)
- 360 mm (35° x 35°)
- 450 mm (28° x 28°)

FOCUSSING

- Continuous focussing by micrometric drum graduated in units of 10μm.
- Focussing range: 1.2 m – ∞, 120 mm
  1.6 m – ∞, 155 mm
  2.5 m – ∞, 240 mm
  4.0 m – ∞, 360 mm
  5.0 m – ∞, 480 mm

LENS CALIBRATION

- Stellar calibration of elements of interior orientation and coefficients of radial and decentering provided for each lens cone for infinity focus.
- Plumb line calibration of coefficients of radial and decentering distortion provided for each lens cone for near field focussing limit.

FILM TRANSPORT

- Digitally controlled drive motor mounted in film magazine
- Two second cycling
- Incremental advance mode in 1.0 mm steps permits execution of multiple exposures on same frame when retroreflective targets used.

MISCELLANEOUS

- Precise roll ring permits rotation about camera areas through ±180° (position of center of projection unaffected by rotation)
- Shutter controlled by cable release, speeds 1 to 1/125 second and bulb
- Auxiliary 35 mm SLR camera serves as viewfinder
- Power, 12 V DC external gel cel battery
- Weight, approx. 22 kg

Non-metric cameras are not designed specifically for photogrammetric applications. These cameras have, as a primary objective, the production of pictures of good pictorial quality. Non-metric cameras usually do not maintain a constant interior orientation, are variable focus, and do not contain fiducial marks (Moffitt and Mikhail (1980)). The lens systems of non-metric cameras are usually not low distortion and the image plane of the camera does not represent a true plane due to the lack of film flattening devices. Non-metric cameras include the multitude of 35mm cameras which are currently available. They produce pictures of good pictorial quality, however these pictures are generally geometrically poor. Factors which contribute to this poor geometric

quality include unstable interior orientations, significant lens distortion and significant film unflatness. These errors are covered in section 2.4. Prior to use of photography from non-metric cameras in an adjustment procedure, application of corrections from calibration, for lens distortion and interior orientation parameters, and from direct measurement, for film unflatness and film deformation, can be applied. In other words the image coordinates are corrected for systematic errors prior to use. However, due to the variable nature of such errors, the calibration may not be valid at the time of photography and hence such a solution will generally not yield results approaching potential accuracy.

As an alternative solution, self-calibrating adjustment procedures may be utilized. Such procedures include in the solution the estimation of interior orientation elements and systematic errors. With the self-calibration approach, parameters, which will model the typical systematic errors in close range photogrammetry, are added to the least squares mathematical model. Approximate estimates of the errors are introduced and the resulting estimation procedure determines the least squares estimates of the parameters which model the systematic errors. Problems with self-calibration procedures are evident if there is high correlation between some systematic errors. If such correlation exists then the resulting least squares process may become unstable and the errors may not be able to be resolved. In selecting parameters, or functions of parameters, to model the systematic errors, care should be taken to ensure that the additional parameters are both necessary and recoverable. If self-calibration procedures adopt an error model which is mathematically significant and allows recovery of parameters, then accuracy of the solution approaches the theoretically expected accuracies of a systematic error free system. The concepts of self-calibration will be covered in more detail in section 2.4.5. With the self-calibration approach of estimating coordinates, interior orientation elements and systematic errors, non-metric cameras provide a cheap, but not necessarily computationally cheap, image acquisition tool for medium accuracy photogrammetric applications.

An extension of the non-metric camera is the *semi-metric camera*. These cameras are designed for photogrammetric applications, but do not exhibit the full stability of the metric cameras. The semi-metric cameras usually have a more stable interior orientation, than non-metric cameras, and are calibrated. Inclusion of a reseau facilitates the measurement and reduction of errors, such as film unflatness and film deformations. Since these cameras are capable of

ensuring a more geometrically correct photograph than non-metric cameras, relatively high positional accuracy on the photograph, approximately 3-5 μm, can be achieved. Semi-metric cameras are usually 35mm to 70 mm format. Examples include the Rollei 3003 and 6006 cameras and the Hasselblad MK70 camera. A relatively new semi-metric camera is the Pentax PAMS 645P. This camera is fitted with a calibrated lens system, film flattening devices, a reseau grid and is electronically driven. The cost of the camera is of the order of $A10K - $A15K and is therefore is out of the financial range of most close range photogrammetrists.

Digital cameras are a new development in close range photogrammetric applications. Such cameras capture a digital image in the form of pixels of varying grey level intensities. These cameras usually employ semi-conductor array sensors or video tubes where, in both cases, conventional photographic emulsion is replaced by electronic sensing devices. Although digital cameras are not routinely implemented in photogrammetric applications, active research is currently taking place into the applicability of such cameras in close range photogrammetry (eg Wong and Ho (1986), Shortis (1988), Fraser (1988b)).

Digital cameras utilizing semi-conductor array sensors, of which the Charge Coupled Device (CCD) is the most common, are preferred to the video sensors due to the high sensor linearity and the higher geometric stability of the semi-conductor array sensor. CCD sensors can be either linear array or area array sensors. Area array sensors are usually preferred, however, due to the problems associated with mechanical scanning requirements for linear array sensors (Shortis (1988)).

Applications of digital cameras to close range metrology are particularly useful for problems requiring automated measurement and real time results. For multi-station convergent networks where large numbers of images, each containing up to several hundred points, are utilized, manual image observations can be time consuming and costly. Automated measurement, by digital correlation techniques based on pattern recognition principles, allow quick, low cost and high precision results. Although still in research stages, target recognition precision from automated measurement of digital images is of the order ±0.2 pixel, as reported by several authors, eg Wong and Ho (1986), Shortis (1988). Under ideal conditions this precision can approach 0.01 pixel (Trinder (1988)).

At present digital cameras have serious limitations for application in close range photogrammetry. A major limitation relates to the small size (9mm x 7mm) and limited resolution of the CCD area-array sensors. Such a limitation means that narrow fields of view result and hence use of a small imaging scale is required (Fraser (1988b), Shortis (1988)). Another limitation of the digital camera relates to the calibration of the digital sensor. Both the degree to which the digital sensor can be calibrated and the stability of the calibration require investigation. Calibration of digital sensors requires assessment of features such as frequency differences between pixel and converter clocks, warm up effects and jitter, or line synchronization effects (Fraser (1988b)).

Hence, although digital camera systems are available and are applicable to close range photogrammetry, limitations relating to camera calibration and imaging geometry must be assessed, and their significance determined, prior to acceptance as a close range photogrammetric image acquisition tool.

2.3.2 Comparators and Analytical Plotters

Photogrammetric cameras are used to acquire photographic images from which data pertaining to the position of points on the image will be determined. Such data, for analytical photogrammetry, is usually in the form of image coordinates with respect to a two dimensional coordinate system. Instruments for the measurement of image coordinates, for analytical photogrammetry, include comparators and analytical plotters and these instruments will be examined in this section.

A *comparator* is a device which allows the measurement of image coordinates on a photograph and can be defined as " an optical instrument, usually precise, for measuring polar or rectangular coordinates of points on any plane surface, such as photographic film" (Slama (ed) (1980);Ch 9). Comparators can be either mono-comparators, where measurements are made on only one photograph, or stereo-comparators, where simultaneous measurement of coordinates in a stereo-pair of photographs is carried out. Detailed descriptions of comparators and their functions in photogrammetry is given in Slama (ed) (1980);Ch 9 and Moffitt and Mikhail (1980).

An *analytical plotter* is "..a photogrammetric plotting system which mathematically solves the relationships between photographic image coordinates, measured in the two dimensional photographic reference

coordinate system and the ground coordinates of the object in the three dimensional 'real' world" (Slama (ed) (1980);Ch 13). An integral component of the analytical plotter is the digital computer which performs, on a real time basis, the computations which satisfy the mathematical relationships between object and image points. Hence no physical reconstruction of the photographic model is undertaken and all measurements are carried out on a computational or analytical basis. Analytical plotter functions and components are covered in Slama (ed) (1980);Ch 13 and Moffitt and Mikhail (1980).

In analytical close range photogrammetry either mono-comparators or analytical plotters are utilized to measure image coordinates from the photograph or image. Both of these instruments require calibration to reduce the effects of systematic instrument error on observed image coordinates. Instrument calibration, accomplished by measurement of a large number of points on a calibrated grid, will usually suppress instrument errors to the level of 1μm or less (Brown (1980)). If the instrument has been calibrated, then the effects of residual instrument errors are considered to be insignificant for close range photogrammetric applications.

Analytical plotters currently on the market include the Wild Aviolyt BC2, the Kern DSR-11,the Zeiss Phocus and the Intergraph Intermap Analytic. Such analytical plotters have the same basic features and are capable of measurement accuracy of the order 3 - 5 μm RMS. Analytical plotters of this type cost in the order of $A300K - $A500K.

A recent advance in analytical plotter technology is the Adam Technology MPS-2. The instrument is a micro photogrammetric system capable of utilizing 35mm to 70mm photography. The unit is small and relatively inexpensive, approximately $A50K, and allows measurement of image coordinates to approximately 5 μm RMS. Consequently the MPS-2 is a viable alternative for small format photogrammetric applications.

Other recent advances in analytical plotter and comparator technology relate to the techniques of automated measurement of analogue images. Automated measurement of analogue images is carried out by video or digital scanning of the analogue image. Pattern recognition techniques allow the detection of targets from which determination of image coordinates can be generated. Well defined targets, for example retro-reflective targets illuminated against a dark background, allow high accuracy in both target detection and measurement of the location of the target centre. Automatic

measurement techniques are generally associated with comparators. For example, GSI has developed the AutoSet-1 automatic mono-comparator specifically for close range photogrammetric applications. Measurement with an accuracy of 0.4 μm RMS and at a rate of one point every 0.8 seconds is possible (Fraser (1988b)). Problems are evident, however, in multi-station convergent photography where target recognition and detection are a problem and the matching of image points in the different scenes becomes difficult. Such problems are due to the distortions in the image geometry caused by convergence.

The accuracy of the output image coordinates is a function of both the camera used for capture of the raw data, and the instrument used for measurement of the image coordinates. Table 2.3 (Fraser (1988b)) depicts the angular measurement precision for different combinations of camera, focal length and image coordinate precision. The angular measurement precision, which is derived from the equation $\sigma_\alpha = \sigma$ / focal length, where σ is the image coordinate precision, allows a direct comparison of photogrammetric and conventional surveying techniques. In conventional surveying, accuracy is usually given in terms of a measured angle, eg theodolite angle measurement.

Table 2.3 Angular measurement precision for different combinations of camera, focal length and image coordinate precision

Camera Focal Length (mm)	Format (mm)	Std. Error of Image Coords. σ (μm)	Angular Std. Error σ_α (")	Representative Camera/ Comparator Combination or Digital Camera
240	230x230	0.5	0.4	CRC-1 with AutoSet automatic monocomparator
200	130x180	1.5	1.5	UMK 20/1318 with 1st order analytical plotter
120	230x230	0.5	0.9	CRC-1 with AutoSet
100	130x180	1.0	2.0	UMK 10/1318 with Rollei RS comparator
100	130x180	2.0	4.1	UMK 10/1318 or P-31 with analytical plotter
80	60x60	2.5	6.4	Hasselblad MK70 or Rollei 6006 Reseau with analytical plotter
40	60x60	1.0	5.2	Rollei RSC reseau-scanning camera
40	60x60	4.0	21.0	70mm semi-metric camera with 2nd order analytical plotter
20	9x7	0.3	3.1	Videk Megaplus CCD camera at 1/20th pixel image measurement accuracy
12.5	8.8x6.6	1.0	16.0	CCD camera with approx. 20 μm pixels and 1/20th pixel accuracy

2.4 Error Sources

Error sources in close range photogrammetry can be classified into five major categories.

1. atmospheric refraction
2. camera errors
3. image measurement errors
4. film errors
5. auxiliary data acquisition errors

Figure 2.4, adapted from Jodoin (1987), illustrates the error sources and the major contributing factors to each error type. Auxiliary data comprise data such as object point coordinates, distances, elevation differences, vertical and horizontal angles and, in general, any data acquired in the object space. Errors associated with the acquisition of auxiliary data include errors such as gross observational error, random measurement error, atmospheric refraction errors, as well as errors such as centring, leveling and pointing errors. The magnitude and effect of these errors is covered in conventional surveying texts and will not be covered here.

The theoretical principles of photogrammetry, as given by the collinearity condition, were developed in section 2.1.1. Conditions which apply at the time of photography are collinearity of object point, perspective centre and image point and coplanarity of all image points. In reality these conditions are not met due to various errors which cause the image point, the perspective centre and the object point to deviate from linearity and cause the reference plane to deviate from being a flat surface. The causes for such differences between theoretical and actual cases are:

1. a light ray traveling from the object to the image is deflected by the medium through which it passes. Such deflections are due to atmospheric refraction and lens distortion.
2. the image point is displaced from its theoretical position in the image plane due to changes within the photograph itself, film shrinkage, expansion or deformation, and due to the lack of flatness of the film in the image plane.
3. systematic errors in the comparator or analytical plotter and random measurement error due to operator / instrument limitations.

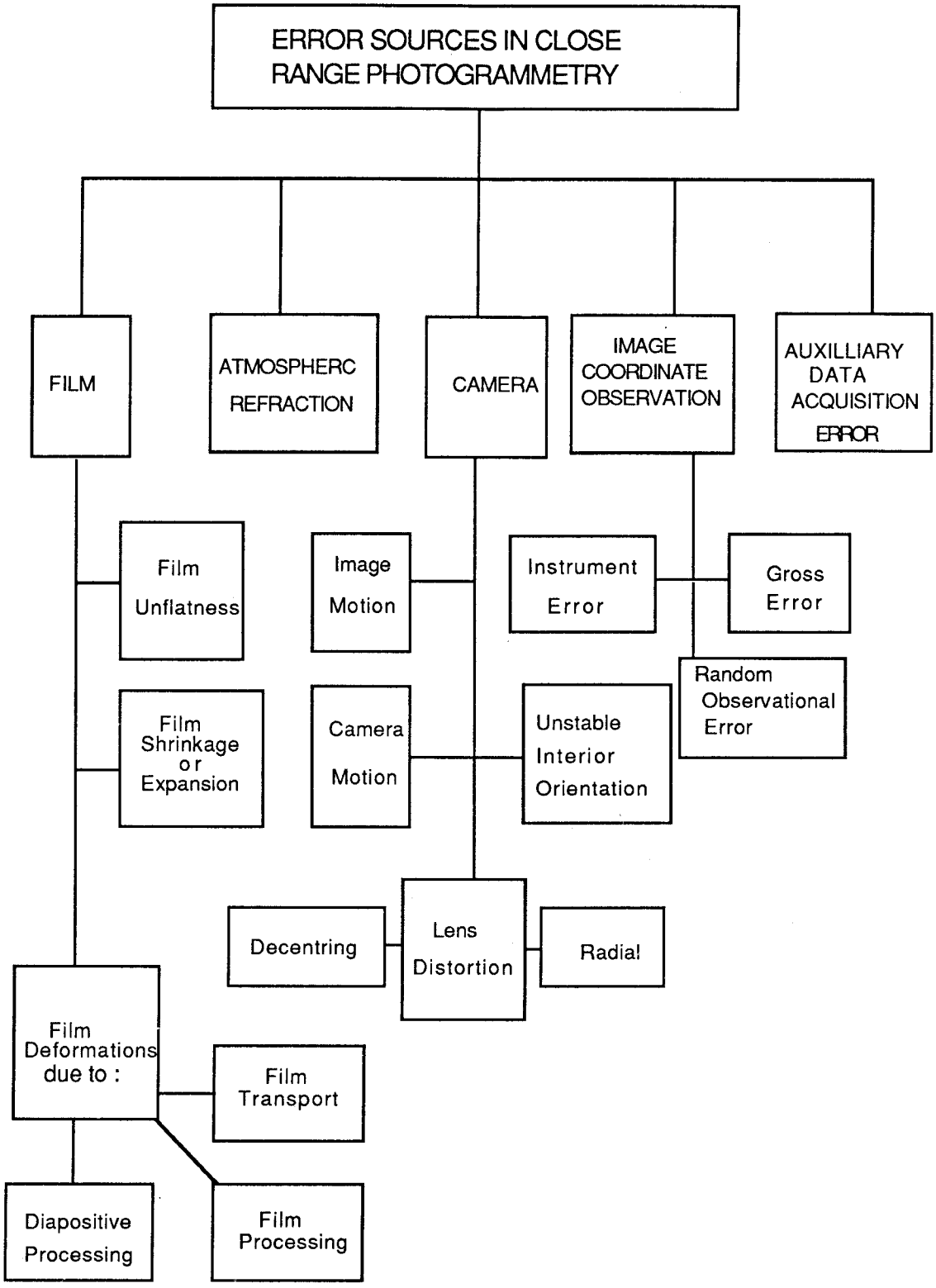

Figure 2.4 Error sources in close range photogrammetry

Image measurement errors comprise two major error sources. These include random observational error and systematic instrument error. Instrument error is covered in section 2.3.2 and the effect of random observational errors is minimized in any least squares adjustment process.

2.4.1 Atmospheric Refraction

A ray of light passing from a point on the object to the camera lens will be refracted due to density gradients in the atmosphere. Such refraction effects will displace the image point on the photograph from its theoretical position, as given by the collinearity condition.

Marzan and Karara (1976) state that for close range photogrammetry, where object to image distances are less than 300 metres, the errors induced by atmospheric refraction are negligible and hence no refraction corrections need to be applied to image coordinates. Therefore unless object to image distances exceed several hundred metres the effects of atmospheric refraction on image position can be ignored.

2.4.2 Lens Distortion

The lens system of a camera will generally contribute as a major error source in close range photogrammetry and is evidenced in the deviation of an image point from its theoretical position, as defined by the collinearity condition. Lens distortion is a term used to describe the bending of an object space ray as it passes through the lens system into the image space. Such bending is due to lens aberrations. Figure 2.5 illustrates the bending of a ray due to lens distortions. Lens distortion consists of two components, namely *radial distortion* and *decentring distortion.*

Radial distortion is inherent in the design and manufacture of the lens and results in radially symmetric displacement of the image from its ideal position. Radial distortion is a function of both radial distance on the image plane and also the distance from the centre of projection to the photographed point (Brown (1980). A complete analysis of radial lens distortion, and its variation with focussed object distance, radial distance and position within the photographic field, is given in Brown (1972).

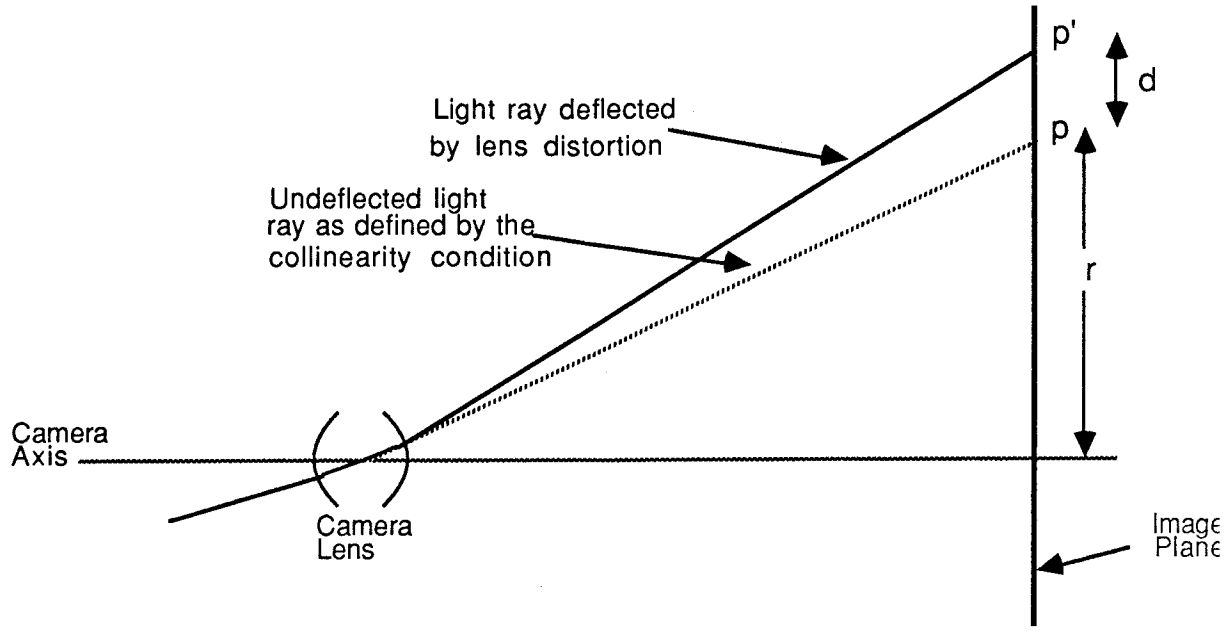

Figure 2.5 Bending of light rays, at the camera lens, due to lens distortion

Decentring distortion is essentially a function of the physical construction of the lens system. Imperfect centring of lenses causes the ray from the object to the image to deviate from its theoretical position, as shown in figure 2.6. Decentring distortion is an individual property of each lens system and can be altered by any blow or knock to the camera. Consequently such distortion cannot be considered constant and regular calibration must be undertaken to determine the magnitude of the distortion and its effect on photographic geometry. Decentring distortion may also vary with changes in focal length and hence, as many non-metric cameras utilize zoom lenses, the effects of errors induced by decentring distortion, as a function of changes in focal length, must be assessed. If the errors due to decentring distortion caused by variable focal length cannot be resolved, then the zoom lenses used for focussing should remain at the one focal length setting. This will ensure a constant focal length for all exposures and hence decentring errors which are not a function of varying focal length. In other words, the errors in the image coordinates due to decentring distortion in the camera lens system will be independent of focal length variations.

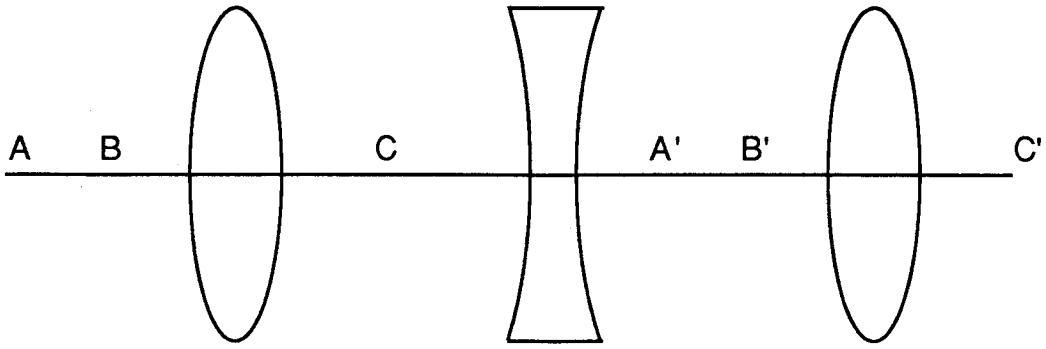

CENTRED LENS SYSTEM

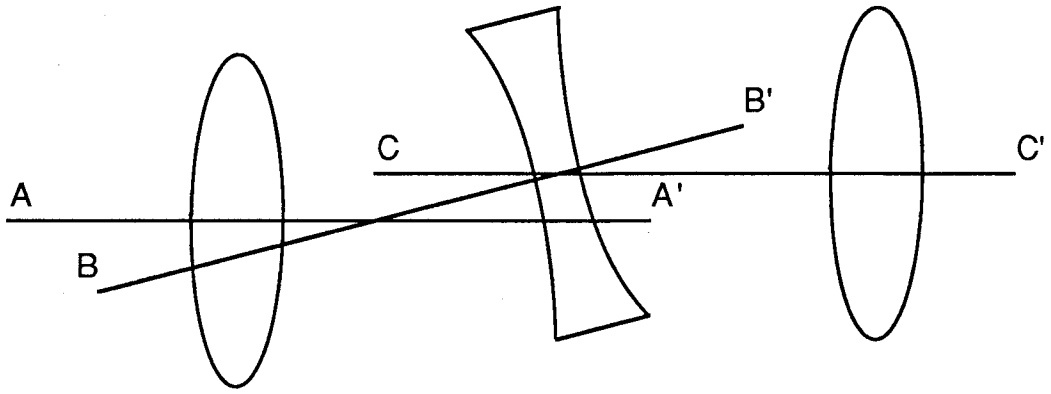

DECENTRED LENS SYSTEM

Figure 2.6 Bending of incident lightrays due to decentring distortion

The corrections to measured image coordinates, for the combined effects of radial and decentring distortion, can be given as :

$$\Delta x = (x_i-x_o)(K_1r^2 + K_2r^4 +..)+[\ P_1\ (r^2 + 2\ (x_i-x_o)^2 + 2P_2(x_i-x_o)(y_i-y_o)][1 + P_3r^2 +..]$$

$$\Delta y = (x_i-x_o)(K_1r^2 + K_2r^4 +..)+[\ 2P_1(x_i-x_o)(y_i-y_o) + P_2(r^2 + 2\ (y_i-y_o)^2][1 + P_3r^2 +..] \quad ..(2.15)$$

where x_i,y_i = image coordinates of point i

x_o,y_o = image coordinates of the principal point

r = radial distance from the principal point

$= \sqrt{(x_i-x_o)^2 + (y_i-y_o)^2}$

$K_1,K_2,...$ = coefficients of radial distortion

$P_1,P_2,...$ = coefficients of decentring distortion

The decentring component of equation 2.15 is valid for an infinite focus. For finite focus the decentring component is multiplied by (1-f/s), where f is the principal distance and s is the distance at which the lens is focussed. This scaling accounts for points in the plane at s. To account for variability within the photographic field, a further scaling factor is used; $\left(\frac{s-cs'}{s'-cs}\right)$, where s' is the distance to the point under consideration (Fryer and Brown (1986)).

Equation 2.15 includes the Brown-Conrady formula for resolving decentring distortion, which assumes focus at infinity. If this is not the case the formula can be extended to include cases where the focus is varying and finite.

The coefficients of distortion in equation 2.15 can be determined by a variety of methods. Such methods include stellar calibration, analytical plumb line calibration, simultaneous multiframe analytical calibration (Brown (1972)) or by simultaneous calibration and adjustment (self-calibration bundle adjustment), which will be covered in section 2.4.5.

2.4.3 Film Unflatness

A basic assumption of the collinearity condition is that all image points lie on a common plane, ie all image points are coplanar. This condition will not hold if the photographic surface is not flat at the instant of photographic exposure. The consequence of this film unflatness is that the image point will be displaced radially from its true position. Figure 2.7 illustrates the radial displacement of an image point due to the departure of the photographic surface from an ideal image plane. Although the error is a systematic error it occurs randomly in the photograph format and hence formulation of a model to define photographic surface unflatness, across a whole photograph format, is not possible.

Most metric cameras can utilize glass plates as the photographic media, with the plates being either micro-flat or ultra-flat. Micro-flat plates are usually flat to within 3 - 4 μm of a best fitting plane while ultra-flat plates are 7 - 10 times coarser than micro-flat plates (Brown (1980)). Ultra-flat plates are usually employed for close range photogrammetric mensuration, where glass plates and not film are used, and departures from flatness can be assumed to be negligible. In high precision applications, micro-flat plates should be utilized to ensure errors due to plate unflatness do not degrade results. The

influence of film unflatness on non-metric imagery is covered in Fraser (1982c).

In both metric and non-metric cameras, where film is used as the photographic media, film unflatness can be a major source of error. To reduce the effect of film unflatness on measured quantities, the film is usually flattened and can be accomplished in several ways.

1. pressing the film against a glass register plate which is located in the camera focal plane. (Register-glass cameras)
2. using atmospheric pressure to press or suck the film against a vacuum platten. (Vacuum-back cameras)

Brown (1980) states that register-glass cameras, utilizing carefully made and maintained pressure pads, ensure film flatness to within 15 to 20 μm, however practical difficulties limit the applicability of the register-glass method. Vacuum-back cameras can ensure film flatness to within 3 - 5 μm of an ideal plane. The degree to which flatness can be achieved is a function of the flatness of the platten itself and the degree to which the actual film can be flattened. These residual errors, ie errors due to remaining film unflatness, are generally negligible for most close range photogrammetric applications however (Brown (1980)).

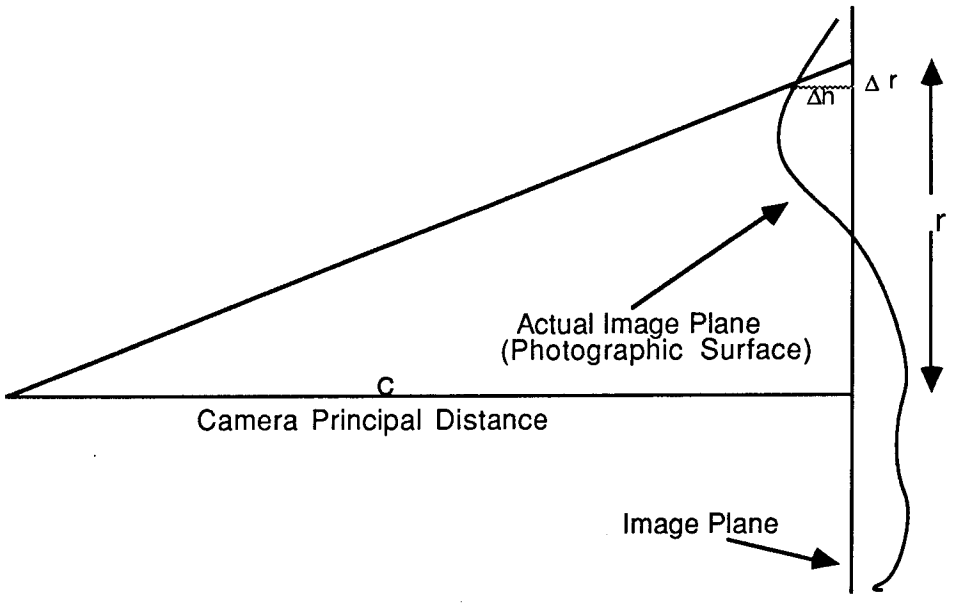

Figure 2.7 Effect of photographic surface unflatness on the position of an image point

A direct approach for the detection and elimination of errors due to film unflatness is to incorporate a reseau in the camera. The reseau either

comprises a plate, mounted in front of the focal plane, consisting of any array of fine crosses in calibrated positions or "back-projected" crosses through the vacuum plate. From the resulting image, which contains superimposed reseau crosses, image coordinates can be measured with respect to the calibrated reseau positions. Cameras which are designed for photogrammetric applications, and which utilize film, are usually fitted with a reseau. Such cameras include the GSI CRC-1 metric camera as well as semi-metric cameras, such as the Rollei 3003, Pentax PAMS 645P and the Hasselblad MK70.

With reference to figure 2.7, equations can be formulated to compute the corrections to the observed image coordinates for a measured departure from flatness. The corrections to image coordinates x_i and y_i become :

$$\Delta x = \frac{x}{c}\Delta h$$

$$\Delta y = \frac{y}{c}\Delta h \qquad ..(2.16)$$

2.4.4 Film Deformations

Film deformations, which are dimensional changes within the plane of the photograph itself, introduce errors into the measured image coordinates. Such errors are due to film expansion and contraction within the camera during photography as well as deformations in the film during processing. Film is extremely sensitive to temperature and humidity and hence changes in either temperature or humidity will cause the film to deform. Such deformations are usually less than 5μm from the ideal or undeformed case. Dimensionally stable film has been developed which is essentially inert with respect to changes in temperature and humidity and for high precision metrology this film is always used. Cameras utilizing glass plates do not have the same degree of problems, due to dimensional deformations, as cameras using film. Glass is much more stable than film and hence any dimensional changes in the glass plates can be assumed to be negligible, ie deformations are generally less than 2μm.

Detection of film deformations is usually carried out by utilizing cameras with a reseau attached, as described in section 2.4.3. Measurement of image coordinates with respect to calibrated reseau positions resolves the majority of

the film deformation effect, with the residual error being of the order 3μm and therefore assumed negligible for close range photogrammetry (Brown (1980)). The fiducial marks on a photograph will give an overall indication of any film deformation that has taken place. Although such measurements give no indication of the actual deformation at any particular point on the photograph, they may be used to indicate if deformation has occurred and the magnitude of this deformation. To minimize film deformation, stable base film can be utilized. Such film is relatively inert to deformations caused by film processing and hence will minimize the effects of film deformation on the measurements.

2.4.5 Correction for Systematic Errors

There are two basic solutions for the correction and compensation of systematic errors in close range photography. The first approach is to either model or measure the errors and apply them to the observed image coordinates prior to adjustment. For example lens distortion errors are modelled by equation 2.15 and the corrections applied to the observed coordinates. If the camera has utilized a reseau then determination of errors due to film unflatness and film deformation can be carried out and corrections applied to the observed coordinates.

Alternatively self calibration procedures can be used. Such procedures use the approach of incorporating additional parameters in the adjustment process, which will model the unresolved systematic errors which exist in the photography. In general, additional parameters are introduced in terms of polynomial functions and take the form of equation 2.17. For high precision applications both methods are utilized. The principle systematic errors are resolved by measurement or prior calibration and then any remaining unresolved systematic errors are modelled by self-calibration procedures.

$$dx = Fx(x,y,r)$$
$$dy = Fy(x,y,r) \qquad \text{..(2.17)}$$

where $r = \sqrt{x^2+y^2}$

x,y = image coordinates (Kilpelä (1981))

Addition of these functions to the collinearity equations gives equations which allow modelling of residual systematic errors in the image coordinates.

The collinearity equations, given by equations (2.12) and (2.13), take the form of the following two equations.

$$x_i - x_o + dx = -f\left(\frac{m_{11}(X_i - X_L) + m_{12}(Y_i - Y_L) + m_{13}(Z_i - Z_L)}{m_{31}(X_i - X_L) + m_{32}(Y_i - Y_L) + m_{33}(Z_i - Z_L)}\right) \quad ..(2.18)$$

$$y_i - y_o + dy = -f\left(\frac{m_{21}(X_i - X_L) + m_{22}(Y_i - Y_L) + m_{23}(Z_i - Z_L)}{m_{31}(X_i - X_L) + m_{32}(Y_i - Y_L) + m_{33}(Z_i - Z_L)}\right) \quad ..(2.19)$$

Problems with this approach become apparent if high correlations between additional parameters exist. High correlations between parameters will make the solution unstable and hence systematic errors will not be resolved accurately. The term "overparameterization", as introduced by Brown (1980), describes ill-conditioning induced by the inclusion in the adjustment of unnecessary or inherently unrecoverable parameters. Overparameterization can be avoided by :

1. setting a loose a priori value and variance on the additional parameters.
2. assessing the covariance structure of the estimated additional parameters and deleting from the model those parameters which exhibit high correlation.
3. deleting from the model those additional parameters which may be recoverable but which do not differ significantly from zero.

Such processes will ensure a stable model for the recovery of a priori unresolved systematic errors, as well as a compact model which contains no extraneous parameters. Another problem associated with overparameterization is that, while the solution may be stable, the increase in the number of parameters can lead to high internal precision but low accuracy.

Typical self calibration parameter sets contain parameters for affinity and non-orthogonality, a model for decentring distortion and a polynomial function for radial distortion. Such parameter sets are given in Kilpelä (1981). As most cameras used in photogrammetric applications either utilize glass plates or have a reseau attached, errors due to film unflatness and film distortion can either be assumed to be negligible (glass plates) or can be measured with respect to a calibrated reseau (film). Consequently parameter sets for the modelling of systematic errors do not usually contain parameters to model systematic film deformation or unflatness errors.

In this chapter the mathematical principles associated with close range photogrammetry have been assessed. The geometric properties of photography and the mathematical relationship between object and image have been developed. Arising from such developments was the basic equation relating object and image points, the collinearity equation, and the structure of the rotational elements which define the orientation of the camera in the object space.

The effect of systematic errors upon the image coordinate data, caused by atmospheric refraction, lens distortion, film unflatness and film deformation have been assessed as have the principles of self-calibration. The computational basis of analytical photogrammetry, especially with respect to network design and evaluation, is the least squares method. This method will be evaluated and developed in detail in Chapter 3.

3. LEAST SQUARES ESTIMATION

The principal estimation technique, for close range photogrammetry, is the least squares adjustment. Both the principles of close range photogrammetry and the principles of network design and analysis are dependent on the form of the least squares estimation methods employed. Consequently to develop the techniques associated with network design, with an emphasis on network optimization, the significance and effect of the least squares adjustment upon the solution must be investigated. In this chapter the basic principles of the least squares process as well as the various estimation techniques, and the implications of such techniques upon the solution, will be analysed in detail. The analysis will be with respect to a general, not necessarily photogrammetric, model and application to close range photogrammetry and photogrammetric network design will be undertaken in the following chapters.

3.1 Least Squares Principles

The technique of least squares estimation was formulated to allow an optimal estimation of a set of parameters, or functions of parameters, based on a set of redundant observations. In other words an estimate is made of the subject parameters from an overdetermined system of observations. For an observation, l, the least squares estimate of the observation will be denoted by $\hat{l}$. The least squares principle, which is based on the principle of maximum likelihood estimation, attempts to minimize the variance of the estimated observations from the actual observations. Such a principle can be expressed as :

$$\Phi = v^T P v \Rightarrow \text{minimum} \qquad ..(3.1)$$

where P = the weight matrix of observations
Φ = the function to be minimized
v = the residual vector (Mikhail (1976))

The residual vector is given by :

$$v = \hat{l} - l \qquad ..(3.2)$$

3.2 Selection of the Least Squares Mathematical Model

In order to estimate parameters or functions of parameters, based on the least squares principle stated in equation 3.1, functional and stochastic models require formulation. Such formulations are generally based on sets of either condition equations and / or observation equations.

A condition equation mathematically expresses the geometrical properties which must be satisfied by a set of observations on a set of physical phenomena. The equation comprises a minimum of two observations and may include unknown parameters. The general form of such an equation is :

$$F(\hat{l}) = F(l + v) \qquad ..(3.3)$$

In equation 3.3 $\hat{l}$ are the adjusted observations, l the observations and v the residuals, as given by equation 3.2. After estimation of observed parameters and observations, unknown parameters can be estimated based on the geometrical relationships established in the conditions applied. An estimation technique based on condition equations is called the *condition method* (Mikhail (1976), Slama (ed) (1980);Ch 2). Condition estimation methods have several problems with respect to practical application of the technique. Such problems include :

1. construction of the least squares formulations requires sound geometrical understanding of the system as only independent conditions can be used.
2. tedious derivation of adjusted parameters from functions of the observables.
3. computer automation for the development of condition equations is not feasible.

Because these problems associated with condition adjustments negate the conceptual simplicity of the technique, alternative estimation techniques are investigated. Derivation of the condition method can be found in Mikhail (1976).

Observation equations are a form of condition equation where only one measured parameter is included in each equation. The equation is formulated on the basis of a measured parameter being a function of several unknown parameters. The general form of the equation is :

$$\hat{l} = F(\hat{X}) \qquad ..(3.4)$$

where $\hat{l}$ = adjusted observations

$\hat{X}$ = parameter estimates

An estimation technique based on observation equations is called the *parametric method* (Mikhail (1976), Slama (ed) (1980);Ch 2). In a case where a mathematical model is formulated based on both condition and observation equations the resulting estimation technique is called the *combined method* (Slama (ed) (1980);Ch 2). The basic equations, relating observations to parameters, in photogrammetry are the *coplanarity condition* and the *collinearity equation.*

The coplanarity condition is a condition equation relating image observations to parameters, such as exterior orientation parameters and object space coordinates. Adjustment processes based upon the coplanarity condition have several problems for solution of close range photogrammetric evaluations. These include complex formulation for more than two photographs, complex image to ground relationships and the fact that the solution is basically sequential. Consequently application of the coplanarity condition to convergent close range photogrammetric networks is not recommended and hence this condition will not be considered. The coplanarity condition is covered in Moffitt and Mikhail (1980), Appendix C.

The collinearity equation, as formulated in Chapter 2, relates image observations to unknown parameters, such as camera orientation parameters and object space coordinates, in the form of observation equations (Equations 2.12 and 2.13). One observation equation is established for each image observation and no specific geometric understanding is required for the application being assessed. In other words each observed image coordinate, x_i or y_i, results in one observation equation and no analysis of the independence of these equations is necessary. Hence automation by computer, for the generation of such equations, is possible.

The collinearity equation is accepted by photogrammetrists as the standard equation in the least squares process for close range photogrammetry and hence will be the fundamental equation in the formulation of a least squares mathematical model. Such a model will be developed on the basis of the parametric method of least squares.

3.3 Formulation of the Least Squares Model

The notation used in photogrammetric and least squares textbooks is often not compatible. In this report an attempt has been made to unify the notation throughout, including application to both least squares and photogrammetric evaluations. Unless explicitly stated otherwise, the following notation will apply throughout this report. The order is given in brackets.

$E(.)$ = expectation operator

X = unknown parameters (u)

$\hat{X}$ = estimated parameters (u)

X^o = approximate estimates of the parameters (u)

$\Delta\hat{X} = \hat{X} - X^o$ = corrections to parameters (u)

l = observations (n)

$\hat{l}$ = adjusted observations (n)

A = design or coefficient matrix $= \left.\frac{\partial F}{\partial x}\right|_{X=X^o}$ (n,u)

b = constant vector (misclosure vector) $= l - F(X)\big|_{X=X^o}$ (n)

v = residual $= \hat{l} - l$ (n)

σ_o^2 = a priori variance factor

$\hat{\sigma}_o^2$ = a posteriori variance factor

Σ = variance -covariance matrix of observations (n,n)

Q = cofactor matrix of observations (n,n)

P = weight matrix of observations $= Q^{-1}$ (n,n)

$\Sigma_{\hat{x}}$ = variance-covariance matrix of adjusted parameters (u,u)

$Q_{\hat{x}}$ = cofactor matrix of adjusted parameters (u,u)

$Q_{\hat{l}}$ = cofactor matrix of adjusted observations (n,n)

Q_v = cofactor matrix of residuals (n,n)

n = number of observations

u = number of unknown parameters

r = redundancy $= n - u$

ε = true error (n)

d = rank deficiency

The basic mathematical model in the least squares estimation process is the Gauss-Markov model (GMM). Such a model is a linear mathematical model relating stochastic observations, l, to parameters, X. The model can be expressed as :

$$E(l) = AX \qquad ..(3.5)$$

$$E(\varepsilon \varepsilon^T) = \sigma_o^2 Q = \Sigma \qquad ..(3.6)$$

The following assumptions are made with respect to the model :

1. the number of observations exceeds the number of unknown parameters. $(n > u)$
2. the observational errors are random with expectation zero. $\varepsilon \sim N(0, \sigma_i^2)$ where σ_i^2 is the variance of an observation
3. the observations are normally distributed with expectation AX and variance Σ. $l \sim N(AX, \Sigma)$
4. the observations are mutually independent.

As a requirement for the model the observation equations must be linear. In cases where the observation equations are not linear an approximate linear equation can be formulated by application of a Taylor series expansion. Such an expansion is of the form :

$$F(X^o) + \left.\frac{\partial F}{\partial x}\right|_{X=X^o} . \Delta\hat{X} + \text{higher order terms} = F(X) \qquad ..(3.7)$$

By neglecting second and higher order terms the above equation provides a linear approximation of the non-linear observation equation. An approximation such as this means that any estimation process will not be a single step process. As $X^o + \Delta\hat{X}$ will only provide an improved estimate of the parameters, X, iterations of the estimation procedure will be required until the corrections $\Delta\hat{X}$ become negligibly small. It is then that the resulting estimate of the parameters, $\hat{X}$, given by $X^o + \Delta\hat{X}$, will be the desired solution. Note that in the non-linear least squares case, solution is with respect to $\Delta\hat{X}$, the corrections to the parameters, and b, the misclosure vector. Equations 3.5 and 3.6 give the theoretical expectations of the model. Transformation of these equations to estimable quantities leads to the following equations.

Functional Model

$$v = A\hat{X} - l \qquad ..(3.8)$$

Stochastic Model

$$\Sigma = \sigma_o^2 Q = \sigma_o^2 P^{-1} \qquad ..(3.9)$$

The weight matrix of observations, P, is determined from σ_i, the standard deviation of observation i. In formulating the matrix it is usually assumed that no correlations exist between observations and hence the weight matrix reduces to a diagonal matrix of terms $\frac{\sigma_o^2}{\sigma_i^2}$.

Equations 3.8 and 3.9 represent an overdetermined system of equations according to assumption 1 on the previous page. Optimal estimation of parameters can then be formulated on the basis of the estimates of the unknown parameters being unbiased and of minimal variance. Such criteria can be expressed mathematically as :

$$E(\hat{X}) = X \qquad \text{(unbiased)} \qquad ..(3.10)$$

$$\sigma_{\hat{X}}^2 = \text{minimum} \qquad \text{(minimum variance)} \qquad ..(3.11)$$

On the basis of such criteria the mathematical derivation of equations to give optimal estimates of the parameters can be undertaken. Such derivation can be found in most statistical texts, such as Searle (1971), as well as in Mikhail (1976). Caspary (1987) gives a descriptive analysis of the formulation. The parameter and variance estimates can be written as :

$$\hat{X} = (A^T P A)^{-1} A^T P l = Q_{\hat{X}} A^T P l = N^{-1} A^T P l \qquad ..(3.12)$$

(BLUE : Best Linear Unbiased Estimator)

Equation 3.12 is of type BLUE and conforms with equation 3.10 since, by rearranging equation 3.12 in terms of equation 3.10 and equation 3.5, the following characteristics can be developed.

$$E(\hat{X}) = (A^T P A)^{-1} A^T P E(l) \qquad ..(3.13)$$

$$E(l) = AX \qquad ..(3.5)$$

therefore

$$E(\hat{X}) = (A^T P A)^{-1} A^T P AX = I X = X \qquad ..(3.14)$$

hence the result is within its expectation value and unbiased.

$$\hat{\sigma}_o^2 = \frac{V^T P V}{n-u} \qquad ..(3.15)$$

(BIQUE : Best Invariant Quadratic Unbiased Estimator)

The cofactor matrices associated with equation 3.12 are :

$$Q_{\hat{x}} = (A^T P A)^{-1} \qquad ..(3.16)$$

$$Q_{\hat{l}} = A (A^T P A)^{-1} A^T \qquad ..(3.17)$$

$$Q_v = Q - A(A^T P A)^{-1} A^T = Q - Q_{\hat{l}} \qquad ..(3.18)$$

(Caspary (1987))

The variance-covariance matrix of the unknown parameters, $\Sigma_{\hat{x}}$, is a scalar function of the cofactor matrix of the unknown parameters, $Q_{\hat{x}}$. Scaling is carried out by premultiplication of $Q_{\hat{x}}$ by either the a priori variance factor or the a posteriori variance factor.

Scaling by the a priori variance factor, σ_o^2, is conditional upon the factor being statistically significant. The a posteriori variance factor, $\hat{\sigma}_o^2$, is statistically tested, by using the F-test at some predetermined level of significance, to determine if it is consistent with σ_o^2. If the test passes then σ_o^2 is used as the scaling factor otherwise $\hat{\sigma}_o^2$ is used (Mikhail and Gracie (1981)). In adopting this technique for determining the scaling factor, care should be taken to ensure that the sample size, over which the test is carried out, is large, ie greater than approximately 20 to 30 observations. For a small sample size statistical compatibility may be assumed from the F-test, however, in reality the two factors may be significantly different. In close range photogrammetric applications sample sizes are usually very large and hence problems associated with the statistical testing of small samples do not occur.

Scaling by the a posteriori variance factor relies on the assumption that σ_i, the accuracy of observation i, can never be known precisely unless it is determined from multiple observations, on the same instrument and by the same observer. In the process of scaling by $\hat{\sigma}_o^2$, the variance factor is assumed to be an unknown. An initial estimate of the a priori variance factor is made and an adjustment carried out, from which $\hat{\sigma}_o^2$ is determined. If $\hat{\sigma}_o^2$ is not equal to σ_o^2 then the observational accuracy is varied, the system of equations readjusted and the sequence continued until $\hat{\sigma}_o^2$ is approximately equal to σ_o^2. In such a process not only are the unknown parameters and their associated

variances estimated but the observational accuracy is estimated as well. A difficulty arises, with scaling by $\hat{\sigma}_o^2$ if observations are of different types, and hence different σ_i apply. Here an ambiguity arises as it cannot be resolved which observational accuracies require reweighting if the a priori and a posteriori variance factors are not approximately equal after the first adjustment (Rüeger (1989)).

In close range photogrammetry the observational accuracies of the typical observations are generally well known. For example image coordinate observations on a first order analytical plotter, eg Wild Aviolyt BC2, are known to have a standard deviation of the order of 3 - 5 μm and for inexperienced operators this can be increased to reflect the estimated increase in observational error. Consequently it can be assumed that σ_o^2 would be a valid estimate of observational precision and hence a valid a priori estimate of the variance factor. For such reasons, and because the resulting processes are numerically simpler, scaling by the a priori variance factor will be carried out. Note however that the requirements for testing of statistical significance of the factor must still be undertaken.

The variance-covariance matrix of adjusted parameters, $\Sigma_{\hat{x}}$, becomes :

$$\Sigma_{\hat{x}} = \sigma_o^2 Q_{\hat{x}} \qquad ..(3.19)$$

The model can be adapted to the case where the estimated quantities are corrections to the unknown parameters. This is achieved by including the corrections to the unknown parameters, $\Delta\hat{X}$, where $\hat{X} = X^o + \Delta\hat{X}$ and X^o is an approximate to the unknown parameter, and the constant term b, where $b = l - F(X)^o$ and $F(X)^o$ is from equation 3.7 evaluated at some approximate value, in the model. Equations 3.15 to 3.19 remain unchanged but equation 3.12 becomes :

$$\Delta\hat{X} = (A^T P A)^{-1} A^T P b \qquad ..(3.20)$$

It should be noted that for equation 3.20 :

$$Q_{\Delta\hat{x}} = Q_{\hat{x}} \text{ and hence } \Sigma_{\Delta\hat{x}} = \Sigma_{\hat{x}} \qquad ..(3.21)$$

(Harvey (1987))

In photogrammetric least squares applications, observation equations are usually non-linear. Therefore observation equations are formulated in terms of corrections to the parameters, $\Delta\hat{X}$. In the least squares developments which follow, the vector $\hat{X}$ will refer to the corrections to the parameters and the vector l will refer to the difference between the observed and the calculated observations, determined at the approximate parameter value. This notation has been adopted in order to simplify the development of the various least squares solutions and will apply unless explicitly stated otherwise.

3.4 Concept of Rank and Rank Deficiency

The rank of a matrix can be defined as " the order of the largest non-zero determinant that can be formed from the elements of the matrix by appropriate deletion of rows or columns (or both)" (Mikhail (1976)). An alternative, and more applicable definition, states that rank is the maximum number of linearly independent row or column vectors in a matrix. The rank deficiency of a matrix can be defined mathematically by considering a matrix A which is related to a vector of u unknowns. For the rank of A denoted by R(A), the rank deficiency is defined by the following relationship.

$$d = u - R(A) \qquad ..(3.22)$$

Linear dependence can be defined mathematically by considering a matrix, A, of u-d linearly independent columns, ie d dependent columns which is equal to the rank deficiency. Then a vector S exists, where the vector $S = (s_1, s_2, ..., s_u)^T$, with at least one $s_i \neq 0$ such that :

$$A\,S = 0 \qquad ..(3.23)$$

To extend the previous definitions of rank to one in terms of eigenvalues, the rank of a matrix becomes equivalent to the number of non-zero eigenvalues in the matrix. The rank deficiency is therefore, by definition, the number of zero eigenvalues in the matrix. The basic eigenvalue equation is:

$$(A - \lambda_i I)\, s_i = 0 \quad \text{for } i = 1,u \qquad ..(3.24)$$

where u = number of unknowns
λ_i = ith eigenvalue
s_i = eigenvector of λ_i

In cases where the rank deficiency is greater than zero the rows and columns of A are not linearly independent. For a rank deficiency greater than zero the matrix cannot be inverted and by definition is singular. Cayley matrix algebra, as utilized here, defines the inverse of a square matrix A as the unique matrix A^{-1} based on the property :

$$A A^{-1} = A^{-1} A = I \qquad \text{for } \det(A) \neq 0 \qquad ..(3.25)$$

where I is the identity matrix of order equal to A.

Consider equation 3.8 for a system of rank deficiency d. By partitioning the equation into two components, A_1 of order (n,u-d) ; $\hat{X}_1$ of order (u-d) and A_2 of order (n,d) ; $\hat{X}_2$ of order (d), then the equation becomes :

$$v = (A_1, A_2) \begin{pmatrix} \hat{X}_1 \\ \hat{X}_2 \end{pmatrix} - l \qquad ..(3.26)$$

The parameters $\hat{X}_1$ are estimable and relate to the rank R(A) and the parameters $\hat{X}_2$ are inestimable quantities and relate to the rank defect d. The linear dependence of the system is formulated from the expression :

$$A_1 L = A_2 \qquad ..(3.27)$$

where L is a matrix defining the dependence of parameters $\hat{X}_2$ on parameters $\hat{X}_1$.

The properties of rank deficiency do not affect many of the formulations of the least squares model. For example the inverse P^{-1}, in equation 3.9, is not affected by singularity. P is usually formulated as $P = Q^{-1} = I$ or $P = Q^{-1}$ = constant. For either case the matrix is non-singular and inversion is elementary (Welsch (1979)).

One area of the model for which rank deficiency is potentially a problem relates to the normal equations of equation 3.12. The equation involves calculation of the inverse $(A^TPA)^{-1}$. In a case where the matrix is non-singular the parameters X are unbiased and estimable, from equation 3.14. In such a case the parameters X will relate to relative quantities and parameters defining absolute quantities are not included in the model. Problems become evident, however, when the matrix A^TPA is rank deficient, ie $R(A^TPA) < u$. In cases where some or all of the parameters define absolute quantities the least

squares method can only find $A^TPA\,\hat{X} = A^TPl$ unbiased. In other words the only unbiased solution to a rank deficient system of equations is a solution in which unknown parameters are an uninverted function of the normal equation coefficient matrix. Unbiased estimation of the parameters, as separate entities, is not possible (Grafarend and Schaffrin (1974)).

Where the rank deficiency of the system, d, is not equal to zero then there can only be an unbiased solution for R(A) of the parameters, X, ie an unbiased solution is only possible for $\hat{X}_1$ in equation 3.26 or, in general terms, an unbiased solution only exists for u-d parameters . As a further complication, if a rank deficiency exists then A^TPA is singular, and therefore cannot be inverted by classical inversion techniques. Hence the parameters are inestimable.

There are two basic solutions to the problems of singular, and hence undefined, systems. The first solution involves the explicit imposition of constraints on the parameters. Such constraints define relationships between the relative quantities, as supported by a least squares functional model, and the absolute quantities as defined by the unknown parameters. Constraints can be applied in various forms with the basic condition being that the applied constraints have to remove the full rank defect of the system. If such a condition is met the the system becomes non-singular and inversion of the normal equation matrix can be carried out by the Cayley inverse (Equation 3.25).

An alternative solution involves the use of generalized matrix algebra. Such formulations allow the inversion of singular matrices and hence can be directly implemented to allow solution of the functional model. In this process no defined or explicit constraints are applied to allow definition of absolute quantities. However the relationships between relative and absolute quantities are implicitly applied in the process of determining the generalized inverse of the singular normal equation.

3.5 Least Squares Model for Observation Equations with Constrained Parameters

The constraint of parameters will be carried out by the imposition of constraint equations upon the basic mathematical model. Such equations

contain no observations and are functions of only parameters and constraints. Considering equation 3.26, constraints may be applied to the equation to remove the rank deficiency and hence allow solution of the system. Constraints can either be minimal, ie a minimum number of constraints to allow a solution of the system, or the system can be over-constrained. If constraints are minimal no distortions are introduced into the estimated parameters. However if redundant constraints are imposed the sum of squares of the residuals will usually be larger than residuals from minimal constraint imposition and distortions are introduced into the estimated parameters (Papo and Perelmuter (1982)). Fraser (1984) defines minimal constraints as those constraints which introduce no information into the adjustment which have the potential of distorting the estimated parameters.

The constraints may be applied in two forms, either absolute or relative. Absolute constraints take the form of a mathematical criterion which must be met by the parameters to which the constraint is applied. For example an absolute constraint may take the form of fixing the parameter at its approximate value. Consequently the constraint will be formulated such that the normal equation is affected so as to induce no correction to the approximate value of the subject parameter. Relative constraints are also referred to as weighted constraints. They take the form of observations to the parameters and are applied to the least squares model in the form of observation equations. Consequently the subject parameters are constrained by the applied weights to the observed values. It should be noted that variance estimates from a least squares adjustment will not be optimal unless absolute minimal constraints are applied.

3.5.1 General Solution for Observation Equations with Constrained Parameters

The basic model, as defined by equation 3.8, is extended to include a constraint equation. The revised model takes the following form :

$$v = A\hat{X} - l \qquad ..(3.8)$$

$$\Sigma = \sigma_o^2 Q = \sigma_o^2 P^{-1} \qquad ..(3.9)$$

$$G^T\hat{X} = c \qquad ..(3.28)$$

The definition of symbols used in equation 3.28 and in the subsequent derivations are defined below and in section 3.3.

Φ' = function to be minimized

k, k_1, k_2 = vectors of Lagrange multipliers

G^T = coefficient matrix of the constraint equation

c = constant term of the constraint equation

Solution of the system is carried out by the method of constrained minima by Lagrange multipliers. Such a method requires minimization of the basic least squares equation, equation 3.1, in the following form :

$$\Phi' = v^T P v - 2k_1 (v + l - A\hat{X}) - 2k_2 (c - G^T \hat{X}) \Rightarrow \min \qquad ..(3.29)$$

Note that the quantities $(v+l - A\hat{X})$ and $(c - G^T \hat{X})$ become zero when equations 3.8 and 3.28 are satisfied, hence equation 3.29 becomes identical to equation 3.1.

To minimize the function Φ', partial derivatives with respect to $\hat{X}$ and v are equated to zero.

$$\frac{\partial \Phi'}{\partial \hat{X}} = 2k_1A + 2k_2G^T = k_1A + k_2G^T \qquad ..(3.30)$$

$$\frac{\partial \Phi'}{\partial v} = 2v^TP - 2k_1 = v^TP - k_1 \qquad ..(3.31)$$

This leads to the system defined by equations 3.8, 3.28, 3.30 and 3.31 and can be expressed as in the following form.

$$\begin{pmatrix} P & 0 & -I & 0 \\ 0 & 0 & A^T & G \\ -I & A & 0 & 0 \\ 0 & G^T & 0 & 0 \end{pmatrix} \cdot \begin{pmatrix} v \\ \hat{X} \\ k_1 \\ k_2 \end{pmatrix} = \begin{pmatrix} 0 \\ 0 \\ l \\ c \end{pmatrix} \qquad ..(3.32)$$

Application of matrix operations then leads to a system of normal equations in terms of $\hat{X}$ and k_2. The derivation of these equations is :

1. multiplication of row 3 by P and addition of row 1, to eliminate v

$$\begin{pmatrix} PA & -I & 0 \\ 0 & A^T & G \\ G^T & 0 & 0 \end{pmatrix} \cdot \begin{pmatrix} \hat{X} \\ k_1 \\ k_2 \end{pmatrix} = \begin{pmatrix} Pl \\ 0 \\ c \end{pmatrix} \qquad ..(3.33)$$

2. multiplication of row 1 by A^T and addition of row 3, to eliminate k_1

$$\begin{pmatrix} A^TPA & G \\ G^T & 0 \end{pmatrix}\begin{pmatrix} \hat{X} \\ k_2 \end{pmatrix}=\begin{pmatrix} A^TPl \\ c \end{pmatrix} \qquad ..(3.34)$$

Simplification of the system given by equation 3.34 results in the following system of normal equations in terms of the parameters $\hat{X}$ and k_2.

$$N.\begin{pmatrix} \hat{X} \\ k_2 \end{pmatrix}=\begin{pmatrix} A^TPl \\ c \end{pmatrix} \qquad ..(3.35)$$

where $$N=\begin{pmatrix} A^TPA & G \\ G^T & 0 \end{pmatrix}$$

Provided that the constraint equations meet the following two conditions, equation 3.35 can be solved to give a solution for the unknown parameters, X. The conditions require that :

1. G^T consists of d independent rows, where d is the rank deficiency of the system defined by equation 3.12.
2. The rows of G^T must be linearly independent of the rows of A. (ie R(A) + R(G) = u) (Caspary (1987))

The above conditions mean that the system defined by equation 3.35 is non-singular and solution is possible by application of the Cayley inverse. A zero on the leading diagonal of the matrix N is of no concern as the rows and columns of the matrix can be interchanged to give a non-zero diagonal term. Care should be taken at this stage, however, to ensure consistency of the equations when rearranging the N matrix.

Although equation 3.35 can be solved directly it is both a numerically inefficient solution and involves solution of the parameters k_2, which are essentially nuisance parameters. By considering the N matrix of equation 3.35, in terms of the Cayley inverse relationship of equation 3.25, the following relationship can be established.

$$\begin{pmatrix} A^TPA & G \\ G^T & 0 \end{pmatrix}\begin{pmatrix} Q_{11} & Q_{12} \\ Q_{21} & Q_{22} \end{pmatrix}=I=\begin{pmatrix} I_u & \\ & I_d \end{pmatrix} \qquad ..(3.36)$$

As the matrix A has rank deficiency d, with respect to equation 3.23, there exists a matrix G, of rank d, such that AG = 0. The matrix G is not unique, however, as there is an infinite solution to the equation AG=0. For example the matrix G may be selected as :

$$G = \begin{pmatrix} 0 \\ I_d \end{pmatrix} \qquad ..(3.37)$$

(Caspary (1987))

Such a constraint matrix leads to a solution based upon the absolute minimal constraint of the parameters affected by the I_d submatrix.

The following solution can be derived for any selected constraint matrix.

$$\hat{X} = Q_{11} A^T P l + Q_{12} c \qquad ..(3.38)$$

$$Q_{11} = (A^T P A + G G^T)^{-1} A^T P A (A^T P A + G G^T)^{-1} \qquad ..(3.39)$$

$$Q_{12} = (A^T P A + G G^T)^{-1} G \qquad ..(3.40)$$

and

$$Q_{\hat{X}} = Q_{11} \qquad ..(3.41)$$

Derivation of the solution can be found in Caspary (1987) section 3.4 and an alternative derivation in Mikhail (1976).

Analysis of the results achieved by imposing constraints shows that the solution is biased. Substitution of equation 3.5 into equation 3.38 gives :

$$E(\hat{X}) = Q_{11} A^T P E(l) + Q_{12} c = Q_{11} A^T P A X + Q_{12} c \neq X \qquad ..(3.42)$$

and

$$Q_{\hat{X}} = (A^T P A + G G^T)^{-1} A^T P A (A^T P A + G G^T)^{-1} \qquad ..(3.43)$$

Equations 3.42 and 3.43 show that the estimated parameters, $\hat{X}$, are biased, not of minimum variance and are not independent of constraint selection.

3.5.2 Minimum Mean Variance Solution for Observation Equations with Constrained Parameters

From equation 3.42 it can be seen that the solution of the parameters, X, is biased and dependent on the choice of constraints. Extension of the model,

as derived in section 3.5.1, is therefore proposed in order to determine a solution for the parameters based on a specific set of constraint equations, $G^T\hat{X} = c$, such that the estimated parameters, $\hat{X}$, are of minimum bias and minimum mean variance.

To achieve such a model a solution of the unknown parameters is investigated such that the trace of the cofactor matrix, $Q_{\hat{X}}$, is a minimum, the trace of the matrix being the sum of the terms on the principal diagonal.

$$tr\,(Q_{\hat{X}}) = \text{minimum} \qquad ..(3.44)$$

where $Q_{\hat{X}}$ is defined by equations 3.39 and 3.41.

Note that if the trace of the cofactor matrix of unknown parameters is a minimum then the sum of the squares of the root mean square errors of the unknowns is also a minimum (Mittermayer (1972)). Hence the proposed solution is a minimum mean variance solution, where the mean variance is $\bar{\sigma}_{\hat{X}}^2 = \sigma_o^2 \frac{tr(Q_{\hat{X}})}{u}$, u = the number of unknown parameters and σ_o^2 is the a priori variance factor.

For such a condition, ie $tr\,(Q_{\hat{X}}) = \text{minimum}$, the Euclidean norm of the estimated parameters, $\|\hat{X}\|$, would be a minimum. The minimum Euclidean Norm condition means that the changes to the a priori parameters, or approximate parameter values, are a minimum.

$$\|\hat{X}\| = (\hat{X}^T\hat{X})^{\frac{1}{2}} = \text{minimum} \qquad ..(3.45)$$

(Caspary (1987))

The constraints which provide such a minimum bias and minimum mean variance condition, as derived by Caspary (1987), can be written as:

$$G^T\hat{X} = 0$$
$$AG = 0 \qquad ..(3.46)$$

where R(G) = d

and the matrix G is composed of the d linearly independent eigenvectors associated with the d zero eigenvalues of A^TPA, as given by equation 3.23.

The solution equations of such a system are given as :

$$\hat{X} = Q_{11}\, A^T P l \qquad ..(3.47)$$

$$Q_{\hat{X}} = Q_{11} = (A^T P A + G G^T)^{-1}\, A^T P A\, (A^T P A + G G^T)^{-1} \qquad ..(3.48)$$

Analysis of the results shows that the estimated parameters are still biased.

$$E(\hat{X}) = Q_{11}\, A^T P l = Q_{11}\, A^T P A X \neq X \qquad ..(3.49)$$

However imposition of the minimum norm condition, $\| \hat{X} \|$ is a minimum, means that a minimum biased estimate of the parameters results. Such a solution is called BLIMBE (Best Linear Minimum Biased Estimate). By definition the resulting solution provides a minimum trace for the cofactor matrix of unknowns and hence a minimum mean variance solution results (Mittermayer (1972), Welsch (1979), Fraser (1980b)). For the case of full rank, and considering equation 3.48, $GG^T = 0$.

$$Q_{\hat{X}} = (A^T P A)^{-1}\, A^T P A\, (A^T P A)^{-1} = (A^T P A)^{-1}$$

and

$$\hat{X} = (A^T P A)^{-1}\, A^T P l \qquad ..(3.50)$$

Equations 3.50 are equivalent to equation 3.12 and equation 3.16, hence BLIMBE becomes BLUE. Note that any system of equations based on the formulations presented here will be biased. However this is of no significance if the unknowns themselves are not important but some invariant function of the unknowns is required. Such functions will define the shape or equivalent relative function, as opposed to an absolute position or quantity, and hence an unbiased estimate of such functions can be achieved (Granshaw (1980)).

3.6 Minimum Mean Variance Solution Based on Generalized Matrix Algebra

As described in section 3.4 the normal equations of the least squares functional model are singular if a rank deficiency exists in the system. A method of solution for the singular matrix $N = A^T P A$ is by use of *generalized inverses*. Generalized inverses allow the solutions to systems of less than full rank, ie they allow inversion of singular matrices.

A matrix N^- can be defined as a generalized inverse if it meets the following condition.

$$N N^- N = N \qquad ..(3.51)$$

(Bjerhammar (1973))

Upon application of equation 3.51 to a rank deficient system, where $R(A^TPA) < u$, equation 3.12 can be written as :

$$\hat{X} = (A^TPA)^- A^TPl = N^- A^TPl \qquad ..(3.52)$$

Grafarend and Schaffrin (1974) state that $\hat{X}$ is unique if the following conditions are met.

$$N N^- N = N \quad \text{and} \quad N^- N = (N^- N)^T \qquad ..(3.53)$$

An inherent problem with the conditions imposed by equation 3.53 is that although $\hat{X}$ is unique N^- is *not* unique. In fact N^- can be defined by a manifold of generalized inverses, each of which is generally not unique. Generalized inverses include inverses such as the Bjerhammar inverse, the Rao inverse and the Moore-Penrose inverse (Bjerhammar (1973)). As stated above these inverses are themselves generally not unique. The Bjerhammar inverse, for example, is based on the deletion of the linearly dependent rows and columns of a singular matrix. The selection of which rows and columns to delete is arbitrary with the only condition being that the remaining matrix be non-singular and hence invertable by the Cayley inverse. The inverse of the singular matrix is then formed by appending the inverted sub-matrix with zero elements for all previously eliminated elements.

An exception to the concept of non-uniqueness of the generalized inverse is the *Moore-Penrose inverse*, or as it is alternatively called the *pseudo inverse* . The Moore -Penrose inverse will be defined by the following notation, N^+. The inverse is a special case of a generalized inverse where the following conditions are applied.

1. $N N^{-} N = N$
2. $N^{-} N N^{-} = N^{-}$ ..(3.54)
3. $(N N^{-})^{T} = N N^{-}$
4. $(N^{-} N)^{T} = N^{-} N$ (Bjerhammar (1973), Welsch (1979))

If the inverse N^{+} were applied to a singular system, equation 3.12 could be rewritten in the following way.

$$\hat{X} = (A^{T}PA)^{+} A^{T}Pl = N^{+} A^{T}Pl \quad ..(3.55)$$

Characteristics of such a system would include :

1. the inverse N+ would be a generalized inverse. (from condition 1 and equation 3.51)
2. the least squares solution, $v^{T}Pv$ = minimum, would apply. (from condition 1 and condition 3)
3. a minimum Euclidean norm would apply, $X^{T}X$ = minimum. (from condition 1 and condition 4)
4. the inverse of the inverse would be the original matrix and R(N) = R(N^{+}). (from condition 1 and condition 2)

(Welsch (1979))

The characteristic of the minimum Euclidean norm condition, $||\hat{X}||$ = minimum, as applied to the estimated parameters, $\hat{X}$, is that the trace of the matrix to which the minimum norm condition is applied is a minimum (ie tr (N^{+}) = minimum). Such a condition would mean that application of the Moore-Penrose inverse to the singular normal equations would result in a minimum trace for the cofactor matrix of the adjusted parameters, ie tr ($Q_{\hat{X}}$) = minimum.

As with the solution of observation equations with constraint equations, the solution of a system defined by equation 3.34, based on generalized inverses, is biased as shown below.

$$E(\hat{X}) = (A^{T}PA)^{-} A^{T}P E(l) \quad ..(3.56)$$

$$E(l) = AX \quad ..(3.5)$$

therefore

$$E(\hat{X}) = (A^{T}PA)^{-} A^{T}P AX = N^{-} A^{T}PA X = N^{-}N X \neq X \quad ..(3.57)$$

For a generalized inverse of the form of a Moore-Penrose inverse, the minimum Euclidean norm condition means that the solution to the singular system will result in a minimum biased estimate of the parameters (BLIMBE : Best Linear Minimum Biased Estimate) and of the parameter variance. For a system of full rank the generalized inverse becomes identical with the Cayley inverse, $N^- = N^{-1}$, and BLIMBE becomes BLUE. The solution requires that the cofactor matrix of unknowns is implicitly minimized and hence the solution, based on generalized inverses of the Moore-Penrose type, will be minimum mean variance solutions (Fraser (1980b)). Indeed any solution based on a generalized inverse is biased or the solution is inestimable (Grafarend and Schaffrin (1974)). Marquardt (1970) substantiates use of the generalized inverse by stressing that a small amount of bias is introduced but with the benefit of large reductions in the variance of parameter estimates.

Solution of the generalized inverse can be carried out by the singular value decomposition of the singular matrix. Such a process is especially useful for determining the Moore-Penrose inverse as all of the conditions defined by equation 3.54 are retained in the decomposition process. Derivation of singular value decomposition can be found in Bjerhammar (1973).

A solution, defined by Caspary (1987), states that the Moore-Penrose inverse, N^+, as defined by equations 3.54, can be calculated from the following equation :

$$A^+ = A^TA\,(\,A^TAA^TA\,)^-\,A^T = A^T\,(\,A^TAA^T\,)^-\,A^T \qquad ..(3.58)$$

where the generalized inverses can be any of the generalized inverses meeting the conditions of equation 3.51.

Solution by the Moore-Penrose inverse is mathematically equivalent to the minimum bias solution by constrained parameters (section 3.5.2). Both cases are of type BLIMBE and in both cases implicit minimal constraints, of the type $||\hat{X}||$ = minimum, are applied.

3.7 Functions Independent of Constraints

As detailed in sections 3.4, 3.5 and 3.6, for a model of rank deficiency d, only u-d unbiased and estimable parameters exist. Hence the estimated parameters, $\hat{X}$, and the associated cofactor matrix, $Q_{\hat{X}}$, are dependent on the choice of constraints $G\hat{X} = c$.

Invariant functions are those functions of $\hat{X}$ which do not vary as a function of the selection of constraints, whether absolute or relative. These functions are of type BLUE and include the adjusted observations, the residuals and their associat6ed cofactor matrices. Following the derivation of Caspary (1987), it can be shown that the cofactor matrices of the adjusted observations, $Q_{\hat{l}}$, and residuals, Q_v, are both independent of constraint selection. Consequently both the function $\Phi = v^TPv$, given by equation 3.1, and the a posteriori variance factor, given by equation 3.15, are also independent of constraint type and form and hence are also invariant functions of the model. Note that such invariant properties apply only to minimal constraints. For over-constrained solutions, resulting in hierarchical adjustments, functions of residuals and observations become dependent upon constraint type and magnitude.

Another form of invariant function is defined by Welsch (1979) in stating "all vectors of linear independent quantities are linear unbiased estimable if and only if they are invariant in respect to any transformation which leaves the observation vector invariant." For example distances, directions, elevation differences or any relative function of the unknown parameters, in the case of the unknown parameters being coordinate positions, are invariant functions and hence can be unbiased estimated.

A detailed analysis of least squares methods, and implications of such methods with respect to parameter and variance estimates, has been carried out. The basic solution for a positive definite system of equations has been established with definition of parameter estimates of type BLUE (Best Linear Unbiased Estimator) and variance estimates of type BIQUE (Best Invariant Quadratic Unbiased Estimator).

Due to the fundamental deficiencies in the least squares model, the system of equations given by $v = A\hat{X} - l$ is often singular, especially in photogrammetric and surveying applications where observations of relative quantities are required to define absolute position. This singularity, which is due to rank deficiency in the system of equations, means that the estimation of the unknown parameters is impossible. Solution techniques based on the general solution for explicit parameter constraints, the minimum bias, minimum mean variance solution for explicit parameter constraints and the minimum bias, minimum mean variance solution based upon generalized matrix algebra have been developed in detail. Finally an analysis is given of the parameters and functions of the least squares solution which are invariant with the selection of minimal constraint.

Having developed the least squares process in detail, the close range photogrammetric principles of Chapter 2 will be applied to the general least squares formulations of this chapter. Observation equations, for the variety of observations in close range photogrammetry, will be established along with algorithms for the least squares solutions of photogrammetric systems.

4. DEVELOPMENT OF THE LEAST SQUARES SOLUTION FOR CLOSE RANGE PHOTOGRAMMETRY

In Chapter 3 the mathematical fundamentals of the least squares model and the least squares estimation process were established. Solution using the parametric method of adjustment was adopted and observation equations, in the form of equation 3.8, are to be utilized, ie $v=A\hat{X} - l$ where v are the residuals, A is the coefficient matrix, $\hat{X}$ are the estimates of the unknown parameters and l are the observations. In the development of observation equations for the least squares model, partitioning of the unknown parameter set is carried out. The estimates of the parameters are partitioned into $\hat{X}_1$, which are the parameters of exterior orientation, and $\hat{X}_2$, which are parameters relating to the coordinates of the object points in the object space coordinate system. The typical form of the observation equation is therefore :

$$v = (A_1, A_2) \begin{pmatrix} \hat{X}_1 \\ \hat{X}_2 \end{pmatrix} - l \qquad ..(4.1)$$

Observation equations are formulated with respect to the typical observations which are evident in close range photogrammetric applications. The observations which will be considered include :

1. image point coordinates
2. exterior orientation parameters (ie measurement of the geographic location and/or orientation of the camera station)
3. control or object point coordinates
4. straight line distances
5. elevation differences
6. azimuths
7. horizontal angles
8. vertical angles

In the development of the mathematical model it has been assumed that observations of all types have taken place. In reality this would not occur but deletion of unnecessary observation equations from the model, for each specific application, is an elementary task.

4.1 Observation Equations for Close Range Photogrammetry

Observation equations, for typical close range photogrammetric observations, have been developed in full in the appendix . Following is a summary of the observation equations in terms of the notation developed. Note that the observation equations relating to distance measurement, elevation differences, azimuth measurement,horizontal angle measurement and vertical angle measurement have been developed in two forms. One form is independent of the camera station, hence for these equations no measurements either from or to the camera station can occur. An alternative form is developed to allow distance, elevation difference, azimuth or angle measurement from or to a camera station. The second form of the equation is not often applied in close range photogrammetry. It is a more common practice to take such measurements between object points alone in order to provide datum control independent of the camera station position. Hence development of the close range photogrammetric mathematical model will be restricted to image coordinate observation, exterior orientation parameter observation, object point coordinate observation and distance, elevation difference, azimuth, horizontal angle and vertical angle observation between object points only.

Image Point Coordinate Observation Equation

The observation equations, relating **n** image coordinate observations on **m** photographs to the unknown parameters, in matrix notation are :

$$\underset{(2mn,1)}{V_1} + \underset{(2mn,6m)}{A_{11}} \cdot \underset{(6m,1)}{\hat{X}_1} + \underset{(2mn,3n)}{A_{12}} \cdot \underset{(3n,1)}{\hat{X}_2} = \underset{(2mn,1)}{c_1} \qquad ..(A.9)$$

Exterior Orientation Parameter Observation Equation

For observations at **m'** camera stations the observation equation for exterior orientation parameters can be written, in matrix notation, as :

$$\underset{(6m',1)}{V_2} - \underset{(6m',1)}{\hat{X}_1} = \underset{(6m',1)}{c_2} \qquad ..(A.12)$$

Control or Object Point Coordinate Observation Equation

The observation equation for **n'** control observations can be expressed in matrix notation as :

$$V_3 - \hat{X}_2 = c_3 \qquad \text{..(A.15)}$$

(3n',1) (3n',1) (3n',1)

Straight Line Distance Observation Equation

The observation equation for **d** measured distances can be expressed in matrix notation as :

$$V_4 - A_4 . \hat{X}_2 = c_4 \qquad \text{..(A.23)}$$

(d,1) (d,3n) (3n,1) (d,1)

Elevation Difference Observation Equation

The observation equation for **e** measured height differences can be expressed in matrix notation as :

$$V_5 - A_5 . \hat{X}_2 = c_5 \qquad \text{..(A.29)}$$

(e,1) (e,3n) (3n,1) (e,1)

Azimuth Observation Equation

In matrix notation, for **a** measured azimuths, the observation equation is :

$$V_6 - A_6 . \hat{X}_2 = c_6 \qquad \text{..(A.38)}$$

(a,1) (a,3n) (3n,1) (a,1)

Horizontal Angle Observation Equation

In matrix notation, for **b** measured clockwise horizontal angles, the observation equation is :

$$V_7 - A_7 . \hat{X}_2 = c_7 \qquad \text{..(A.47)}$$

(b,1) (b,3n) (3n,1) (b,1)

Vertical Angle Observation Equation

The observation equation, for **e** measured vertical angles, can be expressed in matrix notation as :

$$V_8 - A_8 . \hat{X}_2 = c_8 \qquad \text{..(A.56)}$$

(e,1) (e,3n) (3n,1) (e,1)

4.2 Formulation of the Mathematical Model for Close Range Photogrammetry

In Chapter 3 the mathematical model for the least squares solution was developed in general terms. Observation equations of the form $v = A\hat{X} - l$ were formulated and a solution, in terms of estimates of the unknown parameters and the variance of these estimates, was given as :

$$\hat{X} = (A^TPA)^{-1} A^TPl$$
$$Q_{\hat{X}} = (A^TPA)^{-1} \qquad ..(3.12)$$

where $Q_{\hat{X}}$ is the cofactor matrix of the estimated parameters

In this section observation equations, developed in the appendix, will be applied to the model and a solution algorithm developed. From section 4.1 the complete set of observation equations can be given as :

$$\begin{aligned}
V_1 + A_{11}\hat{X}_1 + A_{12}\hat{X}_2 &= c_1 \quad \text{(image coordinates)} \\
V_2 - \hat{X}_1 &= c_2 \quad \text{(exterior orientation parameters)} \\
V_3 - \hat{X}_2 &= c_3 \quad \text{(object space coordinates)} \\
V_4 - A_4\hat{X}_2 &= c_4 \quad \text{(straight line distance)} \\
V_5 - A_5\hat{X}_2 &= c_5 \quad \text{(elevation difference)} \\
V_6 - A_6\hat{X}_2 &= c_6 \quad \text{(azimuth)} \\
V_7 - A_7\hat{X}_2 &= c_7 \quad \text{(horizontal angle)} \\
V_8 - A_8\hat{X}_2 &= c_8 \quad \text{(vertical angle)}
\end{aligned} \qquad ..(4.2)$$

The resulting mathematical model, in the form of equation 4.1, is :

$$\begin{pmatrix} V_1 \\ V_2 \\ V_3 \\ V_4 \\ V_5 \\ V_6 \\ V_7 \\ V_8 \end{pmatrix} + \begin{pmatrix} A_{11} & A_{12} \\ -1 & 0 \\ 0 & -1 \\ 0 & -A_4 \\ 0 & -A_5 \\ 0 & -A_6 \\ 0 & -A_7 \\ 0 & -A_8 \end{pmatrix} \begin{pmatrix} \hat{X}_1 \\ \hat{X}_2 \end{pmatrix} = \begin{pmatrix} c_1 \\ c_2 \\ c_3 \\ c_4 \\ c_5 \\ c_6 \\ c_7 \\ c_8 \end{pmatrix} \qquad ..(4.3)$$

or in a general form :

$$V + A\hat{X} = c \qquad ..(4.4)$$

For a weight matrix of the form :

$$P = \begin{pmatrix} p_1 & & \\ & \ddots & \\ & & p_8 \end{pmatrix} \qquad ..(4.5)$$

where p_j, j=1,8 are the individual weight matrices associated with each observation type. The structure and form of the weight matrices can be found in Slama (ed) (1980);Ch 2.

The resulting least squares solution, of the system of equations given in equation 4.3, is :

$$\hat{X} = (A^TPA)^{-1} A^TPc = N^{-1} A^TPc \qquad ..(4.6)$$

with an associated cofactor matrix of :

$$Q_{\hat{X}} = (A^TPA)^{-1} = N^{-1} \qquad ..(4.7)$$

This system of equations is solvable if the system is not rank deficient. The system will not be rank deficient if observations have been included which allow the datum, ie the scale, orientation and translation, of the network to be determined. The concept of rank deficiency, and its implication on the solution, have been discussed in section 3.4. Application of such concepts, to the solution of rank deficient systems in close range photogrammetry, will be analysed in Chapter 5.

4.3 Solution Algorithms

The solution given by equations 4.6 and 4.7 is consistent with the bundle adjustment technique described in section 2.2. In such a technique a simultaneous least squares solution is carried out for the bundle of rays from all exposure stations to all points as well as all auxiliary or control observations. For close range photogrammetric applications where several hundred points may be imaged on up to ten convergent photographs the derived solution becomes computationally inefficient. For example, the direct solution of equations 4.6 and 4.7 will involve the solution of (6m+3n) simultaneous equations, where m is the number of photographs and n the number of points. For a typical close range configuration of 100 points and 5

photographs, storage for the normal equation coefficient matrix requires 330 x 330, or 108900, locations and the solution is both inefficient and time consuming.

4.3.1 Total Error Propagation - Uncorrelated Object Points

Slama (ed) (1980); Ch 2 derives in detail the solution algorithm developed by Brown (1958). The solution is based on reducing the normal equations to a function of one set of unknowns, solving for these unknowns and then substituting the results back into the system for solution of remaining unknowns. The solution is based on the assumption that all object points are uncorrelated and mutually independent, as the solution requires the form of the normal equation coefficient matrix, with respect to the object point coordinate parameters, to be in the form of 3 by 3 diagonal submatrices. The remaining portions of the object point normal sub-matrix must be null, as shown in figure 4.1. As these portions carry inter-point correlation information, and in Brown's formulation are null, object points cannot be correlated if a rigorous solution is desired. Consequently, for such an assumption to be valid, observations between object points or which are a function of more than one object point, cannot be included in the model. Hence the only observations which can be utilized for a rigorous solution are the image observations, exterior orientation parameter observations and the object control observations. Equation 4.3 is therefore reduced to the form of the following equation.

$$\begin{pmatrix} V_1 \\ V_2 \\ V_3 \end{pmatrix} + \begin{pmatrix} A_{11} & A_{12} \\ -1 & 0 \\ 0 & -1 \end{pmatrix} \begin{pmatrix} \hat{X}_1 \\ \hat{X}_2 \end{pmatrix} = \begin{pmatrix} c_1 \\ c_2 \\ c_3 \end{pmatrix}$$

$$V + A\hat{X} = c \qquad ..(4.8)$$

with a solution equation of :

$$\hat{X} = (A^T P A)^{-1} A^T P c = N^{-1} A^T P c \qquad ..(4.9)$$

The form of the normal equation coefficient matrix is given in figure 4.1.

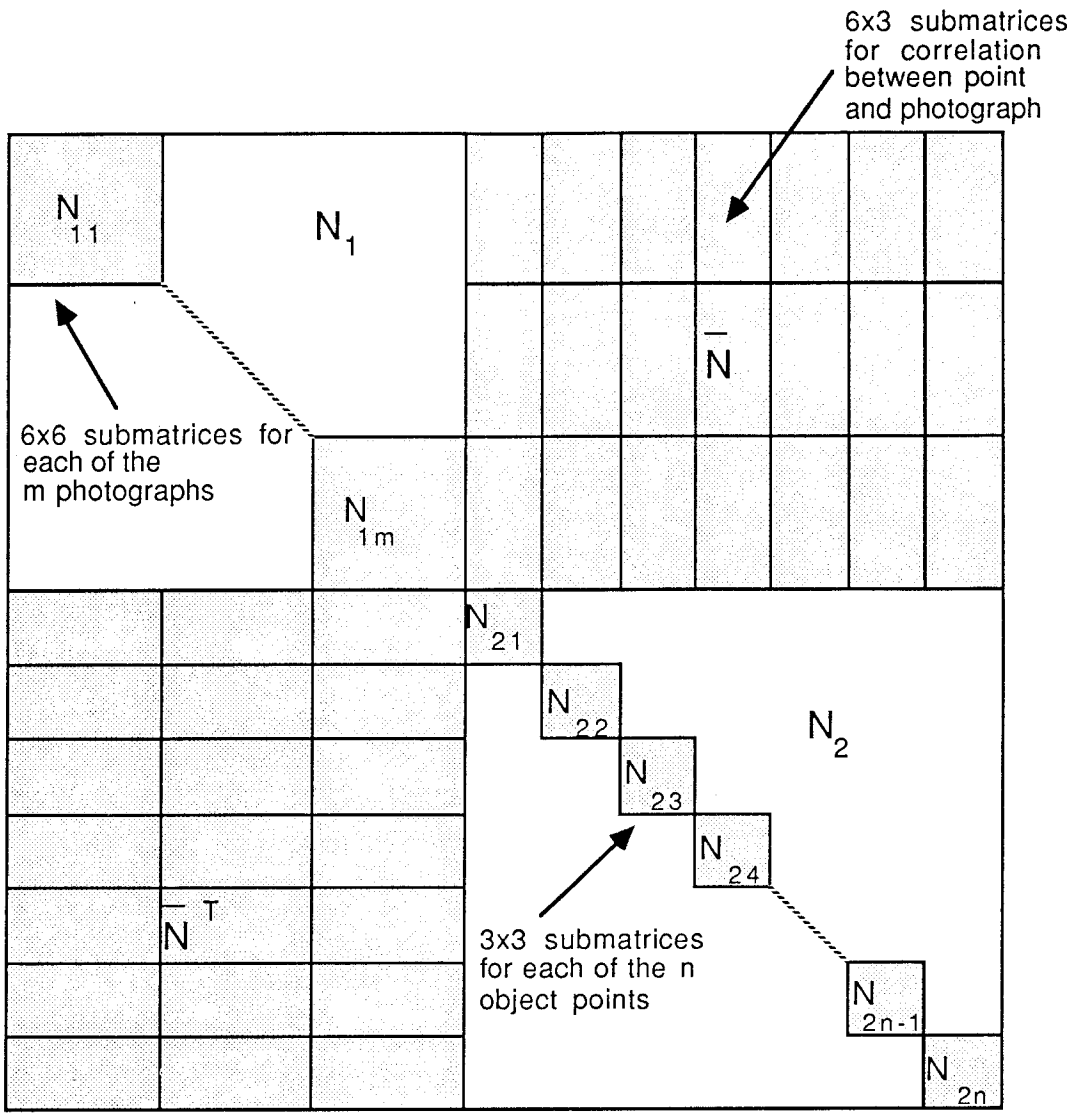

Figure 4.1 Form of the normal equation coefficient matrix for uncorrelated object points

From figure 4.1 it can be seen that the N matrix :

1. is symmetrical about the principal diagonal.
2. comprises 6x6 submatrices on the principal diagonal, in the upper left, corresponding to a particular photograph. (N_{11} to N_{1m} for m photographs)
3. comprises 3x3 submatrices on the principal diagonal, in the lower right, corresponding to a particular point. (N_{21} to N_{2n} for n object points)
4. comprises 6x3 submatrices off the diagonal which relate to the correlation between a point and a photograph. If a point is not imaged on a photograph this will be a null matrix.

Note that, with reference to figure 4.1 and the features of the normal equation matrix listed above, all the sections in the figure which are not shaded represent null elements.

Based on the form of the N matrix, and with respect to equation 4.8, the following solution can then be formulated :

$$N_1 \hat{X}_1 + \bar{N}\ \hat{X}_2 = K_1 \qquad ..(4.10)$$

$$\bar{N}^T \hat{X}_1 + N_2 \hat{X}_2 = K_2$$

where $N_1 = A_1^T P_1 A_1 + P_2$

$N_2 = A_2^T P_1 A_2 + P_3$

$\bar{N} = A_1^T P_1 A_2$

$K_1 = A_1^T P_1 c_1 - P_2 c_2$

$K_2 = A_2^T P_1 c_1 - P_3 c_3$

and P_j, j=1,3 defined by equation (4.5)

By partitioning the system of equations above, solution of the parameters $\hat{X}_1$ can be carried out. The normal equations of the partitioned system are the "reduced normal equations".

$$\hat{X}_1 = (N_1 - \bar{N}\ N_2^{-1} \bar{N}^T)^{-1}\ (K_1 - \bar{N}\ N_2^{-1} K_2) \qquad ..(4.11)$$

Because of the diagonal structure of the N matrix, which is due to the absence of correlation between object points, the object points can be solved sequentially from the following equation.

$$\hat{X}_{2j} = (N_{2j})^{-1}\ (\ K_{2j} - \bar{N}_j\ \hat{X}_1) \qquad ..(4.12)$$

(3,3)

for j=1,n

and n=number of object points

The associated cofactor matrices can be determined from :

$$Q_{\hat{X}_1} = (N_1 - \bar{N}\ N_2^{-1} \bar{N}^T)^{-1} \qquad ..(4.13)$$

$$Q_{\hat{X}_{2j}} = (N_{2j})^{-1} + ((N_{2j})^{-1} \bar{N}_j)\ Q_{\hat{X}_1}\ ((N_{2j})^{-1} \bar{N}_j)^T$$

Full derivation of the reduced normal equations and the solution of such equations is given in Slama (ed) (1980);Ch 2. The term "Total Error Propagation" arises because, if the assumption that all object points are uncorrelated is valid, then the algorithm presented here represents a full propagation of all errors into the final solution. Hence the solution will give a realistic assessment of accuracy and precision as all error sources are represented in the solution. If object points are correlated then solution using this algorithm will not represent a total error propagation as errors based on correlation between points will not be reflected in the final solution. Note that solution of equation 4.8 without forming reduced normals, ie a direct solution to the full system of equations, is also a total error propagation and does not rely upon the assumption that object points are uncorrelated.

4.3.2 Total Error Propagation - Correlated Object Points

Solution of the system of reduced normal equations given by Brown's algorithm have, as previously stated, the limitation that no observations which introduce correlations between object points can be included if a mathematically rigorous solution is required. Wong and Elphingstone (1972) introduce a variation of Brown's algorithm based on the addition of an observation equation of the form $V_g + G_2 \hat{X}_2 = c_g$, which comprises all observation equations which introduce correlations between object points. This equation is restricted to observations between object points. A similar solution could be established for an equation of the form $V_g + G_1 \hat{X}_1 + G_2 \hat{X}_2 = c_g$ to allow observations between exposure station and object point as well as between object points.

The system of observation equations becomes :

$$\begin{pmatrix} V_1 \\ V_2 \\ V_3 \\ V_g \end{pmatrix} + \begin{pmatrix} A_{11} & A_{12} \\ -1 & 0 \\ 0 & -1 \\ 0 & G_2 \end{pmatrix} \begin{pmatrix} \hat{X}_1 \\ \hat{X}_2 \end{pmatrix} = \begin{pmatrix} c_1 \\ c_2 \\ c_3 \\ c_g \end{pmatrix} \qquad ..(4.14)$$

with a weight matrix :

$$P = \begin{pmatrix} p_1 & & & \\ & p_2 & & \\ & & p_3 & \\ & & & p_g \end{pmatrix} \qquad \text{where } p_g = \begin{pmatrix} p_4 \\ \cdot \\ \cdot \\ p_8 \end{pmatrix} \qquad ..(4.15)$$

from equation (4.5)

If all points for which correlation between points exists are grouped together, the unknown parameters can be partitioned as :

$$\hat{X} = \begin{pmatrix} \hat{X}_1 \\ \hat{X}_g \\ \hat{X}_2 - \hat{X}_g \end{pmatrix} = \begin{pmatrix} \hat{X}_1 \\ \hat{X}_{21} \\ \hat{X}_{22} \end{pmatrix} \qquad ..(4.16)$$

where $\hat{X}_1$ = exterior orientation parameters

$\hat{X}_{21}$ = object points with correlation between points

$\hat{X}_{22}$ = object points with no correlation between points

On the basis of this partitioning, equation 4.14 becomes :

$$\begin{pmatrix} V_1 \\ V_2 \\ V_3 \\ V_g \end{pmatrix} + \begin{pmatrix} A_1 & A_{21} & A_{22} \\ -1 & 0 & 0 \\ 0 & -1 & -1 \\ 0 & G_{21} & 0 \end{pmatrix} \begin{pmatrix} \hat{X}_1 \\ \hat{X}_{21} \\ \hat{X}_{22} \end{pmatrix} = \begin{pmatrix} c_1 \\ c_2 \\ c_3 \\ c_g \end{pmatrix} \qquad ..(4.17)$$

Solution of the above system leads to normal equations of the form :

$$\begin{aligned} N_1 \hat{X}_1 + \bar{N}_1 \hat{X}_{21} + \bar{N}_2 \hat{X}_{22} &= K_1 \\ \bar{N}^T_1 \hat{X}_1 + N_{21} \hat{X}_{21} + \bar{N}_3 \hat{X}_{22} &= K_2 \\ \bar{N}^T_2 \hat{X}_1 + \bar{N}^T_3 \hat{X}_{21} + N_{22} \hat{X}_{22} &= K_1 \end{aligned} \qquad ..(4.18)$$

where $N_1 = A_1^T P_1 A_1 + P_2$

$N_{21} = A_{21}^T P_1 A_{21} + P_3 + G_{21}^T P_g G_{21}$

$N_{22} = A_{22}^T P_1 A_{22} + P_3$

$\bar{N}_1 = A_1^T P_1 A_{21}$

$\bar{N}_2 = A_1^T P_1 A_{22}$

$\bar{N}_3 = A_{21}^T P_1 A_{22}$

$K_1 = A_1 P_1 c_1 - P_2 c_2$

$K_2 = A_{21} P_1 c_1 - P_3 c_3 + G_{21} P_g c_g$

$K_3 = A_{22} P_1 c_1 - P_3 c_3$

and P_j, j=1,3 defined by equation 4.15

Note 1) only the term $\bar{N}_3$ carries correlations between object points.

2) if no correlations between object points are evident, for a point j the submatrix $\bar{N}_{3j}$ is null.

The form of the lower portion of the normal equations, ie the section of the normal equations relating to object coordinates, is shown in figure 4.2a, with the correlated object points being the first g of the n points. Figure 4.2b shows the same section of the normal equations but depicts the structure if selective rearrangement of the parameter order had not occurred.

The solution of the system of equations, given by equation 4.18, is similar to Brown's algorithm in that reduced normals are formed with respect to the exterior orientation parameters $\hat{X}_1$. Solution is carried out for these parameters and then reduced normals are formed for the parameters $\hat{X}_{21}$, the correlated object space coordinates, which are solved as a group. For g correlated points then 3g parameters require simultaneous solution. The remaining parameters, the uncorrelated object points $\hat{X}_{22}$, are solved sequentially using Brown's solution (equation 4.13). Hence the algorithm presented here allows a rigorous solution for any form or combination of observation equation, irrespective of correlation. The algorithm also allows a quick and efficient solution because as the number of uncorrelated points becomes equal to the total number of points, then the solution becomes identical with Brown's solution. As the number of uncorrelated points becomes small, however, the initial problems of storage and inefficiency arise again. In most close range photogrammetric applications, observations which introduce correlations between object points are usually only applied to a small portion of the total number of points and so this solution technique is viable and efficient for most applications.

Therefore, if the unknowns are partitioned as in equation 4.16, the solution is given by the following equations :

$$\hat{X}_1 = (N_1 - \bar{N} N_2^{-1} \bar{N}^T)^{-1} (K_1 - \bar{N} N_2^{-1} K_2) \quad ..(4.11)$$

$$\hat{X}_{21} = (N_{21})\text{-}1(K_2 - \bar{N}_2 \hat{X}_1) \quad ..(4.19)$$

$$\hat{X}_{22j} = (N_{2j})^{-1} (K_{2j} - \bar{N}_{1j} \hat{X}_1) \quad ..(4.12)$$

(3,3)

for j=g+1,n

and n=number of object points,

g=number of correlated object points

Note that the solution is equivalent to Brown's solution, section 4.3.1, except for the g correlated object points.

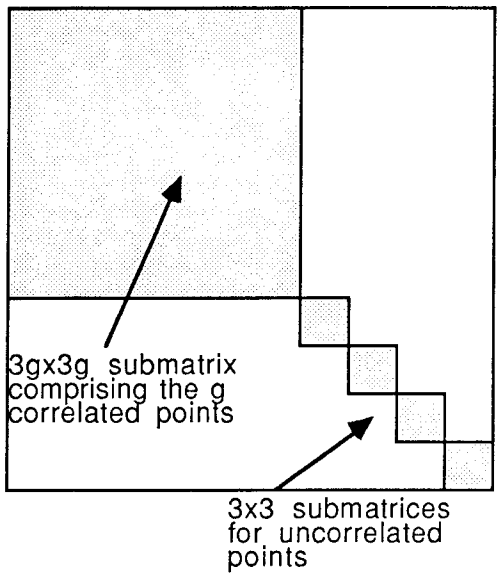

Figure 4.2a Form of the lower portion of the normal equation matrix with the (g) correlated points preceding the (n-g) uncorrelated points.

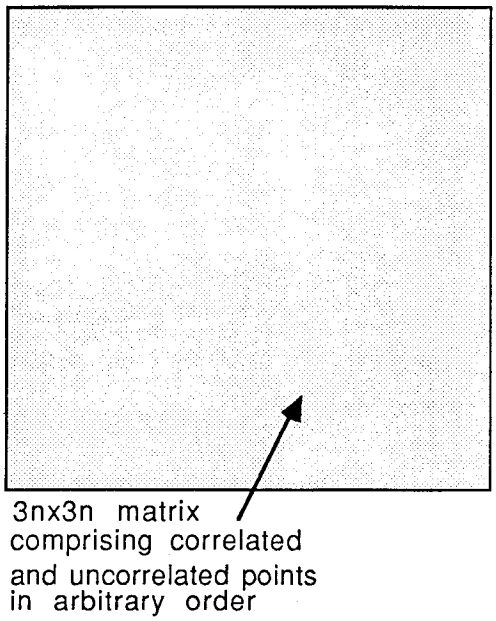

Figure 4.2b Form of the lower portion of the normal equation matrix with the (g) correlated points arbitrarily located in the parameter vector.

4.3.3 Limiting Error Propagation - Uncorrelated Object Points

The concept of Limiting Error Propagation was developed by Brown (1980) and Fraser (1987). The concept is based on the assumption that the camera exterior orientation, or projective, parameters are recovered perfectly in the adjustment process. Hence the process of limiting error propagation will express the limiting result to be expected from error free projective parameters. In other words the limiting error propagation solution will yield the best possible results for a particular imaging geometry. In cases where the projective parameters can be perfectly recovered, the limiting error propagation solution becomes rigorous and identical to a total error propagation solution. Limiting error propagation can be described in terms of the total error propagation of equation 4.13 :

$$Q_{\hat{X}_{2j}} = (N_{2j})^{-1} + ((N_{2j})^{-1}\bar{N}_j)\, Q_{\hat{X}_1}\, ((N_{2j})^{-1}\bar{N}_j)^T \qquad ..(4.13)$$

From this equation, which defines the cofactor matrix of the object point coordinates, it can be seen that for error free projective parameters the cofactor matrix of the projective parameters is a null matrix, ie $Q_{\hat{X}_1} = 0$, and therefore the limiting error propagation solution becomes :

$$Q_{\hat{X}_{2j}} = (N_{2j})^{-1} \qquad ..(4.20)$$

Hence it can be seen that the only errors which will be reflected in the object point coordinate precision estimates will be the effects of errors in the image coordinates. Expressions, similar to equations 4.11 to 4.13, can be developed for the limiting error solution.

Limiting error propagation, despite being a non-rigorous solution, has the valuable advantage that computational time is drastically reduced. The process has applications in close range photogrammetric network design where representative precision estimates are required rather than definitive precision estimates. In Chapter 9 the concepts of limiting error propagation will be examined to determine if the solution gives a representative precision estimate for a variety of close range photogrammetric networks.

Chapters 2, 3 and 4 involved development of close range photogrammetric principles, least squares principles and the close range photogrammetric least squares mathematical model. These chapters have provided the theoretical basis for the development and evaluation of the network design procedures to follow. The introduction of network design principles, with respect to the least squares method and primarily for close range photogrammetry, is covered in Chapter 5.

5. NETWORK DESIGN PRINCIPLES

In preceding chapters the basic tools associated with close range photogrammetry have been analysed in specific terms. The basic structure of the photogrammetric principles, the mathematical formulation of such principles and estimation and adjustment techniques, based primarily on the least squares method, have been developed in detail. Considering such formulations it would seem that the development of a system for photogrammetric mensuration would be a straight forward task. For example, based on the mathematical principles of close range photogrammetry a system of observation equations, as a function of the observations which are available, could be formulated and estimation of the unknown parameters could be carried out via the least squares principles of Chapter 3. However solution of this type of system would invariably lead to either a costly mensuration process, which far exceeds both cost and accuracy criteria, or a system which does not meet accuracy criteria at all. Working Group 1 of Commission V of the International Society of Photogrammetry and Remote Sensing " revealed numerous cases where extremely high accuracy (and cost) were used to accomplish rather simple tasks with moderate accuracy requirements, while in numerous other cases the specified accuracy requirements could not be met because of misjudgment of the capabilities of the instruments employed to accomplish the task" (Marzan and Karara (1976)). Hence it would seem that a major role in developing a system for close range photogrammetric mensuration involves the planning and pre-analysis of the acquisition and adjustment system. In any mensuration project the network, ie the observational configuration and imaging geometry, estimation technique, instrument type and capability etc, must be planned and designed to produce the best or optimal solution to the problem. Given a set of user specified criteria or specifications, which may include precision, accuracy, reliability, sensitivity and economy criteria, a network which optimally meets such criteria must be formulated. This planning and network analysis phase forms the basis of *network design*, and forms the basis of further investigation in this project.

5.1 Network Quality Criteria

An optimally designed network is one in which all design criteria are simultaneously optimized. In most close range photogrammetric applications such criteria include precision, accuracy, reliability, economy and, in the case of deformation analysis, sensitivity.

Precision can be defined as the degree of conformity among a set of observations of the same random variable. Hence the spread of the probability distribution is an indication of precision which is a function of only random effects. With respect to network design, precision represents quality of design and can be estimated by analysing the variance-covariance matrix of adjusted parameters, $\Sigma_{\hat{x}}$. Precision is a function of only random errors in the variable being assessed.

Accuracy can be defined as the extent to which an estimate approaches its true value and is a function of both random and systematic errors in the variable being assessed. With reference to figure 5.1 the distinction between precision and accuracy is clearly depicted.

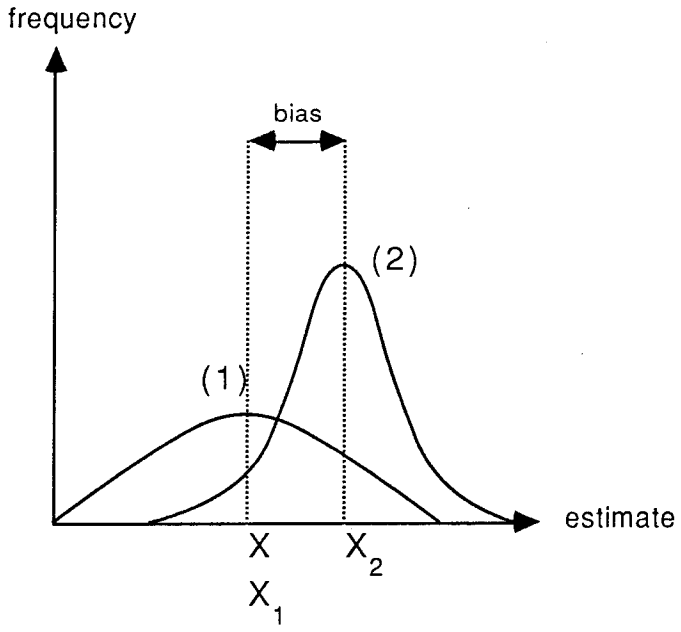

Figure 5.1 Relationship between precision and accuracy on a probability distribution curve

Curve (1) has a high accuracy, no bias, and low precision. Curve (2) has a low accuracy, large bias, and high precision. Consequently the difference between precision and accuracy lies in the presence of systematic error or bias. Accuracy is a function of both precision and bias and can be expressed in the following form.

$$\sigma^2_a = \sigma^2_p + (\text{bias})^2$$
$$\text{accuracy} = \text{precision} + (\text{bias})^2 \qquad ..(5.1)$$

(Mikhail (1976))

Note that if all components of survey measurement, either photogrammetric or classical surveying, are free of bias caused by systematic error, the variance estimates from $\Sigma_{\hat{X}}$ can be used as measures of both accuracy and precision (Mikhail and Gracie (1981)).

Reliability is related to the conformance of an observed network to its design. Hence reliability represents the potential of a network to detect gross and systematic errors by adequate testing procedures and is reflected in the self-checking capabilities, with respect to gross error detection, of the network (Niemeier (1987)). Reliability measures can be divided into two groups, namely internal reliability and external reliability. Internal reliability is assessed by boundary values, which are the smallest gross errors which can be detected with a certain probability in each observation if data snooping techniques are applied. External reliability indicates the effect of an undetected gross error, with the magnitude of the boundary value, on the final results (Amer (1979)). Reliability measures are determined from analysis of the variance-covariance matrix of residuals, Q_v.

Sensitivity relates to the ability of a network to detect movement in a point. Such a quality measure is applicable in deformation analysis where observations occur at two different epochs and the detection of movement of points is required. Hence unless deformation, or time dependent, analysis is required, sensitivity is not considered in assessment of network quality.

Economy relates to the total expenditure in establishing, measuring and assessing a network. To include such a quality criterion in network design, a mathematical cost function requires formulation. Such a cost function must relate cost to variables and estimates in the mathematical and stochastic models of the least squares adjustment. If such a function is formulated,

simultaneous optimization of all design criteria will yield a total cost which is optimal with respect to optimal estimates of precision, accuracy, reliability and sensitivity. A mathematical cost function is relatively easy to formulate for simple networks. For example the cost function for a levelling network can easily be formulated. Here the cost becomes a minimum for a minimum length of levelling. For close range photogrammetry, however, cost functions are complex and, if not formulated in detail, do not represent the true relationship between network configuration and cost. Hence both formulation and integration of the cost function, into the design process, is difficult. Consequently network design, in close range photogrammetry, does not usually simultaneously consider the economic criteria with the network quality criteria.

In general a network is designed and optimized with respect to the quality criteria, and then an a posteriori assessment is made to see if the network meets economic constraints. If such constraints are not met then expert knowledge is required to determine how the design will be altered to maintain conformance with the criteria of network quality yet meet the desired economic specifications. The network, after the design process, will be optimal in terms of precision, accuracy, reliability and sensitivity (if required) but it will not be optimal with respect to all quality criteria. As a final comment on economic considerations it should be noted that, in general, network cost and quality are directly proportional. For example maximum network quality, in terms of accuracy, precision, reliability and sensitivity, will correspond to a maximum cost and any reduction in these quality criteria will result in a corresponding decrease in network cost. Such a concept is shown in figure 5.2.

It is stressed that optimal network design, in the theoretical sense, is not possible unless all quality criteria are simultaneously considered (Cross (1982)). Schmitt (1982) states that precision, accuracy, reliability, sensitivity and economic criteria are difficult to assess simultaneously in the process of network design and optimization. Usually networks are designed with respect to precision criteria and then assessed to determine conformance with the other desired quality criteria. Investigations relating to assessment of network quality, in this project, will be restricted to design based upon precision criteria. The remaining quality criteria, accuracy, reliability, sensitivity and economy, will be assessed after the network has been designed.

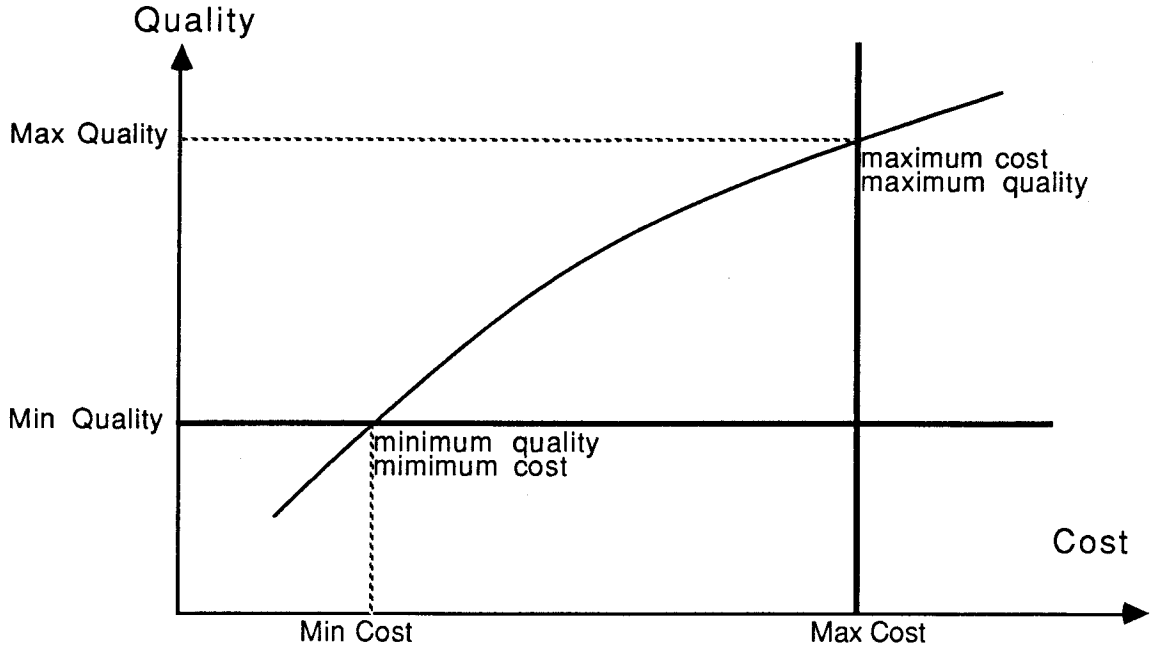

Figure 5.2 Typical cost - quality relationship in network design

In assessing network quality the type and magnitude of constraints applied to define the datum must be known. If constraints are absolute and minimal then optimal estimates of precision can be determined. Application of minimal constraints mean that the inner geometry of the network will not be distorted. This means that residuals and adjusted observations and their associated cofactor matrices will be invariant with respect to constraint selection and consequently any reliability analysis carried out will be valid. If the network is over-constrained then the inner geometry of the network will be destroyed and a hierarchical adjustment will result. Consequently precision estimates will be over determined and reliability estimates will be over estimated (Niemeier (1987)).

A detailed analysis of the measures of network quality, and methods of assessing such measures, will be given in Chapter 6.

5.2 Network Design Methods

The importance of network design in close range photogrammetry has been recognized since the mid 1970's and investigation into methods for close range photogrammetric network design have been under development since then. An early solution to the problems associated with network design is

presented by Marzan and Karara (1976). The network design methodology formulated is the, so called, rational design. The method is based on a set of empirical formulae which output expected precision of object space coordinates of points as functions of certain system or network parameters. These parameters include average image scale, overlap angle, convergence angle and image coordinate observation precision. Tables of estimated object point coordinate precision were generated on the basis of all possible combinations of the chosen system parameters. From these tables a designer was able to determine if the chosen camera type, imaging geometry and reduction technique would meet precision requirements and alter any component arbitrarily in order to either upgrade or degrade the network. Such a network design method has the advantage of simplicity and economy, however the concept has several inherent problems for high precision close range photogrammetric applications. These include :

1. lack of flexibility. (network design can only be determined for tabulated overlap and convergence angles, scales etc)
2. the solution is not mathematically rigorous.
3. the effect of errors, both systematic and gross on the network cannot be assessed.
4. the influence of the adjustment on the network cannot be assessed. (ie effects of varying datum definitions, effects of unstable imaging geometry)
5. design is based on a specific set of system parameters while other, probably less significant, system parameters are not included in the design process.

Due to these fundamental limitations in the rational design process, further development has not occurred and the process is not currently implemented in the design of close range photogrammetric networks.

An alternative, more flexible and mathematically rigorous, network design method was formulated by Grafarend (1974), primarily for the design of geodetic networks. Application of the design method has been applied successfully to close range photogrammetric networks.

The design method, as proposed by Grafarend, classifies the design problems into different orders with respect to the free and fixed parameters of the least squares adjustment. The basic design orders can be classified as follows.

Zero-Order Design (**ZOD**)	: the datum definition problem
First-Order Design (**FOD**)	: the network configuration problem
Second-Order Design (**SOD**)	: the observation "weight" problem
Third-Order Design (**TOD**)	: the network densification problem

With reference to the functional and stochastic models of the least squares adjustment process, postulated in Chapter 3, the following equations can be given.

$$v = A\hat{X} - l \qquad ..(3.8)$$

$$\Sigma = \sigma_o^2 Q \qquad ..(3.9)$$

where
- v = residuals
- A = observation equation coefficient matrix
- $\hat{X}$ = estimates of the unknown parameters
- l = observations
- Σ = variance-covariance matrix of observations
- σ_o^2 = a priori variance factor
- Q = cofactor matrix of observations
- $Q_{\hat{X}}$ = cofactor matrix of unknown parameters

The estimates of the unknown parameters and their associated cofactor matrix being :

$$\hat{X} = (A^T P A)^{-1} A^T P l \qquad ..(3.12)$$

$$Q_{\hat{X}} = (A^T P A)^{-1} \qquad ..(3.16)$$

The classification of the various design orders can be reviewed with respect to the least squares estimation process.

ZOD : the datum problem - involves the choice of an optimal reference system for parameters and their variance-covariance matrix.

Parameters	A,Q	fixed
	$\hat{X},Q_{\hat{X}}$	free

FOD : the configuration problem - involves the optimal positioning of points and the design of an optimal observation plan.

Parameters	$Q,Q_{\hat{X}}$	fixed
	A	free

SOD : the weight problem - involves the identification of optimal precision and distribution of observations.

Parameters	$A,Q_{\hat{X}}$	fixed
	Q	free

TOD : the densification problem - involves the optimal improvement of an existing network via addition of observations or points.

Parameters	$Q_{\hat{X}}$	fixed
	A,Q	partly free

(Schmitt (1982))

The order presented above is not fixed, although it is accepted by most geodesists and photogrammetrists as the chronological order for assessing network design problems. In practice the design problems are interrelated and solution of the various design problems may occur in a different sequence. For example, addition of object points may be carried out in the FOD phase to strengthen the imaging configuration, however this process is essentially a TOD (densification) problem. It should be noted that the datum problem is not independent of the configuration problem. A change in the datum will influence object point precision and the magnitude of such changes is dependent upon the imaging geometry. Hence, prior to evaluation of the datum definition, a good estimate of the imaging geometry should be available. If, after the ZOD analysis, the imaging geometry changes in the FOD analysis, then the effect of such changes upon the datum definition should be determined, ie repeat the datum definition.

In the design of close range photogrammetric networks, the accuracy of the various solutions, with respect to datum definition and imaging geometry

etc, is assessed on the assumption that only random errors are present in observations. In other words, the effect of the network, and only the network, upon estimates of the parameters is assessed. In such a case, where observations do not include systematic or gross errors, precision rather than accuracy estimates are required.

Two solution techniques are possible for the design of networks utilizing the classification scheme and processes previously postulated. These techniques can be classified as either direct or indirect (iterative) solutions.

5.2.1 Direct Solutions

This technique involves a direct solution and hence a direct output of an optimal configuration. Given an initial object point configuration, an estimate of precision of image coordinate observations and an ideal variance-covariance matrix of the coordinate parameters, a solution is derived for an optimal imaging geometry and number of cameras (Fraser (1987)). If all design stages are solved directly then an optimal variance-covariance matrix of observations and an optimal solution to the datum unknowns is also achieved. For practical implementation of a direct solution significant practical restrictions and limitations are evident. The major restrictions include :

1. the FOD or configuration problem cannot be solved directly. The variables associated with imaging geometry and object point location are complex and the inter-relationships between these variables are difficult to quantify in order to allow a direct solution. Usually direct solution of the imaging configuration, ie the FOD design, is restricted to the same number of object points and camera stations in "optimal" locations. In other words no new object points or camera stations can be added and changes in the position of such points can only be minor.

2. the variance-covariance matrix of observations, as determined in a direct solution, is usually fully populated and is frequently singular. In other words the variance-covariance or the weight matrix of observations gives observations which are correlated. Such a form is inconsistent with surveying measurements as,

in reality, such observations are uncorrelated and, by definition, their variance-covariance matrix is non-singular.

3. the design matrix can be affected by various anomalies. These include the absence of redundancy at some stations and the splitting of single networks into several independent networks. Such anomalies do not correspond with practical designs (Mepham and Krakiwsky (1982)).

5.2.2 Indirect (Iterative) Solutions

An alternative solution is based upon an indirect or iterative method and is reliant upon network simulation. In network simulations all observables are simulated and then a conventional adjustment is carried out. The resulting parameter estimates will not give accurate parameter values, however the variance-covariance matrix of parameters will provide an accurate estimate of parameter precision. Therefore, if object points and camera stations are selected such that they represent the anticipated "real" configuration, then the simulation process provides a method of assessing network quality and the precision of object point recovery prior to actual photography and network establishment. A common criticism of simulation methods is that the techniques employed are pseudo-scientific and that the results achieved are never absolutely optimal. This is of no practical concern as the method provides a technique whereby a network can be designed to both meet quality criteria and which will be feasible.

In the indirect simulation process no special computer software is required, as a conventional adjustment program can be used to adjust and output the results of simulated data for a particular network design. Such a procedure has the advantage that all existing network design specifications can be assessed simultaneously, allowing a mathematically rigorous assessment of the network being simulated. Interactive computer graphics can be incorporated into an existing adjustment program to allow efficient network design. Such integration is especially applicable in the FOD, or network configuration phase, and can be utilized for display of existing imaging geometry as well as precision estimates in the form of error ellipses (Cross (1982), Mepham and Krakiwsky (1982), Fraser (1984)). The combination of interactive computer graphics and simulation methods is

widely accepted as the "best" solution for network design problems at the present time (Cross (1982)). This is because well tried and easily understood design methods can be combined with a clear graphics display to allow the network designer the capability to use his own expertise to design a network which meets specified quality criteria. Networks designed in this way will be "observable" as nothing which cannot be observed is simulated. As previously stated, networks designed by indirect methods will not be optimal and therefore further investigation into direct solutions, for the recovery of an optimal network, is required.

Disadvantages of the indirect solution include :

1. the solution is not necessarily optimal.
2. a lengthy time delay between the modification of the previous design and the receipt of the results of the preanalysis of the modified design. Consequently a loss of time and continuity in the network design process results (Mepham and Krakiwsky (1982)).

The indirect network design and simulation procedure is based on the following steps, which are graphically depicted in figure 5.3 (adapted from Fraser (1984)).

1. Coordinates of points of interest, on the object, are specified.
2. Coordinates for the camera stations are specified along with associated principal distances and photographic format.
3. The object points are projected onto the photographic format.
4. The imaging geometry is graphically displayed, if a graphics terminal is available, and the imaging geometry and network configuration is altered as necessary.
5. If the network configuration is satisfactory then image coordinates are written to a file in the same format as if generated by a comparator or analytical plotter.
6. Network quality criteria is specified.
7. Solution to the ZOD problem is carried out (ie specify datum definition).

8. The resulting system of equations is adjusted, via a least squares bundle adjustment, and estimates of network quality are formulated with respect to precision criteria.
9. If the network quality fails the precision criteria, determine if scaling is required (SOD) or if densification is required (TOD). If SOD and TOD are not required then redesign the observational scheme and/or datum definition and readjust.
10. If network meets precision quality criteria determine if accuracy, reliability, sensitivity and economic specifications can be met. If accuracy, reliability, sensitivity and economic specifications cannot be met then redesign ZOD or FOD based on expert judgement.
11. Continue until all quality criteria can be satisfied or conclude that desired quality criteria cannot be met under the allowable conditions.

It should be noted again that networks designed by indirect techniques, based on simulation, are rarely optimal, ie the designed network does not optimally meet quality criteria. This is because an observational configuration is developed such that it meets quality criteria however it is not developed on the basis of any mathematical relationship to optimality. Hence although the designed network may meet all design specifications it may not, and indeed is generally not, the optimal design.

5.3 Zero-Order Design - the Datum Problem

As described in the previous section, the ZOD problem is that of defining an optimal reference system for the object space coordinates, given the imaging geometry and observational plan, defined by the coefficient matrix A, and the precision of observations, defined by the cofactor matrix of observations Q. Such an objective is achieved by selection of a datum which gives an optimal form of the cofactor matrix of parameters, $Q_{\hat{X}}$, and which is assessed via the mean variance of the parameters, $\bar{\sigma}^2_{\hat{X}}$.

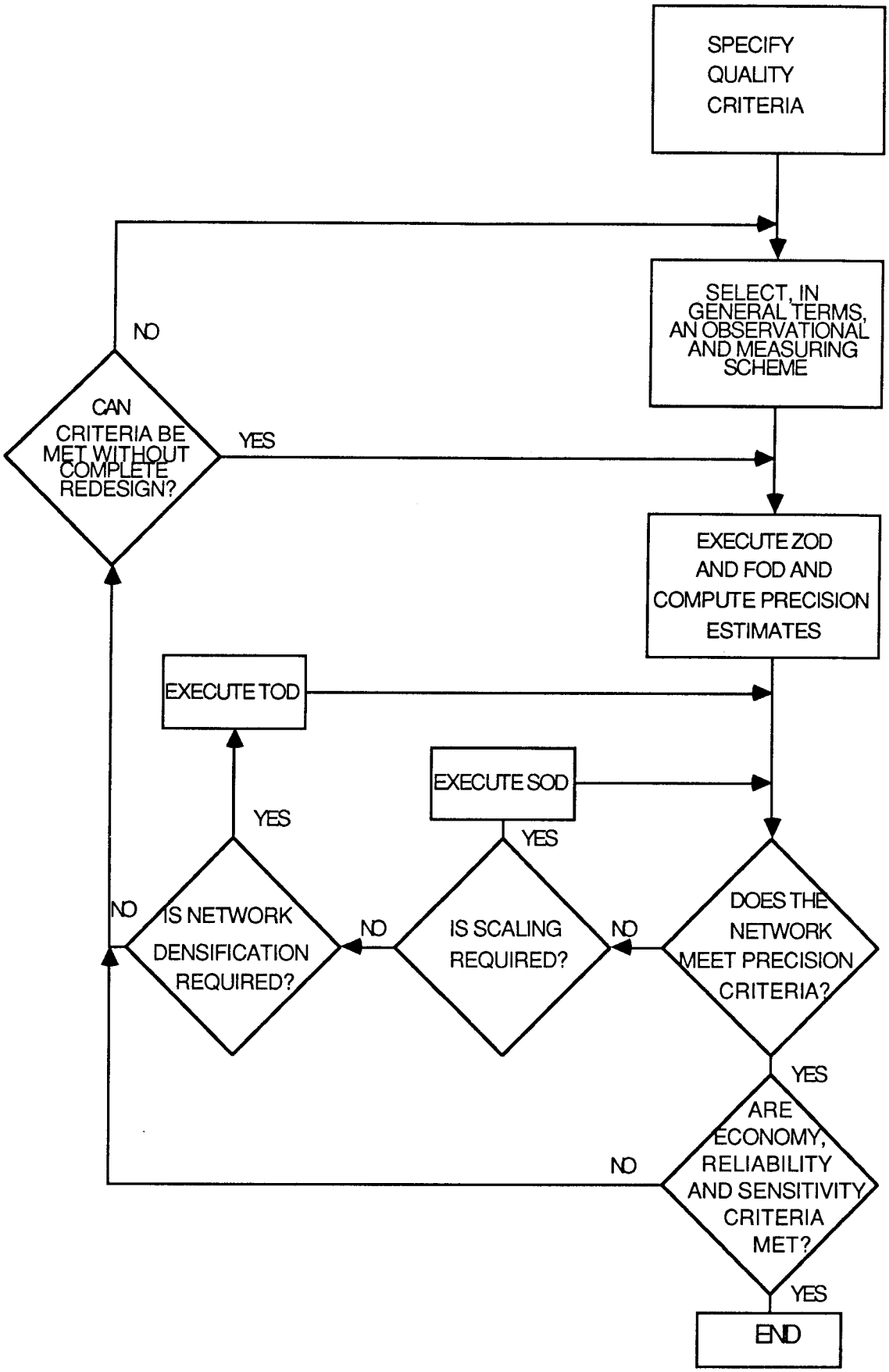

Figure 5.3 Flow diagram of network design based upon simulation procedures

In Chapter 4 the mathematical model of the close range photogrammetric least squares adjustment was developed, with the observation equations being formulated in terms of parameters for the spatial position of the object points and camera stations in a three dimensional rectangular cartesian coordinate system. The basic problem is associated with the lack of information inherent in observations, capable of defining the object space coordinate system to which the unknown parameters, object space coordinates and orientations, refer. The basic observation in photogrammetric applications is the image coordinate observation. Image observations contain no information about the absolute positions of the object points and therefore only relative positions can be defined from such observations. Hence relationships between the relative information, provided by the image coordinates, and the absolute information, with respect to the reference system, require formulation. Such relationships are achieved by defining the origin, orientation and scale of the reference system and applying such a definition to the relative quantities, defined by the image coordinates, to give object space coordinates with respect to some absolute system.

The basic concept of the ZOD, or the datum problem, can be addressed in terms of the mathematical concepts of section 3.4. The coefficient matrix, A, of the close range photogrammetric least squares mathematical model is singular and has a rank defect equal to the number of linearly dependent rows or columns in the matrix. Such a rank deficiency means that, in general, the resulting solution to the system of equations, defined by the model, is both biased and not of minimum variance. This is due to the techniques used to eliminate the effects of rank deficiency from the system. The techniques usually employed to constrain the system, induce a bias to the estimates of the parameters and, as a result, the parameter and precision estimates are not optimal. The theoretical solutions to rank deficient systems have been presented in Chapter 3 and applications of such concepts will be applied to photogrammetric applications in Chapter 8.

The rank deficiency of a system of equations can be thought of, in practical terms, as being equivalent to the lack of datum definition for the system and hence the term datum deficiency or datum defect is used. This means that the design matrix, A, will have a number of linearly dependent rows or columns equal to the number of unknown datum defining elements. The magnitude of the datum defect is a function of the order of the network

and is seven, if no additional information is added into the system, for a three dimensional network. To define a three dimensional reference coordinate system three translations, from the coordinate system origin with respect to the X, Y and Z axes, three rotations, about the X, Y and Z axes, and a scale must be defined. Hence to remove the datum defect of the system, seven independent quantities must be added to the system to define the relationship of the relative quantities to the reference coordinate system. Figure 5.4 illustrates the elements required to define the datum of a three dimensional rectangular cartesian coordinate system.

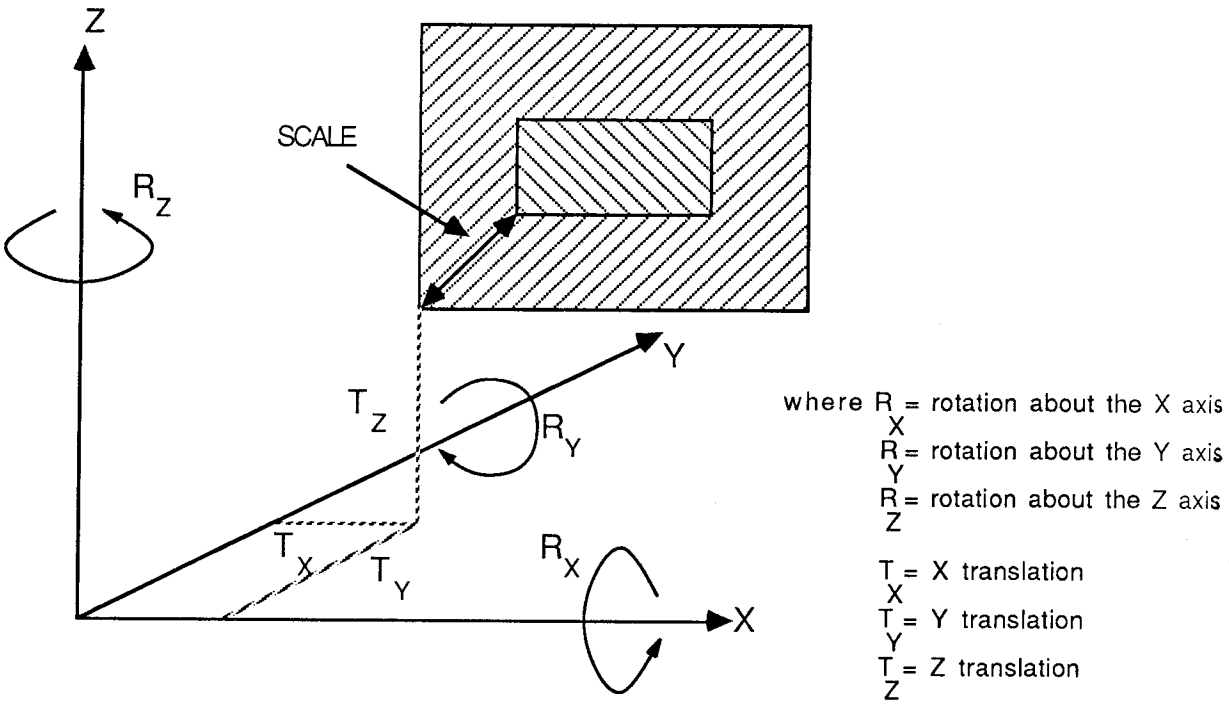

Figure 5.4 Datum definition elements for a three dimensional rectangular cartesian coordinate system

Solutions to the ZOD, or datum, problem will be covered in Chapter 8. The effect of the various forms of datum constraint, with respect to parameter and variance estimation, will be assessed.

5.4 First-Order Design - the Configuration Problem

In section 5.2 the first-order design (FOD) problem was introduced. For the task of designing a close range photogrammetric network the FOD problem involves optimal positioning of object points and the design of an optimal observation plan. The mathematical principles of the first-order

design, with respect to the functional and stochastic models of the least squares process, require that the design matrix, A, is optimally formulated for a given weight matrix of observations, P, to yield a cofactor matrix of unknown parameters, $Q_{\hat{x}}$, which meets specified network quality criteria. As covered in section 5.1, initial design of a network is usually restricted to quality criteria relating to precision. Conformance with the remaining quality criteria, accuracy, reliability, sensitivity and economy, are carried out after initial network design if required. Precision criteria, for example, may be that object space points must be resolved such that a three dimensional Taylor-Karman structure applies to the point coordinates. In other words the coordinates should have circular error ellipsoids (isotropic) and all ellipsoids should be of equal radius (homogeneous) (Koch (1982)).

Solution of the first-order design problem is based upon the indirect simulation method (section 5.2.2). Although such a solution does not offer the optimal configuration it does yield a configuration which is flexible, feasible and which meets specified quality criteria. The solution is basically trial and error, whereby a configuration is proposed, simulated, assessed for conformance with quality criteria and then altered if necessary. This process is continued until all quality criteria are satisfied.

Although all photogrammetric networks, and nearly all geodetic networks, have configurations designed by indirect methods some investigations have been carried out with respect to direct FOD solutions (Schmitt (1982)). Such solutions involve formulation of a criterion matrix, which is an ideal artificial variance-covariance matrix, and are based upon optimal precision criteria. The design matrix is then analytically modified until the cofactor matrix of the unknown parameters is consistent with the criterion matrix, for a given weight matrix of observations. Note that modifications can only be minor and no new points can be added. Consequently, unless a very good initial estimate of the network configuration is available, the direct solution does not offer enough flexibility for configuration design. For close range photogrammetry the formulation of criterion matrices is not elementary and to date no direct solution to the configuration problem, for close range photogrammetry, can be regarded as being practically feasible. For such reasons the solutions to the configuration problem, in this project, are assessed exclusively via the trial and error simulation (indirect) method.

In assessing the first-order design problems all components which influence the network configuration must be evaluated. In other words all components which will affect the structure or form of the least squares design matrix must be assessed. Such assessments are with respect to the effect of change in configuration components upon network quality.

The components which affect network configuration, for close range photogrammetry, include :

1. imaging geometry.
2. number of camera stations.
3. base-distance ratio (for "normal" photography).
4. image scale, focal length and image format
5. number of object points.
6. object point clusters.
7. multiple exposures.
8. self-calibration parameters.

Of the above network configuration components several can be assessed in terms of alternative problems in the network design process. For example, multiple exposures can be assessed as a second-order design ("weight") problem as multiple exposures are directly related to the precision of image observations. Likewise target clusters can be considered as a third-order design (densification) problem as the target cluster effectively densifies the object point array. These two components will, however, be assessed as first-order design problems, with the effect of the components upon other design problems being carried out in the following sections. It is convenient to again emphasize that the sequence of the design process is not definitive and that, for many applications, both SOD and TOD problems can be solved in the FOD phase.

The effect of the configuration components upon network design will be assessed in Chapter 9. As the simulation method requires expert knowledge by the designer of the network, the factors which influence the network configuration must be evaluated in detail. Evaluations will cover both significance to the close range photogrammetric configuration and effect upon parameter and variance estimates.

5.5 Second-Order Design - the Weight Problem

The second-order design ("weight") problem involves the definition of the precision and distribution of observations. In terms of the least squares mathematical models this involves optimizing the weight matrix of observations, P, for a given design matrix, A, such that the cofactor matrix of the unknown parameters, $Q_{\hat{x}}$, meets some predetermined quality criteria.

Direct solutions to the second-order problem have been developed, eg Cross and Whiting (1982), Wimmer (1982). Such solutions are based upon iterative techniques where the weight matrix of observations is analytically modified until results are consistent with a given criterion matrix. As detailed in section 5.2.1 such solutions are inconsistent with "real" observations as the resulting weight matrix of observations is usually fully populated, ie correlated observations, and singular. Direct solutions are therefore not generally applicable to the solution of second-order design problems.

The second-order design problem is of primary concern for geodetic networks. In such networks the second-order design problem involves determination of distribution of observations, precision of observations and repetition number, ie number of repetitions for each observation, for a variety of observations, which include distances, angles, levelling, GPS observations etc. For photogrammetric applications the observations of primary interest are the image observations. Additional observations, such as distances, angles, elevation differences etc, strengthen the network but are not of primary concern in network design. In close range photogrammetry, if additional observation types are neglected, the weight matrix of observations, P, is usually of the form :

$$P = Q^{-1} = \frac{1}{\sigma^2} I \qquad ..(5.2)$$

where Q is the cofactor matrix of observations

Consequently the solution to the second-order design problem merely involves optimal selection of the scale factor, σ (Fraser (1984)). There are three basic methods for improving image coordinate observations in close range photogrammetry.

1. the use of a higher precision comparator or analytical plotter.
2. multiple image coordinate measurements.
3. multiple exposures.

The upgrading of comparator or analytical plotter is not a realistic solution for the improvement of observational precision. Most organizations do not have the flexibility in hardware to allow such a solution. As covered in section 2.3.2 most first-order analytical plotters have observational precision in the 3 - 5 μm range, while high precision comparators offer observational precision in the 1 - 2.5 μm range (Fraser (1984)). Although a change from analytical plotter to comparator would allow an increase in observational precision, change within each group offers little flexibility. Consequently, unless an organization has a range of hardware, offering various measuring precision ranges, this option is not viable.

Multiple image coordinate measurements can be used to scale σ to some predetermined or desired value. If all points are re-observed and these observations averaged, then the observational precision at each point i will become $\frac{\sigma_i}{\sqrt{k}}$, where k is the number of observations to each point and σ_i is the observational precision for one measurement at each point. From section 3.3 the weight matrix of observations was :

$$P = \frac{\sigma_o^2}{\sigma_i^2} I \qquad ..(5.3)$$

Therefore if the observational precision becomes $\frac{\sigma_i}{\sqrt{k}}$, for k image observations, the weight matrix of observations for the multiple observations, P', becomes :

$$P' = k \frac{\sigma_o^2}{\sigma_i^2} I = kP \qquad ..(5.4)$$

Hence the effect of multiple image coordinate measurements is to increase the "weight" of observations by the value k. Therefore the number of observations for each image point can be varied to allow desired observational precision.

Multiple exposures are conceptually similar to multiple image coordinate observations. For k images, taken at the same exposure station, the solution becomes equivalent to observation of an image point k times. One important difference exists however. In the case of multiple exposures not only will observational precision improve but systematic errors which change from exposure to exposure, eg film deformations, will be averaged and hence the effect of such errors will be reduced. Multiple exposures offer a method of both improving observational precision and decreasing the effect of systematic errors and is therefore recommended as the preferred method, if observational precision must be increased in the SOD design (Fraser (1984)). Slama (ed) (1980);Ch 13 observes that about a 30% improvement in observational precision is obtained by two exposures. From two to three exposures an improvement of 16% is expected and from three to four exposures 7% improvement is expected.

The influence of multiple exposures or multiple image observations upon precision estimates of the unknown parameters will be evaluated. For these evaluations several close range photogrammetric networks will be utilized. These include a two photograph "normal" configuration and two, three and four photograph convergent configurations. The convergent configurations have a convergence angle of 100° and are symmetric about the object. The camera used for the evaluations was the Wild P32, which has a 64.1mm focal length and a 90 mm x 65 mm format. It is assumed that the observational accuracy for a single exposure is 5μm. The precision of the various evaluations is made with respect to the mean standard error, which is described in Chapter 6. The evaluation of the networks was carried out using the program SIMPAC, which is described in Chapter 7.

Figure 5.5 depicts the effect of multiple exposures upon object point coordinate precision. Note that the influence of multiple exposures in reducing exposure dependent systematic errors is not considered. From the results of the evaluations the significance and importance of multiple exposures is evident. For three and four exposure networks the influence of multiple exposures is minimal, of the order 1 - 2 mm in each coordinate determination for the above case, and hence would not be utilized. For two photograph configurations, both "normal" and convergent, the influence of multiple exposures is significant. For cases where physical or practical restrictions limit the number of camera stations to two or three, multiple exposures or multiple image observations offer a way to significantly improve coordinate precision.

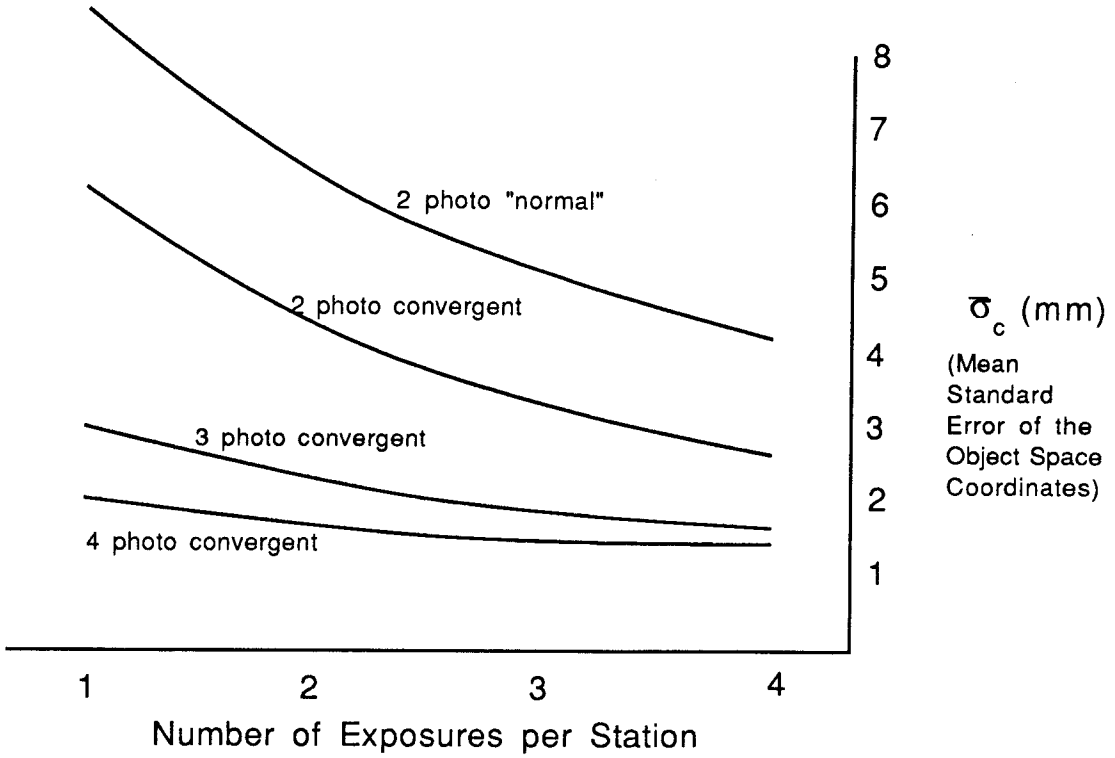

Figure 5.5 The effect of multiple exposures or multiple image observations on precision estimates.

5.6 Third-Order Design - the Densification Problem

The third-order design (densification) involves the improvement of network precision and quality via addition of object points and observations. With respect to the least squares model, the cofactor matrix of the unknown parameters, $Q_{\hat{X}}$, is fixed and both the design matrix, A, and the observation weight matrix, P, are updated to improve network quality.

In most close range photogrammetric networks, object point arrays are dense and typically an object is covered by up to several hundred points. For "strong" networks the effect of incorporating additional object points, and hence additional observations, to the network has only a minimal effect upon network precision (Fraser (1984)). In cases where network geometry is "poor', eg possibly due to physical configuration restrictions imposed at the FOD phase, the target array can be densified and the addition of object points and observations will improve network quality. For such a case, however, the densification would occur at the first-order design phase by increasing the

number of object points or incorporating object point (target) clusters. For cases where object point arrays are not dense, ie only several tens of points, densification will improve network quality but, once again, this is undertaken in the first-order design phase.

As previously stated object point precision and network quality are largely independent of object point density and distribution, for networks of "strong" geometry. Consequently the third-order design problem does not usually arise in close range photogrammetry and is effectively solved at the first-order design stage should it be significant.

The purpose of this chapter is to introduce the basic principles and requirements for network design The criteria for assessing network quality are precision, accuracy, reliability, sensitivity and economy; the design process is primarily concerned with precision. A posteriori evaluation with respect to the remaining quality criteria is then carried out if required.

The network design method is based upon the following classification :

Zero-Order Design (ZOD) - the datum problem
First-Order Design (FOD) - the configuration problem
Second-Order Design (SOD) - the "weight" problem
Third-Order Design (TOD) - the densification problem

In close range photogrammetry the network design process is simplified. The SOD problem merely involves scaling of the weight matrix of observations by a constant scaling term, equal to the number of times an image has been observed or the number of multiple exposures taken. The TOD problem does not usually arise and if it does is effectively solved at the FOD stage. Measures of network quality, with an emphasis on precision measures, will be formulated in the next chapter.

6. MEASURES OF NETWORK QUALITY

Network quality criteria, as introduced in section 5.1, include precision, accuracy, reliability, economy and sensitivity. Such quality criteria do not apply to all network design applications however. In many close range photogrammetric applications absolute definition of the network is not required. For example, position estimates may be required to define the shape, as opposed to absolute position with respect to a given reference coordinate system, of a particular object. In such cases the bias component in an estimate is not significant and consequently accuracy criteria reduces to precision criteria. In other words the bias component of the accuracy measure, as given by equation 5.1, is not significant and hence accuracy criteria is not considered.

Sensitivity criteria are only considered in cases where deformation analysis or where network monitoring is required. For most close range photogrammetric applications, position is required at a single epoch and no time dependent analysis is required. Hence sensitivity criteria are only considered in network design for deformation analysis applications.

In all network design applications an implicit requirement exists to minimize the cost associated with network observation and analysis. Consequently economic considerations are fundamentally important in the process of designing photogrammetric networks. As covered in section 5.1, economic criteria are difficult to assess simultaneously with other quality criteria in network design. After the initial design of the network, assessment is made to determine if financial and cost constraints can be met. Due to the large number of variables in any cost assessment consideration, formulation of measures for assessment of economy is not possible. To assess the cost of network implementation, each network is considered separately and cost is calculated based upon the skill and expertise of the designer. Consequently a measure of economic criteria, as an overall indicator of economy, is not feasible and hence will not be investigated further.

In all close range photogrammetric network design and analyses , precision and reliability form the basis of assessment of network quality.

Measures to represent quality of design, or the degree of conformity among a set of observations of the same random variable, and the conformance of an observed network to its design, or the potential of a network to detect gross and systematic errors via adequate testing procedures, are required.

In this chapter measures of precision, accuracy, reliability and sensitivity will be developed. Even though all measures may not, and indeed will not, be simultaneously utilized they are developed to allow the network designer the flexibility to choose the particular quality measures applicable to each specific application.

6.1 Precision Measures

As previously stated, precision refers to the quality of a network and reflects the degree of conformity among a set of observations of the same random variable. Precision measures are determined exclusively from the variance-covariance matrix of the adjusted parameters, $\Sigma_{\hat{X}}$. Such measures are therefore an indication of the "strength" of recovery of the unknown parameters, as a function of the particular network being analysed. Prior to developing precision measures two points should be noted.

1. The variance-covariance matrix of the unknown parameters, $\Sigma_{\hat{X}}$, is not invariant with respect to datum selection. Consequently the precision measures developed are datum-biased measures and are dependent upon both configuration and type of datum constraint being employed. The fact that $\Sigma_{\hat{X}}$ is datum dependent, and hence not unique, causes problems in assessing the precision of the adjusted object point position.

2. The variance-covariance matrix of the unknown parameters is given by equation 3.19 as $\Sigma_{\hat{X}} = \sigma_o^2 Q_{\hat{X}}$, where $Q_{\hat{X}}$ is the cofactor matrix of unknown parameters and σ_o^2 the a priori variance factor. In analysing $\Sigma_{\hat{X}}$ it is important to have statistically verified the a priori variance factor as this factor has a direct scalar influence on precision measures. Any error in σ_o^2 will directly influence precision measures and therefore must be statistically significant. If the a priori variance factor cannot be verified then the a posteriori variance factor, $\hat{\sigma}_o^2$, should be used.

Precision measures can be analysed as being local measures of precision, ie precision measures which relate to the individual unknown parameters, or global measures of precision, which relate to the set of unknowns as a whole.

6.1.1 Eigenvalue Decomposition

The fundamental approach to precision estimation involves determination of the eigenvalues of the variance-covariance matrix of the estimated parameters. This is achieved by the eigenvalue decomposition of $\Sigma_{\hat{X}}$. From equation 3.24 the basic eigenvalue equation of $\Sigma_{\hat{X}}$ becomes :

$$(\Sigma_{\hat{X}} - \lambda_i I)\, s_i = 0 \qquad \text{for } i=1,u \qquad ..(6.1)$$

where $\Sigma_{\hat{X}}$ = variance-covariance matrix of X.

λ_i = ith eigenvalue of $\Sigma_{\hat{X}}$.

s_i = eigenvector associated with λ_i.

u = number of unknowns.

The characteristic equation of $\Sigma_{\hat{X}}$ is formulated based on $(\Sigma_{\hat{X}} - \lambda_i I)$ being singular. Hence the characteristic equation becomes :

$$\det (\Sigma_{\hat{X}} - \lambda_i I) = 0 \qquad ..(6.2)$$

Solution of the eigenvalues is carried out from the above equation, with solution for the associated eigenvectors being carried out by substitution of the eigenvalues, λ_i, into equation 6.1 (Caspary (1987)).

The eigenvalues are formed into a u by u diagonal matrix of the form :

$$\Lambda = \begin{pmatrix} \lambda_1 & & \\ & \ddots & \\ & & \lambda_u \end{pmatrix} \qquad ..(6.3)$$

The associated eigenvector matrix becomes :

$$S = (s_1 \; . \; . \; s_u) \qquad ..(6.4)$$

The matrix $\Sigma_{\hat{X}}$ can be written in terms of Λ and S as :

$$\Sigma_{\hat{X}} = S\Lambda S^T \qquad ..(6.5)$$

(Caspary (1987))

Properties of eigenvalues include :

1. The sum of the eigenvalues equals the trace of the variance-covariance matrix of unknown parameters.

$$\sum_{i=1}^{u} \lambda_i = tr\, \Sigma_{\hat{X}} \qquad ..(6.6)$$

2. The product of the eigenvalues equals the determinant of the variance-covariance matrix of the unknown parameters.

$$\prod_{i=1}^{u} \lambda_i = det\, \Sigma_{\hat{X}} \qquad ..(6.7)$$

3. $$\lambda_i = \frac{s_i^T \Sigma_{\hat{X}} s_i}{s_i^T s_i} \qquad ..(6.8)$$

(Bjerhammar (1973), Caspary (1987))

Eigenvalues will be used in both local and global precision analysis, as measures of network precision.

6.1.2 Local Measures of Precision

Local measures of precision will be developed in order of evaluation complexity. In selecting a precision measure it should be noted that measures which are easy to compute usually contain a minimum of relevant information. Consequently, in selection of a local precision measure, a compromise between complexity and information content arises.

The simplest measure of precision is the **Standard Deviation of Coordinates**. For this measure, consider a cofactor matrix of unknown parameters, $Q_{\hat{X}}$,of the form:

$$Q_{\hat{X}} = \begin{vmatrix} q_{x1} & q_{x1y1} & q_{x1z1} & \cdots & q_{xu} & q_{xuyu} & q_{xuzu} \\ q_{y1x1} & q_{y1} & q_{y1z1} & \cdots & q_{yuxu} & q_{yu} & q_{yuzu} \\ q_{z1x1} & q_{z1y1} & q_{z1} & \cdots & q_{zuxu} & q_{zuyu} & q_{zu} \end{vmatrix} \quad ..(6.9)$$

where diagonal terms are the variance estimates and the off-diagonal terms are the covariance estimates of the subject parameters. For an a priori variance factor, σ_o^2, the standard deviation of coordinates of point i can be expressed in terms of three equations.

$$\begin{aligned} \sigma_{xi} &= \sigma_o \sqrt{q_{xi}} \\ \sigma_{yi} &= \sigma_o \sqrt{q_{yi}} \\ \sigma_{zi} &= \sigma_o \sqrt{q_{zi}} \end{aligned} \quad ..(6.10)$$

(Mikhail (1976))

If σ_o^2 is unknown it is replaced by $\hat{\sigma}_o^2$, the a posteriori variance factor, and the standard deviation of coordinates becomes the **Root Mean Square (RMS) Error** of coordinates, S_x, S_y, S_z (Caspary (1987)). The standard deviation precision measures are dependent upon the redundancy in the least squares model and hence are neither model nor datum independent precision measures. The standard deviation is referred to as a point estimate, (Mikhail (1976)), as one scalar value is returned for each parameter or coordinate being assessed.

Confidence Intervals provide a precision measure based upon an interval estimation. It provides a measure of how good the estimate is and how much it can be relied upon. To meet such requirements the probability distribution of the sample, and of the ratio $(X - \hat{X}) / \sigma_x$, where X is the unknown parameter, $\hat{X}$ is the estimate of the parameter and σ_x is the parameter standard deviation, is required. The confidence interval measure takes the form of the following probability relationship.

$$P\{ \hat{X}_i - Z_{\alpha/2}\, \sigma_{xi} < X_i < \hat{X}_i + Z_{\alpha/2}\, \sigma_{xi} \} = 1 - \alpha \qquad ..(6.11)$$

where $Z_{\alpha/2}$ = normal distribution coefficient at significance level α

X_i = unknown X coordinate of point i

$\hat{X}_i$ = estimate of X_i

σ_{xi} = standard deviation of X coordinate for point i

(Walpole and Myers (1972))

Similar equations can be formulated for the X,Y and Z coordinates for all unknown points. The confidence interval is based upon the normal distribution, as the a priori variance factor is a population variance measure. If the a posterior variance factor, $\hat{\sigma}_o^2$, is used then the confidence interval is expressed in terms of the root mean square error and the t-distribution, as the a posteriori variance is a sample variance measure.

$$P\{ \hat{X}_i - t_{r,\alpha/2}\, S_{xi} < X_i < \hat{X}_i + t_{r,\alpha/2}\, S_{xi} \} = 1 - \alpha \qquad ..(6.12)$$

where r = redundancy

α = level of significance

S_{xi} = RMS error for the X coordinate of point i

(Mikhail (1976))

Similar expressions can be formulated for all object point coordinates.

Error Ellipses provide a method of graphically displaying precision. Ellipses are used as a precision measure in two dimensional networks and can be developed as either standard or confidence error ellipses. Standard error ellipses are a generalization of the standard deviation while confidence ellipses are a generalization of confidence intervals.

Point error ellipses refer to a point as a single entity while relative error ellipses reflect the relative precision of a pair of, usually adjacent, points. For a two dimensional network, standard point error ellipses can be calculated from the eigenvalue decomposition of section 6.1.1. For the subset of the cofactor matrix relating to a point i, in a two dimensional network :

$$Q_i = \begin{pmatrix} q_{xi} & q_{xiyi} \\ q_{yixi} & q_{yi} \end{pmatrix} \qquad ..(6.13)$$

The associated eigenvalues can be calculated from equation 6.2 as :

$$\lambda_1 = \frac{1}{2}(q_{xi} + q_{yi} + \sqrt{(q_{xi} - q_{yi})^2 + 4q_{xiyi}^2})$$
$$\lambda_2 = \frac{1}{2}(q_{xi} + q_{yi} - \sqrt{(q_{xi} - q_{yi})^2 + 4q_{xiyi}^2}) \quad ..(6.14)$$

where λ_1 = the square of the semi-major axis of the error ellipse
λ_2 = the square of the semi-minor axis of the error ellipse

The direction of the semi-major axis is given by :

$$\tan 2\alpha = \frac{2q_{xiyi}}{(q_{xi} - q_{yi})} \quad ..(6.15)$$

where α = the bearing of the semi-major axis
(Ashkenazi (1976), Slama (ed) (1980);Ch 2, Caspary (1987))

The form of the error ellipse is shown in figure 6.1.

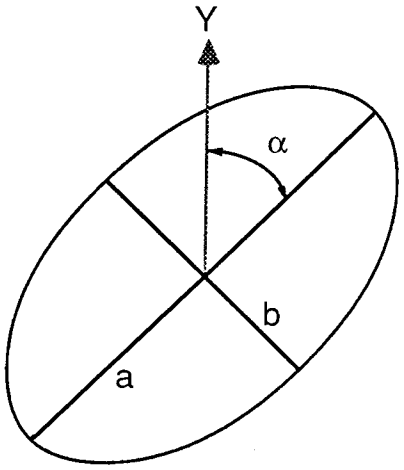

where $a = \sigma_o \sqrt{\lambda_1}$
$b = \sigma_o \sqrt{\lambda_2}$
α =bearing of semi-major axis

Figure 6.1 Standard point error ellipse

The probability of the point lying within the standard point error ellipse reaches a maximum for a redundancy of infinity and is 39.4%. Due to the relatively small probability of the true position being within the standard ellipse it is usually replaced by a **Confidence Error Ellipse**. Such an ellipse is a function of the required probability of the true position of the point lying within

the ellipse. For a probability 1-α, where α is the level of significance, the semi-major and semi-minor ellipse axes become :

$$a = \sigma_o \sqrt{\lambda_1 \chi^2_{2\ .1-\alpha}}$$
$$b = \sigma_o \sqrt{\lambda_2 \chi^2_{2\ .1-\alpha}} \qquad ..(6.16)$$

where a = semi-major axis
b = semi-minor axis
$\chi^2_{2\ .1-\alpha}$ = Chi-squared distribution coefficient at significance level α

(Caspary (1987), Niemeier (1987))

For the case where the a posteriori variance factor, $\hat{\sigma}_o^2$, is used the standard point error ellipse becomes :

$$a = \hat{\sigma}_o \sqrt{\lambda_1}$$
$$b = \hat{\sigma}_o \sqrt{\lambda_2} \qquad ..(6.17)$$

and the confidence point error ellipse becomes :

$$a = \hat{\sigma}_o \sqrt{\lambda_1 F_{2.r.1-\alpha}}$$
$$b = \hat{\sigma}_o \sqrt{\lambda_2 F_{2.r.1-\alpha}} \qquad ..(6.18)$$

where r = redundancy
$F_{2.r.1-\alpha}$ = F (Fischer) distribution coefficient

(Caspary (1987), Niemeier (1987))

For three dimensional networks, as is the case for close range photogrammetric networks, **Error Ellipsoids** are required. The sub-matrix of the cofactor matrix of unknown parameters relating to point i becomes :

$$Q_i = \begin{pmatrix} q_{xi} & q_{xiyi} & q_{xizi} \\ q_{yixi} & q_{yi} & q_{yizi} \\ q_{zixi} & q_{ziyi} & q_{zi} \end{pmatrix} \qquad ..(6.19)$$

The orientation of the error ellipsoid is defined by a 3 by 3 rotation matrix, R, which defines the orientation of the ellipsoid in space. If the magnitude of three orthogonal axes of the ellipsoid are denoted by a', b', and c', the solution takes the following form.

$$\begin{pmatrix} a' & & \\ & b' & \\ & & c' \end{pmatrix} = R\, Q_i\, R^T \qquad ..(6.20)$$

Solution of this expression involves six non-linear independent equations. As the system is non-linear it must be linearized and the solution is therefore iterative. Solution yields the three orientation elements, which define the orientation of the ellipsoid, and the magnitude of the three orthogonal ellipsoid axes (Slama (ed) (1980);Ch 2).

The probability that the true position of a point lies within the ellipsoid is 20%. Confidence ellipsoids, similar to the confidence ellipses developed previously, therefore require formulation. Computation of error ellipsoids, however, is computationally expensive and intensive and is therefore not undertaken, except for the highest precision photogrammetric applications.

An alternative method of graphically representing precision for three dimensional networks is by utilizing error ellipses, for the X and Y axes, with an error vector, to show the direction and magnitude of the error in the Z direction. Such a concept is shown in figure 6.2.

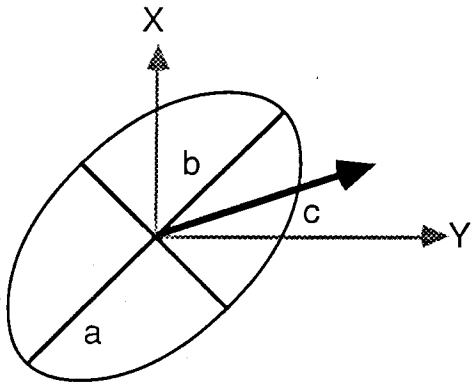

Figure 6.2 Graphical representation of precision for three dimensional networks, (error ellipse (X,Y) ; error vector (Z)).

The problem with such a representation is that it may not depict the principal error magnitude or direction. Figure 6.3 shows a case where the error ellipse and error vector combination do not accurately represent precision of three dimensional networks. Although a simple approach for displaying three dimensional point precision, the procedure is not recommended unless the network designer is aware of the limitations of the graphical representation.

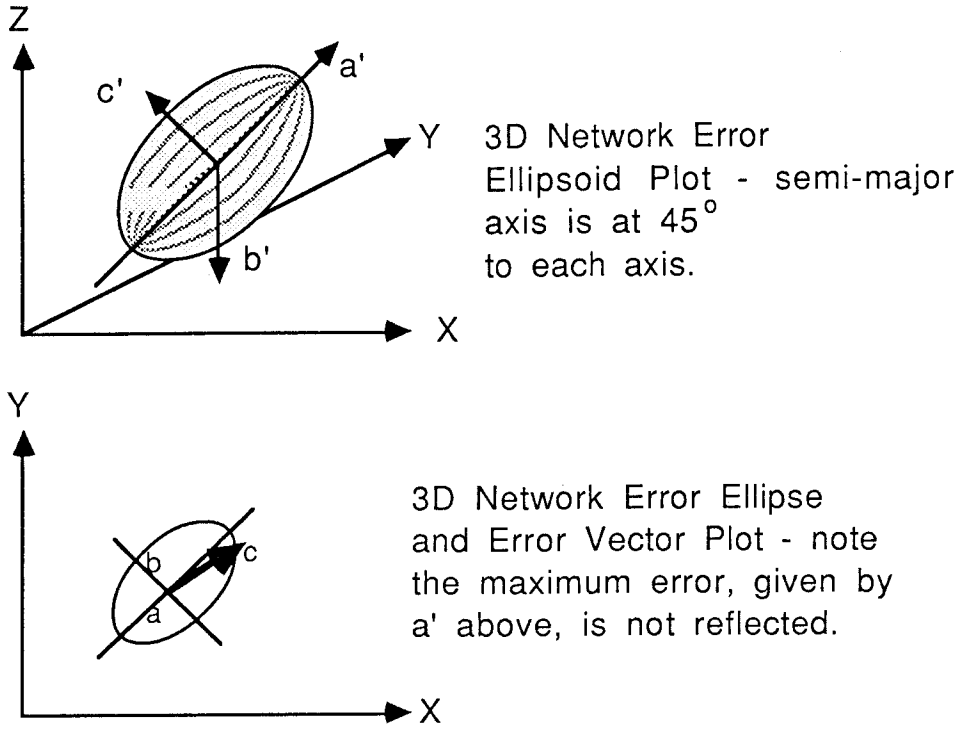

Figure 6.3 Comparison of error ellipsoid and error ellipse / error vector measures for three dimensional networks

Error Circles and **Error Spheres** are precision measures approximating error ellipses and error ellipsoids respectively. Error spheres are of value for three dimensional networks due to their computational simplicity compared with ellipsoid determination. Typical sphere radii for three dimensional networks include :

1. spherical standard error
   $r = \frac{1}{3}(\sigma_X + \sigma_Y + \sigma_Z)$
   where σ_X, σ_Y and σ_Z are the standard deviations in X,Y and Z respectively.

2. mean square standard error
   $r = \sqrt[3]{\sigma_X^2 + \sigma_Y^2 + \sigma_Z^2} = \sigma_o \sqrt[3]{\text{tr } Q_i}$
   where Q_i = cofactor sub-matrix for point i

3. generalized point error
   $r = \sigma_o \sqrt[3]{\det Q_i}$ (Caspary (1987))

A disadvantage of precision measures detailed so far is that no inter-point covariance information is incorporated in the measures. Relative precision measures incorporate inter-point covariances and correlation.

Relative Error Ellipses and Ellipsoids express the relative precision of two points. The computation of standard and confidence ellipses is carried out as for point ellipses with the difference being in the form of the cofactor matrix of unknown parameters, as given by equation 6.13. The cofactor sub-matrix represents the difference between the two points i and j, for two dimensional networks, and takes the form :

$$Q_{i,j} = Q_i + Q_j - Q_{ij} - Q_{ji} \qquad ..(6.21)$$

where Q_i or Q_j is the 2x2 sub-matrix for each point

Q_{ij} or Q_{ji} is the 2x2 covariance sub-matrix between the points i and j

This formulation is a two dimensional representation with graphical plot of the ellipse on the midpoint of the line joining the two subject points (Caspary (1987)). Development of the three dimensional case is identical to the above case except that a relative error ellipsoid is formulated and the cofactor sub-matrix of equation 6.21 is a function of four 3 by 3 sub-matrices.

The local precision measures developed to date are datum dependent measures. A local precision measure, invariant with respect to datum orientation and translation but not datum scale, is the **Distance Standard Error** between two points. For a distance between points i and j, d_{ij}, the distance standard error is :

$$\sigma_{dij} = \sqrt{\sigma_o^2 \, G_{ij} \, Q_{i.j} \, G_{ij}^T} \qquad ..(6.22)$$

where σ_{dij} = standard error of distance d_{ij}

$Q_{i.j}$ = sub-matrix of $Q_{\hat{X}}$ as given by equation 6.21

G_{ij} = row vector of direction cosines *l,m,n* for points i and j

$= (-l, -m, -n, l, m, n)_{ij}$

(Ashkenazi (1976), Fraser (1980b))

6.1.3 Global Measures of Precision

Global measures of precision reflect the precision of the network as a whole. These measures are especially significant for network design as they provide a measure which, although not necessarily absolute, reflects the quality of the network.

The basic, and simplest, global precision measure is the **Mean Variance** of the parameters, $\bar{\sigma}_{\hat{X}}^2$.

$$\bar{\sigma}_{\hat{X}}^2 = \frac{1}{u} \operatorname{tr} \Sigma_{\hat{X}} \qquad ..(6.23)$$

where u = number of unknown parameters
$\Sigma_{\hat{X}}$ = variance-covariance matrix of the parameters

(Mikhail (1976), Fraser (1980b), Caspary (1987))

The mean variance measure can be decomposed into measures for all object space coordinates, $\bar{\sigma}_c^2$, and further decomposed into measures for object space X and Y coordinates, $\bar{\sigma}_{XY}^2$, and object space z coordinates, $\bar{\sigma}_z^2$.

$$\bar{\sigma}_c^2 = \frac{1}{u_c} \operatorname{tr} (\Sigma_{\hat{X}})_c$$
$$\bar{\sigma}_{XY}^2 = \frac{1}{u_{XY}} \operatorname{tr} (\Sigma_{\hat{X}})_{XY}$$
$$\bar{\sigma}_z^2 = \frac{1}{u_z} \operatorname{tr} (\Sigma_{\hat{X}})_z \qquad ..(6.24)$$

where the subscripts denote the parameter components which are relevant for each measure.

The mean variance is usually expressed in terms of the **Mean Standard Error**, $\bar{\sigma}_{\hat{X}}$. A mean standard error can be formulated for both equations 6.23 and 6.24, and is of the form :

$$\bar{\sigma}_{\hat{X}} = \frac{1}{\sqrt{u}} \sqrt{\operatorname{tr} \Sigma_{\hat{X}}} \qquad ..(6.25)$$

For the purposes of assessing global precision relative to the dimension of the object being measured, the **Proportional Precision** is a useful global precision measure. The proportional precision is especially useful in close range photogrammetry where overall precision requirements may be

expressed as one part in a critical dimension of the object or with respect to the principal diameter of the object as a whole. For the object diameter denoted by D, the proportional precision becomes :

$$1 \text{ part in } \frac{D}{\bar{\sigma}_c} \qquad ..(6.26)$$

where $\bar{\sigma}_c$ = mean standard error for X,Y and Z object space coordinates

D = average object diameter

A global precision measure which is useful for assessing coordinate precision homogeneity is the **Standard Deviation Range** or **Root Mean Square Error Range** (Fraser (1982a), (1984)). The measure gives the range, between maximum and minimum values, for XY, Z and XYZ coordinates. In order to achieve maximum point homogeneity a network should be designed which gives a minimum standard deviation range. The measure is of the following form.

$$\begin{aligned} \Delta\sigma_c &= \max(\sigma_{Xi}, \sigma_{Yi}, \sigma_{Zi}) - \min(\sigma_{Xi}, \sigma_{Yi}, \sigma_{Zi}) \\ \Delta\sigma_{XY} &= \max(\sigma_{Xi}, \sigma_{Yi}) - \min(\sigma_{Xi}, \sigma_{Yi}) \\ \Delta\sigma_Z &= \max(\sigma_{Zi}) - \min(\sigma_{Zi}) \\ &\text{for all points } i \end{aligned} \qquad ..(6.27)$$

Maximum object point precision homogeneity is achieved when these values approach zero, ie when the difference between the largest and smallest precision value approaches zero. This measure gives no indication of the absolute precision of the values being assessed as it is a relative measure and hence is not applicable in assessing precision criteria based upon absolute magnitudes.

The **Generalized Variance** , $\bar{\sigma}_{\hat{X}}^2$, is a global precision measure based upon the determinant of the variance-covariance matrix of unknown parameters.

$$\bar{\sigma}_{\hat{X}}^2 = \sqrt[u]{\det \Sigma_{\hat{X}}} \qquad ..(6.28)$$

The generalized variance is dependent upon the smallest eigenvalue of $\Sigma_{\hat{x}}$ and the measure becomes zero for a singular variance-covariance matrix. The geometric significance of this measure is that it relates to the volume of the overall network error ellipsoid (Caspary (1987)). A problem with the generalized variance measure is that it does not reflect the worst possible case for the subject network, as the measure is primarily influenced by the smallest eigenvalue of $\Sigma_{\hat{x}}$. Consequently the generalized variance will usually give an optimistic estimate of network precision.

A global precision measure which is often recommended is the **largest eigenvalue of** $\Sigma_{\hat{x}}$. Caspary (1987) details the motivation for acceptance of λmax as a global precision measure. The maximum eigenvalue, λmax, represents the maximum variance for any function of the parameters and is therefore a measure of the "worst case" for any anticipated precision estimates in a network. λmax can be thought of as a global precision measure as it reflects the upper limit of variance estimates for the network.

For many network design applications an optimal network is one where point estimates are isotropic and homogeneous. Such criteria mean that all error ellipsoids should be spheres and all error spheres should have the same radii. Isotropous and homogeneous precision estimates can be achieved by considering several functions of the eigenvalues. To achieve the above criteria, and hence achieve optimal network design, the following relationships should hold.

1. $\lambda max = \min$ (minimize upper limit of variance)

2. $\frac{\lambda max}{\lambda min} \Rightarrow 1$ (isotropic condition)

3. $\lambda max - \lambda min = \min$ (homogeneity condition)

(Niemeier (1987), Caspary (1987))

Fraser (1980b), (1982a), (1984) has formulated a **photogrammetric network strength factor** based upon network scale, the mean standard error and the image coordinate measurement precision. From this measure an approximate expression for $\bar{\sigma}_{\hat{x}}$ can be formulated.

$$\tilde{\sigma}_{\hat{x}} = q\, S\, \sigma \qquad ..(6.29)$$

where
- q = network strength factor
- S = scale number
- σ = image coordinate measurement precision
- $\tilde{\sigma}_{\hat{x}}$ = approximate mean standard error

The network strength factor, q, is dependent on network geometry and hence a direct relationship between network geometry and mean standard error can be established. For multi-station convergent networks, network strength values of $0.5 < q < 1.5$ are acceptable and represent "strong" networks. Consequently, if the mean standard error is derived in the estimation process, it can be included in equation 6.28 to yield an approximate precision measure, ie the network strength factor, which reflects network geometry and configuration. In practical cases a change in image scale will alter imaging geometry, however corresponding changes in the mean standard error will not be proportional (Fraser (1984)). The relationship of equation 6.29 is therefore only approximate, however for network design applications where a coarse estimate of network quality is required, the effect of this approximation can be neglected.

In assessing global network precision via scalar precision measures, care should be taken as the measures are not consistent and can give different indications of network quality. For example, Caspary (1987) presents the case of two networks A and B, the error ellipses of which are given in figure 6.4.

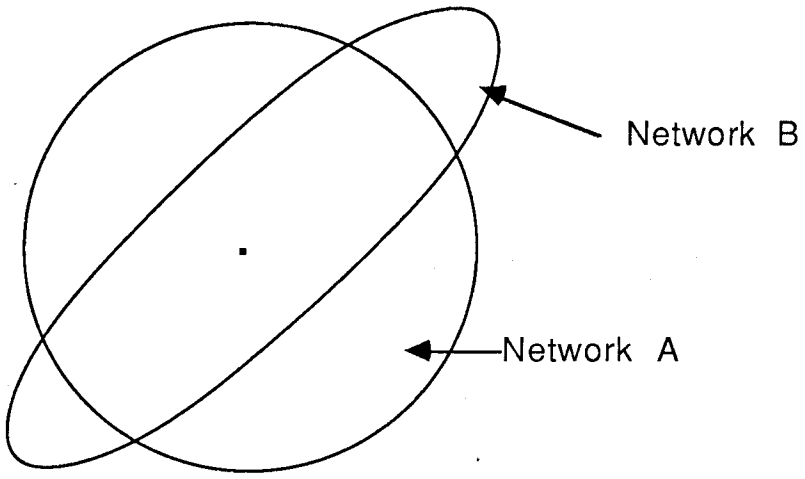

Figure 6.4 Network error ellipses for global precision evaluation

From the results, given in table 6.1, it can be seen that scalar global precision measures are not definitive and in the process of network design the limitations of each measure should be accounted for.

Table 6.1 Results of global precision assessment

Network	$\tilde{\sigma}_{\hat{x}}^2$	error ellipse	$\bar{\bar{\sigma}}_{\hat{x}}^2$	λmax
A	25	a=b=5	25	25
B	25	a=7,b=1	7	49
Conclusion	A = B	A better than B (precision homogeneity)	B better than A	A better than B

A more complete measure of network precision is available from **Criterion Matrices**. Criterion matrices are artificial variance-covariance matrices of the parameters and represent the desired form of the actual variance-covariance matrix. The criterion matrix is usually formulated with a Karman-Taylor structure, ie isotropous and homogeneous coordinate precision. Note that the comparison of the criterion and actual variance-covariance matrix must be carried out with respect to the same datum. The estimation of network precision, via criterion matrix analysis, is computationally intensive but yields an accurate measure of network precision relative to a given benchmark. All variance and covariance components of the point estimates can be assessed to determine overall network quality. Criterion matrix formulation is given in Caspary (1987) and Niemeier (1987).

Principal Component Analysis is another non-scalar method of assessing network quality and network precision. Based upon eigenvalue decomposition of the variance-covariance matrix of unknown parameters, $\Sigma_{\hat{x}}$, the magnitude and direction of the first principal component, ie the "worst case" for each point, is determined. Precision measures are then based upon assessment of the principal component analysis (Niemeier (1987).

6.1.4 Summary of Precision Measures

All precision measures, whether local or global, are based upon decomposition in some form of the variance-covariance matrix of the parameters. Figure 6.5 represents the structure of the cofactor matrix of the parameters, $Q_{\hat{x}}$, and lists the portion of the matrix which contributes to each precision measure.

In the process of network design it is necessary to select precision measures which are applicable to the network requirements, are easy to formulate and which can readily be presented in a easily decipherable form. In network design for three-dimensional networks, as is the case for close range photogrammetric networks, the graphic display of precision information is difficult to both compute and display. Error ellipsoids fall into this category.

Measures based upon eigenvalue decomposition are regarded as good overall indicators of network precision. The problem with such measures, however, is the computational difficulty associated with their formulation. In free network adjustments based upon the Moore-Penrose inverse, eigenvalues are formed in the matrix inversion process and use of the resulting eigenvalues for precision assessment is therefore recommended. In close range photogrammetry the free network solutions are not based upon the Moore-Penrose inverse and hence eigenvalue decomposition especially for precision estimation is required. Precision measures based upon eigenvalues are therefore not practical for close range photogrammetric network design.

In the majority of network design cases several global estimates of network precision are desired. These measures should indicate the overall network quality, the degree of precision homogeneity between point coordinates and the precision with respect to X, Y and Z coordinates separately. For the purposes of network evaluation in this project a combination of global and local precision measures have been used. These measures will allow a good overall assessment of the network quality. The measures chosen include the following.

Global

1. the photogrammetric network strength factor ; q
2. the mean standard error in X,Y,Z ; $\bar{\sigma}_c$
   X,Y ; $\bar{\sigma}_{XY}$
   Z ; $\bar{\sigma}_Z$
3. the coordinate standard deviation range in X,Y ; $\Delta\sigma_{XY}$
   Z ; $\Delta\sigma_Z$

Local

4. the coordinate standard deviation ; $\sigma_{Xi},\sigma_{Yi},\sigma_{Zi}$

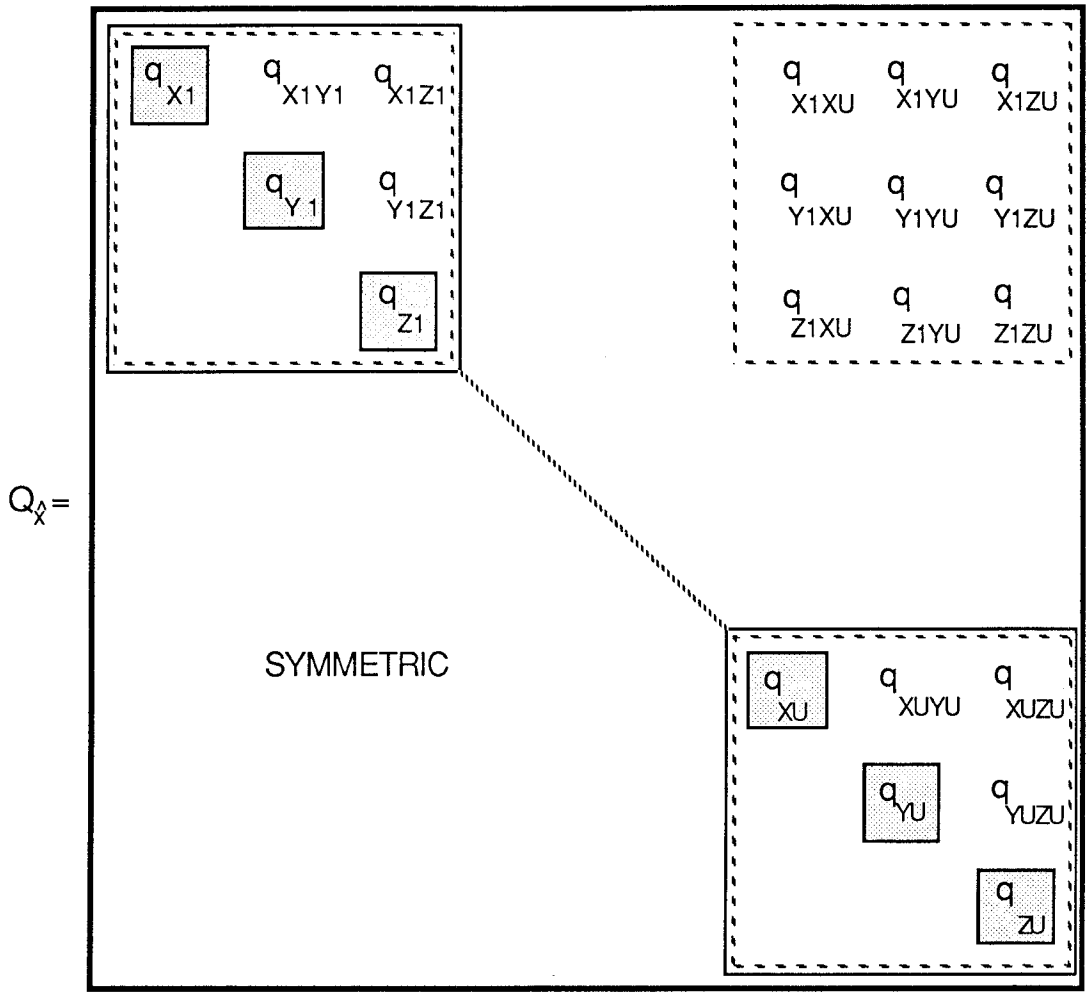

Standard deviation of coordinates
Mean Variance
Mean Standard Error
Photogrammetric network strength factor
Standard Deviation Range
Proportional Precision

Standard point error ellipse / ellipsoid
Confidence point error ellipse / ellipsoid
Error circle / sphere
Confidence interval

Relative error ellipse / ellipsoid
Relative confidence ellipse / ellipsoid
Distance Standard Error

Principal component analysis
Criterion matrix analysis
Eigenvalue analysis
Generalized variance

Figure 6.5 Precision measures as a function of the cofactor matrix of unknown parameters

6.2 Accuracy Measures

Accuracy measures for close range photogrammetric networks have been the neglected component in formulation of measures for network quality. In many cases where network quality is assessed, precision and accuracy are confused. However these quality measures are distinctly different. Precision is directly related to the dispersion of a distribution while accuracy reflects the closeness of an estimate to the true value of the parameter being assessed (Mikhail (1976). As covered in section 5.1, accuracy includes precision and bias terms, with the most significant component of the accuracy measure to be assessed being the bias, or systematic error. If a measure of network accuracy is to be formulated then an indication of the deviation of the estimated coordinates from the true coordinates is required.

There are two features which reduce the significance of accuracy assessment in close range photogrammetry. These include the following.

1. Many close range photogrammetric applications only require the relative position of the object to be assessed. In other words only the shape of the object is important. Many of the systematic errors which affect the object point coordinate determinations in the same manner, ie systematic errors which are invariant with changing exposure station, are therefore not significant. Systematic errors which vary between exposure station, eg film deformation, and which vary from object point to object point will be significant and will affect object shape.

2. Self-calibrating bundle adjustments allow for the detection and compensation of significant systematic errors. If such an adjustment procedure is utilized, with an additional parameter set which will facilitate modelling of the significant systematic errors, then the effect of systematic errors on the final point estimates will be minimized. Although a residual systematic error may still be evident the effect can usually be considered to be negligible and hence accuracy assessment becomes unnecessary.

There are four principal components which will affect photogrammetric network accuracy. These components are :

1.	Geometry of the network	- camera focal length - imaging geometry - density of control measurement
2.	Computational method	- self-calibrating v standard bundle adjustment
3.	Physical characteristics	- quality of camera interior orientation - film and emulsion flatness - accuracy of comparator/analytical plotter (neglected for a calibrated instrument)
4.	Redundance of measurements	- number of image observations per point - multiple exposures

(Hottier (1976))

If network design is carried out properly, and "strong" network geometry with adequate measurement redundancy results, then the principal contributor to network accuracy are the physical characteristics of the camera and measurement system. For multi-station close range photogrammetric evaluations there are two basic methods of assessing network accuracy. The first method is the control check method. Although conceptually simple the method requires the availability of object point coordinates, to a higher degree of precision and accuracy than could be anticipated from a photogrammetric evaluation. To allow adequate accuracy assessment 10 - 15 such points are required. Determination of accuracy is then computed by comparison of photogrammetric and control coordinates and determination of the systematic component if any is evident (Hottier (1976)).

An alternative method is based upon simulation procedures. Image coordinates for a network identical to the "real" network are simulated, with a random error included in simulated observations to allow for anticipated observational errors. The resulting object point coordinates, after adjustment of the simulated data, are then compared to the coordinates from the "real" evaluation. Any systematic difference between the two sets of results reflect the accuracy of the network (Hottier (1976)).

For network design applications, where no "real" network has been observed, neither of the above methods can be applied directly, as both methods require comparison of results with "real" photogrammetric data. For network design, if accuracy criteria are of importance, a combination of the two methods can be formulated. The first step involves acquisition of high precision / high accuracy coordinates of 10 - 15 object points. The second stage involves the simulation of image coordinates for these points. Pseudo-errors, which model systematic errors such as film deformation, emulsion irregularities, lens distortions, film unflatness etc, are added to the simulated coordinates along with random errors to simulate observational errors. After these pseudo-observations are adjusted, comparison of the derived object point coordinates with the control coordinates is carried out. Evaluation of the difference between the two sets of coordinates will give an indication of network accuracy. Although the process requires the acquisition of "real" data, in the form of control coordinates, this is a more economical method than acquiring photographs for numerous possible networks in order to assess accuracy for each design.

A more applicable method of assessing network accuracy is via two network simulations, one with added systematic errors and one without such errors. A comparison of the two sets of results will give an indication of network accuracy. This method has the inherent advantage that no "real" information is required and hence the evaluations can be carried out without the time consuming and costly exercise of acquiring "real" data.

For accuracy assessment in "normal" stereo photography, Hottier (1976) has developed predictor formulae as accuracy measures. Such predictors cannot be extended to cover the multi-station convergent case of photogrammetry however.

The accuracy measures which have been covered are practical and physical measures of network accuracy. An alternative approach, which will be introduced in the assessment of reliability measures, involves assessment of the least squares mathematical model. Attempts to resolve systematic effects, by assessing the expected results of an unbiased versus biased solution, will be addressed.

6.3 Reliability Measures

Reliability, in the context of network quality, refers to the conformance of an observed network to its design. The basis of reliability assessment is the potential for detection of systematic and gross errors via adequate testing procedures.

Methods for the detection and compensation of systematic errors have been covered in previous sections. Section 6.2 introduces accuracy measures and outlines the significance of systematic error detection in close range photogrammetric applications. Self-calibration adjustment procedures allow the major photogrammetric systematic errors to be modelled and hence compensated for in the estimated object point coordinates. The principal photogrammetric systematic errors are detailed in sections 2.4.1 to 2.4.4, with development of self-calibration procedures being carried out in section 2.4.5. As the major photogrammetric systematic errors will be assumed to have been adequately reduced by self-calibration and pre-calibration procedures, the reliability measures assessed will primarily be with respect to gross errors.

The effect of gross errors on estimated parameters can be analysed by observing the network and then applying mathematical model testing procedures in order to detect if gross errors exist in one, or more, observations. The testing procedure commences with a global model test, whereby the least squares functional model is tested, based upon the null hypothesis that the model is correct and complete and that distribution assumptions meet reality. If the alternative hypothesis, ie that either systematic or gross errors exist, is accepted, then the residuals are screened in order to detect outliers. Residual screening methods include Baarda's data snooping, Pope's Tau method and the Danish method. The mathematical principles of the three methods are covered, in detail, in Caspary (1987). Analysis of network reliability is covered in Pelzer (1979), Niemeier (1982), Niemeier (1987),Caspary (1987), and with respect to photogrammetric analysis in Amer (1979).

For network design however, the detection of "real" gross errors, or outliers, is not significant. In the network design process reliability assessment is concerned with the influence of gross errors upon parameter estimates, methods of minimizing the effect of gross errors on the network and measures of assessing network reliability.

Network reliability can be assessed as in terms of either internal or external reliability. Internal reliability refers to the desired properties of the least squares model to facilitate the detection of systematic and gross errors without requiring additional information. External reliability is a measure of the response of the least squares model to undetected systematic and gross errors, or the influence on the parameter estimates (Caspary (1987)).

Caspary (1987) develops reliability measures for global, ie the model as a whole, and local, ie with respect to individual observations, in terms of internal and external reliability. A summary of these measures is given in table 6.2. Note that these measures are based upon Baarda's data snooping methods.

Table 6.2 Network reliability measures

	Internal	External
Global	$\Lambda_{max}(P\,Q_v\,P) = max$ $tr(P\,Q_v\,P) = max$	$\Lambda_{max}(P\,\hat{Q}_l\,P) = min$ $tr(P\,\hat{Q}_l\,P) = min$
Local	$f_i = p_i q_{vivi} = max$	$p_i^2\, a_i^T \hat{Q}_x a_i = min$
Local Average= Global	$\bar{f} = \frac{f}{n} = max$	$\frac{1}{n} tr(P\,\hat{Q}_l\,P) = min$

where
Q_v = cofactor matrix of residuals
$\hat{Q}_l$ = cofactor matrix of adjusted observations
$\Lambda_{max}(M)$ = maximum eigenvalue of the matrix M
P = weight matrix of observations
q_{vivi} = ith diagonal element of Q_v
p_i = the a priori weight of observation i
a_i = ith column of the design matrix A
n = number of observations

In utilizing the reliability measures for network design and network reliability assessment, the measures should be used as relative measures. In

other words the difference between the measures for different network designs and not the absolute magnitude of each measure should be assessed.

To achieve a high conformance of an observed network to its design, the network must be self-checking (Niemeier (1982)) and hence must comprise independent redundant observations. For photogrammetric network design, Amer (1979) introduces simple methods to improve network reliability. These include increasing the number of observations, hence increasing redundancy, and using object point clusters instead of single well spaced object points. A simple method of increasing network redundancy, and hence network reliability, is via multiple exposures. With respect to improvement in network reliability, one of the most important consequences of multiple exposures is that exposure dependent systematic errors are averaged and therefore reduced.

In assessment of network reliability, measures are based upon analysis of functions of either the cofactor matrix of residuals, Q_v, or the cofactor matrix of adjusted observations, $Q_{\hat{l}}$. These matrices are invariant with respect to datum selection as long as the applied constraints are minimal. If the network is over-constrained both Q_v and $Q_{\hat{l}}$ become datum dependent and reliability assessment may not be valid.

Förstner (1985) covers the influence of imaging configuration upon network reliability. For high accuracy photogrammetric applications, two and three photograph, convergent or "normal", imaging configurations do not give sufficient internal reliability to be routinely implemented in close range photogrammetric evaluations. It is recommended that a minimum of four photographs are utilized to ensure high internal reliability (Fraser (1987)).

6.4 Sensitivity Measures

Until recently, assessment of network sensitivity for close range photogrammetric networks has not been required. Due to the increase in precision from close range photogrammetric evaluations in recent years, monitoring and deformation analysis have become possible. Applications of close range photogrammetry for deformation analysis are given in Fraser (1983), and for industrial monitoring in Fraser (1988b), (1988c).

Sensitivity, with respect to network quality criteria, can be defined as the potential of a network to determine or resolve deformations. The fundamental measure of sensitivity is the sensitivity criterion, or the minimum magnitude of deformations for a given model at which deformations are just detectable (Niemeier (1982)). For the purposes of determining such a measure, measurements at two epochs are considered. The parameter and variance estimates at the two epochs are :

$$\begin{aligned} &\text{Epoch 1} : \quad \hat{X}_1 \; ; Q_{\hat{X}1} \\ &\text{Epoch 2} : \quad \hat{X}_2 \; ; Q_{\hat{X}2} \end{aligned} \qquad ..(6.30)$$

The difference measures, between epochs, take the following form.

$$\begin{aligned} &\text{difference} = d = \hat{X}_1 - \hat{X}_2 \\ &\text{cofactor matrix of the difference} = Q_{dd} = Q_{\hat{X}1} + Q_{\hat{X}2} \end{aligned} \qquad ..(6.31)$$

In order to determine if deformation has occurred, a Global Congruency test Fraser (1983), Caspary (1987)), (Niemeier (1987) is carried out. Such a test is based upon the null hypothesis that the expected value of the difference metric is zero. The alternative hypothesis is that the difference metric is not zero, and equals the deformation d_A. If the alternative hypothesis is accepted then at least one point has undergone movement or change. Based upon the results of the Global Congruency test, further tests can be carried out to isolate the deformation or movement.

For the design of networks the detection of deformations is not significant. The significant aspect, with respect to network design, is to be able to design a network which will allow maximum sensitivity and consequently maximum likelihood of detecting significant deformations. To allow a measure for sensitivity the deformation, d_A, is expressed as :

$$d_A = a\, g \qquad ..(6.32)$$

where a = the unknown scale factor

g = the known form of critical movements

In order to determine the minimum detectable deformation, $d_{min}=a_{min}\, g$, a minimum scale, a_{min}, requires determination.

$$a_{min} = \sigma_o \sqrt{\frac{\lambda_o}{g^T Q_{dd}^+ g}} \qquad ..(6.33)$$

where σ_o = the a priori variance factor

λ_o = the F-distribution non-centrality parameter

Q_{dd}^+ = the Moore-Penrose inverse of Q_{dd} (Niemeier (1987))

A measure has been developed for sensitivity, namely the minimum detectable deformation. In designing a network for application in monitoring and deformation analysis, the following steps should be carried out in conjunction with the conventional design procedure.

1. develop the deformation model
2. develop the vector g of critical movements
3. select the risk level of the test
4. determine a_{min}
5. determine the minimum detectable deformation

Design of deformation networks can also be carried out via principal component analysis of the cofactor matrix of parameters. The principal component of each point determination will indicate the "worst" direction and magnitude of any point estimate. The sensitivity criteria then has the requirement that anticipated critical movements should be orthogonal to the principal component, to allow maximum likelihood of detecting the subject deformation (Niemeier (1987)).

In this chapter, methods of assessing network quality have been described. Precision measures have been covered in detail as such measures indicate the quality of the network. Precision measures are predominantly datum dependent and therefore the effect of the datum definition upon precision measures should be determined prior to selecting a particular measure.

Measures for accuracy, reliability, and sensitivity have not been developed in detail as they are essentially secondary network quality measures. Sufficient references have been included if detailed analysis of these quality criteria is required. Measures of network economy have not been developed. The cost of network establishment and evaluation is left to the network designer and is determined by considering all cost components individually, based upon the expert opinion of the designer.

7. INTERACTIVE GRAPHICS, SIMULATION AND ADJUSTMENT SOFTWARE

Interactive computer graphics and network simulation provide a convenient method of designing and assessing network configuration and ultimately, network quality. The process provides an indirect solution to the problems associated with close range photogrammetric network design. A network can be designed interactively with the computer, with graphic displays of the imaging geometry, target array, camera orientations etc, and the network design problems, introduced in section 5.2, are then solved by iteratively, utilizing network simulations.

For the purposes of assessing the various components of close range photogrammetric network design, such as datum definition, quality measures, configuration influence, observation quality etc, a close range photogrammetric computer software package was developed. The package, called SIMPAC (Simulation Package) for identification purposes, was designed in order to allow assessment of network design problems and has a range of options to allow evaluation of the majority of the factors influencing network design.

SIMPAC is an interactive computer graphics and simulation package. The software specifications are :

1. written in Fortran 77 for use on a VAX 11 / 780 computer.
2. graphics are established from Plot 10 Graphical Kernel System (GKS) subroutines. These subroutines are Fortran 77 library subroutines which comply with the GKS standard for computer graphics.
3. the software runs on a Tektronix 4107 graphics terminal. If adjustment routines are used independent of graphics, then any computer terminal may be used.

Flowcharts to demonstrate the capabilities of SIMPAC are given in figures 7.1a and 7.1b. The flowcharts are not detailed but give an overall indication of the package features and software structure.

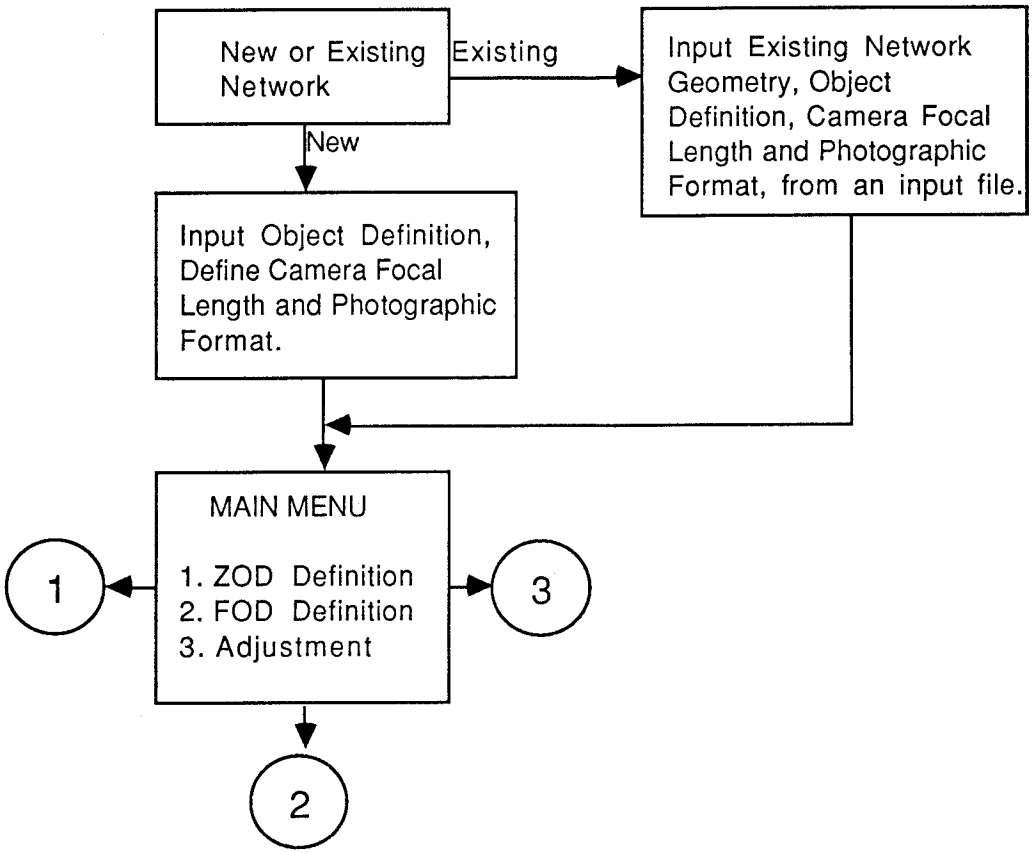

Figure 7.1a Flowchart of the interactive computer graphics network design and simulation package - SIMPAC

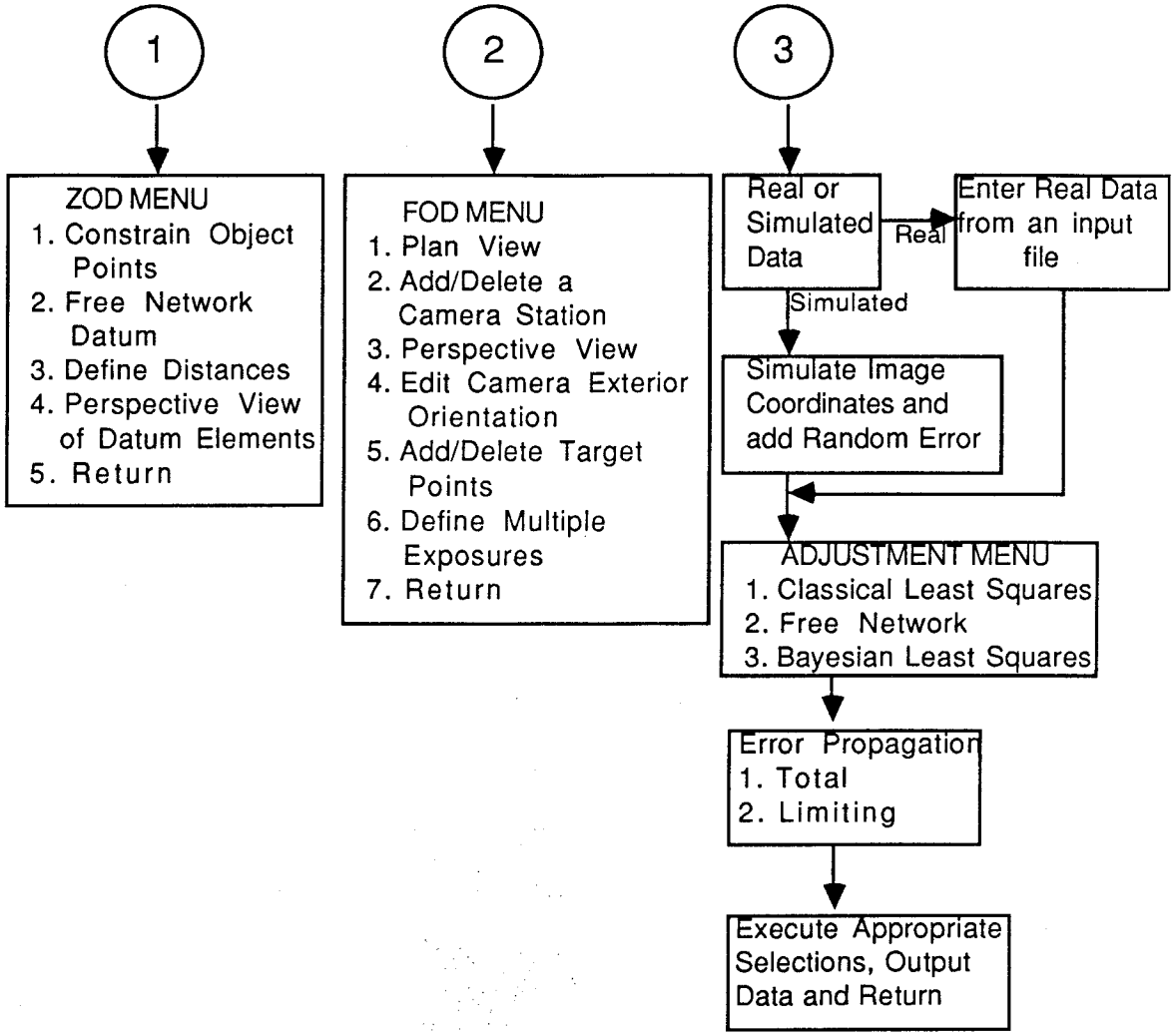

Figure 7.1b Flowchart of SIMPAC options

The basic software features of SIMPAC will be described briefly with an emphasis on applicability to network design. The package will be analysed in terms of the two basic components of the software, namely the interactive computer graphics component and the adjustment component.

7.1 SIMPAC - Interactive Computer Graphics Component

To illustrate the various features of the graphics capabilities of SIMPAC, consider the following example. An object, being a 50m cube, is to be photographed. A Wild P32 metric camera is used, with 64.1mm focal length and a offset photographic format of 90mm x 65mm. Included in the example are several obstructions, for example a wall and a pole. The influence of these obstructions can be graphically seen from the plots. The plots show various

design stages in the network configuration definition, from initial plan view of the object through to the object with added targets and defined camera station locations.

An object is defined, external to the program, in a format compatible with input requirements. Also defined are the internal camera parameters of focal length and image format. A plan view of the object is plotted, along with any obstructions or restricting features.

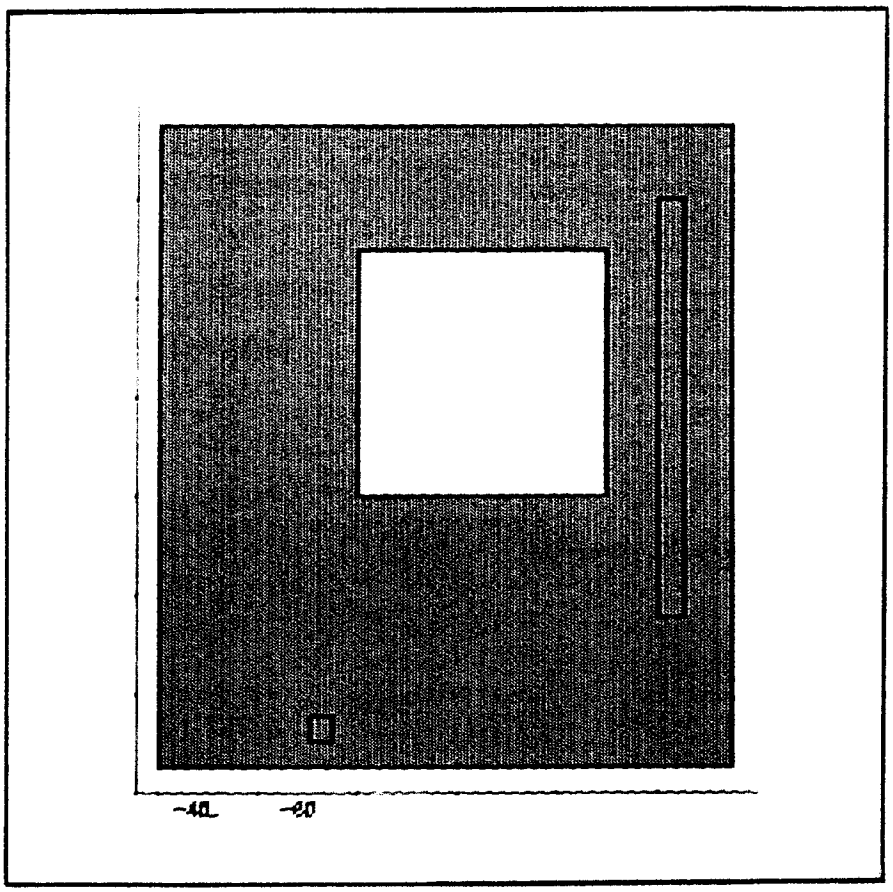

Figure 7.2 SIMPAC plot - Plan view of the object with no camera stations or object points defined.

Camera stations can be specified, by definition of the exterior orientation parameters, and a planimetric plot of the configuration is carried out. The plot shows position of the camera stations relative to the object, and includes camera field of view to aid in configuration design and to assess photographic coverage of the object. Camera stations can be added to or deleted from the configuration.

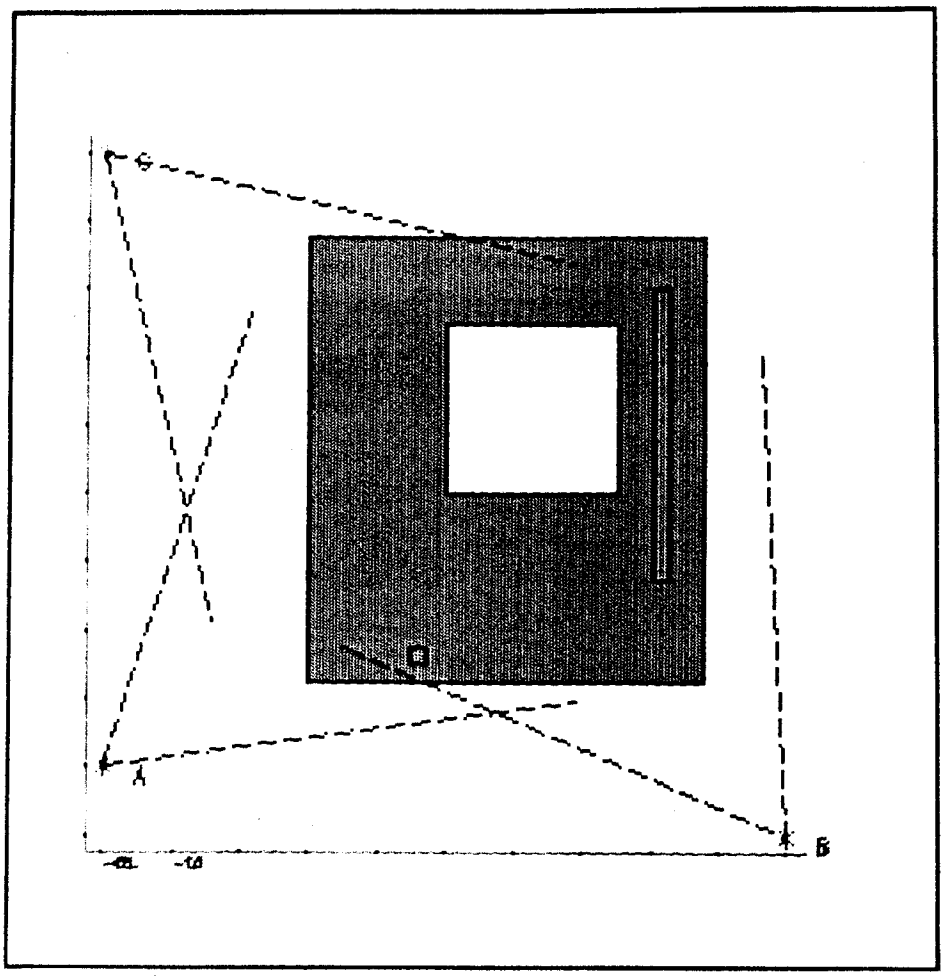

Figure 7.3 SIMPAC plot - Plan view of the object with defined camera stations and network configuration.

A perspective view from each camera station can be plotted. The view is overlaid by the photographic format, and hence the coverage of the object, by each photograph, can be established. Obstructing features, such as walls, poles, buildings etc, are also included in the perspective plot. Consequently any obstruction of the object, by any feature, can be modeled and a configuration as close as possible to reality achieved. The plot of the perspective view is carried out via a two stage hidden polygon removal procedure. The first stage involves detection and flagging of all "back" polygon faces for a given view direction. "Back faces" are those polygons which face away from the observer's position and which therefore cannot be seen. The second stage involves depth sorting, in order of increasing distance from the observer's position. The plotting of polygons is then carried out in order of decreasing distance from the observer and only for front face polygons. The resulting perspective view consists of near polygons being overlaid on distant polygons with a consequent "realistic" perspective view.

This process is called the painter's algorithm, and is developed in Pavlidis (1982) and Hearn and Baker (1986). Along with the perspective plot, from the subject camera station, the camera exterior orientation parameters are also output.

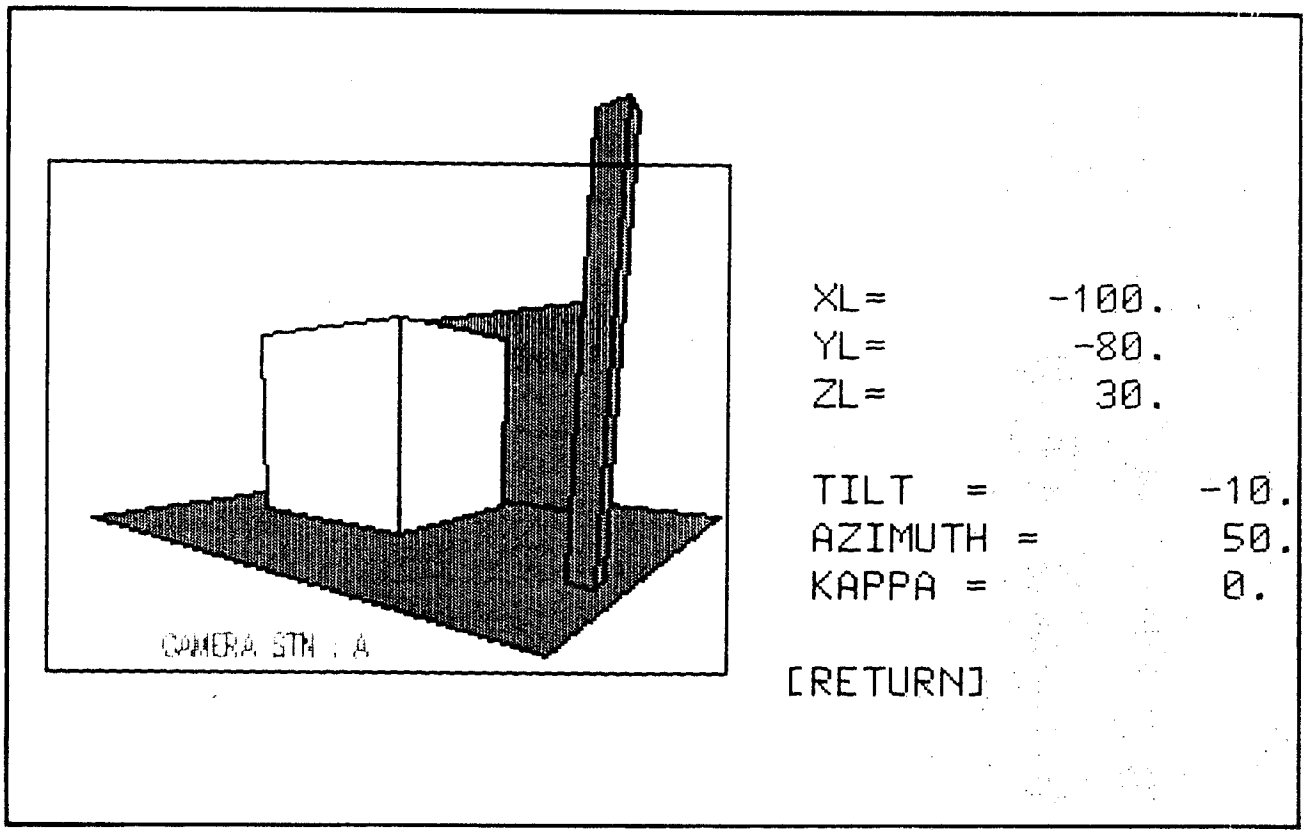

Figure 7.4 SIMPAC plot - Perspective view of the object

Camera exterior orientation parameters can be edited to allow optimal coverage of the object in question. Perspective views after each edit stage are possible.

Having devised an initial network configuration, target points can be added to the object. This is achieved by generating a perspective view from a camera station and selecting a polygon upon which targets are required. The subject polygon is then plotted normal to the view direction and targets are interactively added to the polygon using the cursor on the computer terminal. After all targets have been added the perspective view from the camera station is regenerated in order to define which points can or cannot be seen.

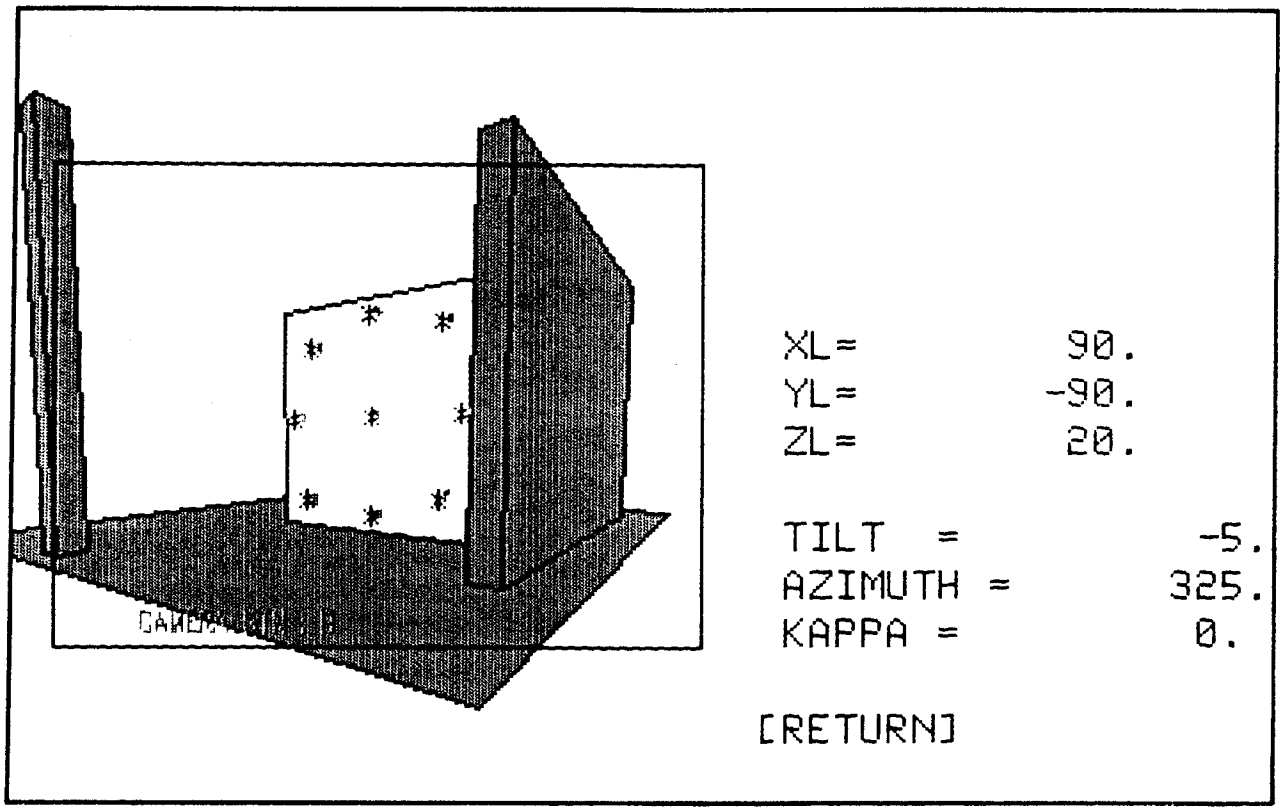

Figure 7.5 SIMPAC plot - Perspective view of the object with defined object points plotted.

The software has a semi-automatic target visibility feature. If a target falls on a back face or is outside the photographic format then it is automatically deleted from the target array of points which can be seen from that particular station. Editing facilities allow manual deletion of targets, on a front face and within the photographic format, but which are either obstructed or not required.

After definition of the imaging configuration and the target array, which is essentially the first-order design, the datum can be defined. The datum, or zero-order design, definition allows :

a) object point coordinate constraint, for any combination of X,Y or Z, and in either minimal or over-constrained form.
b) definition of observed distances.
c) inner constraints (free network) datum definition.

If object point coordinates are constrained or distances observed then a plot of the datum defining elements is possible. The perspective view which results aids in determination of the geometric strength of the datum definition.

The final stage, of the graphics component of SIMPAC, involves the simulation of observations, which include image coordinates and distances, with respect to the previously designed network configuration. The simulated observations have a pseudo-random, normally distributed, error added in order to model the anticipated observational precision of both image coordinate and distance observations. The simulated image coordinates, simulated distances, camera orientation data and any other relevant information are then automatically transferred to the adjustment component of the package. As an addition feature, an output file of simulated image coordinates, in the format of the Wild Aviolyt BC2 analytical plotter, is formed in order to allow analysis of the network by any other conventional adjustment program.

7.2 SIMPAC - Adjustment and Network Evaluation Component

The adjustment component of SIMPAC will be described via the following steps.

An initial selection is made from the three available adjustment types.

a) Classical Least Squares
b) Free Network (Inner Constraints)
c) Bayesian Least Squares

An option is available to introduce "real" image coordinates, instead of simulated image coordinates. Hence the package allows analysis of both "real" and simulated networks.

An option is also available for either a total error propagation (TEP) or limiting error propagation (LEP) solution. Note that all adjustments are mathematically rigorous with respect to inter-point covariance and related error propagation.

Free network adjustment is carried out with respect to the object point coordinates, or a chosen subset of the object point coordinates. Camera exterior orientation parameters are not included in the free network conditions, and hence a partial minimum trace datum with respect to the object points is formulated. The free network method utilized is the free network constraint elimination method, described in section 8.5.3.

The output of results from the chosen adjustment includes :

a) adjusted observations and residuals.
b) the a posteriori variance factor, number of unknowns, number of observations.
c) control equation residuals, for classical least squares adjustments.
d) estimated exterior orientation parameters and associated variance estimates.
e) estimated object point coordinates and associated variance estimates. The points to which the minimum condition is applied, in free network adjustments, are flagged.
f) the mean standard error, in terms of XY, Z and XYZ components ($\bar{\sigma}_{XY}, \bar{\sigma}_{Z}, \bar{\sigma}_{XYZ}$).
g) the standard deviation ranges, in terms of XY, Z and XYZ components ($\Delta\sigma_{XY}, \Delta\sigma_{Z}, \Delta\sigma_{XYZ}$)
h) the photogrammetric network strength factor.

After the adjustment the program control is returned to the interactive graphics component and any, or all, of the network configuration and datum elements can be redefined if necessary.

SIMPAC will be used to illustrate many of the features of close range photogrammetric network design, with an emphasis on zero-order design and first-order design, in the following chapters. The illustrations will include both simulated data and real data and will be designed to verify the software and to demonstrate the significant aspects of network design and analysis.

8. ZERO-ORDER DESIGN SOLUTIONS

The datum problem of the close range photogrammetric network can be solved by various techniques, based upon different forms of the least squares adjustment process. The techniques do not give identical solutions for parameter and variance estimates as the function minimized, the base form of which is given by equation 3.1, usually varies for each technique. Moreover, as both the estimates of the unknown parameters, $\hat{X}$, and the cofactor matrix of these estimates, $Q_{\hat{X}}$, are not invariant functions with respect to constraint selection, the solution will differ as a function of the magnitude and type of constraints which are applied to remove the network datum deficiency.

The mathematical fundamentals of the various constrained estimation techniques have been developed, in detail, in sections 3.5 to 3.7. Such solutions are based upon either absolute or relative constraints, in either explicit or implicit form, which are of a magnitude and type capable of removing the datum deficiency of the network.

In this section, solution of the datum problem for close range photogrammetric networks will be developed. Such developments will be in terms of both the mathematical fundamentals of the least squares solution and the mathematical model for close range photogrammetry. Solutions for the various techniques will be analysed in terms of the type of parameter and variance estimates that result. Note that, in general, the various solutions to the datum problem will be assessed with respect to minimal constraints. Solutions based upon over-constrained parameters result in a hierarchical adjustment in which the inner geometry of the network is destroyed. Over-constrained solutions are applicable in certain circumstances however, and imposition of such constraints is merely an extension of the procedures which will be developed. Note also that invariant functions of the least squares model are only invariant under application of minimal constraints. In an over-constrained network, functions such as residuals, adjusted observations and their associated cofactor matrices become datum dependent and hence dependent upon constraint selection.

8.1 Relative Datum Constraints

Solutions to the problems associated with rank, or datum, deficient systems and the implications of such solutions have been presented in sections 3.5 to 3.6. The application of such techniques depends on the magnitude of the datum defect of the system after all observations have been applied. Observations can act as constraints for the datum definition. Such constraints are relative or weighted constraints (Blaha (1971)). Alternatively constraints which represent certain mathematical conditions, as applied to the parameters, which must be fulfilled are called absolute constraints. For example, if a system is developed based solely on image coordinate observations then a datum defect of seven exists. However if object space distances are observed along with image coordinate observations, then the resulting datum defect will not be seven. Observed distances can define the scale of the network resulting in a network with six datum defects, three translations and three rotations, with the scale being implicitly determined by distance observations. Table 8.1 lists observations applicable to close range photogrammetry and gives the effect of such observations on the datum deficiency of the network. All combinations of possible observations are not included in the table, however an indication of the significance of each observation type, for datum definition, is listed.

Table 8.1 Datum information in observables and combinations of observables (The datum parameters are defined in figure 5.4).

OBSERVATION	DATUM DEFECT	FREE DATUM PARAMETERS	REMARKS
Image observations	7	T_X, T_Y, T_Z R_X, R_Y, R_Z Scale	No datum information in image coordinate observations.
Image observations and one object point in XYZ.	4	R_X, R_Y, R_Z Scale	Coordinates of one point define translation from the origin.

Table 8.1 (cont)

Image observations and two object points in XYZ.	1	Rotation about the line between the two points.	Coordinates of two points define all elements except the rotation about the axis of the line between the two points which may be a function of R_X and R_Y.
Image observations and two object points in XYZ and one non-collinear object point in Z.	-	-	Defines all 7 datum definition elements.
Image observations and exterior orientation parameter observation of one camera station.	1	Scale	Defines orientation and origin of the reference system.
Image observations and distances	6	T_X, T_Y, T_Z R_X, R_Y, R_Z	Observed Distances define scale of the network. Care should be taken to ensure observed distances are representative of the whole network.
Image observations and elevation differences.	7(6)	T_X, T_Y, T_Z R_X, R_Y, R_Z (Scale)	No datum information is inherent in elevation differences unless the points are vertically above one another, in which case the observation can define scale.

Table 8.1 (cont)

Image observations and horizontal angle measurements	7	T_X, T_Y, T_Z R_X, R_Y, R_Z Scale	No datum information is inherent in horizontal angle or direction measurements.
Image observations and two vertical angle measurements	5	T_X, T_Y, T_Z R_Z Scale	Vertical angles can define the direction of the vertical axis.Ensure vertical angles are in both X and Y directions to resolve rotations R_X and R_Y.
Image observations and azimuth observation.	6	T_X, T_Y, T_Z R_X, R_Y Scale	Azimuth defines rotation about the Z axis.
Image observations and one object point in XYZ, azimuth and two vertical angles.	1	Scale	One point defines the translations T_X, T_Y, T_Z, azimuth defines rotation R_Z, vertical angles can define rotations R_X and R_Y
Image observations and elevation difference + distance between the same points.	4	T_X, T_Y, T_Z R_Z	Elevation difference and a distance, between the same points, uniquely define the direction of the vertical axis.
Image observations and one object point in XYZ, azimuth and elevation difference + distance between the same points.	-	-	One point defines the translations T_X, T_Y, T_Z., azimuth defines rotation R_Z, distance defines scale and elevation difference and distance define direction of the vertical axis

One important criterion of the datum definition is that application of datum defining elements must not affect the geometry of the network. In other words the datum must not impose strain upon the network (Caspary (1987)). As described in section 3.5, such a condition is achieved by application of minimal constraints, ie a minimum number of constraints must be applied to remove the datum defect but add no more information into the system. Observations which contain datum information implicitly apply a constraint to the network. For example an observed distance can be utilized to constrain the scale in the network. Hence only six more constraints can be applied to both define the datum and at the same time maintain the criterion for minimal constraints, as the distance observation has been used to implicitly apply one constraint. For a system consisting of image coordinate observations, seven, and only seven, constraints may be applied to both define the datum and maintain the criteria for minimal constraints. If, for example, observations are carried out on three object points, defining the X, Y and Z coordinates of each, as well as image coordinate observations and the object point coordinates are used to define the network datum, then the system would be over constrained, ie nine constraints, and the resulting network geometry would be affected.

With reference to equation 3.22, for a network of rank or datum deficiency, d, then for :

d constraints	- the inner geometry of the network is maintained. (ie the network is not distorted)
<d constraints	- the network is still singular and the parameters are non-estimable.
>d constraints	- the inner geometry of the network is not maintained and a hierarchical adjustment results.

Only that information which is introduced into the network by the actual observations is preserved without change under minimal constraints. As detailed in section 3.7, functions which are invariant with changes in constraints include adjusted observations and residuals. Network reliability assessment, which is based upon assessment of the cofactor matrix of residuals or the cofactor matrix of adjusted observations, can be carried out for any constraint configuration as long as it is minimal. This is because residuals and functions of residuals are invariant with respect to minimum constraint configuration (Blaha (1971)). For over-constrained networks, residuals and

adjusted observations and their associated cofactor matrices will be larger than minimal constraint values and hence reliability assessment will be in error. Additional parameters associated with the camera interior orientation are also invariant with respect to constraint change. Functions, such as those listed above, will not remain invariant, however, if constraints are not minimal. In summary, for an over-constrained network, quantities invariant under minimal constraints become dependent on constraint type and magnitude.

In close range photogrammetric applications, where the network is often independent of existing object space reference systems, provision of datum constraints may be difficult and time consuming and hence minimal constraints are applicable. Also the actual position of the object, with respect to a reference system, may not be required and only the relative shape of the object may be of interest. A partial datum may therefore be explicitly applied to define scale and direction of the vertical (Papo and Perelmuter (1982)). Techniques for minimal constraint solutions, in the form of both absolute and relative constraints, in either explicit or implicit form, and the implication of such solutions in terms of parameter and variance estimation, require assessment.

The datum deficiency of a network has been established as a function of the observables, and the methods for solution of the system of equations for such a network will be investigated.

8.2 Zero-Variance Computational Base

The classical solution to singular adjustment problems, characterized by the datum problem, is the solution obtained by specifying a particular zero-variance computational base, equivalent to the datum deficiency of the network, and solving the system based upon such constraints. In other words a minimum number of parameters required to define the network datum are held fixed and a solution is carried out relative to the fixed parameters. The solution is achieved by suppressing or deleting d appropriate columns of the design matrix, A, where d is the number of datum unknowns (Caspary (1987), Niemeier (1987)). Consequently the zero-variance computational base solution takes the form of a solution based upon absolute minimal constraints. The form of the zero-variance computational base solution, in terms of the constraint equations of section 3.5.1, is given by equation 3.37.

The mathematical model of the least squares solution is then equivalent to the system of equations given by equation 3.26, where :

$$v = (A_1\ A_2)\begin{pmatrix}\hat{X}_1\\ \hat{X}_2\end{pmatrix} - l \qquad ..(3.26)$$

where $\hat{X}_1$ = vector of estimated parameters of order (u-d)

$\hat{X}_2$ = vector of estimated parameters of order (d)

A_1 = design matrix of order (n,u-d)

A_2 = design matrix of order (n,d)

n = number of observations

u = number of unknowns

d = datum deficiency

Section 3.4 develops the assumption that the parameters $\hat{X}_1$ are estimable and the parameters $\hat{X}_2$ are non-estimable. This is due to the linear dependence of the design matrix A_2 upon the design matrix A_1, as given by equation 3.27. As an absolute minimal constraint adjustment, the zero-variance computational base solution involves the deletion of the A_2 design matrix from the least squares mathematical model. Consequently the A_2 design matrix will be a null matrix and hence the parameters X_2 are fixed at their approximate values. Hence the solution is constrained by the fixed points, which will define the scale, orientation and translation of the reference coordinate system. Note that, as given by table 8.1, for a datum deficiency of seven, two points must have their X, Y and Z coordinates placed into $\hat{X}_2$ and a further non-collinear point must have its Z coordinate placed into $\hat{X}_2$, to allow the datum definition. This selection of coordinates for $\hat{X}_2$ is only one of many possible sets of parameters for defining the zero-variance computational base. Although it is the most common constraint selection, almost any combination of parameters may be selected, providing that the selected parameters allow definition of the origin, orientation and scale of the network.

In close range photogrammetric adjustments the observation equations are developed in terms of corrections to the unknown parameters, as for example in equation 4.9. Consequently the solution can be simplified by holding fixed the parameters $\hat{X}_2$. This is achieved by constraining $\Delta\hat{X}_2$ to zero, ie no correction will be applied to the approximate values, X_2^o. Therefore the solution for parameter and variance estimates take the following form.

$$\hat{X} = \begin{pmatrix} \Delta\hat{X}_1 \\ \Delta\hat{X}_2 \end{pmatrix} = \begin{pmatrix} \Delta\hat{X}_1 \\ 0 \end{pmatrix} \qquad ..(8.1)$$

$$Q_{\hat{X}} = \begin{pmatrix} Q_{\Delta\hat{X}1} & 0 \\ 0 & 0 \end{pmatrix}$$

where
$$\Delta\hat{X}_1 = (A_1^T P A_1)^{-1} A_1^T P l$$
$$\Delta\hat{X}_2 = 0 \qquad ..(8.2)$$
$$Q_{\Delta\hat{X}1} = (A_1^T P A_1)^{-1}$$
$$Q_{\Delta\hat{X}2} = 0$$

The cofactor matrix, $Q_{\Delta\hat{X}2}$, is by definition a null matrix. Hence the term "Zero-Variance Computational Base".

Note that this solution is numerically equivalent to the case where d additional rows are appended to the linear model. These rows can be viewed as fictitious observations on the unknown parameters of X_2. Consequently, if the weight applied to the fictitious observation is numerically large enough to "fix" the coordinates, then the two solutions become equivalent (Fraser (1982)). The mathematical model for this formulation is :

$$\begin{pmatrix} v_1 \\ v_2 \end{pmatrix} = \begin{pmatrix} A_{11} A_{12} \\ 0 \quad A_{22} \end{pmatrix} \begin{pmatrix} \hat{X}_1 \\ \hat{X}_2 \end{pmatrix} - \begin{pmatrix} l_1 \\ l_2 \end{pmatrix} \qquad ..(8.3)$$

where
- v_1, v_2 = residuals of image observation and control equations respectively
- l_1, l_2 = observations of image observation and control equations respectively
- A_{11}, A_{12} = design matrices for the image observation equations
- A_{22} = design matrix for the fictitious control equation

From equation 3.42 it can be seen that the solution based upon definition of a zero-variance computational base, which comprises explicit absolute constraint of the parameters, is biased and depends upon constraint selection. Equation 3.43 shows that the cofactor matrix of estimated parameters is not a minimum variance estimate and also depends upon constraint selection. In other words both parameter and variance estimates are not invariant with respect to datum constraint and vary according to which zero-variance computational base is chosen, ie which coordinates are held fixed.

Solutions based upon the specification of a zero-variance computational base have the advantage that they are conceptually simple and easy to implement. Disadvantages, however, include :

1. definition of the datum is restricted to definition by absolute constraint of d components of the unknown parameters.
2. the estimates of the parameters, $\hat{X}$, and the cofactor matrix of the estimated parameters, $Q_{\hat{X}}$, depend upon the arbitrarily selected points used to define the datum. Consequently definition of a zero-variance computational base does not clearly reflect the inner precision, or quality, of the network, and hence is not ideally suited for assessment of network design and quality.

As discussed above, both parameter and variance estimates from a zero-variance computational base datum definition, are datum biased and datum dependent. If a zero-variance computational base is to be used for photogrammetric datum definition it would be logical to define the datum with respect to those coordinates which would allow the "best" possible solution. This "best" solution will not be optimal, ie the solution will not provide a minimum mean variance estimate, however it would result in the smallest mean variance estimate for the available zero-variance computational base configurations.

In selecting a zero-variance computational base for close range photogrammetric datum definition, a quantitative relationship between constraint configuration and precision estimates would be useful. A method for determining which three object points would form the best control configuration is required. Fraser (1982a) observed the following qualitative relationships with respect to the mean standard error and distribution of the minimal constraints or control.

1. as the centroid of the control point triangle approaches the centroid of the object point target array, the mean standard error of the object points, $\bar{\sigma}_c$, decreases.
2. as the area of the control point triangle increases so the mean standard error decreases.

Quantitatively these requirements can be expressed in the following way. For the target array centroid denoted by Xc, Yc, Zc, and a plane defined by the three chosen control points, then the minimum distance between the plane and the centroid is normal to the plane and is denoted by d. The area of the triangle defined by the control points can be determined from $A = \frac{1}{2} b\, c \cos\alpha$, where the notation is defined in figure 8.1.

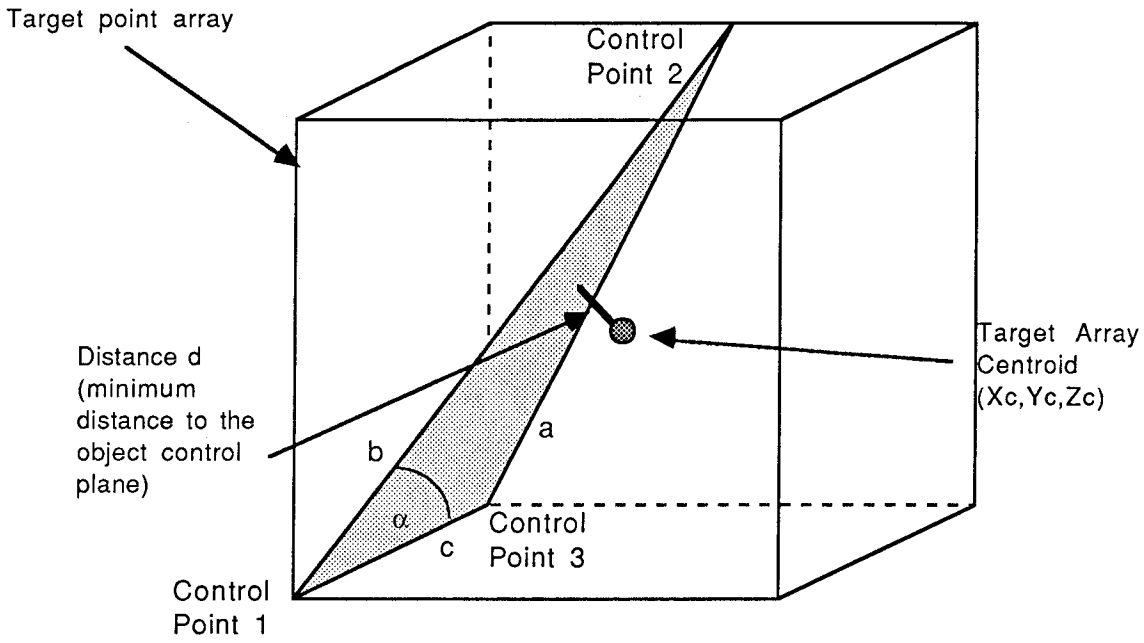

where a,b,c = control point triangle side lengths
α = angle subtended by sides b and c

Figure 8.1 Requirements for the "best" control configurations for zero-variance computational base datum definitions

Consequently, if the "best" or one of the "best" control configurations is to be determined analytically, then the following two relationships should hold simultaneously.

1. d = minimum
2. A = maximum

where d = the minimum distance from the target array centroid to the control point plane
A = area of the control point triangle

For complex target arrays these relationships may not be applicable, however for network design purposes, where an initial coarse estimate of

suitable datum definition configurations is required, the relationships can be used to estimate several applicable control configurations from which the "best" configuration can be ascertained by network simulation.

8.3 Ridge Regression Models

In all cases of least squares estimation characterized by datum or rank deficiency, the coefficient matrix of the normal equations is singular and ill-conditioned. To eliminate the singularity problem of the normal equation coefficient matrix, mathematical models have been proposed which, in general terms, comprise the addition of non-negative values to the main diagonal elements of the singular matrix. Such a process will enable constraint of the parameters if the added values can remove the rank deficiency of the matrix, and hence an estimate for the parameters and their cofactor matrix can be formulated. The magnitude and type of values which are to be added to the diagonal of the singular matrix will be analysed, as will the form of the parameter and variance estimates which result.

Two basic forms of the ridge regression model will be evaluated. These include Bayesian formulations, whereby the non-negative values are determined from prior information of the variance of the unknown parameters, and generalized ridge regression formulations, whereby the non-negative values are in fact constants which can be varied to numerically form a non-singular normal equation coefficient matrix (Draper and Van Nostrand (1979)).

8.3.1 Bayesian Least Squares

Bayesian least squares is an estimation process whereby a good a priori knowledge of the unknown parameters can be included in an adjustment process in order to ensure that the estimated parameters do not differ significantly from their a priori value. In other words the Bayesian approach combines sample information (observations) with other available prior information which may be available. Such an estimation procedure is subjective as the "degree of belief" in the unknown parameters is used (Walpole and Myers (1972)). Bayesian estimates are therefore biased estimates. For a priori knowledge, comprising prior estimates of the parameters, X', and the associated cofactor matrix, Q_X^{-1}, the quadratic form to be minimized is of the following form.

$$\phi = v^T P v + X'^T P_X X' \Rightarrow \text{minimum} \qquad ..(8.4)$$

(Krakiwsky (1982))

where v = residuals

ϕ = function to be minimized

P = weight matrix of observations = Q^{-1}

P_X = a priori weight matrix of parameters = Q_X^{-1}

X' = a priori values of parameters

The extension of the least squares quadratic form,given by equation 3.1, to that given by equation 8.4, means that Bayesian estimation is a form of constrained least squares. Constraints are relative and are in the form of weighted observations, and the Bayesian formulation therefore allows implicit definition of the datum unknowns. Instead of the augmented quadratic form, given by equation 8.4, observation equations could have been established for the "observed" parameters and then added to the existing system of equations. Solution of such a system would rely on least squares, minimization of $v^T P v$, with constraints implicit in the added observations of the parameters. In terms of the method of constrained minima by Lagrange multipliers, the minimum function of equation 8.4 becomes :

$$\phi' = v^T P v + \hat{X}^T P_X \hat{X} - 2k(v + l - A\hat{X}) \qquad ..(8.5)$$

where k = Lagrange multipliers

$\hat{X}$ = estimates of the parameters,X

Partial derivatives, with respect to v and $\hat{X}$, are equated to zero to give:

$$\frac{\partial \phi'}{\partial \hat{X}} = 2\hat{X}^T P_X + 2kA = \hat{X}^T P_X + kA = 0 \qquad ..(8.6)$$

$$\frac{\partial \phi'}{\partial v} = 2v^T P - 2k = v^T P - k = 0 \qquad ..(8.7)$$

The system of equations, in terms of the Lagrange multipliers, k, the unknown parameters, $\hat{X}$, and the residuals, v, becomes :

$$\begin{pmatrix} 0 & P_X & A \\ P & 0 & -I \\ -I & A & 0 \end{pmatrix} \begin{pmatrix} v \\ \hat{X} \\ k \end{pmatrix} = \begin{pmatrix} 0 \\ 0 \\ l \end{pmatrix} \qquad ..(8.8)$$

The solution of equation 8.8 is similar to that developed in section 3.5.2 and hence will not be covered again here. The resulting solution equations become :

$$\hat{X} = (A^TPA + P_X)^{-1} A^TPl$$
$$Q_{\hat{X}} = (A^TPA + P_X)^{-1} \qquad ..(8.9)$$

$$\hat{\sigma}_o^2 = \frac{v^TPv + \hat{X}^TP_X\hat{X}}{n - u + m} \qquad ..(8.10)$$

where n = number of observations
u = number of unknowns
m = number of parameters with prior weights
(Krakiwsky (1982), Harvey (1987))

Equations 8.9 apply to linear observation equations and therefore only one iteration is required to achieve a solution. In non-linear cases, where several iterations may be required, equations 8.9 contain additional terms. The Bayesian formulations can easily be compared with classical least squares by noting that the fundamental difference between the two solutions is that the Bayesian case merely involves addition of terms to the diagonal of the classical least squares normal equation coefficient matrix. Consequently the Bayesian estimate can be determined by forming the least squares normal equations, adding the prior parameter weighting to the appropriate diagonal terms and then solving the system as for the least squares case.

The design matrix, A, is evaluated at the prior values for the parameters, X', and at some approximate value, X^o, if no prior information is available. Note that the degrees of freedom, given by r= n-u+m, is equal to the number of observations minus the number of free unknowns. This is an approximate formulation which can lead to significant errors in the a posteriori variance factor, $\hat{\sigma}_o^2$, if the degrees of freedom are small. An explanation of the degrees of freedom, for Bayesian formulations, is given by Harvey (1987). It depends upon the degree of prior weighting of the observed parameters. In most close range photogrammetric applications the degrees of freedom is large and any small error in r, depending upon the magnitude of prior weighting, will generally have an insignificant effect on $\hat{\sigma}_o^2$.

The Bayesian estimate is based upon a two stage linear model, both of which rely on normality of distribution. The first stage requires observations to be normally distributed, with expectation AX and variance Σ ($l \sim N(AX,\Sigma)$). The

second stage requires the prior estimates of the parameters, X', to be normally distributed with weight matrix P_X^{-1} ($X \sim N(X', P_X^{-1})$) (Fraser (1980)). Consequently the resulting Bayesian estimates have the structure of a multivariate weighted average between the standard least squares estimate and the prior value, X'.

The Bayesian solution does not provide an optimal solution to the datum problem as the solution is dependent upon the structure and magnitude of the weight matrix P_X. In other words the solution depends upon which parameters have an a priori weighting and the magnitude of this weighting. For seven parameters, with strong a priori weighting, the solution takes on the form of a zero-variance computational base solution, as the seven constrained parameters effectively fix the datum. For such a solution prior weights must only be applied to just enough parameters to resolve the datum. The case just described is a form of the Bayesian solution in which minimal constraints apply, with the constraints taking the form of relative or weighted constraints. In all other cases the network is over-constrained and a hierarchical adjustment results. Bayesian estimation solutions are not designed specifically for solution of the datum problem, however the benefit of such formulations become evident when prior knowledge of the parameters is available and needs to be included in the estimation procedure.

For close range photogrammetric network design applications the Bayesian estimation process does not provide the best solution. An estimate of the quality of the network, as given by the mean variance, is not optimal unless constraints are absolute and a minimum (Fraser (1980b), Fraser (1982a)). In Bayesian formulations, constraints are neither absolute nor minimal and hence an optimal estimate of network quality is not possible. As a hierarchical adjustment usually results from a Bayesian formulation, the residuals and adjusted observations are not invariant with selection of constraint. Consequently optimal estimates of reliability, which are based upon the analysis of the cofactor matrix of residuals, Q_v, is not unbiased in Bayesian adjustment procedures. The statistical principles of the Bayesian estimation procedure are given in detail in Leonard (1975).

8.3.2 Ridge Regression Estimation

Ridge regression least squares is similar to Bayesian least squares, with the difference being that the weighting matrix, P_X, in equation 8.9 is replaced by k^2I. Here k is an arbitrary constant which is numerically added to the main diagonal elements of the normal equation coefficient matrix and I is the identity matrix. In ridge regression formulations a constant term is added to each diagonal term while in the Bayesian case, the term added to the normal equation coefficient matrix may be different for each parameter. The constant, k, will have an "optimal" value. However usually there will be a range of k values which will allow the transformation of the singular matrix into a numerically non-singular matrix, therefore allowing solution to the subject system of equations. The "loading" of the main diagonal of the singular matrix in effect implicitly defines the datum, as the addition of the non-negative constants can be thought of as weighted or relative constraints which implicitly define the network orientation, origin and scale. As the constraints are neither minimal nor absolute the ridge regression solution does not provide variance estimates which are optimal. As the constraints are not minimal a hierarchical adjustment will result and the inner geometry of the network will be destroyed. In ridge regression solutions the value of k is usually an arbitrary value, with a magnitude to just allow the solution of the singular normal matrix, while in Bayesian least squares the added value is not arbitrary and is derived from real a priori information.

In a manner similar to the Bayesian formulation a function to be minimized can be established in terms of the constant k, and a solution for parameter and variance estimates derived. The ridge regression solution becomes :

$$\hat{X} = (A^TPA + k^2I)^{-1} A^TPl$$
$$Q_{\hat{X}} = (A^TPA + k^2I)^{-1} \qquad ..(8.11)$$

(Marquardt (1970), Fraser (1980b))

In contrast to least squares estimation, ridge regression estimates introduce a small amount of bias in order to achieve a major reduction in variance (Marquardt (1970)) and consequently give a smaller mean square error than least squares. This can be evaluated in terms of the the constraints. As the system is over-constrained, in fact every parameter is subject to

constraint, the residuals and adjusted observations are no longer invariant quantities. Consequently the sum of squares of the residuals will be larger than the minimal constraints solution and the solution will not be "least squares". As with the Bayesian formulation, whose estimates are dependent upon the structure and magnitude of the prior value of the weight matrix, P_X, the ridge regression solution depends upon the value of the constant k. In selection of the constant k several theorems, relating to the properties of the ridge regression solution as detailed by Marquardt (1970), will be given. Such theorems will aid in optimal selection of k.

1. the function to be minimized, ϕ, is a monotone increasing function of k, ie the ridge solution will have a larger sum of the squares of the residuals over the least squares sum of the squares of residuals.

2. the mean variance of the estimates, $\bar{\sigma}_X^{\wedge 2}$, is a continuous monotone decreasing function of k.

The mean variance of theorem 2 comprises a variance and a bias component and is seriously inflated for a singular, or near singular, normal equation coefficient matrix. As k is increased the matrix becomes non-singular and the mean variance approaches a minimum. Hence in search of an optimal value for k, assessment of bias and variance requirements must be determined. In a case where an optimal ridge regression solution is required, with respect to both variance and bias, a value for k is chosen such that the mean variance approaches a minimum but also so that the minimum function is not seriously inflated.

Ridge regression solutions, for solution of numerically singular normal matrices, are difficult to assess in terms of the requirements for datum definition. In other words the selection and addition of the constant k to the singular normal equation matrix does not have a conceptual or geometric relationship with the physical concept of datum definition. The solution is basically mathematical and k is selected such that practical and numerical prerequisites are met. Despite this, the ridge regression solution can be thought of as a weighted constraint solution where all the parameters are constrained to allow the datum to be resolved, with the condition that k is kept as small as possible.

8.3.3 Summary of Bayesian and Ridge Regression Solutions

The application of Bayesian and ridge regression methods, to solve datum definition problems for close range photogrammetry, is not recommended. The reasons for this are :

1. In ridge regression solutions the value of k^2, for addition to the diagonal of the singular normal equation coefficient matrix, is often an arbitrary value. In such solutions a range of values for k can suffice, all of which result in different solutions.

2. The solutions of both Bayesian and ridge regression formulations do not give optimal estimates of either parameters or variances, an optimal estimate being a minimum bias, minimum mean variance solution. Optimal estimates of variance are only possible under application of minimal and absolute constraints and neither Bayesian nor ridge regression solutions offer this. Assessment of network quality is therefore not feasible.

3. The solutions of both Bayesian and ridge regression formulations are usually based on an over-constrained datum. Consequently the inner geometry of the network is not maintained and functions, such as adjusted observations and residuals, become dependent upon constraint selection and magnitude. Assessment of network reliability, based upon residual analysis, is therefore not possible.

4. With respect to ridge regression models in general, Draper and Van Nostrand (1979) condemn mechanical application of regression solutions merely to improve conditioning of the network or system. Application of such solutions should be restricted to cases where prior or practical information is available, and for such a case Bayesian least squares solutions are acceptable. Doubt is cast upon the value of ridge regression analysis as it is claimed that ridge estimators only provide suitable results in cases where the regressions are significant and the ridge estimates close to the least squares estimates.

In close range photogrammetric network design, optimal estimates of the variance of the parameters are required. Both Bayesian and ridge regression solutions fail to meet the required form of the estimates for network design. For this reason, and because of the problems listed above, Bayesian estimation and ridge regression estimation should not be utilized in close range photogrammetric network analysis to solve the datum problem. If, however, prior knowledge of the parameters is available then the Bayesian solutions provide a convenient and simple method for incorporating such information in the estimation process.

8.4 Free Network Solutions

Solutions to the datum problem, thus far, have been based upon the explicit constraint of selected or arbitrary parameters in order to resolve the datum unknowns of scale, orientation and translation of the reference coordinate system. Such constraints will result in variation of both parameter and variance estimates as a function of the selected constraints. Consequently the parameter estimates are usually biased and the variance estimates are not minimal. Free network solutions are based on the concept that there should be no overall translation, rotation and scale change with respect to the approximate values in any estimation procedure (Granshaw (1980)). Physically this means that all parameters in the adjustment are "free" or unconstrained and hence the resulting parameter and variance estimates will be on the basis of all parameters being able to shift to a value which results in no overall scale, rotation and translation change. Parameter and variance estimates therefore, are referred not to selected points but to the network of points as a whole. Free network solutions are conceptually difficult to assess with respect to the origin of the reference coordinate system. If coordinates are fixed in order to define the datum, then the origin of the reference system will be relative to these points. In a free network solution such a relationship is not evident and the reference system is relative to the centre of gravity of the object space coordinates. The geometric significance of this is that the centroid, or centre of gravity, of the network does not move. The mathematical significance of a free network adjustment is that the trace of the cofactor matrix of the unknown parameters is a minimum and consequently that the mean variance of the unknown parameters, $\bar{\sigma}_{\hat{x}}^2$, is a minimum (Granshaw (1980), Caspary (1987), Mittermayer (1972), Welsch (1979)). Due to the above mentioned properties of the free network adjustment, the term

minimum trace datum is used for describing a free network adjustment, in conjunction with analysis of the datum problem, where the inner geometry of the network is based upon all approximate values and hence all parameters.

For the purposes of close range photogrammetric network design, free network solutions provide a useful evaluation tool as the solution provides both a minimum bias and a minimum mean variance solution. The minimum mean variance solution is especially useful as it can be used in the process of evaluating network quality. The constraints applied for a free network solution are both absolute and minimal, as covered in sections 3.5.2 and 3.6, and consequently the inner geometry of the network is preserved and the precision estimates derived can be used as precision estimates for the inner geometry of the network. As constraints are minimal the residuals and adjusted observations remain invariant with respect to constraint selection, and therefore reliability assessment can be carried out from residual analysis.

With respect to the concept of inner precision (Granshaw (1980)) the effect of an arbitrary set of parameters can be filtered out of the cofactor matrix. If the filter parameters are chosen as rotational, translational and scaling parameters, as is the case for close range photogrammetry, then inner precision refers to the internal precision of a network which is not affected by choice of coordinate system. Inner precision therefore refers to the precision of a free network adjustment (Granshaw (1980)).

Free network solutions, of the close range photogrammetric datum problem, can be classified depending on the form of the constraints applied. The first technique involves the application of generalized matrix algebra for the solution of the singular system of equations. The Moore-Penrose inverse is applied to ensure a minimum mean variance solution. Such a solution is covered, in general terms, in section 3.6. The second technique involves the application of a specific constraint equation to the least squares mathematical model in order to achieve a minimum mean variance solution. This technique is covered, in general terms, in section 3.5.2. Note that both solutions will yield identical results if the constraint applied, in both cases, is that of the minimum Euclidean Norm of the parameters.

8.4.1 Moore-Penrose Inverse Solution

The Moore-Penrose inverse allows solution of singular matrices based upon the concepts of generalized matrix algebra. The resulting solution is of type BLIMBE (Best Linear Minimum Biased Estimate) and gives a minimum mean variance solution. In terms of the cofactor matrix of the estimated parameters this means that the trace of the cofactor matrix is a minimum ($tr(Q_{\hat{X}}) = minimum$).

From equation 3.55 the solution vector is :

$$\hat{X} = (A^T P A)^+ A^T P l = N^+ A^T P l \qquad ..(3.55)$$

where N^+ is the Moore-Penrose inverse of the singular matrix N

The Moore-Penrose inverse can be determined from the singular value decomposition of the subject matrix (Bjerhammar (1973), Fraser (1980b), (1982a)). The Moore-Penrose inverse, N^+, is of the following form.

$$N^+ = \sum_{i=1}^{u} \frac{1}{\lambda_i} S_i S_i^T \qquad ..(8.13)$$

where u = order of matrix N (u,u)

λ_i = ith eigenvalue of N, for i=1,u

S_i = ith eigenvector of N, corresponding to eigenvalue λ_i.

In the singular value decomposition the eigenvalues, λ, are selected such that the smallest eigenvalue attains its maximum value. If this is the case then the resulting mean variance of the estimated parameters will be a minimum, as required. Note that a disadvantage of the solution based on the Moore-Penrose inverse, determined by singular value decomposition, is that the solution is computationally time consuming.

Fraser (1980b), (1982a) defines the inverse N^+ as :

$$N^+ = \lim_{k^2 \to 0} (N + k^2 I)^{-1} \qquad ..(8.12)$$

Equation 8.12 is similar to the Bayesian and ridge regression solutions of section 8.3.2. In these solutions, however, the term added to the diagonal

elements of the normal equation coefficient matrix is either arbitrary or based upon some prior knowledge of the parameters. In the Moore-Penrose solution, the terms k^2I are selected such that an optimal estimate of the mean variance of parameters results. Fraser (1980b), (1982a) shows that $N^+ \neq (N + k^2I)^{-1}$ over a broad range of values of k and consequently the Moore-Penrose inverse solution is not equivalent to a solution based upon explicit ridge regression analysis. For most values of k, the inverse $(N + k^2I)^{-1}$ is an unsatisfactory, typically seriously inflated, estimate of the variance of the unknown parameters.

For the selected minimal constraint for the Moore-Penrose inverse being a minimum Euclidean Norm, or the changes to the a priori parameters is a minimum, a minimum value is attained for the mean variance of the estimated parameters, $\bar{\sigma}^2_{\hat{X}}$, when the constraint is absolute. The minimum Euclidean Norm condition is always absolute and minimal, and hence a minimum $\bar{\sigma}^2_{\hat{X}}$ results.

With respect to photogrammetric applications and especially photogrammetric network design, free network solution via the Moore-Penrose inverse has an inherent disadvantage. The solution detailed above gives a minimum for the mean variance estimate for all the parameters, X. For close range photogrammetric network analysis the parameters of interest are the object space coordinates. Hence a minimum of the variance component of the cofactor matrix relating to these parameters is required. As the free network properties will be based, in this case, upon a subset of the approximate coordinates, and hence upon a subset of the parameters, the term partial minimum trace datum is used.

The estimate $\bar{\sigma}^2_{\hat{X}}$ can be expressed in terms of the three basic parameter sets of the close range photogrammetric model. Such parameters include exterior orientation parameters, denoted by X_{eo}, object space coordinates, denoted by X_c, and additional parameters, denoted by X_a. In terms of the above parameters the mean variance can be expressed as :

$$\bar{\sigma}^2_{\hat{X}} = \bar{\sigma}^2_{\hat{X}_{eo}} + \bar{\sigma}^2_{\hat{X}_c} + \bar{\sigma}^2_{\hat{X}_a} \qquad ..(8.14)$$

From the above equation it can be seen that a minimum $\bar{\sigma}^2_{\hat{X}}$ does not necessarily imply minimum $\bar{\sigma}^2_{\hat{X}_c}$. In fact in most cases the estimate $\bar{\sigma}^2_{\hat{X}}$ will be

influenced primarily by the $\bar{\sigma}^{2}_{\hat{X}eo}$ component as $\bar{\sigma}^{2}_{\hat{X}eo}$ is usually much larger than $\bar{\sigma}^{2}_{\hat{X}c}$. In other words the mean variance of the object space coordinates will be degraded and the mean variance of the exterior orientation parameters will be improved until an overall optimal mean variance results. As implied previously, for close range photogrammetric network analysis, parameters other than object space coordinates can be considered as nuisance parameters and hence to optimize their solution is of no value. For accurate network analysis an optimal form of $\bar{\sigma}^{2}_{\hat{X}c}$ is required and although the estimates of the object space coordinates will be optimal the estimates of the remaining parameters will not be optimal. The Moore-Penrose inverse cannot facilitate such an evaluation as the solution provided is with respect to optimal variance estimates of the parameter set as a whole. Therefore free network solution, utilizing the concepts of generalized matrix algebra, may be applicable in terms of providing an overall minimum mean variance, however for the special case of close range photogrammetry where a minimum mean variance for a particular subset of the parameters is required, the Moore-Penrose inverse solution is not acceptable.

8.4.2 Free Network Constraint Method

The free network constraint method is based upon the minimum bias, minimum mean variance solution for observations with constrained parameters, as given in section 3.5.2. The technique involves the imposition of absolute minimal constraints which will result in the Euclidean Norm of the parameters, $\| \hat{X} \|$, being a minimum. Such constraints will result in a minimum trace of the cofactor matrix of the estimated parameters and consequently a minimum mean variance. As the technique involves the imposition of minimal constraints, which means that the inner geometry of the network is maintained, and the constraints are of the form which give a minimum mean variance of parameters, the solution will reflect the inner precision of the network. The solution is therefore also referred to as the "Inner Constraints" solution, (Blaha (1971), Fraser (1982a), (1984)), and is developed in full in Blaha (1971).

From section 3.5.2 it has been shown that the constraints which provide a minimum Euclidean Norm of the parameters are of the form:

$$G^T\hat{X} = 0$$
$$AG = 0 \qquad ..(3.46)$$

where R(G) = d

and G = the constraint coefficient matrix, and is composed of the d linearly independent eigenvectors, associated with the d zero eigenvalues of the singular normal matrix.

The solution for such constraints is given by equation 3.35 and is of the form :

$$\begin{pmatrix}\hat{X}\\ k\end{pmatrix} = \begin{pmatrix}N & G\\ G^T & 0\end{pmatrix}\begin{pmatrix}A^TPl\\ 0\end{pmatrix} \qquad ..(8.15)$$

where k is a vector of Lagrange multipliers

(Ashkenazi (1976), Fraser (1982a))

The solution is conceptually simple as it merely involves the bordering of the singular normal equation coefficient matrix with the constraint matrix G. Solution of the system of equations, as given by equations 3.47 and 3.48, is :

$$\hat{X} = Q_{\hat{X}} A^TPl \qquad ..(3.47)$$
$$Q_{\hat{X}} = (A^TPA + GG^T)^{-1} A^TPA (A^TPA + GG^T)^{-1} \qquad ..(3.48)$$

The inverses in this formulation are based upon the Cayley inverse, ie the matrix to be inverted is non-singular. In the processes of formulating the inner constraints solution the form of the constraint matrix, G, must be assessed. The constraint matrix, G, can be formed from the d linearly independent eigenvectors corresponding to the d zero eigenvalues of N, as previously stated. Alternatively Papo and Perelmuter (1982) give a solution for the constraint coefficient matrix as :

$$G = \begin{pmatrix}G_1\\ G_2\end{pmatrix} = \begin{pmatrix}G_1\\ I\end{pmatrix} \qquad ..(8.16)$$

where $G_1^T = (A_2^TA_1)\,(A_1^TA_1)^{-1}$

A_1 = design matrix of (u-d) parameters

A_2 = design matrix of the d parameters used to define the datum

This formulation obtains a minimum for the Euclidean Norm of the parameters and meets the constraint requirements of equation 3.46.

Where the parameters, X, include corrections to coordinates in three dimensional space there is an alternative, geometrically meaningful, approach to evaluating G. Numerous authors, including Granshaw (1980), Fraser (1982a), Papo and Perelmuter (1982) and Caspary (1987), have shown that a Helmert transformation matrix meets the requirements for a minimum Euclidean Norm of the parameters if applied as the constraint matrix, G, in equation 8.15. The geometrical significance of the Helmert transformation matrix can be assessed via three basic properties which state that the sum of the translations in each coordinate direction will be zero, the sum of the rotations about each coordinate axis will be zero and there will be no overall scale change. These properties of the Helmert transformation matrix mean that the matrix will provide results consistent with free network adjustment requirements. The rows of the Helmert transformation matrix relate to three origin translations, three small orientation rotations and a scale change.

The Helmert transformation matrix, for u points, is of the form :

$$\left(\begin{array}{ccc|c|ccc} 1 & 0 & 0 & \cdots & 1 & 0 & 0 \\ 0 & 1 & 0 & \cdots & 0 & 1 & 0 \\ 0 & 0 & 1 & \cdots & 0 & 0 & 1 \\ 0 & -Z_1 & Y_1 & \cdots & 0 & -Z_u & Y_u \\ Z_1 & 0 & -X_1 & \cdots & Z_u & 0 & -X_u \\ -Y_1 & X_1 & 0 & \cdots & -Y_u & X_u & 0 \\ X_1 & Y_1 & Z_1 & \cdots & X_u & Y_u & Z_u \end{array}\right) \Rightarrow \begin{array}{l} \text{X translation} \\ \text{Y translation} \\ \text{Z translation} \\ \text{X rotation} \\ \text{Y rotation} \\ \text{Z rotation} \\ \text{Scale} \end{array} \qquad ..(8.17)$$

where X_i, Y_i, Z_i are the approximate coordinates for the parameters

For close range photogrammetric applications it is meaningful to partition G into two components, which refer to the exterior orientation parameters and the object space coordinate parameters.

The constraint matrix then becomes :

$$G = \begin{pmatrix} G_{eo} \\ G_c \end{pmatrix}$$

where, for photograph i :

$$G^T_{eoi} = \begin{pmatrix} 1 & 0 & 0 & 0 & 0 & 0 \\ 0 & 1 & 0 & 0 & 0 & 0 \\ 0 & 0 & 1 & 0 & 0 & 0 \\ 0 & -Z_{Li} & Y_{Li} & 1 & 0 & 0 \\ Z_{Li} & 0 & -X_{Li} & 0 & 1 & 0 \\ -Y_{Li} & X_{Li} & 0 & 0 & 0 & 1 \\ X_{Li} & Y_{Li} & Z_{Li} & 0 & 0 & 0 \end{pmatrix} \quad ..(8.18a)$$

where X_L, Y_L, Z_L are the perspective centre coordinates for photograph i

and for object point j :

$$G^T_{cj} = \begin{pmatrix} 1 & 0 & 0 \\ 0 & 1 & 0 \\ 0 & 0 & 1 \\ 0 & -Z_j & Y_j \\ Z_j & 0 & -X_j \\ -Y_j & X_j & 0 \\ X_j & Y_j & Z_j \end{pmatrix} \quad ..(8.18b)$$

where X_j, Y_j, Z_j are the coordinates of object point j.

(Granshaw (1980), Fraser (1982a))

Hence the constraint equation coefficient matrix, in terms of the typical photogrammetric parameters of exterior orientation parameters, object space coordinates and additional parameters, becomes :

$$G^T = (G^T_{eo}, G^T_c, G^T_a) \quad ..(8.19)$$

where G^T_{eo}, G^T_c are defined by equation 8.18.

If the constraint matrix, G, is not a null matrix with respect to the three components in equation 8.19, then a free network solution will be based upon all approximate coordinates and hence upon all parameters and a minimum trace datum results. In close range photogrammetry, G^T_a is usually set to zero since the additional parameters, under minimal constraints, are invariant with respect to datum or constraint selection. Hence the G matrix takes the form :

$$G^T = (G^T_{eo}, G^T_c, 0) \quad ..(8.20)$$

This, therefore, constitutes a partial minimum trace datum where the free network conditions are applied to a subset of the parameters, namely the exterior orientation parameters and the object space coordinates.

The general solution of the system given by equation 8.15, based upon the constraints of equation 8.20, suffers from the same basic deficiency as the Moore-Penrose inverse solution. Such a deficiency relates to the fact that a minimum mean variance results for both exterior orientation parameters and object space parameters. The parameters of interest, in close range photogrammetric network design, are the object space coordinates. From equation 8.14, the mean variance of the object space coordinates is given by $\bar{\sigma}_c^2$ and, for the purposes of assessing photogrammetric network quality, this quantity should be a minimum. Several authors, including Papo and Perelmuter (1982) and Fraser (1982a), formulate the solution for a minimum mean variance of the object space coordinates. Such a solution utilizes a constraint coefficient matrix in the following form.

$$G^T = (0 , G^T_c , 0) \qquad ..(8.21)$$

Consequently a partial minimum trace datum results, with the free network conditions being applied only to the object space coordinates. If this form of the G matrix is utilized then the partial trace of the cofactor matrix, relating to object space coordinates, is minimized and the aim of achieving a minimum $\bar{\sigma}_c^2$ is realized.

In many cases an inner constraints solution may only be required for a chosen subset of the object space coordinates. For c object space points, a minimum mean variance may be required for c' of the points. To achieve such a solution G^T_c is partitioned into two components to reflect the 3c' parameters, for which ||X|| = minimum is required, and the 3(c-c') parameters, for which no minimum condition applies. Consequently, for m photographs and a additional parameters, the constraint matrix becomes :

$$G^T = \underset{(d\,,\,6m)}{(\ 0\ ,} \quad \underset{(d\,,\,3(c-c'))}{0\ \ ,} \quad \underset{(d\,,\,3c')}{G^T_{c'}\ ,} \quad \underset{(d\,,\,a)}{0\ )} \qquad ..(8.22)$$

A partial minimum trace datum results whereby the free network conditions apply only to a chosen subset of the object space coordinates. Note that 3c', the number of object space coordinates to which the free network conditions apply, must be greater than d, the datum deficiency of the network, otherwise the network will still be singular and hence solution will not be possible. Note also that estimates of all parameters, excluding the 3c'

object space coordinates to which the free network conditions apply, will be dependent upon the free network solution for the 3c' object space coordinates. Hence, while the mean variance $\bar{\sigma}_{c'}^2$ will be a minimum and therefore optimal, the remaining parameters will not have optimal variance estimates.

The technique for the inner constraints solution has been developed in section 3.5.2 in general terms. This involves the simultaneous solution of all parameters based upon the technique of constrained minima by Lagrange multipliers. An alternative solution is based upon the principle of linear dependence between parameters which define the datum and the remaining parameters. Such a solution is called the free network constraint elimination method (Papo and Perelmuter (1982)). The advantage of the technique is that it is conceptually simple and distinguishes clearly between dependent and independent parameters. Consequently, for implementation of free network solutions by photogrammetrists who are unfamiliar with advanced estimation techniques, the solution provides a mathematically simple solution which can be implemented easily and which can be clearly understood.

8.4.3 Free Network Constraint Elimination Method

The free network constraint elimination method is based upon the principle of eliminating dependent parameters from the solution and then carrying out a solution based upon the (u-d) estimable parameters which remain. The solution for the d dependent parameters is based upon the linear dependence properties of the two parameter sets, as given by equation 3.27, and can be written in the form :

$$X_{23} = G_{\bullet}^{T} X_{22}$$
$$\text{or} \qquad \text{..(3.27)}$$
$$G_{\bullet}^{T} X_{22} - X_{23} = 0$$

The system of equations, for the free network constraint elimination method, takes the form :

$$\begin{pmatrix} v \\ 0 \end{pmatrix} = \begin{pmatrix} A_1 & A_{21} & A_{22} & A_{23} \\ 0 & 0 & G_{\bullet}^{T} & -I \end{pmatrix} \begin{pmatrix} \hat{X}_1 \\ \hat{X}_{21} \\ \hat{X}_{22} \\ \hat{X}_{23} \end{pmatrix} - \begin{pmatrix} l \\ 0 \end{pmatrix} \qquad \text{..(8.23)}$$

where v = residuals

X_1 = the 6m exterior orientation parameters of m camera stations(X_{eo})

X_{21} = the 3(c-c') object space coordinates

$\begin{pmatrix} X_{22} \\ X_{23} \end{pmatrix}$ = the 3c' object space coordinates upon which the ||X|| = minimum condition is applied($X_{c'}$)

X_{22} = 3c'-d object space coordinates

X_{23} = the d object space coordinates used to define the datum

A_{ij} = the individual design matrices corresponding to the above parameter sets

c = number of object space points

c' = number of object space points to which the ||X|| = min condition applies

d = the number of datum defects

$G_\bullet^T$ = constraint coefficient matrix

Equation 8.23 does not account for any additional parameters which may be required in the solution. These parameters can be included, and a constraint matrix of the form of equation 8.22 applied, if required. In terms of equation 8.23, the constraint coefficient matrix G becomes:

$$G^T = (\underset{(d,6m)}{0} , \underset{(d,3(c-c'))}{0} , \underset{(d,(3c'-d))}{G^T_{22}} , \underset{(d,d)}{G^T_{23}}) \qquad ..(8.24)$$

Note that G^T_{23}, which relates to the d selected datum definition elements, is by definition square and non-singular. Therefore $G_\bullet^T$ can be determined by :

$$G_\bullet^T = -(G^T_{23})^{-1}(G^T_{22}) \qquad ..(8.25)$$

The first step in the solution involves the transformation of the system from a biased system into an unbiased system, ie transformation of equation 8.23 into a system of full rank. Equation 8.23 becomes :

$$v = (A_1 , A_{21} , \bar{A}_{22}) \begin{pmatrix} \hat{X}_1 \\ \hat{X}_{21} \\ \hat{X}_{22} \end{pmatrix} - l \qquad ..(8.26)$$

where $\bar{A}_{22} = A_{22} + A_{23} G_\bullet^T$

Normal equations are established, and take the form :

$$\begin{pmatrix} A_1^T P A_1 & A_1^T P A_{21} & A_1^T P \bar{A}_{22} \\ A_{21}^T P A_1 & A_{21}^T P A_{21} & 0 \\ \bar{A}_{22}^T P A_1 & 0 & \bar{A}_{22}^T P \bar{A}_{22} \end{pmatrix} \begin{pmatrix} \hat{X}_1 \\ \hat{X}_{21} \\ \hat{X}_{22} \end{pmatrix} = \begin{pmatrix} A_1^T P l \\ A_{21}^T P l \\ \bar{A}_{22}^T P l \end{pmatrix} \qquad ..(8.27)$$

In a general form, equation 8.27 can be written as :

$$\begin{pmatrix} N_1 & N_{21} & N_{31} \\ N_{21}^T & N_2 & 0 \\ N_{31}^T & 0 & N_3 \end{pmatrix} \begin{pmatrix} \hat{X}_1 \\ \hat{X}_{21} \\ \hat{X}_{22} \end{pmatrix} = \begin{pmatrix} L_1 \\ L_2 \\ L_3 \end{pmatrix} \qquad ..(8.28)$$

N_1, N_{21}, N_{31} and N_3 are usually full matrices, while N_2 is a block diagonal matrix of block size 3 by 3. Solution for the parameters X_1,X_{21} and X_{22}, and their associated variance-covariance matrices can be solved by a number of methods, including the method given in section 4.3.2 for the total error propagation solution based upon correlated object points. Solution for the parameters $\hat{X}_{23}$, and the associated cofactor matrix $Q_{X_{23}}$, is from :

$$\begin{aligned} \hat{X}_{23} &= G_\bullet^T \hat{X}_{22} \\ Q_{X_{23}} &= G_\bullet^T Q_{X_{23}} G_\bullet \end{aligned} \qquad ..(8.29)$$

An advantage of this solution is that the computation time is reduced. The normal equation coefficient matrix which must be inverted, is reduced in size by d rows and d columns. Consequently, as the inversion process is the most time consuming component of the estimation process and as the time for inversion increases approximately as a cube of the size of the matrix to be inverted, the solution based upon the free network constraint elimination method is faster and computationally more efficient than alternative techniques. The solution given here can be extended to include observations which act as relative constraints on the datum. For such added observations, observation equations can be established, as given in Chapter 4, and added to the system of equations given by equation 8.23. The constraint matrix $G_\bullet^T$ will have the rows removed which correspond to the datum unknown defined by the observation. For example, for an observed distance, observation equations of the form of equation A.23 are added to equation 8.23. As such an equation defines network scale the sixth row of equation 8.17 is deleted and the matrix G^T is of reduced order. The solution for such formulations is given in Papo and Perelmuter (1982).

8.5 Datum Transformations

Under application of minimal constraints the inner geometry of a network is not destroyed and hence the shape of the network is not deformed. Consequently it is possible to transform adjustment results, namely the estimates of the parameters, $\hat{X}$, and the cofactor matrix of estimated parameters, $Q_{\hat{X}}$, from one datum to another, as long as both datums are minimally constrained datums.

The transformation is the similarity transformation, S-transformation, and is carried out with respect to the 7 (d) parameters of scale (1), rotation (3) and translation (3). Consider a transformation from datum i to datum k. The adjustment results for datum i are given by :

$\hat{X}^i$ = estimated parameters based on datum i
$Q_{\hat{X}}{}^i$ = cofactor matrix of the estimated parameters, datum i

The solution for these adjustment results is given in sections 3.5.1, for the general solution of constrained parameters, and 3.5.2, for the minimum mean variance solution associated with constrained parameters.

The properties of the S-transformation are :

$$NQ_{\hat{X}}{}^i = S^{iT} = (N + GG^T)^{-1} N$$

where N = the normal equation coefficient matrix
S^{iT} = transformation operator
G = the constraint equation coefficient matrix

and ..(8.30)

$NQ_{\hat{X}}N = N$ for any $Q_{\hat{X}}$

Therefore the solutions for datum k, in terms of the S-transformation, can be determined from :

$$S^i \hat{X}^k = \hat{X}^i$$

and ..(8.31)

$$S^i Q_{\hat{X}}{}^k S^{iT} = Q_{\hat{X}}{}^i$$

Datum transformations are applicable in close range photogrammetric network design. It is possible to transform adjustment results, based on a particular zero-variance computational base, into the corresponding results for

any other minimally constrained datum. For example, it is possible to transform from a zero-variance computational base solution to a free network solution by application of the S-transformation. Note that the solution involves the inversion of a u by u matrix in equation 8.30, and hence, for dense target arrays where the parameter sets will be large, readjustment of the system for a different datum is often more practical than applying an S-transformation. Despite this, for network design processes where solution based upon a variety of minimally constrained datums may be required, the S-transformation allows the solutions of the various datum definitions without having to readjust the system for each.

For minimally constrained datums, functions of constraint invariant quantities, such as residual and adjusted observation cofactor matrices, are also invariant with respect to application of the S-transformation. Consequently such functions do not need to be re-evaluated with each application of a datum transformation. S-transformations are covered in Niemeier (1987) and Caspary (1987).

8.6 Datum Definition Example Evaluations

For the purposes of assessing the various zero-order design solutions, simulated network designs are considered. In such evaluations a network, comprising the imaging geometry and target array definition of figure 8.2, is formulated.

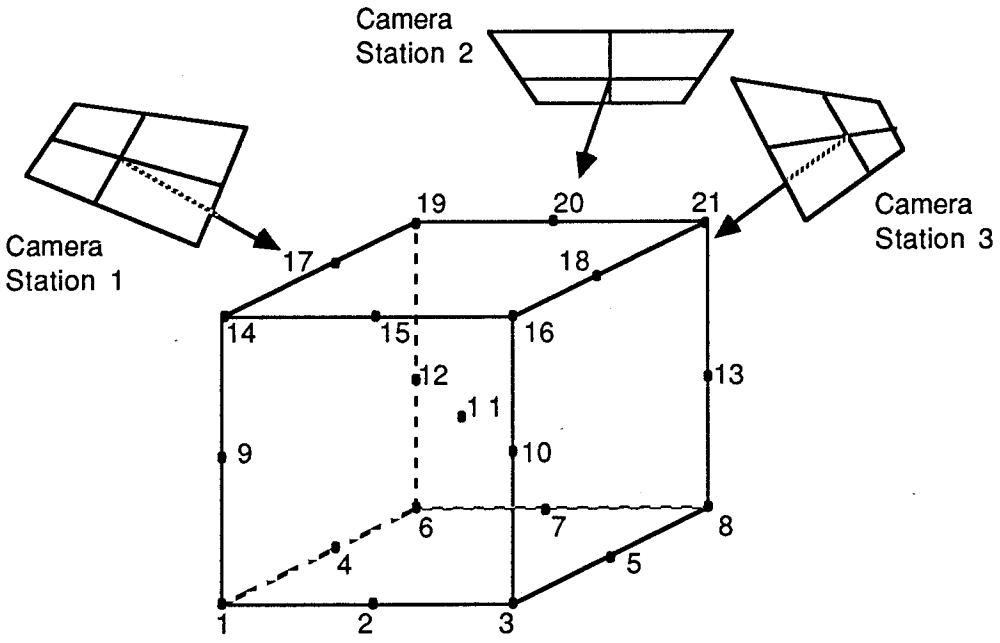

Figure 8.2 Network configuration for the datum definition evaluations

The target array comprises 21 object points covering a cube of side length 20 metres. The array is imaged by a three photograph convergent configuration which is symmetric about the centre point of the object. Each camera has an angle of 50° between the vertical axis and the camera optical axis, which corresponds to a convergence angle of 100° between camera optical axes. The camera used for the simulations is the Wild P32 which has a 64.1mm focal length and a 40,40mm x 20,40 mm format. The average image scale is 1:1000, ie a camera focal length of 64.1mm with the camera stations being approximately 60 metres from the object centroid. The estimated observational precision for each simulation is 3μm.

In assessing the results of the various zero-order design solutions, the absolute magnitude of the precision measures is not of primary significance. This is because the observation configuration employed is essentially arbitrary and a different absolute precision estimate would be achieved if the observation configuration was altered. The influence of a variety of datum definitions, relative to one another, is important to determine.

For the evaluation of the zero-order design problem, several datum configurations have been formulated. These include zero-variance computational base solutions, over-constrained parameter solutions, free network solutions based upon all or a chosen subset of the object points, and Bayesian solutions. The precision measures used to evaluate the resulting network quality include the mean standard error of the object points, the standard deviation range and the photogrammetric network strength factor. The results of the simulations are given in tables 8.2, 8.3, 8.4 and 8.5, and were generated by SIMPAC.

The notation used in tables 8.2 to 8.5 is as follows.

q = photogrammetric network strength factor
$\bar{\sigma}_c$ = mean standard error, of the c object points, in X,Y,Z
$\bar{\sigma}_{XY}$ = mean standard error, of the c object points, in X,Y
$\bar{\sigma}_Z$ = mean standard error, of the c object points, in Z
$\Delta\sigma_{XY}$ = standard deviation range in X,Y
$\Delta\sigma_Z$ = standard deviation range in Z
$\bar{\sigma}_{c'}$ = mean standard error, of the subset of c' object points, in X,Y,Z

Table 8.2 Zero-variance computational base solutions - ZOD results (ref : section 8.2)

ZERO-VARIANCE COMPUTATIONAL BASE SOLUTIONS								
No	Fixed XYZ	Fixed Z	q	$\bar{\sigma}_c$ mm	$\bar{\sigma}_{XY}$ mm	$\bar{\sigma}_Z$ mm	$\Delta\sigma_{XY}$ mm	$\Delta\sigma_Z$ mm
1	9, 13	10	1.0	2.59	2.60	2.57	3.04	3.73
2	1, 21	6	1.1	2.84	2.92	2.68	4.14	4.39
3	12, 9	5	1.2	3.06	3.17	2.83	4.50	3.89
4	1, 8	6	1.2	3.13	3.17	3.06	4.15	4.49
5	14,21	6	1.2	3.17	3.26	2.99	4.88	5.39
6	17,10	19	1.2	3.24	3.30	3.10	5.04	4.90
7	14,19	5	1.4	3.51	3.79	2.86	6.66	3.84
8	21,16	1	1.4	3.55	3.83	2.93	6.73	4.18
9	14,16	7	1.4	3.61	3.88	2.99	6.84	4.11
10	3, 19	7	1.5	4.02	4.08	3.91	6.34	6.70
11	11, 6	4	1.8	4.62	4.74	4.38	7.49	6.77
12	6, 5	7	2.5	6.41	6.24	6.74	10.87	11.77

Table 8.3 Over-constrained parameter solutions - ZOD results

OVER-CONSTRAINED PARAMETER SOLUTIONS									
No	Fixed XYZ	Fixed XY	Fixed Z	q	$\bar{\sigma}_c$ mm	$\bar{\sigma}_{XY}$ mm	$\bar{\sigma}_Z$ mm	$\Delta\sigma_{XY}$ mm	$\Delta\sigma_Z$ mm
13	14,19,3	-	-	1.4	3.76	3.76	3.76	2.89	2.71
14	14,8	6	16	1.5	3.77	3.78	3.75	2.83	2.77
15	1,21,6	-	-	1.5	3.80	3.82	3.77	2.88	2.56
16	9,13,10	-	-	1.6	4.08	3.92	4.38	2.34	3.57
17	19,16	-	3,1	1.8	4.79	4.99	4.35	4.61	4.82
18	1,6,11	-	-	1.9	4.93	4.85	5.08	4.42	4.05

Table 8.4 Bayesian solutions - ZOD results (ref : section 8.3.1)

BAYESIAN SOLUTIONS									
No	Prior parameter precision	Points XYZ	Points Z	q	$\bar{\sigma}_c$ mm	$\bar{\sigma}_{XY}$ mm	$\bar{\sigma}_Z$ mm	$\Delta\sigma_{XY}$ mm	$\Delta\sigma_Z$ mm
19	0.001mm	9,13	10	1.0	2.59	2.60	2.57	3.04	3.73
20	5mm	1,3,8,21 16,14 19, 6	-	1.2	3.09	3.10	3.07	0.72	0.86
21	10mm	all	all	1.5	3.73	3.74	3.72	1.23	1.44
22	3mm	9,13,10	-	1.6	4.08	3.92	4.38	2.34	3.57
23	3mm	14,2,10 16	-	1.7	4.14	4.15	4.13	3.31	3.52
24	3mm	1,6,11	-	1.9	4.93	4.85	5.08	4.42	4.05

Table 8.5 Free network (Inner Constraint) solutions - ZOD results (ref : section 8.4.3)

FREE NETWORK (INNER CONSTRAINT) SOLUTIONS									
No	Points for $\|\|\hat{X}\|\| = \min$	Datum points	q	$\bar{\sigma}_c$ mm	$\bar{\sigma}_{c'}$ mm	$\bar{\sigma}_{XY}$ mm	$\bar{\sigma}_Z$ mm	$\Delta\sigma_{XY}$ mm	$\Delta\sigma_Z$ mm
25	all	21,19,18	0.7	1.72	-	1.73	1.68	0.41	0.73
26	all	14,21,6	0.7	1.72	-	1.73	1.68	0.41	0.73
27	11,3,16 14,6,8 21,19,18	21,19,18	0.7	1.83	1.62	1.84	1.79	0.76	1.06
28	9,13,10	9,13,10	1.0	2.49	0.85	2.45	2.55	2.08	3.75

The results of the various datum definition solutions, given in tables 8.2 to 8.5, lead to a number of observations and conclusions.

- Changes in control configuration alter both object point coordinate standard errors as well as the object point coordinate precision homogeneity. Results show that precision estimates are biased and dependent upon datum constraint magnitude and configuration. Free

network (inner constraint) solutions yield a higher degree of object point precision and homogeneity than either zero-variance computational base solutions, over-constrained solutions or Bayesian solutions. Consequently free network evaluations offer an "optimal" solution to the zero-order design problem. For high precision close range photogrammetric applications, free network solutions are recommended for the solution of the datum problem (Fraser (1989)).

• Table 8.2 lists several zero-variance computational base configurations. The estimates of precision and homogeneity are dependent upon the configuration of the control and hence such estimates are datum-biased. The "best" configurations are achieved when the centre of the control point triangle is approximately at the target array centroid and when the control point triangle area is a maximum. Configurations 1 to 6 can be considered as acceptable datum definitions, while configurations 7 to 12 can be considered to be poor datum definitions as both precision and homogeneity measures are over-estimated. Of note is configuration 12, which has both a small triangle area and is a maximum distance from the target array centroid. This configuration can be considered as very poor and both precision and homogeneity estimates support this.

• Free network solutions yield the optimal object point coordinate precision and homogeneity estimates. Note that configurations 25 and 26, from table 8.5, give identical results. Although both are free network solutions, a different set of points has been used in each case for datum definition. Consequently, with respect to equation 8.23, any subset of points can be used to define the datum as long as the points chosen can resolve the network scale, translation and orientation. With reference to figure 8.2 , points 1, 2 and 3 could not be used to resolve the datum and hence would not be acceptable for use in the free network solution.

• Free network solutions can be applied to a chosen subset of the object point coordinates, for example in configuration 27 and 28 of table 8.5. If the object points included in the subset of minimum condition points are both geometrically "strong" and have good approximate coordinate estimates, then the resulting mean standard error , $\bar{\sigma}_{c'}$, will be smaller than for the case where a free network solution applies to all

object points. This is useful for applications where one or more object points are undesirable for datum definition. These points can then be removed from the minimum condition set and will not influence datum definition. Of note is configuration 28, where the set of points to which the minimum condition is applied is a minimum, ie three points. The resulting mean standard error of these points is optimal, however the precision estimates for the object points as a whole is larger than for full free network evaluations. Consequently, all points should be subject to the free network minimum condition unless point removal is based upon poor initial approximate values or poor geometry with respect to network configuration.

- Bayesian solutions offer a large amount of flexibility in varying datum definition. The only minimal constraint Bayesian solution results when seven parameters are effectively fixed by the prior weighting. Configuration 19, from table 8.4, is such a case. Note that this solution is equivalent to configuration 1, from table 8.2, where the same points define a zero-variance computational base. For configurations 20 and 21, from table 8.4, large numbers of object points with a loose prior weighting define the datum. These configurations do not yield high coordinate precision however they do give high precision homogeneity estimates. At this point it is pertinent to note that Bayesian solutions yield identical results to corresponding explicit constraint solutions. For example, configurations 1 and 19, 16 and 22, 18 and 24. Consequently, for applications where over-constrained solutions are required, Bayesian least squares offers a conceptually simple and computationally simple method of applying such constraints. For most close range photogrammetric applications, however, minimal constraints are desired and definition of a zero-variance computational base is computationally simpler and more efficient.

- Both over-constrained parameter solutions and Bayesian solutions require extra surveying work, over minimal constraint solutions, in order to establish object point control. It is worth noting therefore, that minimal constraint solutions offer the best datum definitions and hence provision of control, other than minimal control, is not necessary. This can be shown via three control configurations, namely 1, 16 and 22. In all cases the same points are used with different constraint forms applied. The

minimal constraint configuration yields the highest precision. With respect to precision homogeneity, however, the over constrained solutions usually offer improved coordinate precision homogeneity. Consequently, if this requirement is of importance in photogrammetric evaluations, an increase in control will improve precision homogeneity. As a comparison with the above three configurations, consider configuration 28. This configuration is a free network evaluation with the minimum condition being applied to the same points as in configurations 1,16 and 22. Precision estimates are better than the explicit constraint cases, however precision homogeneity is not as good. Note however that full free network solutions yield the "best" precision homogeneity estimates.

- As a final comment, the value of the precision measure, q, is assessed. The photogrammetric network strength factor would appear to be a coarse estimate of network quality. This estimate is dependent upon network geometry and hence for imaging scales such as the scale in this example, ie 1:1000, the factor is relatively invariant with change in network precision. As an initial estimate of network quality, ie "strong" networks yield a q value of between 0.5 and 1.5, the factor has merit.

From the comments and conclusions presented, the solution of the zero-order design problem is based upon free network solutions, for all or for a chosen subset of the object point coordinates, or zero-variance computational base solutions in the "best" control configurations.

Solutions to the zero-order, or datum, problem have been developed in detail. In close range photogrammetry, datum definition is usually carried out with respect to minimal constraints. Constraints are applied in either absolute or relative form and allow fixation of a reference coordinate system to which the estimated coordinates refer. The definition of a reference coordinate system is carried out by definition of an origin, orientation and scale of the coordinate system.

Parameter and variance estimates are dependent upon the type and magnitude of constraint applied. For network design applications it is

desirable to minimize the variance estimates to allow determination of network quality. Free network solutions are minimum mean variance solutions and hence are applicable for determination of network quality.

If minimal constraints are utilized, the inner geometry of the network will be maintained. Consequently the solution of parameter and variance estimates, relating to a particular datum, can be transformed to another datum via the S-transformation.

For close range photogrammetry the following solutions to the datum definition problem are recommended.

1. definition of an optimal zero-variance computational base, where optimal implies the "best" control configuration.
2. application of relative constraints, in the form of observations to parameters, with the remaining datum unknowns being defined by a "best" zero-variance computational base.
3. free network evaluations.
4. application of relative constraints with a free network solution to resolve the remaining datum unknowns.

Bayesian and ridge regression solutions, and over-constrained adjustments in general, are not recommended for close range photogrammetric datum definition. The solution to the datum problem in close range photogrammetry is usually achieved by free network (inner constraint) solutions. In cases where the point coordinate estimates are required with respect to an absolute datum, zero-variance computational base solutions utilizing optimal control configurations are used.

9. FIRST-ORDER DESIGN SOLUTIONS

The first-order design problem, with respect to close range photogrammetric network evaluation, is essentially a problem of configuration. In theory it involves the optimal positioning of object points and the optimal design of an observation plan and imaging geometry. With respect to the indirect solution method, based upon trial and error simulations, optimal configurations, and therefore optimal first-order design solutions, are not achieved. Solution of the first- order design problem is such that results meet quality requirements as well as physical and practical requirements, but do not meet such criteria in an optimal or "best" manner.

With respect to the least squares mathematical model, the first-order design involves formulation of a design matrix, A, such that quality criteria, derived from the cofactor matrix of parameters, $Q_{\hat{x}}$, are met. In formulating the design matrix, assessment of all factors which affect the structure of the matrix must be carried out. The magnitude of these factors and the influence of change in these factors upon network configuration and network quality require investigation.

The factors influencing network configuration, and therefore first-order design, are listed in section 5.4. The primary factors are imaging geometry and the number and location of camera stations, however less significant factors are also evaluated. Prior to such evaluations the concept of configuration defect will be covered. The presence of a configuration defect implies a weak configuration, and consequently an unstable mathematical solution, and therefore must be detection and eliminated.

9.1 Configuration Defect

A configuration defect, like the datum defect, will cause an unstable solution to the least squares evaluation process. Unlike the datum defect, however, the configuration defect is not a consequence of improper mathematical modelling. A configuration defect is caused by a critical configuration in the network geometry. If such a defect exists then absolute estimates of the parameters cannot be resolved. The mathematical

consequence of this, with respect to least squares estimation, is that the normal equation coefficient matrix becomes singular, or near singular, and the solution becomes either unsolvable or unstable.

The concept of configuration defect is best explained by an example. Consider the case of a 20 metre cube, targeted on all corners and on the midpoint of all edges. An imaging geometry and configuration was established, as shown in figure 9.1, and an adjustment carried out using SIMPAC. Note that the configuration established is by no means desirable and is used for illustrative purposes only. The resulting solution is poor and is due to the presence of a configuration defect. Figure 9.2 shows a perspective view from SIMPAC. From this plot, in conjunction with the configuration of figure 9.1, it can be seen that points 3 and 19 and the two camera stations are nearly collinear. As there are only two camera stations, and one or more points lie on the line joining the two stations, then an absolute determination of the position of the points on the line is not possible. Consequently a configuration defect exists.

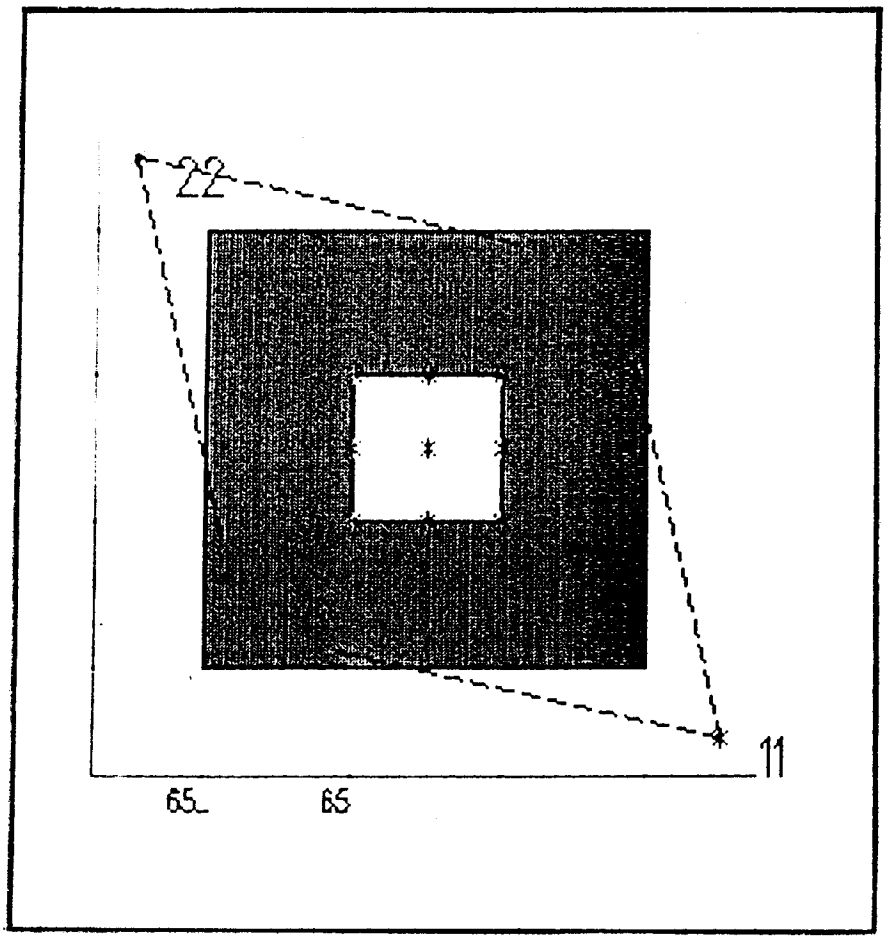

Figure 9.1 Network geometry for the configuration defect example

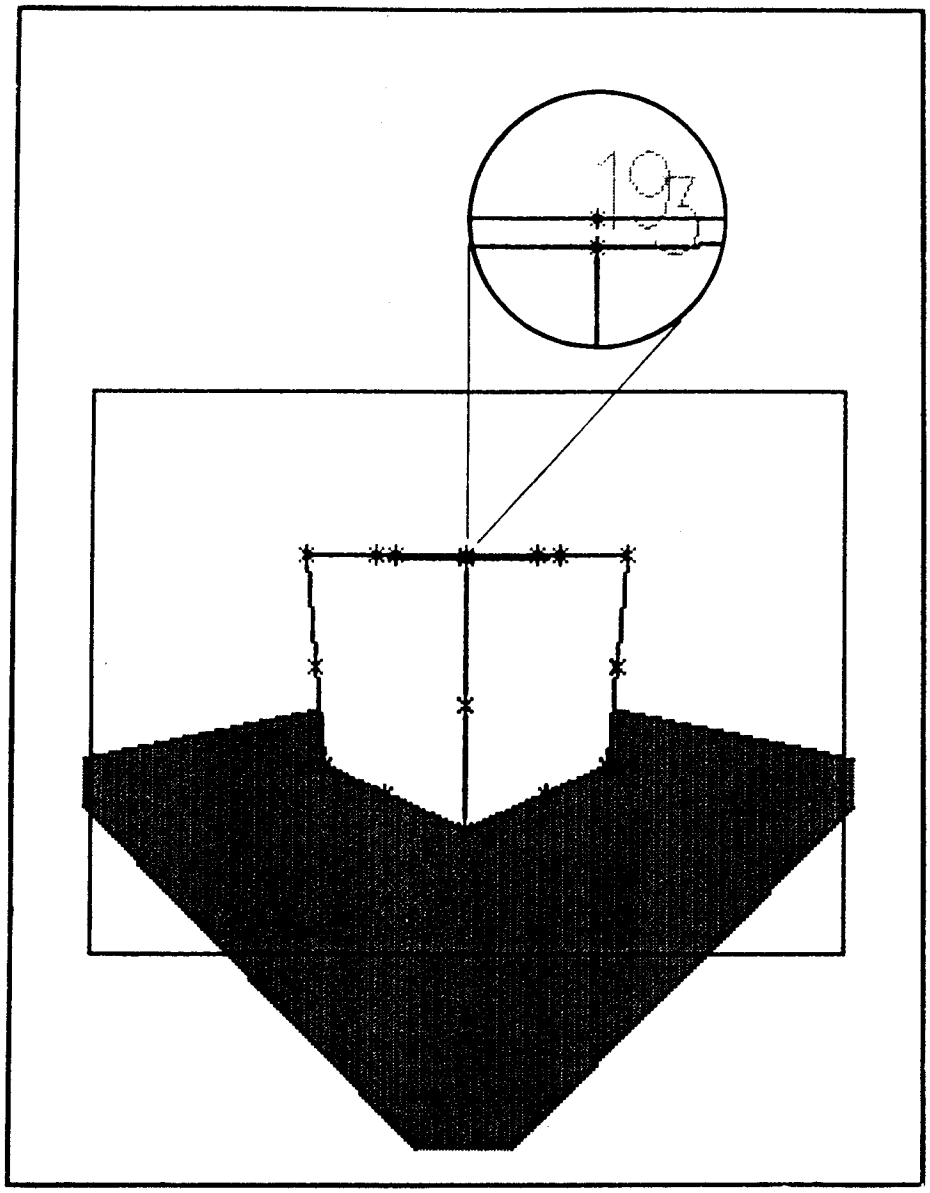

Figure 9.2 SIMPAC perspective view - Configuration defect of points 3 and 19

Table 9.1 shows the estimates of the parameters and estimates of the object point coordinate precision. Note that the precision, in terms of the standard deviations σ_{Xi}, σ_{Yi}, σ_{Zi}, of points 3 and 19, is of the order of ten times worse than the precision of the other points. For a similar configuration, altered only enough to remove the configuration defect, the precision of point coordinates is of the order of 5 - 10 mm, which is approximately a ten fold improvement over the configuration defect case. Therefore a configuration defect will influence not only those points directly affected by the defect but will degrade all estimates in the parameter set.

In close range photogrammetric applications, where up to ten exposure stations and several tens of object points are utilized for a typical network, critical configurations are not expected. However in designing networks,

especially if only two or three camera stations are involved, the designer should be aware of configuration defects and should be able to detect and remove such configurations if they exist.

Table 9.1 Results showing Influence of a configuration defect upon object point precision

Point	σ_{Xi} (mm)	σ_{Yi} (mm)	σ_{Zi} (mm)
1	19.0	19.0	3.2
2	22.4	21.2	31.4
3	**265.6**	**266.3**	**29.8**
4	32.6	34.9	22.8
5	19.3	20.6	28.9
6	26.4	24.6	22.7
7	37.8	35.3	22.9
8	24.5	10.4	25.5
9	8.8	22.6	25.5
10	30.4	38.4	24.9
11	25.8	28.1	3.1
12	25.3	25.2	20.5
13	10.7	22.7	24.0
14	32.0	37.1	25.1
15	23.2	23.2	18.7
16	23.2	23.2	18.7
17	20.7	8.9	24.0
18	36.2	30.2	25.1
19	**265.1**	**264.4**	**29.9**
20	38.6	31.9	24.9
21	22.0	23.9	22.7

9.2 First-Order Design Influencing Factors

The solution to the first-order design problem, for close range photogrammetric network analysis, is solved by an iterative or indirect solution method. As the solution is basically trial and error, it is necessary to evaluate those configuration factors which influence the network configuration and to determine the significance of such factors upon the precision of recovery of the object point coordinate parameters.

For close range photogrammetry, the primary factors influencing network configuration include :

1. imaging geometry.
2. number of camera stations.
3. base-distance ratio (for "normal" photography).
4. image scale, focal length and image format
5. number of object points.
6. object point clusters.
7. multiple exposures.
8. self-calibration parameters.

For the purposes of these evaluations, numerous networks will be simulated. These simulations will be with respect to the object of figure 9.3, which is a cube of 5 metre side length. The basic target configuration comprises 21 targets and are configured as shown in the figure. With respect to these evaluations it should be noted that the absolute magnitude of the various simulated precision estimates is not of importance. Varying camera types and configurations will be utilized and hence to evaluate results in terms of absolute precision estimates would lead to erroneous conclusions. It is important however, to evaluate the change in precision estimate for each particular configuration and to determine the influence of changing configuration upon object point coordinate precision estimates.

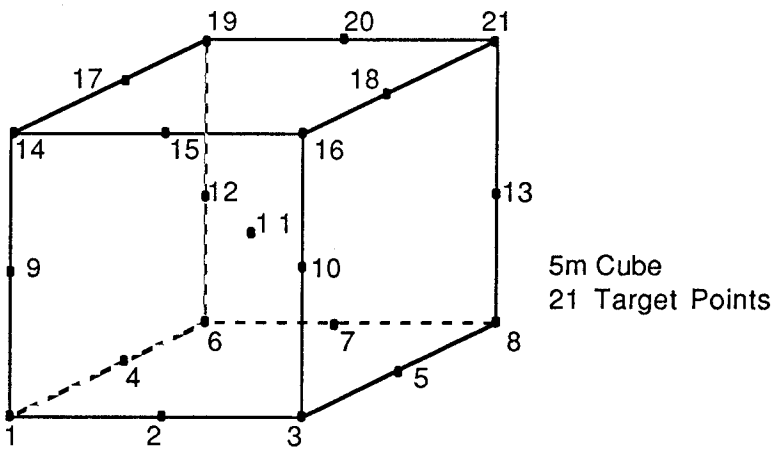

Figure 9.3 Object point array for first-order design analysis

In assessing the influence of varying network configuration upon object point coordinate precision estimates, several global precision measures will be utilized. These include :

q = photogrammetric network strength factor

$\bar{\sigma}_c$ = mean standard error, of the c object points, in X,Y,Z

$\bar{\sigma}_{XY}$ = mean standard error, of the c object points, in X,Y

$\bar{\sigma}_Z$ = mean standard error, of the c object points, in Z

$\Delta\sigma_{XY}$= standard deviation range in X,Y

$\Delta\sigma_Z$ = standard deviation range in Z

$\frac{D}{\bar{\sigma}_c}$ = proportional precision (ie the mean standard error as proportion of the object diameter, D)

9.2.1 Imaging Geometry

Imaging geometry is the central component of first-order design. The geometry of the camera stations with respect to the object being photographed will be the primary factor in determining the resulting object point coordinate precision. For the purposes of assessing the influence of imaging geometry upon the coordinate estimates the concept of a convergent multi-station photogrammetric network needs to be established, a typical configuration of which is shown in Figure 9.4.

The concept of convergence angle, which is fundamental to evaluation of imaging geometry, is shown in figure 9.4. Slama (ed) (1980);Ch 16 defines convergence angle as the angle subtended by the camera optical axis and the normal to the camera base. In the network simulations carried out in this chapter, all convergent networks will be symmetric configurations about the vertical axis through the centre point of the object target array. As a symmetric configuration will be utilized it is appropriate to utilize the convergence angle definition of Brown (1980) and Fraser (1984). This definition assumes a symmetric configuration with equal camera station tilts. If these conditions are met then the convergence angle becomes the angle subtended by the vertex of the cone which is defined by the symmetrically located camera stations and the centre of the object space target array (Brown (1980)), as shown in figure 9.4.

In most convergent networks, 100%, or nearly 100%, of the object can be seen in each exposure. This is not the case with "normal" stereo photography, where the photographs overlap and may not fully cover the object. For the purposes of network simulations covered in this section, it will be assumed that the exposures are optimized to allow maximum object coverage and that all object points are imaged on all photographs.

Prior to evaluation of the influence of imaging geometry on object point coordinate precision it should be noted that several authors, Brown (1980), Granshaw (1980), Fraser (1984), have indicated that a significant overall network precision improvement can be achieved by utilizing convergent rather than "normal" photography. This improvement is dependent upon including camera interior orientation parameters as additional unknowns in the estimation process (Fraser (1984)). In actual evaluation of convergent

networks a reduction in object point precision is usually evident over "normal" networks, due to the instability of the camera interior orientation.

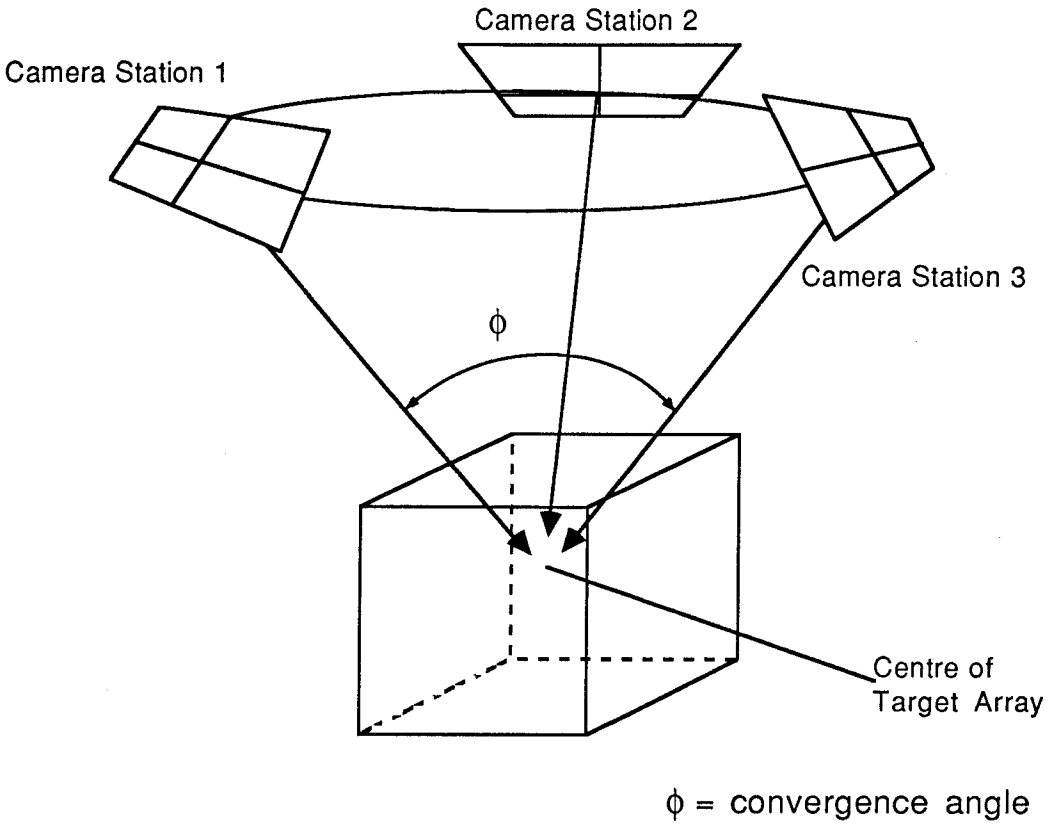

Figure 9.4 A typical multi-station, symmetric and convergent, close range photogrammetric imaging configuration

For the purposes of assessing the influence of image geometry upon object point coordinate precision, consider the imaging geometries depicted in figure 9.5. Note that these configurations are idealized and do not reflect the practical restrictions for many imaging geometries in practice. The camera used is the Jena UMK 10/1318, which has a 13cm x 18cm format and a 100mm focal length. The simulations were carried out by SIMPAC with image coordinate precision of 3μm and using a free network (inner constraints) solution.

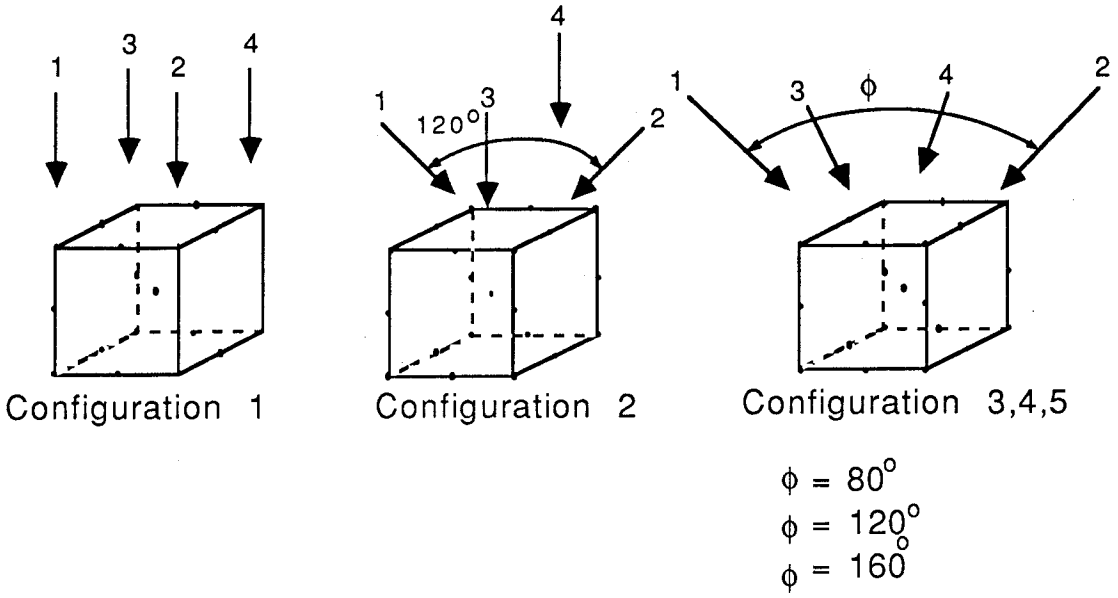

Figure 9.5 Imaging geometry configurations

The imaging geometries to be evaluated are all four photograph configurations and include :

1. Configuration 1 - a "normal" configuration, base/distance ratio = 0.7.
2. Configuration 2 - two "normal" photographs, base/distance ratio = 0.7, and two convergent photographs, $\phi = 120^{o}$.
3. Configuration 3 - convergent geometry, $\phi = 80^{o}$.
4. Configuration 4 - convergent geometry, $\phi = 120^{o}$.
5. Configuration 5 - convergent geometry, $\phi = 160^{o}$.

The simulation results are given in table 9.2.

Table 9.2 The influence of imaging geometry on object point precision

Configuration	q	$\bar{\sigma}_c$ mm	$\bar{\sigma}_{XY}$ mm	$\bar{\sigma}_Z$ mm	$\Delta\sigma_{XY}$ mm	$\Delta\sigma_Z$ mm	$\frac{D}{\bar{\sigma}_c}$
1	0.7	0.18	0.13	0.25	0.08	0.26	1 in 28,000
2	0.6	0.15	0.12	0.20	0.06	0.17	1 in 33,000
3	0.7	0.14	0.10	0.20	0.03	0.19	1 in 36,000
4	0.5	0.11	0.10	0.12	0.02	0.09	1 in 46,000
5	0.5	0.11	0.12	0.09	0.03	0.03	1 in 46,000

The influence of the image geometry on object point coordinate precision can be summarized as follows.

- The difference in precision for planimetry ($\bar{\sigma}_{XY}$) and height ($\bar{\sigma}_Z$), for "normal" configurations, is illustrated in the results of configuration 1. For this particular geometry, a 50% difference in recoverability between planimetric and height position is evident. Coordinate precision homogeneity, given by the standard error ranges $\Delta\sigma_{XY}$ and $\Delta\sigma_Z$, shows that the precision of X and Y coordinates is homogeneous for "normal" cases, however poor precision homogeneity is evident for the Z coordinate.

- The combination of "normal" and convergent geometries does not influence the planimetric precision to any large degree. In the example of configuration 2, an improvement of 0.01mm in the mean standard error for X and Y coordinates resulted over the "normal" case. Similarly the precision homogeneity did not improve to any significant degree. The recovery of the Z coordinate improved significantly however, with an improvement of approximately 20% in the mean standard error of the Z coordinate, resulting in an improvement in the overall mean standard error, $\bar{\sigma}_c$, of approximately 15%. Precision homogeneity of the Z coordinate also improved significantly, ie 35%. The improvement in the Z coordinate precision is directly proportional to changes in the convergence angle (Fraser (1984)).

- Of the five networks evaluated, the convergent network with convergence angle of 160° gave the most homogeneous results. The results for this configuration show that the range of standard errors is 0.03mm for both X,Y ($\Delta\sigma_{XY}$) and Z ($\Delta\sigma_Z$). As the convergence angle increases both $\Delta\sigma_{XY}$ and $\Delta\sigma_Z$ decrease, with this increase in precision homogeneity being more notable in the Z coordinate range. In the process of first-order design, for cases where precision homogeneity is of importance, these results show that homogeneous precision can be achieved by maximizing the convergence angle.

- Evaluation of the convergent configurations show that a convergence angle of 120° is the "best" configuration. This configuration

yields a near isotropic form, ie precision estimates are approximately equal in all three coordinate directions, and has high precision homogeneity. For applications where point recovery must be both isotropous and homogeneous, configurations with a 120° convergence angle provide the "best" solution.

The important information contained in table 9.2 is not the magnitude of the overall precision measures but the precision estimates which reflect recovery of planimetric, $\bar{\sigma}_{XY}$, and height, $\bar{\sigma}_Z$, position. Fraser (1984) states that in the initial stage of first-order design, a configuration should be formulated which meets precision homogeneity and isotropy requirements. Scaling of the overall precision can then be carried out via alternative first-order or second-order design processes. At this initial stage, ie where imaging geometry is specified, unless a configuration is formulated which meets the basic coordinate precision requirements in each of the three coordinate directions, then such criteria will not be met in the network design process.

9.2.2 Number of Camera Stations

The number of camera stations in a close range photogrammetric network is the configuration factor with importance only surpassed by imaging geometry (Brown (1980)). The number of camera stations employed will directly influence the resulting object point coordinate precision estimates and, in general, precision increases for an increasing number of camera stations and hence photographs. As well as improving network precision, an increase in the number of camera stations improves network reliability (Fraser (1984). With an increase in the number of camera stations the number of photographs increases, the network redundancy increases and hence, since network redundancy is directly related to the capability of the network to detect and compensate for gross and systematic errors, the network reliability is improved.

In network design, variations in the number of camera stations cannot, however, be divorced from imaging geometry. With an alteration in the number of camera stations the imaging geometry will change and the resulting spatial intersection geometry will change. In order to assess the relationship between imaging geometry, in the form of varying convergence angles, and the number of camera stations, consider figure 9.6. The data for the figure has

been generated from simulated networks using SIMPAC and the camera type and object are the same as for the imaging geometry examples.

It is important to stress that the absolute magnitude of the proportional precision values is not important. The relationship between varying imaging geometry and number of camera stations upon object point precision is of importance however. Figure 9.6 yields several important conclusions, which include the following.

- Object point precision increases with the number of camera stations. This influence is most evident in progressing from 2 to 3 camera stations and gradually decreases as the number of camera stations increases. For example, a precision improvement of approximately 30% is evident in increasing from 1 to 2 camera stations and drops to approximately 5 % in increasing from 7 to 8 camera stations. Hence for an optimal network there would be a number of camera stations adopted such that precision criteria were satisfied but also such that any expected precision improvement, with inclusion of an additional camera station, would not be warranted with respect to the cost associated with including the extra station.

- Although precision increases with added camera stations there is a function relating the magnitude of such increases to the convergence angle. As the convergence angle increases so the degree of precision improvement also increases.

- Figure 9.6 shows the variation of object point precision with varying convergence angle. It is clear that precision for the Z coordinate is poor at low convergence angles and increases steadily as convergence angle increases. Precision with respect to the X and Y coordinates starts low, increases to be a maximum at a convergence angle of approximately 120° and then falls again. The 120° maximum is due to the strength of the spatial intersection at such a convergence angle, with respect to both X and Y coordinate directions. As the convergence angle increases or decreases from 120°, either X or Y precision estimates decrease and hence the overall planimetric precision decreases. With respect to all coordinate directions it is necessary to select a convergence angle range which will satisfy precision criteria in all three coordinate directions. This range would appear to be from 70° to 150°.

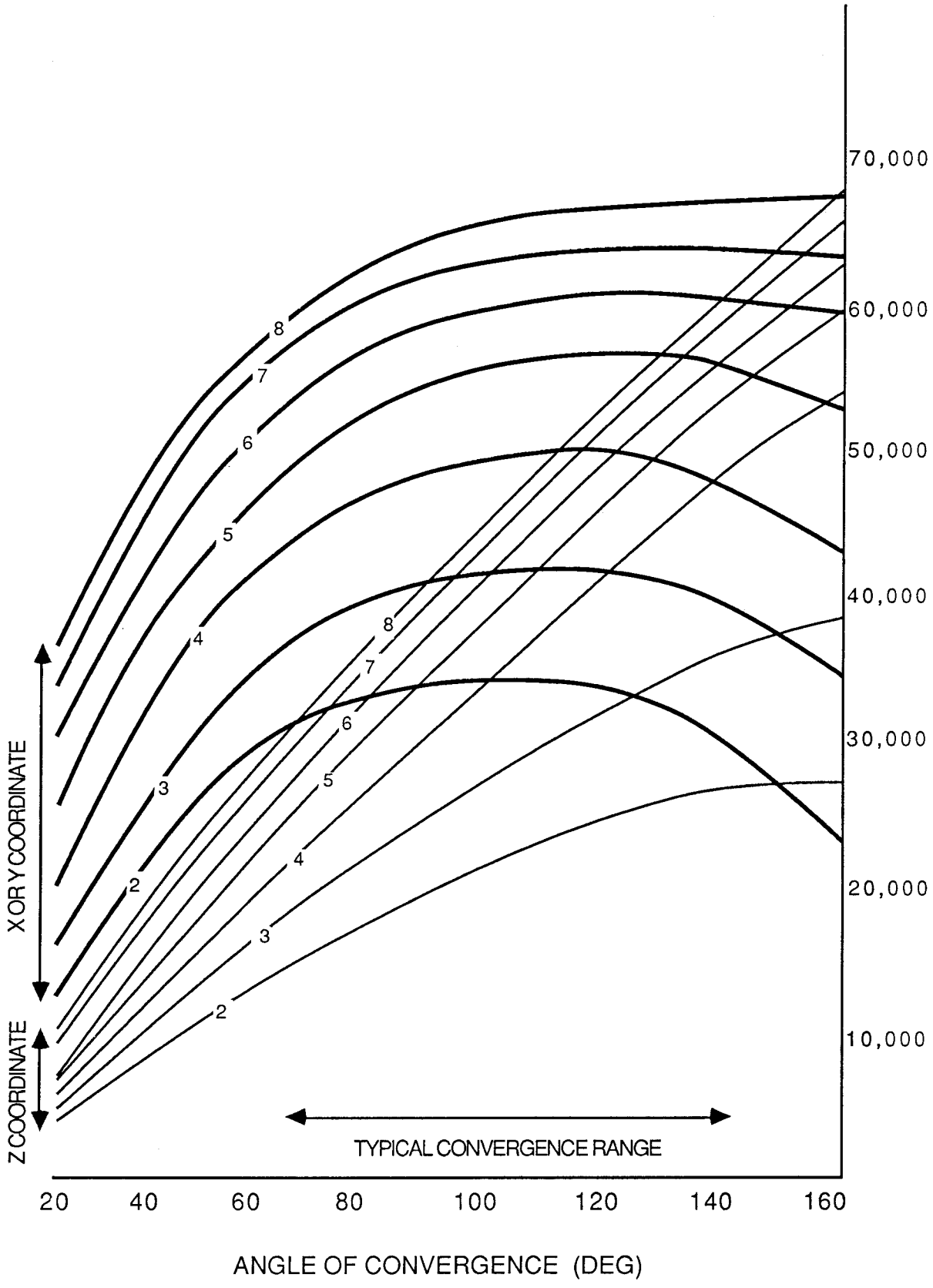

Figure 9.6 Relationship between imaging geometry and the number of camera stations

Table 9.3 has been formulated for the purposes of specifically determining the influence of the number of camera stations upon object point coordinate precision. The table shows results for a symmetric convergent configuration with the number of camera stations varying from 2 to 5. The convergence angle is 90° and the camera type and object point array are the same as for the previous examples. The proportional precision estimates are with respect to the mean standard error of the object points in X, Y and Z, $\bar{\sigma}_c$.

Table 9.3 The influence of the number of camera stations on object point precision

Number of Camera Stns	q	$\bar{\sigma}_c$ mm	$\bar{\sigma}_{XY}$ mm	$\bar{\sigma}_Z$ mm	$\Delta\sigma_{XY}$ mm	$\Delta\sigma_Z$ mm	$\frac{D}{\bar{\sigma}_c}$
2	0.9	0.21	0.19	0.25	0.13	0.20	1: 24,000
3	0.7	0.16	0.14	0.19	0.06	0.15	1: 31,000
4	0.6	0.13	0.12	0.16	0.03	0.13	1: 38,500
5	0.5	0.12	0.11	0.14	0.03	0.12	1: 42,000

Table 9.3 supports the conclusions developed with respect to analysis of figure 9.6, with the following additional conclusions.

- As the number of camera stations increases the mean standard error of the object point coordinates decreases. This precision improvement is not uniform and decreases as the number of camera stations increases. For example, in increasing from 2 to 3 camera stations a precision improvement of approximately 30% results, however in increasing from 4 to 5 camera stations this increase in precision drops to approximately 10%. Fraser (1984) develops a relationship between $\bar{\sigma}_c$ and the number of camera stations, m, with the precision improvement being given by $\sqrt{m}$. For example, in increasing from 2 to 3 camera stations the approximate precision improvement is 25%, while increasing from 4 to 5 camera stations the precision improvement drops to 10%. The practical results above agree with this relationship, however it should be noted that this relationship is approximate and will not hold for all imaging geometries.

- From the results of both figure 9.6 and table 9.3 it can be seen that a minimum of three camera stations is desirable to ensure both precision

homogeneity and precision estimates which reflect the strength of the image geometry. In other words, if a "strong" imaging geometry is utilized with only two camera stations then the resulting precision of the object space coordinates will not reflect the potential precision capabilities of the geometry.

- The results of table 9.3 clearly show that addition of camera stations is merely a scaling of the mean standard error of the object point coordinates. Hence, as previously stressed, it is important to design an imaging geometry which meets the form of the required precision criteria and then scale these estimates by adding camera stations or by alternative first-order or second-order design solutions.

9.2.3 Base / Distance Ratio

Base/distance ratio is a component of first-order design which is applicable only to "normal" photography. The concept of base/distance ratio is directly related to imaging geometry and hence several of the conclusions established here will be similar to those established for convergent configurations.

In "normal" photography, the ratio of the camera to object distance to the distance between the two, or more, camera stations will directly influence the resulting precision estimates. Figure 9.7 shows a typical "normal" configuration. Note that the direction of the camera optical axis need not be vertical and in most close range photogrammetric cases is horizontal. The requirement for "normal" geometry is that the camera optical axis, of two or more camera stations, is perpendicular to the base between the two subject camera stations, ie zero convergence angle.

The base/distance ratio will be evaluated to determine the relationship between this ratio and the mean standard error estimates of the object point coordinates. For such purposes consider the network configurations given in figure 9.8. Two basic configurations will be evaluated, one a four photograph "normal" configuration and the other a two photograph "normal" configuration. The camera type and object point array are the same as previous examples. The simulations were carried out by SIMPAC, with image observation of 3μm and solution was by a free network (inner constraints) adjustment. The

influence of changing base/distance ratio on both two and four photograph configurations will be assessed via the evaluation results of table 9.4.

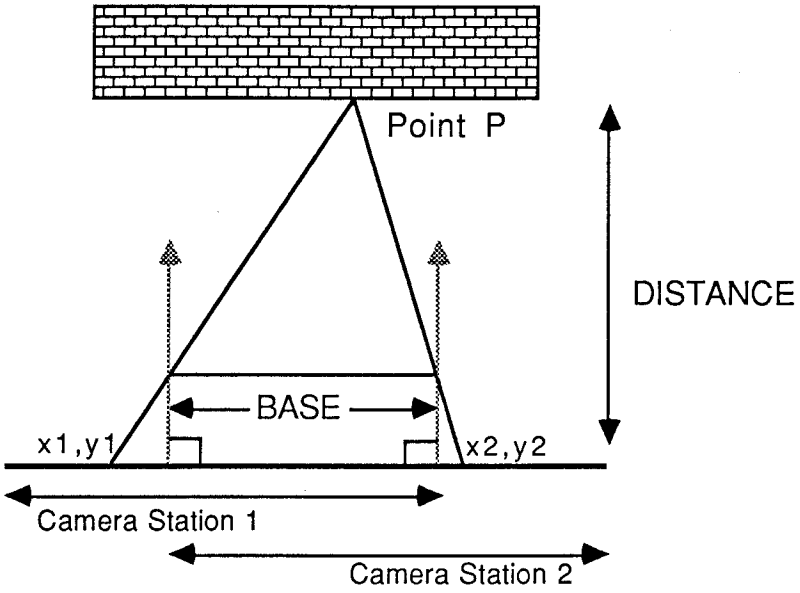

Figure 9.7 The "normal" case of close range photogrammetry

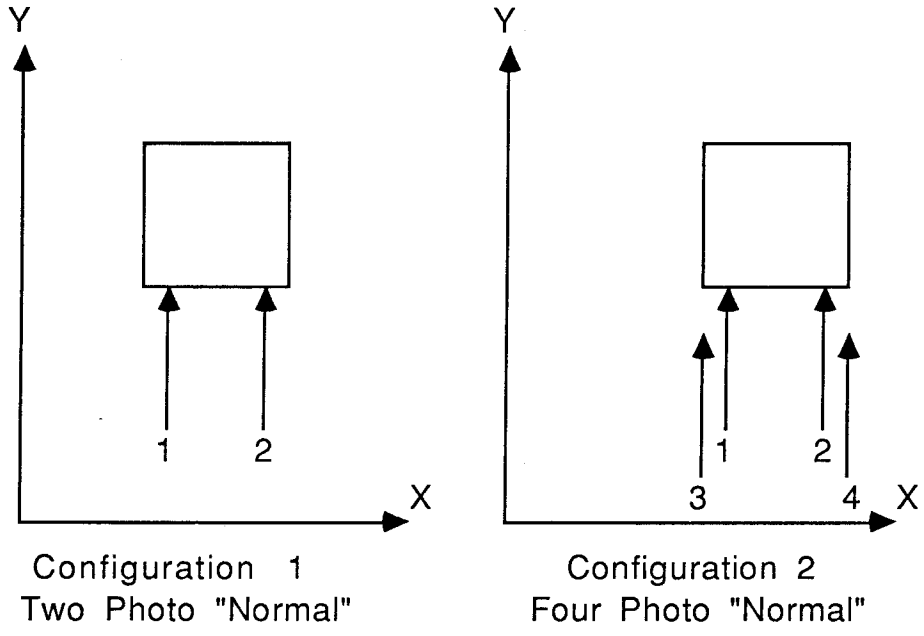

Figure 9.8 "Normal" geometry configurations

Table 9.4 The influence of base / distance ratio of "normal" photography on object point precision

Configuration	B/D Ratio	q	$\bar{\sigma}_c$ mm	$\bar{\sigma}_{XY}$ mm	$\bar{\sigma}_Z$ mm	$\Delta\sigma_{XY}$ mm	$\Delta\sigma_Z$ mm	$\frac{D}{\bar{\sigma}_c}$
1	0.5	3.3	0.72	0.83	0.41	1.47	0.36	1 in 7,000
	0.7	2.9	0.64	0.56	0.33	1.14	0.31	1 in 8,000
	0.9	2.6	0.45	0.51	0.28	0.91	0.28	1 in 11,000
2	0.5	1.6	0.36	0.42	0.21	0.70	0.17	1 in 14,000
	0.7	1.4	0.28	0.32	0.17	0.55	0.15	1 in 18,000
	0.9	1.3	0.23	0.26	0.15	0.44	0.14	1 in 22,000

It has been established (Hottier (1976), Fraser (1984)) that increasing base/distance ratio in "normal" photography both increases object point precision and improves network reliability. The results of table 9.4 support this view. The following conclusions and observations can be made.

- As the base/distance ratio is increased, in both two photograph and four photograph configurations, a corresponding increase in object point precision is achieved. In increasing the base/distance ratio from 0.5 to 0.9 an increase in object point precision of approximately 50% occurs in both four and two photograph configurations. The precision improvement is not linear as the base/distance ratio increases. The object point coordinate precision is better in directions which are perpendicular to the camera optical axis.

- The "normal" configuration influences object point precision homogeneity as well as object point precision. The results in table 9.4 show that approximately 30% difference in precision homogeneity exists between planimetric and height precision, with the better homogeneity being in directions perpendicular to the camera optical axis.

- The network strength factor, q, shows that all the above configurations in fact are poor or undesirable configurations. For typical "strong" close range photogrammetric networks a value of q is expected between 0.5 and 1.5 (Fraser (1982a)). Conflicting with this observation is the "normal" configuration of table 9.2. Here a base/distance ratio of 0.7 was employed and the resulting network strength factor was 0.7, in

fact quite an acceptable network. Distinction must therefore be made between vertical "normal" and horizontal "normal" configurations. Vertical configurations will yield good planimetric position with degraded height position, while horizontal configurations will yield good height position but poor planimetric position with respect to one of the horizontal directions, depending on the direction of the camera optical axis.

- As the base/distance ratio is increased it becomes increasingly difficult to maintain coverage of the object and therefore a practical restriction exists as to the extent to which the base/distance ratio can be increased yet still maintain object coverage. Increasing base/distance ratio is, however, one of the few methods of improving object point precision in "normal" photogrammetric configurations.

Initial selection of an appropriate base, as a function of camera to object distance, has been investigated by Slama (ed) (1980);Ch 16. For the configuration of figure 9.7 an approximate base length can be computed.

$$\frac{D_{max}}{20} < B < \frac{D_{min}}{5} \qquad ..(9.1)$$

where D_{max} = maximum photographic distance
D_{min} = minimum photographic distance
B = camera base

As a conclusion to base/distance ratio discussion, it should be noted that convergent configurations yield both higher object point precision and higher precision homogeneity in all three coordinate directions. Consequently, unless "normal" photography is to be employed due to either practical or physical limitations or because stereoscopic observations are to be carried out, then the implementation of convergent photography should be investigated.

9.2.4 Image Scale, Focal Length and Image Format

The selection of camera type for any particular close range photogrammetric mensuration procedure will directly influence object point precision. The influence of camera type in this section, however, does not cover the capabilities of the particular camera to produce a geometrically

correct image, devoid of any systematic errors. In other words it will be assumed that the image produced by the cameras in question are not influenced by film unflatness, lens distortion, film deformation etc. The investigations of camera selection in the first-order design process will be to determine the influence of varying camera geometrical properties upon the object point precision. Such geometrical properties include variations in focal length, image format and image scale.

Image Scale

An average image scale can be formulated as a function of focal length and average distance to the object as follows.

$$1 : S \qquad ..(9.2)$$

where $S = \frac{D_{av}}{f}$

S = average image scale number

D_{av} = average distance to the centroid of the object point array

f = focal length

The influence upon object point precision, in terms of varying image scale, shows a linear relationship between image scale and object point precision. Equation 6.29 gives an approximate relationship between image scale and object point precision.

$$\bar{\sigma}_c \approx q\, S\, \sigma \qquad ..(6.29)$$

where $\bar{\sigma}_c$ = mean standard error of the object point coordinates

q = network strength factor

S = average image scale number

σ = image coordinate observation precision

Equation 6.29 shows that changes in the average image scale number will have a direct linear influence upon object point precision. Changes in image scale will, however, alter imaging geometry and hence the relationship of equation 6.29 is not rigorous. However for most network design applications the equation yields sufficient accuracy.

Evaluation of equation 6.29 shows that a decrease in the average image scale number will result in a proportional increase in object point precision. Based on the assumption that the object is to be fully covered by the image format, variations in image scale are not possible unless focal length or image format can be varied. Consequently, in assessing the influence of variations in image scale upon object point precision, it is necessary to determine the influence of variations in focal length and image format upon precision estimates.

Focal Length

Equation 9.2 gives the influence of focal length upon image scale, and hence via equation 6.29, upon object point precision. Analysis of focal length variations is, however, not as simple as this. As the focal length is varied it becomes necessary to vary the object to camera distance as well in order to maintain a full image format coverage of the object. When changing focal length it becomes necessary to change the object to camera distance in order to maintain average image scale. Note that only the average scale is maintained because when the focal length is decreased, the camera has a wider angle of coverage and the object to camera distance can be reduced. Consequently greater variations in image scale for individual points will result, despite maintaining the average image scale. Therefore, although the average image scale is maintained, the overall object point precision will decrease due to the greater variation in the image scale for the individual object points.

For the purposes of assessing the influence of focal length variations upon object point precision consider the following example. A four-photograph symmetric, convergent (ϕ=90°) imaging configuration is simulated. The simulation was carried out by SIMPAC using observational precision of 3μm and a free network (inner constraints) adjustment. The camera utilized was the Wild P31 metric camera with image format 10.2 x 12.7 cm. The above network was simulated using two focal length lenses, 100mm and 45mm, and the average image scale was maintained in both cases by varying the average object to camera distance. Also included are the results where focal length is changed but average image scale is not maintained. The results are given in table 9.5.

Table 9.5 The influence of focal length variations on object point precision

Focal Length	Average Image Scale	q	$\bar{\sigma}_c$ mm	$\bar{\sigma}_{XY}$ mm	$\bar{\sigma}_Z$ mm	$\Delta\sigma_{XY}$ mm	$\Delta\sigma_Z$ mm	$\frac{D}{\bar{\sigma}_c}$
100mm	1 : 100	0.5	0.15	0.14	0.17	0.03	0.13	1 in 33,000
45mm	1 : 100	0.6	0.21	0.19	0.24	0.07	0.26	1 in 24,000
45mm	1 : 190	0.6	0.34	0.31	0.39	0.07	0.28	1 in 15,000

From table 9.5 several interesting conclusions can be noted.

- Higher object point precision and precision homogeneity are achievable for longer focal length cameras. In the case where the average image scale has been maintained despite a focal length decrease, object point precision has decreased. This is due to the large variations in scale for the short focal length, wide angle lens (45mm). In increasing the camera focal length from 45mm to 100mm a 35% increase in overall object point precision has resulted. Brown (1980) reports similar precision improvement in increasing focal length from 135mm to 480mm for the CRC-1. Conclusions from these observations are that long focal length cameras are to be preferred over shorter focal length cameras. This is however dependent upon camera and lens availability and upon the physical restrictions for each specific application. As well as object point precision improvement, long focal length cameras have the added advantage of suppressing the influence of film unflatness on coordinate precision estimates (Fraser (1984)).

- With increased camera focal length, precision homogeneity increases. In increasing focal length from 45mm to 100mm the precision homogeneity improves almost 50%. Note however that homogeneity improvement does not result if only image scale is altered. For the case of the 45mm focal length camera the precision homogeneity exhibits negligible improvement when image scale is changed from 1:190 to 1:100. This is because increased focal length tends to create a more homogeneous geometry of multi-ray intersections, and consequently an improvement in precision homogeneity. However variations in average image scale do not significantly alter this geometry.

Image Format

The influence of image format on object point precision is not difficult to assess, as variations in image format require a corresponding variation in average image scale in order to maintain full format coverage of the object. Consequently image format influence upon object point precision can be addressed in terms of the influence of average image scale. A notable influence relates to the fact that most close range photogrammetric cameras have rectangular image formats . This format configuration has the limitation that only the square portion of the format can be utilized in cases where self-calibration adjustments are undertaken (Brown (1980)). In recovering camera interior orientation via self-calibration, it is recommended that orthogonal kappa rotations between exposures is employed (Fraser (1984)). Consequently the actual rectangular format is reduced to an effective square format, of dimension equal to the minimum rectangular dimension.

For the purposes of assessing the influence of image format on object point precision the configuration of the previous example is re-assessed. In these simulations four camera types are used, each with different focal lengths and image formats. The focal lengths vary from long, narrow angle(240mm) to short, wide angle (45mm) lenses. In all cases the object to camera distance is varied to ensure full coverage of the image format by the object. The results of the simulations are included in table 9.6.

Table 9.6 The influence of variations of focal length, image format and average image scale on object point precision

Camera Type	Focal Length mm	Image Format cmxcm	q	$\bar{\sigma}_c$ mm	$\bar{\sigma}_{XY}$ mm	$\bar{\sigma}_Z$ mm	$\Delta\sigma_{XY}$ mm	$\Delta\sigma_Z$ mm	$\frac{D}{\bar{\sigma}_c}$
Wild P32	45	6.5 x 9	0.5	0.22	0.21	0.24	0.05	0.18	1 in 23,000
Image Scale = 1 : 150									
Wild P31	100	10.2x12.7	0.5	0.15	0.14	0.17	0.03	0.13	1 in 33,000
Image Scale = 1 : 100									
UMK 10/1318	100	13 x 18	0.6	0.13	0.12	0.16	0.03	0.13	1 in 39,000
Image Scale = 1 : 80									
CRC-1	240	23 x 23	0.6	0.07	0.06	0.08	0.01	0.06	1 in 72,000
Image Scale = 1 : 40									

The results of table 9.6 enforce the conclusions presented previously. In general it can be concluded that object point precision, and to a lesser degree precision homogeneity, is improved with large image scale. The image scale is a function of both focal length and image format, hence large focal length cameras with large, rectangular image formats are recommended. Note however, that for the purposes of first-order network design, improvement of object point precision by altering focal length and image format depends upon availability of a range of close range photogrammetric cameras, to enable selection of a camera with focal length and image format which optimally meet precision requirements.

In specifying an image format in the first-order design simulations, it should be noted that the full image format should not be utilized. This is because the effect of systematic errors, such as lens distortion and film deformations, are usually greatest at the photograph edges. Consequently in the first-order design process the object coverage is defined such that the extremes of the photograph are not used.

9.2.5 Number of Object Points

The number of object points has little influence of the object point precision in standard adjustment procedures. Consequently, for networks which exhibit "strong" geometry, object point precision can be considered to be independent of the number of object points in the target array. To illustrate this, consider a four photograph symmetric,convergent configuration (ϕ=90°) of the object in figure 9.1. The camera utilized for the following simulations is the UMK 10/1318 with a 100mm focal length. The evaluations were carried out using SIMPAC with 3μm observational precision and a free network (inner constraints) solution. Four separate adjustments have been evaluated, with 10, 20, 30 and 40 object points in the target array. The results of the evaluation is given in table 9.7.

The results of table 9.7 clearly show that, for standard adjustments, object point precision and object point precision homogeneity, are essentially invariant with respect to the number of object points used. In increasing the number of object points from 10 to 40, the object point precision has improved only 0.01mm. Consequently the relative independence of object point precision and number of object points is illustrated. This characteristic can be

utilized to advantage in close range photogrammetric network design. For networks which are likely to require several hundred object points, network design and evaluation can be carried out using 20 to 40 well distributed, "typical", object points. This number of points will allow accurate assessment of network quality and will significantly reduce computation time (Fraser (1984)).

Table 9.7 The influence of the number of object points upon object point precision

Number of Points	q	$\bar{\sigma}_c$ mm	$\bar{\sigma}_{XY}$ mm	$\bar{\sigma}_Z$ mm	$\Delta\sigma_{XY}$ mm	$\Delta\sigma_Z$ mm	$\frac{D}{\bar{\sigma}_c}$
10	0.6	0.13	0.12	0.16	0.04	0.13	1 in 38,500
20	0.6	0.13	0.12	0.16	0.03	0.13	1 in 38,500
30	0.6	0.12	0.11	0.16	0.03	0.12	1 in 42,000
40	0.6	0.12	0.11	0.15	0.03	0.12	1 in 42,000

Although the number of object points does not influence object point precision in standard bundle adjustments the same cannot be said for self-calibrating bundle adjustments. In self-calibration procedures both the density and distribution of the object points will affect object point precision (Fraser (1982a), Fraser (1984)). Systematic error models, included in a self-calibrating bundle adjustment, are usually expressed as functions of the image coordinates. The distribution and density of the image points will influence the strength of recovery of the systematic error model additional parameters. The density and distribution of image points is directly related to the density and location of object points. Therefore, if self-calibrating adjustment procedures are used, the number of object points and the distribution of these object points should be assessed in the first-order design phase. Such assessment is to ensure that the recovery of systematic error model additional parameters is facilitated and that object point coordinates are recovered to satisfactory precision. For self-calibration adjustments, a minimum of 30 to 40 well distributed object points should be incorporated in order to ensure both satisfactory recovery of additional parameters and satisfactory object point precision (Fraser (1989)).

9.2.6 Object Point Clusters

Amer (1979) and Hottier (1976) have introduced the concept of object point clusters for the purpose of improving network accuracy and reliability. Object point clusters are simply clusters of two to five object point targets, densely located around each single object point. For the purposes of improving network reliability this concept has merit, in that the overall network redundancy is increased and the possibility of detecting observation gross errors, or outliers, is greatly enhanced. For geometrically "strong" networks, however, this reason for introducing object point clusters is not relevant. In convergent, multi-station networks high network reliability is evident due to the basic geometric properties of the configuration. Consequently the evaluation of object point clusters reduces to an evaluation of the influence of the number of object points upon object point precision. As covered in section 9.2.5, the density and distribution of object points has only a minimal effect on precision estimates, for standard bundle adjustments. The use of object point clusters is therefore only considered in cases where network reliability is to be strengthened in geometrically poor configurations, as the influence of object point clusters on network precision is not significant.

At this point it is convenient to note that both the number of object points and the use of object point clusters are basically a third-order design problem (densification). Due to the independence of object point precision with respect to object point density and distribution in networks of "strong" geometry, the third-order design problem does not usually arise in close range photogrammetry. If object point densification is required, ie for self-calibration adjustment requirements or to improve network reliability, it is effectively solved at the first-order design phase.

9.2.7 Multiple Exposures

The influence of multiple exposures has been assessed, in Chapter 5, as a second-order design problem. The influence of multiple exposures is to increase the observational precision of the image coordinates and therefore to increase the resulting object point precision estimates.

There are two basic forms of the multiple exposure. The first form is where an additional photograph is acquired at exactly the same camera

station as the previous exposures. In this case the exterior orientation parameters for each exposure are the same and the result of the extra exposures is to scale the weight matrix of observations, P.

$$P' = k\frac{\sigma_o^2}{\sigma_i^2} I = kP \qquad ..(5.4)$$

where
- P = weight matrix of observations for one exposure
- P' = weight matrix of observations for k exposures
- k = number of exposures
- σ_o^2 = a priori variance factor
- σ_i = observational precision

As the influence of this form of multiple exposure is to scale the weight matrix of observations, the process is a second-order design (weight) problem.

The other form of the multiple exposure is when the exterior orientation parameters of the camera station at which the multiple exposures occur are not be maintained between exposures. In such cases an additional set of exterior orientation parameters must be introduced into the least squares mathematical model for each additional exposure. This process is a first-order design problem as the design matrix, A, of the least squares mathematical model is altered with each additional exposure.

In close range photogrammetric networks which already exhibit "strong" geometry, the use of multiple exposures is an easy and convenient method of enhancing object point precision. The common procedure is to take multiple exposures but to assume that a new camera station has been established and to therefore include a new set of exterior orientation parameters in the bundle adjustment (Fraser (1989)). For weak networks which exhibit poor network geometry and reliability, multiple exposures are not necessarily the best method of enhancing object point precision. It would be more applicable to introduce a new, geographically different, camera station in order to enhance the network geometry, and at the same time improve network reliability and object point precision. In most cases multiple exposures are therefore a first-order design problem, although utilization of multiple exposures in a second-order context is acceptable.

9.2.8 Self-Calibration Parameters

For self-calibrating adjustment techniques, the form of the systematic error model will influence the object point precision estimates. In minimally constrained adjustments, additional parameters, both those modelling systematic errors and interior orientation parameters, will be invariant with respect to constraint selection (Fraser (1982a)). With addition of such parameters into the least squares mathematical model, the precision of recovery of object point coordinates and coordinate precision estimates are dependent upon the error model of the systematic errors which has been utilized. This dependence is due to the degree of coupling between additional parameters, exterior orientation parameters and object point coordinates (Fraser (1982a)). Therefore it is necessary to consider the form and impact of the systematic error model upon object point estimates in the first-order design phase.

General rules are difficult to establish with respect to the influence of additional parameters upon precision estimates. Error models are very diverse and additional parameters may be sub-block invariant, photograph invariant or block invariant. Despite the diversity of available systematic error models, several general conclusions can be formulated with respect to first-order design procedures. The general process of self-calibration is covered in section 2.4.5 and the influence of self-calibration, with respect to first-order network design, will be evaluated on the basis of this analysis.

For systematic error models which exhibit high correlation between additional parameters, exterior orientation parameters and object points, object point precision is likely to degrade (Brown (1980), Fraser (1984)). This high correlation is introduced by over-parameterization (Brown (1980)) where additional parameters are either unrecoverable or not statistically significant. The procedures for ensuring over-parameterization does not occur are detailed in section 2.4.5, and in general terms involves the deletion of additional parameters from the error model which either exhibit high correlation or which do not differ significantly from zero. Such processes will ensure a stable model for the recovery of a priori unresolved systematic errors, as well as a compact model which contains no extraneous parameters.

In the first-order design process, networks are simulated in order to estimate achievable object point coordinate precision. In order to estimate the influence of self-calibration parameters upon object point precision, systematic

error models must be formulated and "typical" systematic errors added to the simulated image observations. Such a process allows a comparison of standard and self-calibration approaches, to estimate how well expected systematic errors are being resolved and how well the systematic error model is representing typical systematic errors This allows a realistic assessment of object point precision for self-calibrating bundle adjustments.

In order to ensure a strong recovery of additional parameters both the imaging geometry and the object point array require evaluation. The recovery of interior orientation parameters is dependent upon an object point array which is well distributed in all three coordinate directions (Fraser (1984)). The estimates of both systematic error model additional parameters and object point coordinates is improved if the density of the object point array is increased. Systematic error models are usually expressed as functions of the image coordinates. The distribution and density of the image points will influence the strength of recovery of the systematic error model additional parameters and, as the image point location is dependent upon object point location, the distribution and density of object points will influence resulting precision estimates. The recovery of interior orientation additional parameters in a self-calibrating adjustment is enhanced by introducing mutually orthogonal kappa rotations between each camera station (Fraser (1984)). For high precision close range photogrammetry the introduction of such rotations is necessary for all applications (Fraser (1989)). Orthogonal kappa rotations are required in order to minimize projective coupling between exterior orientation parameters and additional parameters and, in particular, to enable recovery of the principal point location.

In assessing the influence of self-calibration additional parameters upon object point precision it is important to carry out a network simulation based upon a self-calibration adjustment. It is of no use to design a network by a standard evaluation technique if a self-calibration technique is to be employed, as the simulated precision estimates from the standard adjustment will invariably over-estimate object point precision. As a final comment on the influence of self-calibration additional parameters on object point precision estimates, it should be noted that object point precision will not be degraded as long as all additional parameters are statistically significant (Fraser (1984)). Consequently assessment of the network via self-calibration adjustment simulations, and also assessing additional parameter recovery and coupling, is important in the first-order design phase.

9.3 Limiting Error Propagation - Application in Network Design

The concept of limiting error propagation (Brown (1980)) was introduced in section 4.3.3. The limiting error propagation solution is based on the assumption that the projective parameters are recovered perfectly in the adjustment process. Hence the process of limiting error propagation will express the limiting result to be expected from error free exterior orientation parameters. Such assumptions simplify the estimation procedure and the computation time for a given close range photogrammetric bundle adjustment is reduced. Note that the solution is not rigorous and, in general, will over-estimate precision estimates as the influence of all error sources has not been introduced into the solution.

The purpose of this section is to evaluate the applicability of limiting error propagation solutions in network design and evaluation. Although not a strict first-order design problem, the selection of computational method is dependent upon network configuration. For example, if a small object point array exists then a total error propagation solution poses no problems as the computational time is not large. If the object point array approaches several hundred however, then the trial and error simulation process becomes lengthy and alternative, faster, solutions are required. As a direct influence of network configuration upon computational method, the results of the limiting error propagation solution, for a variety of networks, will be assessed.

For the purposes of assessing the influence of limiting error propagation solutions upon object point precision estimates, five networks have been evaluated. These networks range from geometrically "strong", configurations 1, 2 and 3, through to networks which exhibit less than ideal geometric properties, configurations 4 and 5. A plan view of each configuration is given in figure 9.9. The convergence angle adopted in each configuration is 90°.

The assessment of limiting error propagation, as a method for estimating object point precision in the network design phase, has been carried out by three independent adjustment techniques. The adjustments carried out are the limiting error propagation (LEP) solution and the total error propagation (TEP) solution, based upon definition of a zero-variance computational base, and the total error propagation free network (IC) solution. It is proposed to

evaluate the limiting error solution with respect to several factors which include the influence of constraint configuration, the influence of imaging geometry and the relationship of the LEP solution to the TEP and IC solutions. For such purposes several SIMPAC simulations, the results of which are given in table 9.8, were carried out with respect to the object of figure 9.1. The camera utilized was the UMK 10/1318 and the observational precision was 3μm.

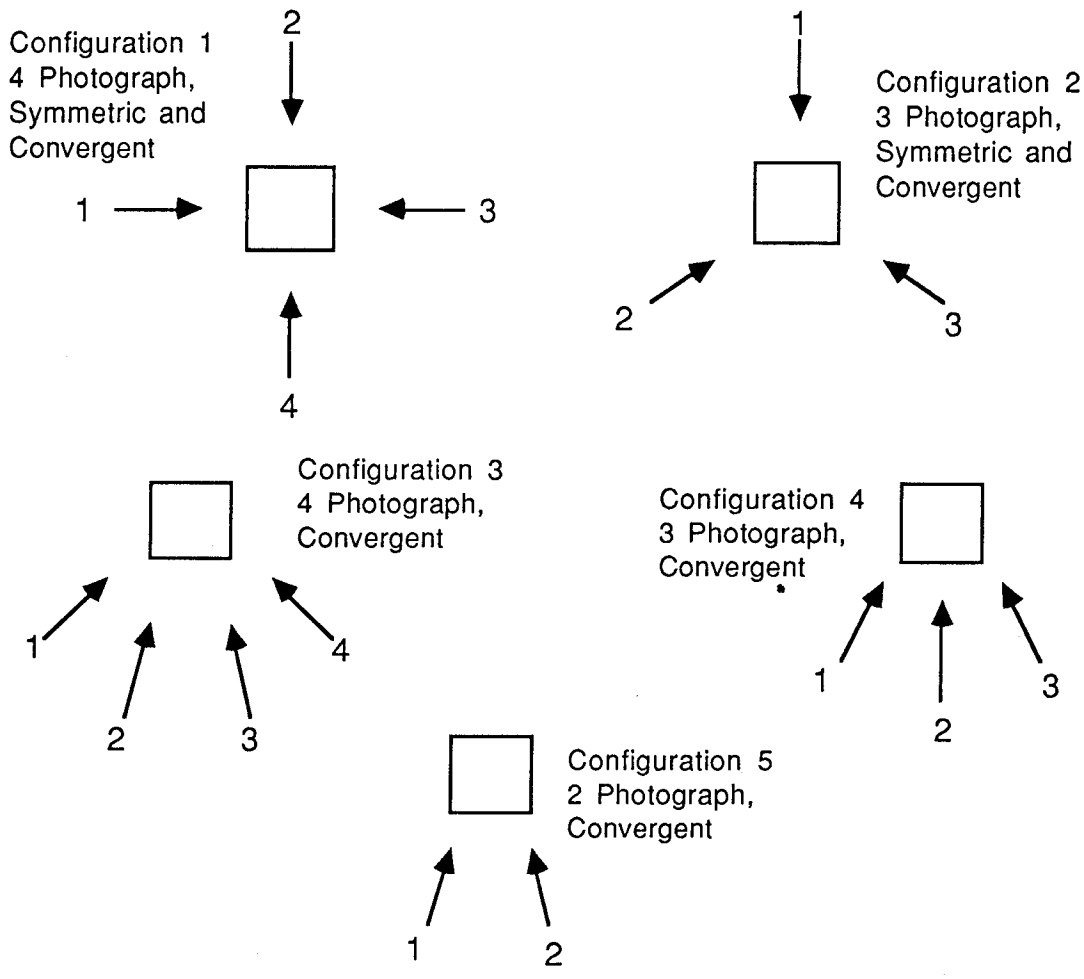

Figure 9.9 Imaging geometry for limiting error propagation (LEP) evaluation

Table 9.8 Comparison of LEP, TEP and free network solutions

No	Solution	Constraint	q	$\bar{\sigma}_c$ mm	$\bar{\sigma}_{XY}$ mm	$\bar{\sigma}_Z$ mm	$\Delta\sigma_{XY}$ mm	$\Delta\sigma_Z$ mm	$\frac{D}{\bar{\sigma}_c}$
1	LEP	3,19,21	0.5	0.13	0.11	0.16	0.14	0.23	1 in 38,500
	TEP	3,19,21	0.8	0.20	0.19	0.23	0.26	0.36	1 in 25,000
	IC	$x^Tx = min$	0.6	0.13	0.12	0.16	0.03	0.13	1 in 38,500
2	LEP	3,19,21	0.6	0.15	0.13	0.19	0.17	0.28	1 in 33,000
	TEP	3,19,21	1.0	0.24	0.22	0.27	0.31	0.42	1 in 21,000
	IC	$x^Tx = min$	0.7	0.16	0.14	0.19	0.06	0.15	1 in 31,000
3	LEP	3,19,21	0.7	0.17	0.15	0.21	0.29	0.34	1 in 29,500
	TEP	3,19,21	1.0	0.26	0.24	0.30	0.42	0.44	1 in 19,000
	IC	$x^Tx = min$	0.7	0.18	0.16	0.21	0.18	0.22	1 in 28,000
4	LEP	3,19,21	0.8	0.19	0.16	0.23	0.31	0.38	1 in 26,000
	TEP	3,19,21	1.2	0.29	0.26	0.33	0.45	0.50	1 in 17,000
	IC	$x^Tx = min$	0.8	0.20	0.17	0.24	0.19	0.24	1 in 25,000
5	LEP	3,19,21	1.6	0.41	0.37	0.48	0.83	0.83	1 in 12,000
	LEP	3,2,12	1.5	0.40	0.37	0.46	0.83	0.83	1 in 12,500
	TEP	3,19,21	2.3	0.62	0.57	0.70	1.19	1.13	1 in 8,000
	TEP	3,2,12	4.5	1.19	1.19	1.17	2.03	2.05	1 in 4,000
	IC	$x^Tx = min$	1.7	0.46	0.42	0.52	0.69	0.69	1 in 11,000

The results of table 9.8 give rise to several observations and comments regarding the applicability of the limiting error solution in first-order close range photogrammetric network design. These include :

- The comparison of the solutions based upon zero-variance computational base datums show that the LEP solution gives precision results which are over-estimated. The absolute magnitude of this over-estimation does not depend upon network configuration and is of the order of 50%, with respect to TEP solutions, for most configurations.

- Of interest is the assessment of configuration 5. Two solutions were carried out, one with respect to a good zero-variance computational base, points 3, 19, 21, and another with a poor zero-variance computational base, points 3, 2, 12. The TEP solution exhibits the expected difference between the good and poor datum solutions,

however the LEP solutions are effectively the same in both cases. This is not unexpected, however, as camera stations are effectively fixed in the LEP solution and therefore implicitly define the datum (Fraser (1989)). The introduction of further datum constraints is therefore unnecessary. In the case of the strong datum, precision was over-estimated by approximately 50% while in the case of the poor datum, precision was over-estimated by over 200%. It is therefore evident that the degree of conformance between TEP and LEP solutions is largely dependent upon the datum adopted.

- Of interest in table 9.8 is the degree of compatibility between free network solutions (inner constraints) and the LEP solution. In all cases, irrespective of network geometry and datum definition, the limiting error propagation solution approximates the free network precision estimates. For the "strong" networks this difference is only of the order of a few percent and increases to 5% to 10% for the weaker networks. Note that, although object point precision for the LEP case is consistent with the free network solution, precision homogeneity is not compatible and, in general, is larger than the free network homogeneity estimates.

From the above observations several conclusions can be made about the applicability of LEP in close range photogrammetric network design. The initial conclusion is that the LEP solution should never be used to approximate the TEP solution, especially in cases of an unfavourable datum definition. Use of LEP in such cases will lead to an over-estimated object point precision estimate, which will not be achieved when the network is implemented. A rigorous equality of LEP and TEP only occurs when the term $((N_{2j})^{-1}\bar{N}_j)\ Q_{\hat{X}_1}\ ((N_{2j})^{-1}\bar{N}_j)^T$, from equation 4.13, is equal to zero. Fraser (1987) states that this condition is never sufficiently realized and hence satisfactory equivalence of LEP and TEP solutions is never achieved.

The high degree of compatibility between the limiting error propagation solution and the free network solution indicate that the limiting error solution does have a place in first-order design. Fraser (1987) attempts to explain the observed compatibility between the LEP and free network solutions, but develops no concrete explanation for the compatibility. An important note in comparing LEP and free network solutions is that an LEP solution will invariably mask the effects of self-calibration over-parameterization (Fraser

(1987)). In such cases the LEP solution will not be influenced by the high correlations between additional parameters, exterior orientation parameters and object points and this high correlation will therefore not influence the recovery or precision of object point coordinates. Consequently the LEP solution will over-estimate the precision of object points and will not indicate the presence of self-calibration over-parameterization.

As the LEP solution is computationally faster than the full inner constraints and total error propagation solutions, Fraser (1987) advocates the use of LEP solutions in the initial network design phases instead of the rigorous free network solution. For example, Fraser (1987) claims that an LEP solution for 231 unknowns takes 21 seconds while a full solution takes approximately 12 minutes. The value of the LEP solution is therefore evident for initial trial and error establishment of the network configuration. Fraser (1987) also emphasizes, however, that a full (total error propagation) solution should be carried out after initial design to verify results, especially in weak networks where LEP and free network solutions may differ by up to 30%, and in self-calibrating adjustments where the effect of over-parameterization will not be detected.

The purpose of this chapter was to develop the methods available to enhance the object point precision estimates in the first-order design process. As the first-order design process in close range photogrammetric network design is based on an indirect solution and is achieved by trial and error simulations, it was necessary to examine those factors which influenced object point precision and to determine the effect of such factors upon network configuration and network quality. The primary factors assessed include imaging geometry and the number and location of camera stations.

Of minimal concern is the concept of configuration defect. Although introduced, such a defect is relatively easy to detect and is not common in convergent, multi-station configurations. Consequently the implications of this are not important in close range photogrammetric network design.

The limiting error propagation solution, of Chapter 4, was assessed in order to determine whether or not the solution gave representative precision

estimates for possible utilization in the design process. Although not representative of the total error propagation solution, the limiting error solution was found to represent the free network solution to a high degree. Consequently, in the network design process, initial precision estimation via the limiting error solution with a final check with the total error propagation solution, is recommended.

In the following chapter all the processes of network design theory will be linked together and illustrated via a practical example. This example will demonstrate the of the whole network design process for close range photogrammetry.

10. CASE STUDY - PORT KEMBLA COAL LOADER

A close range photogrammetric mensuration problem has been selected in order to illustrate the process of network design. In conjunction with this illustration, the example will allow verification of the theory of network design via simulation procedures and will demonstrate the typical problems encountered in close range photogrammetry.

The case study is that of the mensuration of the Port Kembla coal loader. The purpose of the study is not to demonstrate the high precision potential of close range photogrammetry, as this has been clearly demonstrated by Brown (1980), Granshaw (1980), Fraser (1982), (1984), (1985), (1988a) and (1988b). The case study clearly demonstrates both the problems which are often encountered in close range photogrammetry and the necessity for network design prior to data acquisition and evaluation.

10.1 Port Kembla Coal Loader Case History

A close range photogrammetric survey was commissioned in 1987 in order to determine the spatial location of the eight coal loader axles. The position of the axles was required to 10 millimetres in each coordinate direction, and with respect to the railway tracks upon which the coal loader moved. The railway tracks were therefore to act as the datum for the survey. Figure 10.1 shows a plan view of the Port Kembla coal loader, and clearly depicts the physical constraints on the site. The coal loader is surrounded on two sides by water, and the third side is restricted by the physical layout of the wharf. Figure 10.2 shows the coal loader, the target points used for the survey and again illustrates the site constraints. The coal loader itself is approximately 50 metres long and 10 metres wide.

A close range photogrammetric survey was carried out in early 1988. Due to the relatively moderate precision requirements for the task, network simulations were not undertaken and a network was implemented based upon "expert" opinion, such that it could be assumed that precision requirements could easily be met.

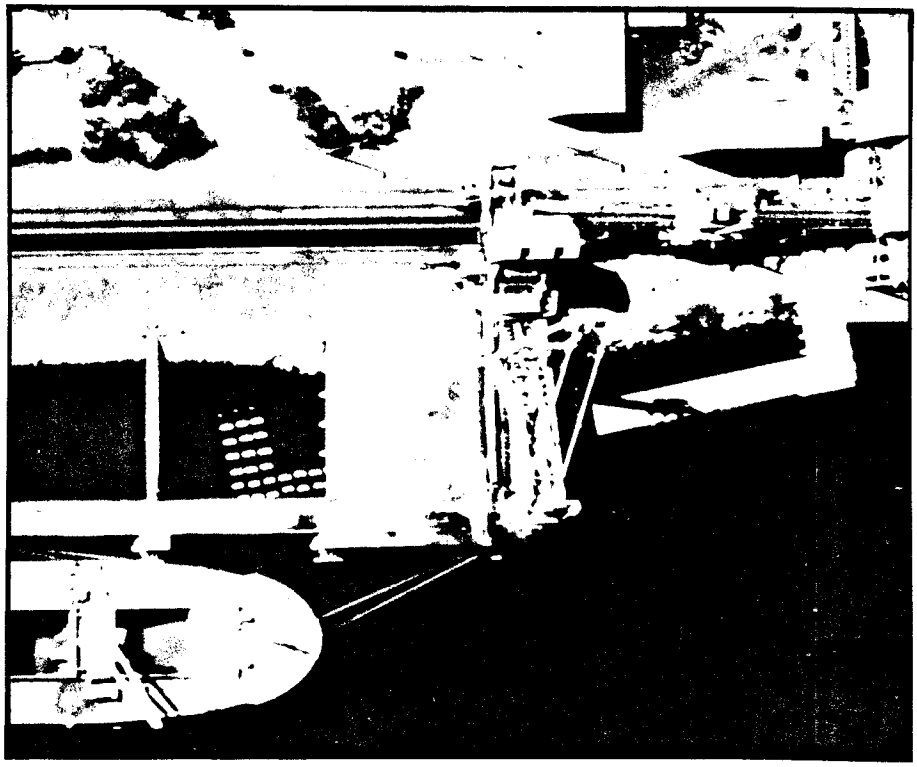

Figure 10.1 Aerial photograph of the Port Kembla coal loader

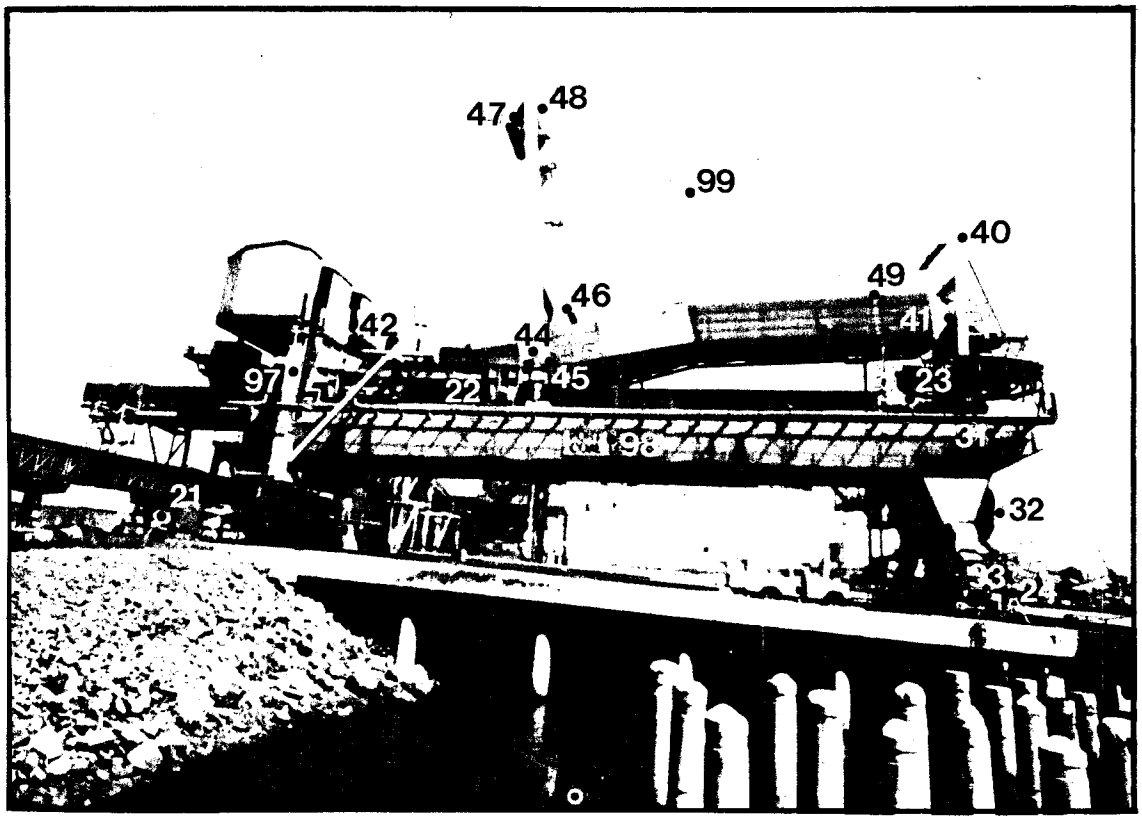

Figure 10.2 Photograph of the Port Kembla coal loader

The SIMPAC plan view, of Figure 10.3, shows the network adopted for this task. Five, essentially "normal", camera stations were situated on the wharf, such that a full coverage of the coal loader was possible from each station. Figure 10.2 is the photograph taken from camera station 44. With respect to this figure and the SIMPAC perspective view, of figure 10.4, note that the object point array does not optimally cover the image format. Consequently a relatively small average image scale, of 1 : 1000 results. This poor format coverage is due to the physical site restrictions in selecting camera locations.

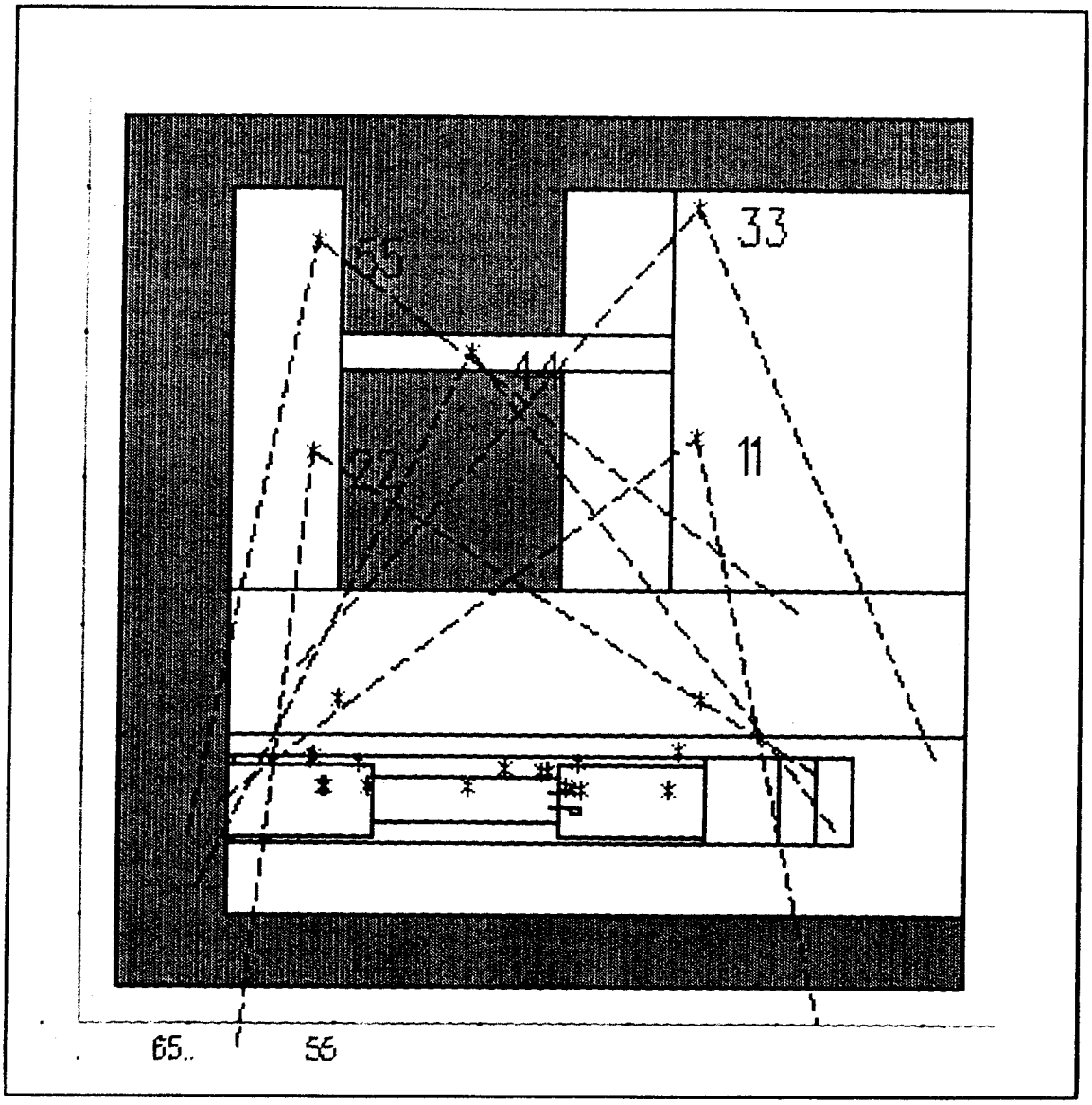

Figure 10.3 SIMPAC plan view - Network configuration for the initial survey

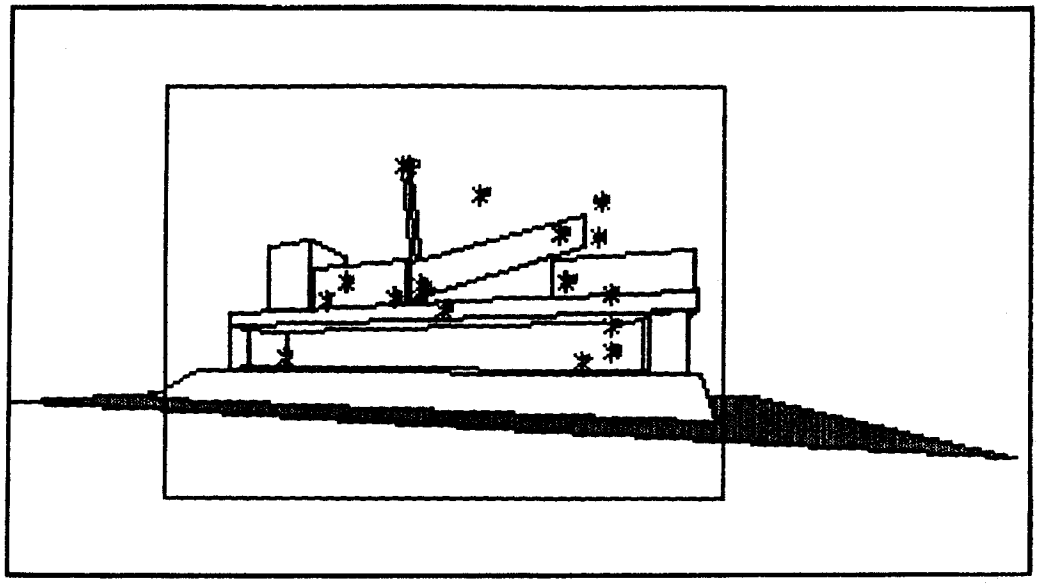

Figure 10.4 SIMPAC perspective view - Port Kembla coal loader

The axles, for which position is required, are the eight points 40, 41, 42, 44, 45, 47, 48 and 49 in figure 10.2. The points are essentially coplanar, ie within 2 metres of a vertical plane through the Y axis. Points 21, 22, 23, and 24 were introduced as control points and define the datum with respect to the coal loader railway tracks. The six additional points were introduced in order to strengthen the solution.

Acquisition and evaluation of the photography was carried out using the Wild P32 metric camera, focal length 64.1 millimetres, and the Kern DSR-11 analytical plotter for image coordinate measurement. The control points 21 to 24 provided an over-constrained least squares solution. Upon analysis of the results it was found that precision specifications had not been met for all points and with respect to the defined datum, the 10 millimetre precision requirement could not be met in all three coordinate directions. Precision estimates in the X and Z directions were approximately 6 and 8 millimetres respectively, both within specifications, however Y coordinate determination could not meet the 10 millimetre requirement and in some cases was nearly twice this value.

Although a network had been established which should have yielded the desired precision, the precision specifications were ultimately not met. In the following sections determination of the reasons for the poor solution from the initial network will be evaluated and amendments to the design proposed in order to achieve the required level of precision.

10.2 Verification of the Simulation Method

Prior to evaluating the Port Kembla coal loader problem it is pertinent to verify the methodology of network design via simulation procedures. As data has been made available from the actual mensuration of the coal loader it is a simple task to evaluate this data and to simulate an identical network with respect to datum and imaging configuration. Verification of the capability of determining network precision a priori, via network simulation, can then be assessed by comparing the precision estimates of the two networks. Both networks were evaluated using SIMPAC. In the "real" network image coordinates and control were those derived in the initial survey. Approximate camera exterior orientation and object point coordinates were determined in the initial adjustment procedure. In the simulated network, object point coordinates and camera exterior orientation parameters were slightly altered in order to illustrate that resulting object point precision estimates will accurately reflect the "real" case despite using only a representative network configuration and object point array. The results of the two evaluations is given in table 10.1. The precision measures used are given in Chapter 6.

Table 10.1 Comparison of "real" and simulated networks

CASE	q	$\bar{\sigma}_c$ mm	$\bar{\sigma}_{XY}$ mm	$\bar{\sigma}_Z$ mm	$\Delta\sigma_{XY}$ mm	$\Delta\sigma_Z$ mm
Real	0.7	3.91	4.26	3.10	3.83	2.51
Simulated	0.7	3.59	3.95	2.73	3.54	2.22

Evaluation of the results of table 10.1 indicate that simulated results are representative of "real" estimates. Simulated precision estimates are all higher than the actual estimates, possible reasons for which include the following.

- Simulated results are based upon a 5μm image observation precision. The least squares estimation results indicate that the "real" image observation precision is approximately 6μm. Consequently a degradation of object point precision estimates would result.

- Image observations were carried out using the Kern DSR-11 analytical plotter, with image observation precision specifications of the order 3 to 5 μm. The difference between simulated and "real" precision estimates is of the order of 0.32 millimetres on the object. At an average object to camera distance of 50 metres and with a focal length of 64.1 millimetres this corresponds to 0.4μm on the image. This difference is essentially negligible and undetectable in the analytical plotter observations.

- The estimation procedure used for both simulated and "real" networks was the standard bundle adjustment. No self-calibration was utilized and hence unresolved systematic errors in the "real" image coordinates could have degraded "real" precision estimates. The simulated network was not influenced by systematic errors and a diference between the precision estimates of the two networks would have therefore resulted.

From this analysis it can be seen that simulated network evaluations are indeed representative of actual network evaluations. The use of network simulation for close range photogrammetric network design allows an accurate a priori estimate of achievable precision from the subject network and ultimately design of a network which meets precision requirements.

10.3 Analysis of the Initial Network

The close range photogrammetric network for the mensuration of the Port Kembla coal loader was introduced in section 10.1. The purpose of this section is to evaluate the network and to determine why precision estimates were lower than expected and did not meet precision criteria. From this analysis a network will be formulated such that the problems evident here are removed and so that the new network will meet precision requirements.

The network to be evaluated, ie the "real" network implemented and observed in 1988, is depicted in the SIMPAC plot, of figure 10.3. For the purposes of determining potential problem areas, several aspects of the network configuration, or first-order design, will be evaluated and the implications of these aspects upon precision estimates will be determined.

- The network imaging geometry is essentially a "normal" configuration, with the camera optical axis being virtually parallel to the ground coordinate system Y axis in all cases. Precision estimates from this configuration would be expected to be relatively poor with respect to the Y coordinate. Precision estimates would not be homogeneous for this configuration as the X and Z coordinates would be resolved to a higher degree of precision than the Y coordinate. In order to improve the recovery of the Y coordinate, introduction of convergent photography is recommended. This will increase both the coordinate precision estimates and the coordinate precision homogeneity.

- The configuration, defined by figure 10.3, does not optimally utilize the image format. This is evident from figures 10.2 and the SIMPAC plot, of figure 10.4. The target array coverage is approximately half the full format and this leads to a less than optimal image scale. This reduction in effective image scale reduces the potential precision capability of the network. Although the image format coverage, and consequently image scale, is dictated to a large degree by physical site constraints, this is an area to be addressed in future network design of the coal loader.

- The object point array utilized is a weakness in the network design. Two problems with the density and distribution of the array are evident. The first problem is that all object points are within approximately 10 metres of being coplanar with all points essentially being in the vertical plane through the Y axis. With the X and Z distributions being approximately 50 metres and 40 metres respectively, this poses a problem for resolution of Y coordinates if the datum is defined on the outer edge object point array. In the subject network, the datum was defined with respect to four points in the lower half of the target array. Consequently the Y coordinates for the points furthermost from the control, or datum, points are severely degraded. In order to strengthen the solution, with respect to recovery of the object point Y coordinate, object points should be added to the network which have a large range in

the Y direction, ie approximately the same as the range in X and Z directions. As the precision of object point determination degrades as the distance from the control increases, the use of control points which cover the whole object point array will improve the precision of points at the top of the coal loader.

The second weakness in the object point array relates to the density of the object points for self-calibration purposes. For adequate recovery of additional parameters, a minimum of 30 well distributed object points is required. In the subject object point array only 18 points are evident, and the array should therefore be augmented by additional points to allow efficient recovery of additional parameters and object points.

The principal causes of poor object point precision, with respect to the network configuration, were the imaging geometry and the distribution of the object points. In order to fully assess the network, however, the zero-order design of the initial network should be evaluated. In order to evaluate the datum definition for the network, several simulations have been carried out, each with a different datum. The influence of the over-constrained datum adopted in the "real" case will be compared to alternative datum solutions. As the precision criterion only applies to a subset of the object point array, the table of simulation results will include both overall precision estimates and estimates with respect to the axle points only. The results are given in table 10.2 and table 10.3.

Table 10.2 Simulation results - all object points

DATUM	q	$\bar{\sigma}_c$ mm	$\bar{\sigma}_{XY}$ mm	$\bar{\sigma}_Z$ mm	$\Delta\sigma_{XY}$ mm	$\Delta\sigma_Z$ mm	Max Point
Free Network (all)	0.7	3.59	3.95	2.73	3.54	2.22	-
Free Network (pts 21,22,23,24)	0.9	5.00	5.50	3.80	8.76	5.27	47
Fixed 21,23,24(Z)	1.1	5.82	6.41	4.41	13.71	7.59	47
Fixed 21,24,22(Z)	1.3	6.92	7.93	4.23	15.76	6.32	48
Fixed 22,23,21(Z)	1.3	6.87	7.86	4.23	16.19	6.91	48
Over-Constrained 21,22,23,24 @ 0.005mm	1.3	6.83	7.36	5.61	11.89	4.55	47

The first simulation of tables 10.2 and 10.3 is a free network evaluation of the existing network. The results of the simulation indicate that that the network, despite the weaknesses previously detailed, does have the potential to meet precision specifications. With respect to the object points of interest, ie the axle points, recovery of X, Y and Z coordinates is to the order of 3 to 4 millimetres. Note that the Y coordinate has poorest recovery, and this is due to the network configuration aspects previously described.

Table 10.3 Simulation results - axle points

DATUM	$\bar{\sigma}_c$ mm	$\bar{\sigma}_{XY}$ mm	$\bar{\sigma}_Z$ mm	$\Delta\sigma_{XY}$ mm	$\Delta\sigma_Z$ mm	MAX σ_X	MAX σ_Y	MAX σ_Z
Free Network (all)	3.80	4.09	3.15	3.42	1.89	3.1	5.6	4.1
Free Network (pts 21,22,23,24)	6.09	6.63	4.83	7.83	3.70	4.9	10.3	6.7
Fixed 21,23,24(Z)	6.82	7.38	5.56	10.91	3.55	4.8	13.7	7.6
Fixed 21,24,22(Z)	8.42	9.64	5.20	13.18	2.97	6.1	15.8	6.3
Fixed 22,23,21(Z)	7.89	9.00	4.97	13.33	3.60	6.8	16.2	6.9
Over-Constrained 21,22,23,24 @ 0.005 mm	8.15	8.81	6.57	11.43	3.99	6.3	15.2	8.4

Additional simulations were carried out with respect to the available control, ie points 21, 22, 23 and 24. For the axle points, none of the control configurations applied allow precision determination to within precision requirements. Once again recovery of the Y coordinate is the poorest with recovery of the points furthermost from the defined control points, ie points 47 and 48, being in excess of 50% worse than specification. None of the possible datum configurations allow precision criteria to be met, including the over-constrained datum applied in the original adjustment.

The primary problem with the network is therefore one of datum definition. The available control points are located at a maximum distance from the axle points, for which position is required, and hence recovery of these points is poor. For a minimal control configuration, the triangle defined by the three control points is neither of maximum area nor does it pass through the centroid of the object point array. Consequently the available control configurations do not allow a "best" zero-variance computational base

definition, and in fact the available definitions can be considered as very poor configurations.

With respect to the initial network design for the photogrammetric mensuration of the Port Kembla coal loader, three basic problems or deficiencies are evident. The first, and principal deficiency, relates to the zero-order design. The datum definition is essentially arbitrary and offers no mathematical "strength" to the points of interest in the object point array. The need for an a priori solution of the zero-order design problem, with respect to precision requirements and the object points of interest, is essential.

The second deficiency in the network relates to the first-order design. In this network a configuration has been utilized which does have the potential of meeting precision requirements. However the form of the configuration, especially the imaging geometry, has not been optimally designed for the purpose of deriving 10 millimetre precision from the axle points. The configuration is essentially a classical network, ie "normal" geometry, with an excess of camera stations in order to ensure recovery of point position to the required precision. A priori evaluation of the network configuration, with respect to precision criteria, is essential in order to ensure precision requirements can be achieved in an economical manner.

The third deficiency is related to the manner of specifying the precision requirements. For the task of determining position on the coal loader, a requirement that position be related to an arbitrary datum, ie the railway tracks, is not the most appropriate method of defining the position of the axle points. This requirement inherently means that point precision estimates will be degraded due to the requirement for reference to an absolute datum. A more applicable solution would be to define the position of the axle points and the railway tracks with respect to the network of points as a whole, via a free network solution. Consequently the shape of the object point array would be defined, a higher object point precision would result, and the network to achieve required precision could be based upon a simpler, more economical configuration and design.

10.4 Network Design for the Port Kembla Coal Loader

With respect to the precision criteria of section 10.1, a close range photogrammetric network will be designed for the Port Kembla coal loader.

An augmented object point array has ben proposed for this design. The array is essentially the same as that for the initial design and is shown in figure 10.5. Twelve points have been added to initial array. These are the ten points, 50 to 59, which have been included to strengthen the object point array for self-calibration purposes. Points 81 and 82 have also been added to the array. These points are well separated in the Y direction and hence will stabilize the solution with respect to poor definition in the Y direction. For axle points at the top of the coal loader, points 81 and 82 will effectively reduce the pivoting effect caused by a datum defined at the base of the coal loader. The object point array is show in figure 10.6. The size of the targets should be 100 to 120 μm on the image (Trinder (1989)). At an anticipated image scale of between 1 : 800 and 1 : 1000, this means that the actual target size should be approximately 0.1 metres in diameter.

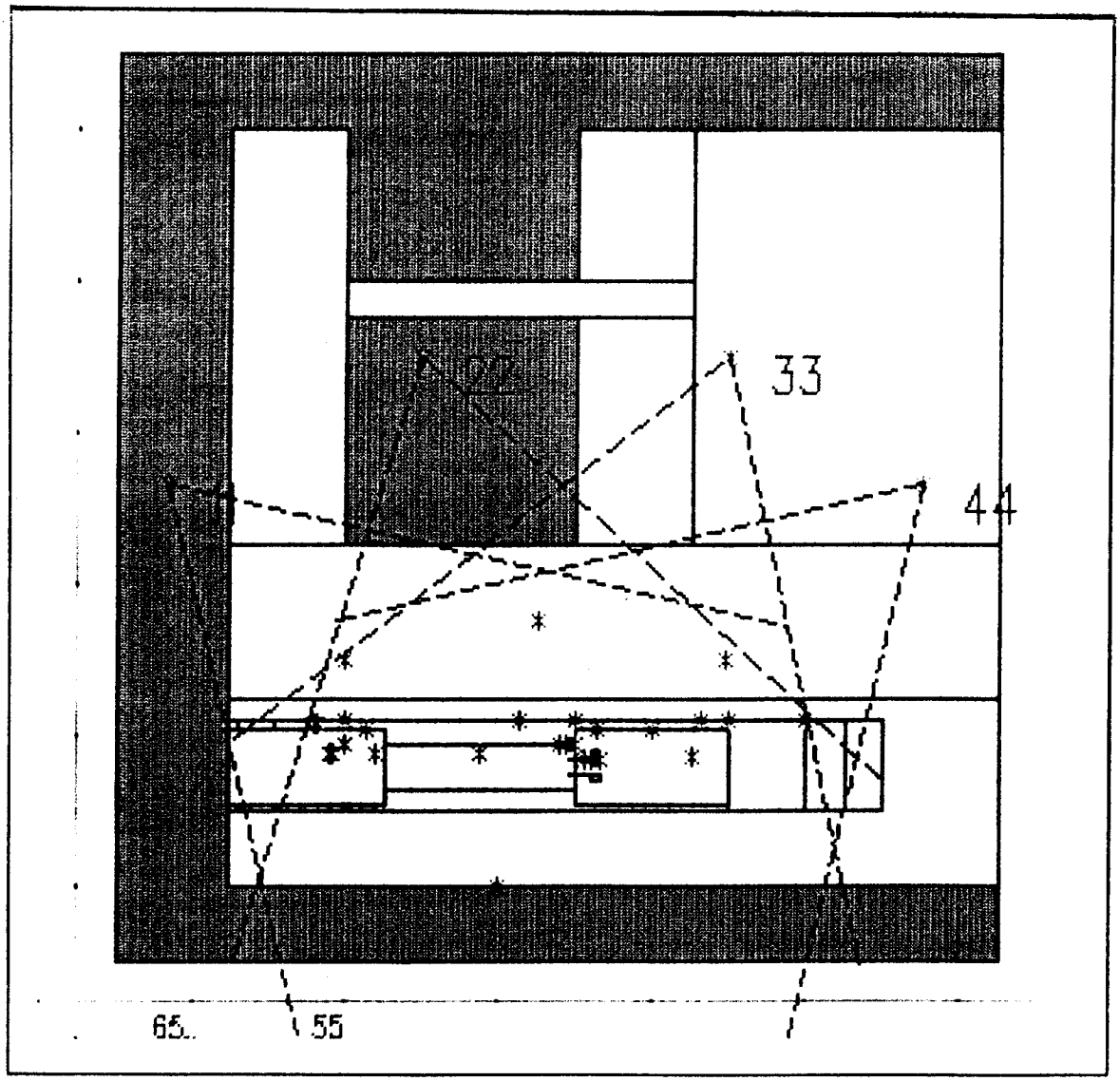

Figure 10.5 SIMPAC plan view - proposed network configuration

Options in photogrammetric image and image coordinate acquisition hardware are as follows.

- Camera - Hasselblad MK70 (Semi-metric)
  - Wild P32 (Metric)
  - CRC-1 (Metric)
- Comparator - Kern DSR-11 Analytical Plotter

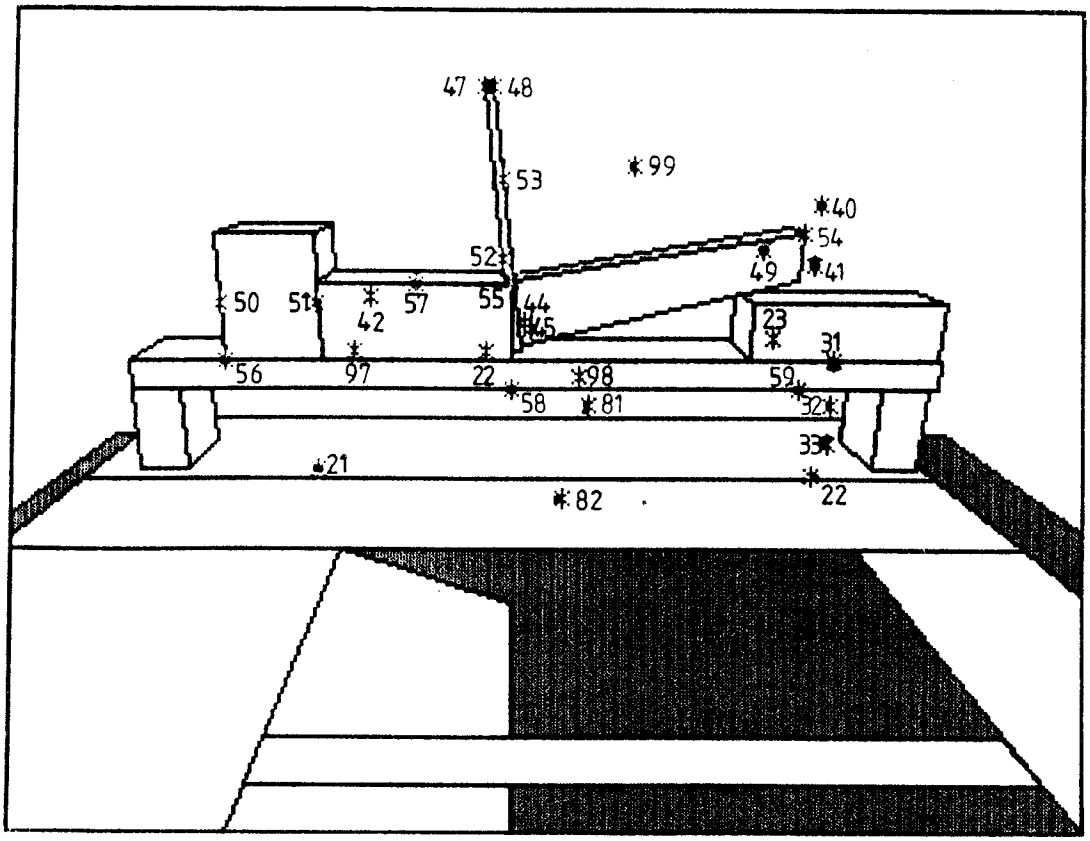

Figure 10.6 SIMPAC perspective view - object point array for the proposed design

No option in analytical plotter is available, and although several camera options are evident, the precision requirements of the task are such that a high precision camera, such as the CRC-1, is not warranted. For this design the Wild P32 will be utilized, with a focal length of 64.1 millimetres and an image format of 80 by 60 millimetres.

Following several trial and error simulations the network configuration, of figure 10.6, was formulated. The configuration comprises four convergent camera stations, each of which has an optimal coverage of the object point array. Figure 10.7 and figure 10.8 show SIMPAC perspective views of the

object from stations 11 and 22 respectively. The configuration has been designed to allow improved recovery of the object point Y coordinate, through utilization of convergent photography. Full object point array coverage has resulted in an increased image scale, 1 : 850, which will facilitate improved overall object point precision. Note that camera stations 11 and 22 will require a "cherry-picker" to allow photography from the desired location.

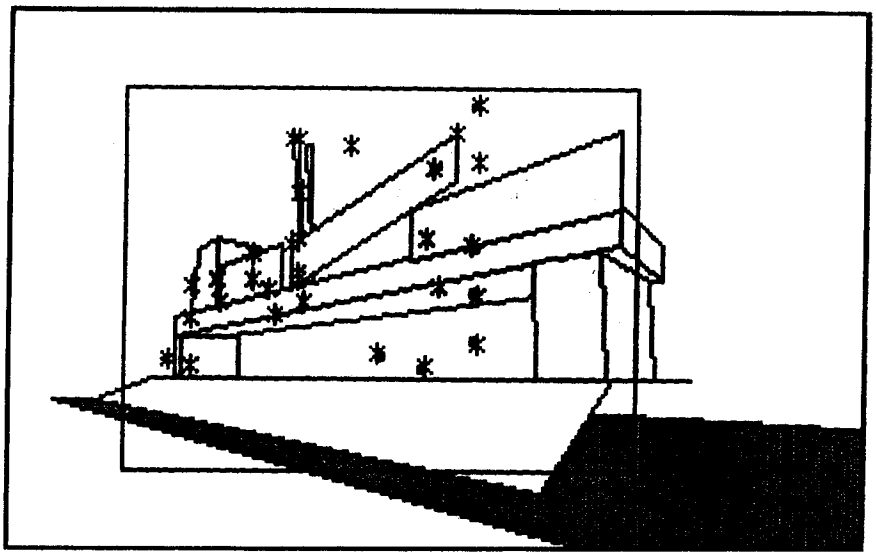

Figure 10.7 SIMPAC perspective view - camera station 11

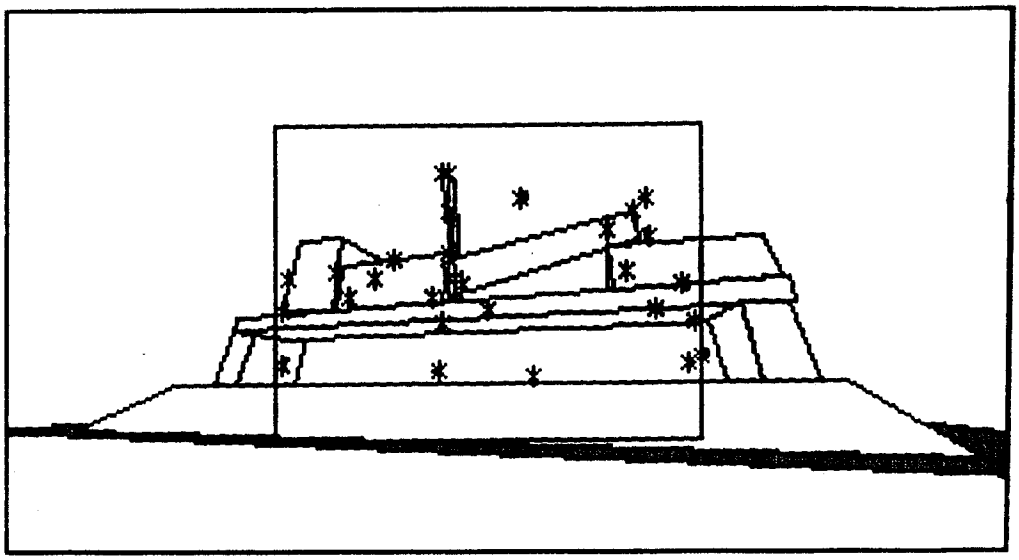

Figure 10.8 SIMPAC perspective view - camera station 22

Based upon this network configuration, simulations by a free network solution and a chosen zero-variance computational base have been carried out. Table 10.4 shows the results for all object points and table 10.5 shows the results for the axle points only. The zero-variance computational base was chosen in the zero-order design phase such that precision criteria were satisfied.

Table 10.4 Simulation results - all object points

DATUM	q	$\bar{\sigma}_c$ mm	$\bar{\sigma}_{XY}$ mm	$\bar{\sigma}_Z$ mm	$\Delta\sigma_{XY}$ mm	$\Delta\sigma_Z$ mm	Max Point
Free Network (all)	0.6	2.71	2.92	2.21	3.06	1.00	-
Fixed 21,52,24(Z)	1.2	5.50	6.32	3.30	12.07	6.35	33

Table 10.5 Simulation results - axle points

DATUM	$\bar{\sigma}_c$ mm	$\bar{\sigma}_{XY}$ mm	$\bar{\sigma}_Z$ mm	$\Delta\sigma_{XY}$ mm	$\Delta\sigma_Z$ mm	MAX σ_X	MAX σ_Y	MAX σ_Z
Free Network (all)	2.71	2.88	2.34	1.00	0.41	2.8	3.4	2.5
Fixed 21,52,24(Z)	5.50	6.19	3.74	6.00	1.42	6.3	9.5	4.3

The free network solution, of tables 10.4 and 10.5, show that the network has the potential to recover axle position to less than 3 millimetres. Despite being one camera station less than the initial network, this configuration offers an improved precision homogeneity, improved recovery of the object point Y coordinate and improved overall precision. For the requirement of relating object points to the required datum, the two object points which define the railway track location have been retained. An additional control point, namely 52, has been selected in the centre of the target array to strengthen the recovery of axle points towards the top of the array.

With the given network configuration, figure 10.6, and the datum definition, based on points 21 and 52 in X, Y and Z and point 24 in Z, precision specifications can be met. For the axle points, the mean standard errors in planimetry and height are 6 millimetres and 4 millimetres respectively. No standard deviation for the axle points, in either X, Y or Z, exceeds 10 millimetres.

10.4 Comments

The case study of the photogrammetric mensuration of the Port Kembla coal loader illustrates the applicability of network design and simulation in close range photogrammetry. The study also illustrates many of the typical problems encountered in close range photogrammetric evaluations. Problems including datum definition, configuration design and the implication of physical and practical constraints can be assessed and solved via network design and simulation methods prior to actual acquisition of data. Consequently a network can be implemented for which all design problems have been solved and which will meet specified precision criteria. The case study not only ties together the various design problems but also illustrates practical design problems evident in many practical applications. Several conclusions can be formulated from the case study.

- For a datum defined by absolute, explicit constraints, excess control does not improve network precision estimates. The "best" precision estimates, with respect to a fixed datum, are achieved by optimal zero-variance computational base configurations.

- For precision criteria which includes equal precision determination in each coordinate direction, Application of "normal" imaging geometries is not applicable. "Normal" configurations have reduced precision estimates in the direction parallel to the camera axis. For isotropic precision, convergent imaging geometries should be utilized.

- For datum definition by a zero-variance computational base, control should be distributed over the whole target array. The control point triangle should be of maximum area and should pass through the centroid of the object point array.

- Many photogrammetrists are either unfamiliar or ignorant of the free network concept. For many close range photogrammetric applications, where position is not required relative to a fixed datum, free networks offer the best solution. Free network precision estimates are always higher than from alternative datum definitions and hence the method is preferred for high precision applications. An education of photogrammetrists is required on the inherent benefits of free network solutions, and the applicability of such solutions in the majority of close range photogrammetric applications.

11. CONCLUSIONS

This study defines the techniques for network design in close range photogrammetry. Many of the developments for these techniques have deliberately been theoretical in nature and were designed to maintain the continuity of theory from first principles through to the final network design principles.

11.1 Summary and Recommendations

(i) The process of close range photogrammetric network design can be fully described via four basic design problems.

Zero-Order Design - datum definition
First-Order design - network configuration
Second-Order design - observation "weight"
Third-Order Design - network densification

In close range photogrammetry the network design process is simplified to a certain extent. The second-order design problem reduces to a simple scaling procedure based upon image observation precision. The basic methods of solving this problem are to upgrade the comparator or analytical plotter, to carry out multiple image observations for each object point or to take multiple exposures at each camera station. If multiple exposures are utilized and a new set of camera exterior orientation parameters are included for each new exposure, as is the usual case, then the second-order design problem is not significant as it is effectively solved in the first-order design phase. For close range photogrammetry the third-order design problem is solved at the first-order design phase. The problem, which involves network densification, is solved during the determination of the density and distribution of the object point array in the first-order design.

(ii) The network design problems which are of fundamental importance in close range photogrammetric network design are the zero-order and first-order design problems. The zero-order design solutions which are applicable in close range photogrammetry include zero-variance computational base

solutions, in optimal control configurations, free network solutions and, in special cases, Bayesian least squares solutions. The optimal solution to the datum problem is dependent upon finding a minimum variance solution. Such a solution is only possible under application of absolute, minimal constraints. Over-constrained solutions require both an excess of surveying for control provision and do not give optimal precision estimates and hence are not applicable for close range photogrammetric datum definition.

Zero-variance computational base solutions are applicable in cases where an absolute datum definition is required. Biased precision estimates will result and will be dependent on the control configuration selected. However this bias can be minimized by selecting a control configuration where the triangle defined by the three control points selected is both of maximum area and passes through the centroid of the object point array.

(iii) Free network solutions offer the optimal solution to the close range photogrammetric network design problem. A free network solution is applicable in cases where the shape of the object point array, as opposed to the position of the object points with respect to a fixed datum, is required. Free network solutions for close range photogrammetry give a partial minimum trace datum with respect to the object points, or a chosen subset of the object points. Free networks yield a minimum mean variance and minimum biased estimates for the parameters to which the free network conditions apply.

(iv) Bayesian least squares is applicable in close range photogrammetry where a good a priori knowledge of the parameters is available. As a solution to the datum problem, however, Bayesian estimation techniques are not applicable. A Bayesian estimation solution usually results in an over-constrained system, from which invariant quantities become dependent on constraint selection and precision estimates are never optimal.

(v) Solution of the first-order design problem is dependent upon the form of the various factors which influence the network configuration. The primary component in the first-order design solution is the imaging geometry. The imaging geometry will define the form of the precision estimates which result from the evaluation process, in terms of precision homogeneity. Precision homogeneity, which refers to the degree of homogeneity in precision estimates in the three coordinate directions, approaches maximum

homogeneity at a convergence angle of the camera axes of 120°. Imaging geometry also influences the magnitude of resulting precision estimates, with a different precision in planimetry and height resulting, depending on the convergence angle.

(vi) Network configuration components, such as number of camera stations, number and distribution of object points, base/distance ratio ("normal" configurations), the influence of self-calibration additional parameters, camera type, image scale, object points clusters and multiple exposures, are merely precision scaling factors. This scaling is essentially with respect to the form of the precision estimates, as defined by the imaging geometry.

(vii) In order to assess the quality of network design, measures have been formulated so that a global assessment of the network, in terms of either precision, accuracy, reliability or sensitivity, is possible. The principal quality criterion is that of precision. In general, assessment of network precision with respect to specifications is carried out during the design process, with evaluation with respect to the remaining network quality criteria being carried out after the initial design. Precision measures which give a global indication of network quality have been developed and evaluated. The pertinent global precision measures include the mean standard error and the photogrammetric network strength factor, which assesses network strength on the basis of precision estimates and network configuration. Local precision measures which have been utilized include the standard deviation and the distance standard error. For the purposes of assessing precision homogeneity, the standard error range offers a global measure which can easily be evaluated.

(viii) The problems of network design are solved by an indirect method. Based upon trial and error simulations, a network can be formulated such that the network meets the imposed quality criteria, which may be in terms of precision, accuracy, reliability, sensitivity and economy. For these solutions interactive computer graphics and network simulation provide an effective method of carrying out a network design. Networks can be formulated, based upon a graphic representation of the network configuration and any physical constraints on the site. This configuration can then be altered based upon assessment of the precision estimates from the simulation and adjustment routines. Although networks designed by trial and error methods are not optimal, with respect to satisfying quality criteria, the networks so designed do

meet quality criteria and represent a network which can easily be implemented in practice.

(iX) Applicable in close range photogrammetric network design process is the adjustment process based upon limiting error propagation. The limiting error propagation procedure gives precision estimates which closely approximate the free network estimates. The advantage of the limiting error propagation solution relates to the vastly reduced computation time for the solution. In evaluation of the first-order design problems, where numerous trial and error simulations may be required, the network can be evaluated by the limiting error propagation solution and time in determining the "best" solution can be reduced. Having solved the first-order design an appropriate total error propagation solution is carried out in order to verify the approximate precision estimates from the limiting error propagation solution.

The techniques presented comprise a viable method for designing networks in close range photogrammetry. A common criticism of the design methodology relates to the trial and error, iterative solution method. This criticism is of no concern, however, as the method allows for the design of a network which can be implemented in practice and for which the photogrammetrist can predict achievable object point precision with assurity.

11.2 Future Research

Several areas pertaining to network design require evaluation and research in the future. The development of these areas will allow the design of networks, in close range photogrammetry, to progress past what is currently a trail and error network design technique.

- Direct solution to the network design problems, especially with respect to first and second order design problems. If a direct solution technique could be formulated then an optimal network design, with respect to the quality criteria of interest, could be implemented.

- Integration of quantitative economy measures, simultaneously with other quality criteria, into the close range photogrammetric network design process. At present economy assessment is essentially qualitative and carried out after the network has been designed, and

therefore the current design techniques do not offer network designs which are optimal with respect to an economic cost function.

- Development of network precision measures based upon datum invariant quantities. At present all precision measures are dependent upon the selected datum constraints and hence give a datum-biased estimate of network quality. Precision measures based upon datum invariant quantities would offer a method of assessing network quality independently of the chosen datum.

The points presented above are a few of the technical considerations which require attention with respect to the technical aspects of close range photogrammetric network design. Also of considerable importance, but not of a technical nature, is the education of possible users of close range photogrammetry of the potential of the technique as a high precision metrology tool. In order to achieve this, photogrammetrists in general should be made aware of the precision capabilities of close range photogrammetry and of the essential requirements for prior network design and analysis in order to ensure such precision.

This study has provided a comprehensive evaluation of the processes involved in close range photogrammetric network design. Utilizing the design process which have been developed, close range photogrammetry becomes a viable alternative to high precision mensuration application in industry and engineering.

APPENDIX

DEVELOPMENT OF OBSERVATION EQUATIONS

Observation equations, based on the least squares mathematical model of Chapter 3, will be formulated in detail. Observation equations relating to measurement of image coordinates, exterior orientation parameters, control or object points, straight line distances, elevation differences, azimuths, horizontal angles and vertical angles will be considered.

A.1 Image Point Coordinates (Collinearity Equation)

The basic observation equation in photogrammetric adjustments is the collinearity equation. The equation, as developed and derived in Chapter 2, relates observations on the image or photograph to the unknown parameters defining the position of a point in a three dimensional rectangular coordinate system in the object space. The collinearity equation, as given in equation 2.12 and 2.13, can be written in the following form.

$$x_i - x_o + f\left(\frac{m_{11}(X_i - X_L)+m_{12}(Y_i - Y_L)+m_{13}(Z_i - Z_L)}{m_{31}(X_i - X_L)+m_{32}(Y_i - Y_L)+m_{33}(Z_i - Z_L)}\right) = F_x = 0 \qquad ..(A.1)$$

$$y_i - y_o + f\left(\frac{m_{21}(X_i - X_L)+m_{22}(Y_i - Y_L)+m_{23}(Z_i - Z_L)}{m_{31}(X_i - X_L)+m_{32}(Y_i - Y_L)+m_{33}(Z_i - Z_L)}\right) = F_y = 0 \qquad ..(A.2)$$

where
- x_i, y_i = coordinates of point i (image space coordinate system)
- x_o, y_o = coordinates of the principal point (image space coordinate system)
- f = focal length
- X_i, Y_i, Z_i = coordinates of point i (object space coordinate system)
- X_L, Y_L, Z_L = coordinates of the perspective centre (object space coordinate system)
- m_{ij} = elements of the 3x3 rotation matrix as given by equation 2.9

For equations A.1 and A.2 to be used in the least squares mathematical model they must be expressed in a linear form and must be presented in the form of equation 3.8, ie $v = A\hat{X} - l$. Linearization of equations A.1 and A.2 is carried out by utilizing the Taylor series expansion of equation 3.7. In developing the observation equations for image coordinate observations the following assumptions are made :

1. All points are imaged on all photographs. Such an assumption can be adapted to a specific case by deleting the appropriate observation equations where necessary.
2. No additional parameters, for the modeling of unresolved systematic errors, are to be included. If additional parameters are to be incorporated, ie for a self-calibrating adjustment as discussed in section 2.4.5, then addition of parameters sets to the model can be carried out as detailed in Kilpelä (1981), Fraser (1982b), Fraser (1982c)).

Prior to linearization of the collinearity equations the observations are established in the form where measured quantities are related to "true" quantities. Therefore the image coordinates x_i and y_i are written in terms of measured quantities x_i^{oo}, y_i^{oo} and residuals v_x and v_y.

$$x_i = x_i^{oo} + v_x \qquad ..(A.3)$$
$$y_i = y_i^{oo} + v_y$$

The unknown parameters are expressed in terms of a correction to an approximate value. For estimates of the unknown parameters $\hat{X}_i$, $\hat{Y}_i$, $\hat{Z}_i$, and $\hat{X}_L$, $\hat{Y}_L$, $\hat{Z}_L$, $\hat{\theta}$, $\hat{\alpha}$ and $\hat{\kappa}$ the following equations can be formulated. Note that approximate values are denoted by the superscript "o" and corrections to the unknown parameters are denoted by the prefix "Δ".

$$\hat{X}_L = X_L^o + \Delta\hat{X}_L$$
$$\hat{Y}_L = Y_L^o + \Delta\hat{Y}_L \qquad ..(A.4a)$$
$$\hat{Z}_L = Z_L^o + \Delta\hat{Z}_L$$

$$\hat{\alpha} = \alpha^o + \Delta\hat{\alpha}$$
$$\hat{\theta} = \theta^o + \Delta\hat{\theta} \qquad ..(A.4b)$$
$$\hat{\kappa} = \kappa^o + \Delta\hat{\kappa}$$

$$\hat{X}_i = X_i^o + \Delta\hat{X}_i$$
$$\hat{Y}_i = Y_i^o + \Delta\hat{Y}_i \qquad ..(A.4c)$$
$$\hat{Z}_i = Z_i^o + \Delta\hat{Z}_i$$

The linearized collinearity equations, in the notation of equations A.3 and A.4, become :

$$v_{x\,i} = \left(\frac{\partial F_x}{\partial X_L}\right)^o \Delta\hat{X}_L + \left(\frac{\partial F_x}{\partial Y_L}\right)^o \Delta\hat{Y}_L + \left(\frac{\partial F_x}{\partial Z_L}\right)^o \Delta\hat{Z}_L + \left(\frac{\partial F_x}{\partial \alpha}\right)^o \Delta\hat{\alpha} + \left(\frac{\partial F_x}{\partial \theta}\right)^o \Delta\hat{\theta} +$$
$$\left(\frac{\partial F_x}{\partial \kappa}\right)^o \Delta\hat{\kappa} + \left(\frac{\partial F_x}{\partial X_i}\right)^o \Delta\hat{X}_i + \left(\frac{\partial F_x}{\partial Y_i}\right)^o \Delta\hat{Y}_i + \left(\frac{\partial F_x}{\partial Z_i}\right)^o \Delta\hat{Z}_i + F_x^o \approx 0 \qquad ..(A.5)$$

$$v_{y\,i} = \left(\frac{\partial F_y}{\partial X_L}\right)^o \Delta\hat{X}_L + \left(\frac{\partial F_y}{\partial Y_L}\right)^o \Delta\hat{Y}_L + \left(\frac{\partial F_y}{\partial Z_L}\right)^o \Delta\hat{Z}_L + \left(\frac{\partial F_y}{\partial \alpha}\right)^o \Delta\hat{\alpha} + \left(\frac{\partial F_y}{\partial \theta}\right)^o \Delta\hat{\theta} +$$
$$\left(\frac{\partial F_y}{\partial \kappa}\right)^o \Delta\hat{\kappa} + \left(\frac{\partial F_y}{\partial X_i}\right)^o \Delta\hat{X}_i + \left(\frac{\partial F_y}{\partial Y_i}\right)^o \Delta\hat{Y}_i + \left(\frac{\partial F_y}{\partial Z_i}\right)^o \Delta\hat{Z}_i + F_y^o \approx 0 \qquad ..(A.6)$$

Equations A.6 and A.7 follow the convention established earlier where the superscript "o" denotes a coefficient evaluated at the approximate value. Likewise the functions F_x^o and F_y^o are the equations A.1 and A.2 evaluated at the approximate values. To simplify the linearized expressions the following notation will be adopted :

$$a_{11} = \left(\frac{\partial F_x}{\partial X_L}\right)^o \qquad a_{21} = \left(\frac{\partial F_y}{\partial X_L}\right)^o$$
$$a_{12} = \left(\frac{\partial F_x}{\partial Y_L}\right)^o \qquad a_{22} = \left(\frac{\partial F_y}{\partial Y_L}\right)^o$$
$$a_{13} = \left(\frac{\partial F_x}{\partial Z_L}\right)^o \qquad a_{23} = \left(\frac{\partial F_y}{\partial Z_L}\right)^o$$
$$a_{14} = \left(\frac{\partial F_x}{\partial \alpha}\right)^o \qquad a_{24} = \left(\frac{\partial F_y}{\partial \alpha}\right)^o \qquad ..(A.7)$$
$$a_{15} = \left(\frac{\partial F_x}{\partial \theta}\right)^o \qquad a_{25} = \left(\frac{\partial F_y}{\partial \theta}\right)^o$$
$$a_{16} = \left(\frac{\partial F_x}{\partial \kappa}\right)^o \qquad a_{26} = \left(\frac{\partial F_y}{\partial \kappa}\right)^o$$
$$a_{17} = \left(\frac{\partial F_x}{\partial X_i}\right)^o \qquad a_{27} = \left(\frac{\partial F_y}{\partial X_i}\right)^o$$
$$a_{18} = \left(\frac{\partial F_x}{\partial Y_i}\right)^o \qquad a_{28} = \left(\frac{\partial F_y}{\partial Y_i}\right)^o$$
$$a_{19} = \left(\frac{\partial F_x}{\partial Z_i}\right)^o \qquad a_{29} = \left(\frac{\partial F_y}{\partial Z_i}\right)^o$$

The partial derivatives listed above, with the exception of the partial derivatives a_{14} to a_{16} and a_{24} to a_{26}, are evaluated in numerous photogrammetric texts, including Moffitt and Mikhail (1980), and will not be evaluated here. The partial derivatives with respect to the rotation elements azimuth, tilt and kappa are not given in such texts however. Consequently the six partial derivatives relating to the rotations will be evaluated.

Equations A.1, A.2 and 2.8 will be utilized in the derivation of the derivatives, where equations A.1, A.2 and 2.8 are :

$$M = M_\kappa M_\theta M_\alpha \qquad ..(2.8)$$

$$F_x = x_i - x_o + f\left(\frac{U}{W}\right) \qquad ..(A.1)$$

$$F_y = y_i - y_o + f\left(\frac{V}{W}\right) \qquad ..(A.2)$$

where $U = m_{11}(X_i - X_L)+m_{12}(Y_i - Y_L)+m_{13}(Z_i - Z_L)$

$V = m_{21}(X_i - X_L)+m_{22}(Y_i - Y_L)+m_{23}(Z_i - Z_L)$

$W = m_{31}(X_i - X_L)+m_{32}(Y_i - Y_L)+m_{33}(Z_i - Z_L)$

A.1.1 Design Matrix Coefficients a_{14} and a_{24} - Azimuth

The partial derivative of 2.8, with respect to α, becomes :

$$\frac{\partial M}{\partial \alpha} = M_\kappa M_\theta \frac{\partial M_\alpha}{\partial \alpha}$$

where $$\frac{\partial M_\alpha}{\partial \alpha} = \begin{pmatrix} -\sin\alpha & -\cos\alpha & 0 \\ 0 & 0 & 0 \\ -\cos\alpha & \sin\alpha & 0 \end{pmatrix} = M_\alpha \begin{pmatrix} 0 & -1 & 0 \\ 1 & 0 & 0 \\ 0 & 0 & 0 \end{pmatrix}$$

$$\text{therefore } \frac{\partial M}{\partial \alpha} = M_\kappa M_\theta M_\alpha \begin{pmatrix} 0 & -1 & 0 \\ 1 & 0 & 0 \\ 0 & 0 & 0 \end{pmatrix} = M \begin{pmatrix} 0 & -1 & 0 \\ 1 & 0 & 0 \\ 0 & 0 & 0 \end{pmatrix}$$

$$= \begin{pmatrix} m_{12} & -m_{11} & 0 \\ m_{22} & -m_{21} & 0 \\ m_{32} & -m_{31} & 0 \end{pmatrix}$$

Therefore $\frac{\partial F_x}{\partial \alpha}$ and $\frac{\partial F_y}{\partial \alpha}$ are determined by substitution of $\frac{\partial M}{\partial \alpha}$ into equations A.1 and A.2 respectively. The resulting partial derivatives, namely a_{14} and a_{24}, become :

$$a_{14} = \frac{\partial F_x}{\partial \alpha} = \frac{f}{W}\left(\frac{\partial U}{\partial \alpha} - \frac{U}{W}\frac{\partial W}{\partial \alpha}\right)$$

$$a_{24} = \frac{\partial F_x}{\partial \alpha} = \frac{f}{W}\left(\frac{\partial V}{\partial \alpha} - \frac{V}{W}\frac{\partial W}{\partial \alpha}\right)$$

where
$$\frac{\partial U}{\partial \alpha} = m_{12}(X_i - X_L) - m_{11}(Y_i - Y_L)$$
$$\frac{\partial V}{\partial \alpha} = m_{22}(X_i - X_L) - m_{21}(Y_i - Y_L)$$
$$\frac{\partial W}{\partial \alpha} = m_{32}(X_i - X_L) - m_{31}(Y_i - Y_L)$$

A.1.2 Design Matrix Coefficients a_{15} and a_{25} - Tilt

The partial derivative of 2.8, with respect to θ, becomes :

$$\frac{\partial M}{\partial \theta} = M_\alpha \frac{\partial M_\theta}{\partial \theta} M_\kappa$$

where
$$\frac{\partial M_\theta}{\partial \theta} = \begin{pmatrix} 1 & 0 & 0 \\ 0 & \cos\theta & \sin\theta \\ 0 & -\sin\theta & \cos\theta \end{pmatrix} = \begin{pmatrix} 0 & 0 & 0 \\ 0 & 0 & 1 \\ 0 & -1 & 0 \end{pmatrix} M_\theta$$

therefore

$$\frac{\partial M}{\partial \theta} = M_\kappa \begin{pmatrix} 0 & 0 & 0 \\ 0 & 0 & 1 \\ 0 & -1 & 0 \end{pmatrix} M_\theta M_\alpha = \begin{pmatrix} 0 & 0 & \sin\kappa \\ 0 & 0 & \cos\kappa \\ -\sin\kappa & -\cos\kappa & 0 \end{pmatrix} M$$

$$= \begin{pmatrix} \sin\kappa.m_{31} & \sin\kappa.m_{32} & \sin\kappa.m_{33} \\ \cos\kappa.m_{31} & \cos\kappa.m_{32} & \cos\kappa.m_{33} \\ -\sin\kappa.m_{11}-\cos\kappa.m_{21} & -\sin\kappa.m_{12}-\cos\kappa.m_{22} & -\sin\kappa.m_{13}-\cos\kappa.m_{23} \end{pmatrix}$$

$$= \begin{pmatrix} L_{11} & L_{12} & L_{13} \\ L_{21} & L_{22} & L_{23} \\ L_{31} & L_{32} & L_{33} \end{pmatrix}$$

Therefore $\frac{\partial F_x}{\partial \theta}$ and $\frac{\partial F_y}{\partial \theta}$ are determined by substitution of $\frac{\partial M}{\partial \theta}$ into equations A.1 and A.2 respectively. The resulting partial derivatives, namely a_{15} and a_{25}, are formed as follows.

$$a_{15} = \frac{\partial F_x}{\partial \theta} = \frac{f}{W}\left(\frac{\partial U}{\partial \theta} - \frac{U}{W}\frac{\partial W}{\partial \theta}\right)$$

$$a_{25} = \frac{\partial F_x}{\partial \theta} = \frac{f}{W}\left(\frac{\partial V}{\partial \theta} - \frac{V}{W}\frac{\partial W}{\partial \theta}\right)$$

where
$$\frac{\partial U}{\partial \theta} = L_{12}(X_i - X_L) + L_{11}(Y_i - Y_L) + L_{11}(Z_i - Z_L)$$

$$\frac{\partial V}{\partial \theta} = L_{22}(X_i - X_L) + L_{21}(Y_i - Y_L) + L_{11}(Z_i - Z_L)$$

$$\frac{\partial W}{\partial \theta} = L_{32}(X_i - X_L) + L_{31}(Y_i - Y_L) + L_{11}(Z_i - Z_L)$$

A.1.3 Design Matrix Coefficients a_{16} and a_{26} - Kappa

The partial derivative of 2.8, with respect to κ, becomes :

$$\frac{\partial M}{\partial \kappa} = \frac{\partial M_\kappa}{\partial \kappa} M_\theta M_\alpha$$

where
$$\frac{\partial M_\kappa}{\partial \kappa} = \begin{pmatrix} -\sin\kappa\cos\kappa & 0 \\ -\cos\kappa - \sin\kappa & 0 \\ 0 \quad 0 & 0 \end{pmatrix} = \begin{pmatrix} 0 & 1 & 0 \\ -1 & 0 & 0 \\ 0 & 0 & 0 \end{pmatrix} M_\kappa$$

$$\text{therefore } \frac{\partial M}{\partial \kappa} = \begin{pmatrix} 0 & 1 & 0 \\ -1 & 0 & 0 \\ 0 & 0 & 0 \end{pmatrix} M_\kappa M_\theta M_\alpha = \begin{pmatrix} 0 & 1 & 0 \\ -1 & 0 & 0 \\ 0 & 0 & 0 \end{pmatrix} M$$

$$= \begin{pmatrix} m_{21} & m_{22} & m_{23} \\ -m_{11} & -m_{12} & -m_{13} \\ 0 & 0 & 0 \end{pmatrix}$$

Therefore $\frac{\partial F_x}{\partial \kappa}$ and $\frac{\partial F_y}{\partial \kappa}$ are determined by substitution of $\frac{\partial M}{\partial \kappa}$ into equations A.1 and A.2 respectively. The resulting partial derivatives, namely a_{16} and a_{26} , become :

$$a_{16} = \frac{\partial F_x}{\partial \kappa} = \frac{f}{W}\frac{\partial U}{\partial \kappa}$$

$$a_{26} = \frac{\partial F_x}{\partial \kappa} = \frac{f}{W}\frac{\partial V}{\partial \kappa}$$

where
$$\frac{\partial U}{\partial \kappa} = m_{21}(X_i - X_L) + m_{22}(Y_i - Y_L) + m_{23}(Z_i - Z_L) = V$$

$$\frac{\partial V}{\partial \kappa} = -m_{11}(X_i - X_L) - m_{12}(Y_i - Y_L) - m_{13}(Z_i - Z_L) = -U$$

$$\frac{\partial W}{\partial \kappa} = 0$$

Equations A.5 and A.6 can be written in matrix notation, in terms of the notation of equation A.7.

$$\begin{pmatrix} v_{xi} \\ v_{yi} \end{pmatrix} + \begin{pmatrix} a_{11} & a_{12} & a_{13} & a_{14} & a_{15} & a_{16} \\ a_{21} & a_{22} & a_{23} & a_{24} & a_{25} & a_{26} \end{pmatrix} \begin{pmatrix} \Delta\hat{X}_L \\ \Delta\hat{Y}_L \\ \Delta\hat{Z}_L \\ \Delta\hat{\alpha} \\ \Delta\hat{\theta} \\ \Delta\hat{\kappa} \end{pmatrix} + \begin{pmatrix} a_{17} & a_{18} & a_{19} \\ a_{27} & a_{28} & a_{29} \end{pmatrix} \begin{pmatrix} \Delta\hat{X}_i \\ \Delta\hat{Y}_i \\ \Delta\hat{Z}_i \end{pmatrix} = \begin{pmatrix} -F_x^o \\ -F_y^o \end{pmatrix}$$

..(A.8)

The observation equations, relating **n** image coordinate observations on **m** photographs to the unknown parameters, in matrix notation becomes:

$$\underset{(2mn,1)}{V_1} + \underset{(2mn,6m)}{A_{11}} \cdot \underset{(6m,1)}{\hat{X}_1} + \underset{(2mn,3n)}{A_{12}} \cdot \underset{(3n,1)}{\hat{X}_2} = \underset{(2mn,1)}{c_1} \qquad ..(A.9)$$

The least squares model, for the linearized collinearity equations, can be found in Burns (1982), Moffitt and Mikhail (1980) and Slama (ed) (1980);Ch 2 and development of the observation equations for self-calibration can be found in Brown (1980), Fraser (1982b), Fraser (1982c) and Kilpela (1981).

A.2 Observation of Exterior Orientation Parameters

Observations of geographic location and orientation of a camera station can be formed into observation equations of the form of equation (3.8). For the "true" parameters X_L, Y_L, Z_L, α, θ and κ equations can be formulated in terms of the observed parameters X_L^{oo}, Y_L^{oo}, Z_L^{oo}, α^{oo}, θ^{oo} and κ^{oo} and residuals V_{XL}, V_{YL}, V_{ZL}, V_α, V_θ,and V_κ.

$$\begin{aligned} X_L &= X_L^{oo} + V_{XL} \\ Y_L &= Y_L^{oo} + V_{YL} \\ Z_L &= Z_L^{oo} + V_{ZL} \\ \alpha &= \alpha^{oo} + V_\alpha \\ \theta &= \theta^{oo} + V_\theta \\ \kappa &= \kappa^{oo} + V_\kappa \end{aligned} \qquad ..(A.10)$$

Equations A.4a and A.4b relate estimates of the parameters to approximate values and corrections to approximate values in the following form :

$$\begin{aligned} \hat{X}_L &= X_L^o + \Delta\hat{X}_L \\ \hat{Y}_L &= Y_L^o + \Delta\hat{Y}_L \\ \hat{Z}_L &= Z_L^o + \Delta\hat{Z}_L \end{aligned} \qquad ..(A.4a)$$

$$\begin{aligned} \hat{\alpha} &= \alpha^o + \Delta\hat{\alpha} \\ \hat{\theta} &= \theta^o + \Delta\hat{\theta} \\ \hat{\kappa} &= \kappa^o + \Delta\hat{\kappa} \end{aligned} \qquad ..(A.4b)$$

For an unbiased estimate of the unknown parameters equation A.10 can be equated to equations A.4a and A.4b to give the observation equation for observations on exterior orientation parameters.

$$\begin{pmatrix} V_{XL} \\ V_{YL} \\ V_{ZL} \\ V_\alpha \\ V_\theta \\ V_\kappa \end{pmatrix} - \begin{pmatrix} \Delta X_L \\ \Delta Y_L \\ \Delta Z_L \\ \Delta\alpha \\ \Delta\theta \\ \Delta\kappa \end{pmatrix} = \begin{pmatrix} X_L^o - X_L^{oo} \\ Y_L^o - Y_L^{oo} \\ Z_L^o - Z_L^{oo} \\ \alpha^o - \alpha^{oo} \\ \theta^o - \theta^{oo} \\ \kappa^o - \kappa^{oo} \end{pmatrix} \qquad ..(A.11)$$

For observations at **m'** camera stations, equation A.11 can be written in matrix notation as :

$$\underset{(6m',1)}{V_2} - \underset{(6m',1)}{\hat{X}_1} = \underset{(6m',1)}{c_2} \qquad ..(A.12)$$

A.3 Control or Object Point Coordinates

Observations on object points, which are in the form of coordinates in the object space coordinate system, are control point coordinate observations. Such observations act as "control" or constraint in any adjustment process. Actual observations are in the form of distances and angles in the object space coordinate system, from which object space coordinates are derived.

Expressing the "true" coordinates X_i, Y_i, Z_i in terms of measured coordinates $X_i^{oo}, Y_i^{oo}, Z_i^{oo}$ and residuals V_X, V_Y, V_Z the following equations can be formed.

$$X_i = X_i^{oo} + V_X$$
$$Y_i = Y_i^{oo} + V_Y \qquad ..(A.13)$$
$$Z_i = Z_i^{oo} + V_Z$$

Equation A.4c relates estimates of the parameters to approximate values and corrections to the approximate values in the following form.

$$\hat{X}_i = X_i^{o} + \Delta\hat{X}_i$$
$$\hat{Y}_i = Y_i^{o} + \Delta\hat{Y}_i \qquad ..(A.4c)$$
$$\hat{Z}_i = Z_i^{o} + \Delta\hat{Z}_i$$

For an unbiased estimate of the unknown parameters equations A.13 and A.4c can be equated to give the control coordinate observation equation.

$$\begin{pmatrix} V_X \\ V_Y \\ V_Z \end{pmatrix} = \begin{pmatrix} \Delta\hat{X}_i \\ \Delta\hat{Y}_i \\ \Delta\hat{Z}_i \end{pmatrix} = \begin{pmatrix} X_i^{o} - X_i^{oo} \\ Y_i^{o} - Y_i^{oo} \\ Z_i^{o} - Z_i^{oo} \end{pmatrix} \qquad ..(A.14)$$

The observation equation for **n'** control observations can be expressed in matrix notation as :

$$\underset{(3n',1)}{V_3} - \underset{(3n',1)}{\hat{X}_2} = \underset{(3n',1)}{c_3} \qquad ..(A.15)$$

A.4 Straight Line Distances

Observation equations to relate a measured distance between two object points in the object space coordinate system to unknown parameters, requires formulation.

A "true" distance S_{jk}, between points j and k on the object, can be expressed in terms of a measured distance S_{jk}^{oo} and a residual V_s.

$$S_{jk} = S_{jk}^{oo} + V_s \qquad ..(A.16)$$

The estimate of the distance $\hat{S}_{jk}$ can be expressed in terms of an approximate distance S_{jk}^{o} and a correction term $\Delta\hat{S}_{jk}$.

$$\hat{S}_{jk} = S_{jk}^{o} + \Delta\hat{S}_{jk} \qquad ..(A.17)$$

For an unbiased estimate of the distance, equations A.16 and A.17 can be equated to give :

$$Vs - \Delta\hat{S}_{jk} = S_{jk}^{o} - S_{jk}^{oo} \qquad ..(A.18)$$

A problem with equations A.16 to A.18 is that they do not directly relate to the unknown parameters, ie X_j, Y_j, Z_j, X_k, Y_k, Z_k which are the coordinates of the points between which the distance was measured. The general form of the equation for a distance between two points in a rectangular coordinate system is given by :

$$S_{jk} = \sqrt{(X_j - X_k)^2 + (Y_j - Y_k)^2 + (Z_j - Z_k)^2} \qquad ..(A.19)$$

Equation A.19 is non-linear and will be linearized by the Taylor series expansion of equation 3.7. Substitution of the linearized equation into equation A.18 gives the observation equation for a straight line distance between two object points.

$$V_s - \left(\frac{\partial S_{jk}}{\partial X_j}\right)^{o} \Delta\hat{X}_j - \left(\frac{\partial S_{jk}}{\partial Y_j}\right)^{o} \Delta\hat{Y}_j - \left(\frac{\partial S_{jk}}{\partial Z_j}\right)^{o} \Delta\hat{Z}_j - \left(\frac{\partial S_{jk}}{\partial X_k}\right)^{o} \Delta\hat{X}_k - \left(\frac{\partial S_{jk}}{\partial Y_k}\right)^{o} \Delta\hat{Y}_k - \left(\frac{\partial S_{jk}}{\partial Z_k}\right)^{o} \Delta\hat{Z}_k = S_{jk}^{o} - S_{jk}^{oo} \qquad ..(A.20)$$

To simplify equation A.20 the following notation will be used :

$$s_1 = \left(\frac{\partial S_{jk}}{\partial X_j}\right)^{o} = \frac{(X_j - X_k)}{S_{jk}} \qquad s_4 = \left(\frac{\partial S_{jk}}{\partial X_k}\right)^{o} = -\frac{(X_j - X_k)}{S_{jk}}$$

$$s_2 = \left(\frac{\partial S_{jk}}{\partial Y_j}\right)^{o} = \frac{(Y_j - Y_k)}{S_{jk}} \qquad s_5 = \left(\frac{\partial S_{jk}}{\partial Y_k}\right)^{o} = -\frac{(Y_j - Y_k)}{S_{jk}} \qquad ..(A.21)$$

$$s_3 = \left(\frac{\partial S_{jk}}{\partial Z_j}\right)^{o} = \frac{(Z_j - Z_k)}{S_{jk}} \qquad s_6 = \left(\frac{\partial S_{jk}}{\partial Z_k}\right)^{o} = -\frac{(Z_j - Z_k)}{S_{jk}}$$

Equation A.20, in terms of the notation of equation A.21, becomes :

$$V_S - (s_1, s_2, s_3, s_4, s_5, s_6) \begin{pmatrix} \Delta\hat{X}_j \\ \Delta\hat{Y}_j \\ \Delta\hat{Z}_j \\ \Delta\hat{X}_k \\ \Delta\hat{Y}_k \\ \Delta\hat{Z}_k \end{pmatrix} = S_{jk}^{o} - S_{jk}^{oo} \qquad ..(A.22)$$

The observation equation for **d** measured distances can be expressed in matrix notation as :

$$\underset{(d,1)}{V_4} - \underset{(d,3n)}{A_4} . \underset{(3n,1)}{\hat{X}_2} = \underset{(d,1)}{c_4} \qquad ..(A.23)$$

From equation A.21 it should be noted that each partial derivative is a function of the distance. Hence as the distance becomes small, ie $S_{jk} \Rightarrow 0$, then the solution based on this observation equation will become unstable.

Note that equation A.23 is a special case for a distance measured between two points on the object. For a more general equation, where distances could be measured from camera stations to the object as well, then extension of equation A.23 to include the parameter set X_1 would be carried out. Such on observation equation would be of the form :

$$V_4 - A_{41}. \hat{X}_1 - A_{42}. \hat{X}_2 = c_4 \qquad ..(A.24)$$

where the coefficient matrix A_{41} would be a null matrix if distances were only measured on the object.

Development of distance observation equations can be found in Mikhail and Gracie (1981) and Faig and El-Hakim (1982) and a solution for aerial photogrammetry can be found in Wong and Elphingstone (1972).

A.5 Elevation Difference

Observation equations to relate an elevation difference, between two points in the object space coordinate system, to unknown parameters requires formulation. A "true" elevation difference h_{jk}, between points j and k in the

object space, can be expressed in terms of a measured elevation difference h_{jk}^{oo} and a residual V_h.

$$h_{jk} = h_{jk}^{oo} + V_h \qquad ..(A.25)$$

The estimate of the elevation difference $\hat{h}_{jk}$ can be expressed in terms of an approximate elevation difference h_{jk}^{o} and a correction term $\Delta\hat{h}_{jk}$.

$$\hat{h}_{jk} = h_{jk}^{o} + \Delta\hat{h}_{jk} \qquad ..(A.26)$$

For an unbiased estimate of the elevation difference equations A.25 and A.26 can be equated to give :

$$V_h - \Delta\hat{h}_{jk} = h_{jk}^{o} - h_{jk}^{oo} \qquad ..(A.27)$$

The term $\Delta\hat{h}_{jk}$ must be expressed in terms of the coordinates of the points j and k, hence giving an equation in terms of the unknown parameters.

$$V_h - (\Delta\hat{Z}_j - \Delta\hat{Z}_k) = h_{jk}^{o} - h_{jk}^{oo}$$

OR ..(A.28)

$$V_h - (0, 0, 1, 0, 0, -1) \begin{pmatrix} \hat{X}_j \\ \hat{Y}_j \\ \hat{Z}_j \\ \hat{X}_k \\ \hat{Y}_k \\ \hat{Z}_k \end{pmatrix} = h_{jk}^{o} - h_{jk}^{oo}$$

The observation equation for **e** measured height differences can be expressed in matrix notation as :

$$\underset{(e,1)}{V_5} - \underset{(e,3n)}{A_5} \cdot \underset{(3n,1)}{\hat{X}_2} = \underset{(e,1)}{c_5} \qquad ..(A.29)$$

Equation A.29 is a special case where elevation differences are only measured on the object. A more general case, involving elevation differences between exposure station and object point and/or between object points, is given by the following observation equation.

$$V_5 - A_{51}\hat{X}_1 - A_{52}\hat{X}_2 = c_5 \qquad ..(A.30)$$

where the coefficient matrix A_{51} would be null for elevation differences observed on the object only.

A.6 Azimuth Observation

The azimuth of a line is defined as the horizontal angle, measured clockwise from the positive Y axis of the ground coordinate system (true north), to the line. (section 2.1.2.2) An observation equation which relates the measured azimuth to the unknown parameters requires formulation.

The "true" azimuth α_{ij} from the object point i to the object point j, as shown in figure A.1, can be expressed in terms of a measured azimuth α_{ij}^{oo} and a residual V_α.

$$\alpha_{ij} = \alpha_{ij}^{oo} + V_\alpha \qquad ..(A.31)$$

The estimate of the azimuth $\hat{\alpha}_{ij}$ can be expressed in terms of an approximate azimuth α_{ij}^{o} and a correction term $\Delta\hat{\alpha}_{ij}$.

$$\hat{\alpha}_{ij} = \alpha_{ij}^{o} + \Delta\hat{\alpha}_{ij} \qquad ..(A.32)$$

For an unbiased estimate of the azimuth equations A.31 and A.32 can be equated to give :

$$V_\alpha - \Delta\hat{\alpha}_{ij} = \alpha_{ij}^{o} - \alpha_{ij}^{oo} \qquad ..(A.33)$$

From figure A.1, the azimuth of the line is given by :

$$\alpha_{ij} = \tan^{-1}\left(\frac{X_j - X_i}{Y_j - Y_i}\right) \qquad ..(A.34)$$

Equation A.34 is non-linear and hence linearization by a Taylor series expansion (equation 3.7) is carried out. Substitution of the solution into equation A.33 gives the observation equation for an azimuth observation.

$$V_\alpha - \left(\frac{\partial\alpha_{ij}}{\partial X_i}\right)^{o}\Delta\hat{X}_i - \left(\frac{\partial\alpha_{ij}}{\partial Y_i}\right)^{o}\Delta\hat{Y}_i - \left(\frac{\partial\alpha_{ij}}{\partial X_j}\right)^{o}\Delta\hat{X}_j - \left(\frac{\partial\alpha_{ij}}{\partial Y_j}\right)^{o}\Delta\hat{Y}_j = \alpha_{ij}^{o} - \alpha_{ij}^{oo} \qquad ..(A.35)$$

To simplify equation A.35 the following notation will be used :

$$\alpha_1 = \left(\frac{\partial \alpha_{ij}}{\partial X_i}\right)^o \qquad \alpha_3 = \left(\frac{\partial \alpha_{ij}}{\partial X_j}\right)^o \qquad \text{..(A.36)}$$

$$\alpha_2 = \left(\frac{\partial \alpha_{ij}}{\partial Y_i}\right)^o \qquad \alpha_4 = \left(\frac{\partial \alpha_{ij}}{\partial Y_j}\right)^o$$

The partial derivatives, defined by equation A.36, are a function of the horizontal distance between the two points. As this distance approaches zero the azimuth becomes undefined and hence an unstable solution for this equation results. Equation A.35, in terms of the notation of equation A.36, becomes :

$$V_\alpha - (\alpha_1, \alpha_2, 0, \alpha_3, \alpha_4, 0) \begin{pmatrix} \hat{X}_i \\ \hat{Y}_i \\ \hat{Z}_i \\ \hat{X}_j \\ \hat{Y}_j \\ \hat{Z}_j \end{pmatrix} = \alpha_{ij}^o - \alpha_{ij}^{oo} \qquad \text{..(A.37)}$$

In matrix notation, for **a** measured azimuths, the equation becomes :

$$\underset{(a,1)}{V_6} - \underset{(a,3n)}{A_6} . \underset{(3n,1)}{\hat{X}_2} = \underset{(a,1)}{c_6} \qquad \text{..(A.38)}$$

Equation A.38 is a special case for an azimuth measured between two points on the object. For a more general solution, where an azimuth is measured from a camera station to an object point or between object points, then extension of equation A.38 to include the parameter set X_1 would be carried out. The observation equation of this form would be :

$$V_6 - A_{61} . \hat{X}_1 - A_{62} . \hat{X}_2 = c_6 \qquad \text{..(A.39)}$$

where the coefficient matrix A_{61} would be null for azimuth observations on the object only.

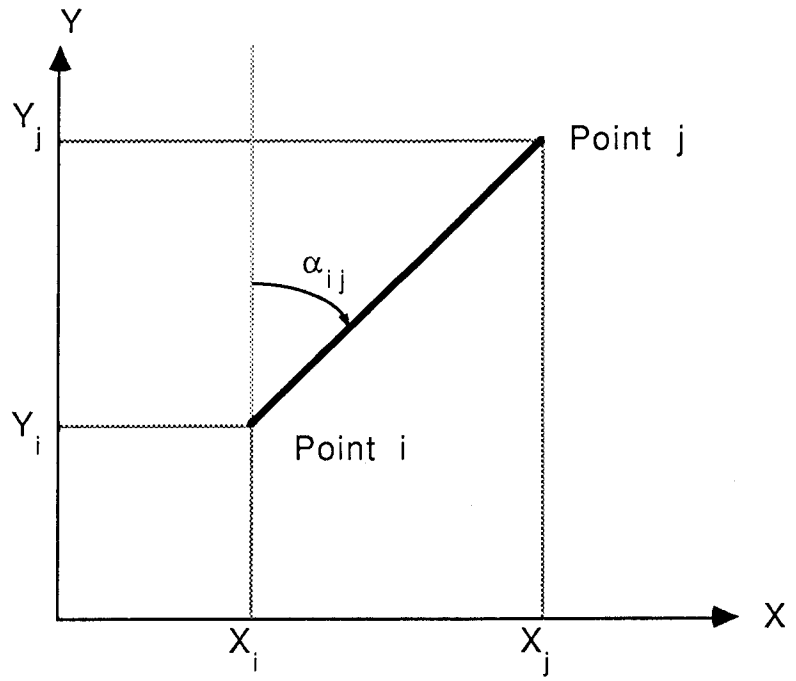

Figure A.1 Azimuth observation between object points

A.7 Horizontal Angle Observation

Observations comprising horizontal angles will be analysed on the basis of clockwise angles at an object point, from one object point to another. The observation equation for horizontal angle measurement is formulated as follows.

A "true" horizontal angle β_{jk}, from an object point i and between object points j and k, as shown in figure A.2, can be expressed in terms of a measured angle β_{jk}^{oo} and a residual V_β.

$$\beta_{jk} = \beta_{jk}^{oo} + V_\beta \qquad ..(A.40)$$

The estimate of the angle $\hat{\beta}_{jk}$ can be expressed in terms of an approximate angle β_{jk}^{o} and a correction term $\Delta\hat{\beta}_{jk}$.

$$\hat{\beta}_{jk} = \beta_{jk}^{o} + \Delta\hat{\beta}_{jk} \qquad ..(A.41)$$

For an unbiased estimate of the horizontal angle equations A.40 and A.41 can be equated to give the following equation.

$$V_\beta - \Delta\hat{\beta}_{jk} = \beta_{jk}^{o} - \beta_{jk}^{oo} \qquad ..(A.42)$$

From figure A.2 it can be seen that the horizontal angle β_{jk} can be expressed in terms of two azimuths, α_{ij} and α_{ik}. The horizontal angle is therefore given by :

$$\beta_{jk} = \tan^{-1}\left(\frac{X_k - X_i}{Y_k - Y_i}\right) - \tan^{-1}\left(\frac{X_j - X_i}{Y_j - Y_i}\right) \qquad ..(A.43)$$

Equation A.43 is non-linear and linearization by a Taylor series expansion (equation 3.7) is carried out. The linearized equation is substituted into equation A.42 to give the observation equation for a horizontal angle.

$$V_\beta - \left(\frac{\partial\beta_{jk}}{\partial X_i}\right)^{o}\Delta\hat{X}_i - \left(\frac{\partial\beta_{jk}}{\partial Y_i}\right)^{o}\Delta\hat{Y}_i - \left(\frac{\partial\beta_{jk}}{\partial X_j}\right)^{o}\Delta\hat{X}_j - \left(\frac{\partial\beta_{jk}}{\partial Y_j}\right)^{o}\Delta\hat{Y}_j - \left(\frac{\partial\beta_{jk}}{\partial X_k}\right)^{o}\Delta\hat{X}_k - \left(\frac{\partial\beta_{jk}}{\partial Y_k}\right)^{o}\Delta\hat{Y}_k = \beta_{jk}^{o} - \beta_{jk}^{oo} \qquad ..(A.44)$$

To simplify equation A.44 the following notation will be used :

$$\beta_1 = \left(\frac{\partial\beta_{jk}}{\partial X_i}\right)^{o} \qquad \beta_3 = \left(\frac{\partial\beta_{jk}}{\partial X_j}\right)^{o} \qquad \beta_5 = \left(\frac{\partial\beta_{jk}}{\partial X_k}\right)^{o} \qquad ..(A.45)$$

$$\beta_2 = \left(\frac{\partial\beta_{jk}}{\partial Y_i}\right)^{o} \qquad \beta_4 = \left(\frac{\partial\beta_{jk}}{\partial Y_j}\right)^{o} \qquad \beta_6 = \left(\frac{\partial\beta_{jk}}{\partial Y_k}\right)^{o}$$

The partial derivatives, defined by equation A.45, are functions of the horizontal distance between the points. As these distances become small the horizontal angle will be undefined and the solution will be unstable.

Equation A.44 in terms of the notation of equation A.45 becomes :

$$V_\beta - (\beta_1,\beta_2, 0,\beta_3,\beta_4, 0, \beta_5,\beta_6, 0)\begin{pmatrix}\hat{X}_i\\ \hat{Y}_i\\ \hat{Z}_i\\ \hat{X}_j\\ \hat{Y}_j\\ \hat{Z}_j\\ \hat{X}_k\\ \hat{Y}_k\\ \hat{Z}_k\end{pmatrix} = \beta_{jk}^{o} - \beta_{jk}^{oo} \qquad ..(A.46)$$

In matrix notation, for **b** measured clockwise horizontal angles, the observation equation becomes :

$$V_7 - A_7 . \hat{X}_2 = c_7 \qquad ..(A.47)$$

(b,1) (b,3n) (3n,1) (b,1)

Equation A.47 is a special case for a horizontal angle measured between two points on the object, at an object point. For a more general solution, where a horizontal angle is measured from a camera station between two object points or at an object point between two object points, then extension of equation A.47 to include parameter set X_1 would be carried out. In the derivations above the point i would be replaced by camera station L and hence the observation equation would be partially in terms of the geographic location of camera station L. The observation equation of this form would be :

$$V_7 - A_{71}.\hat{X}_1 - A_{72}.\hat{X}_2 = c_7 \qquad ..(A.48)$$

where the coefficient matrix A_{71} would be null for horizontal angles measured independent of a camera station.

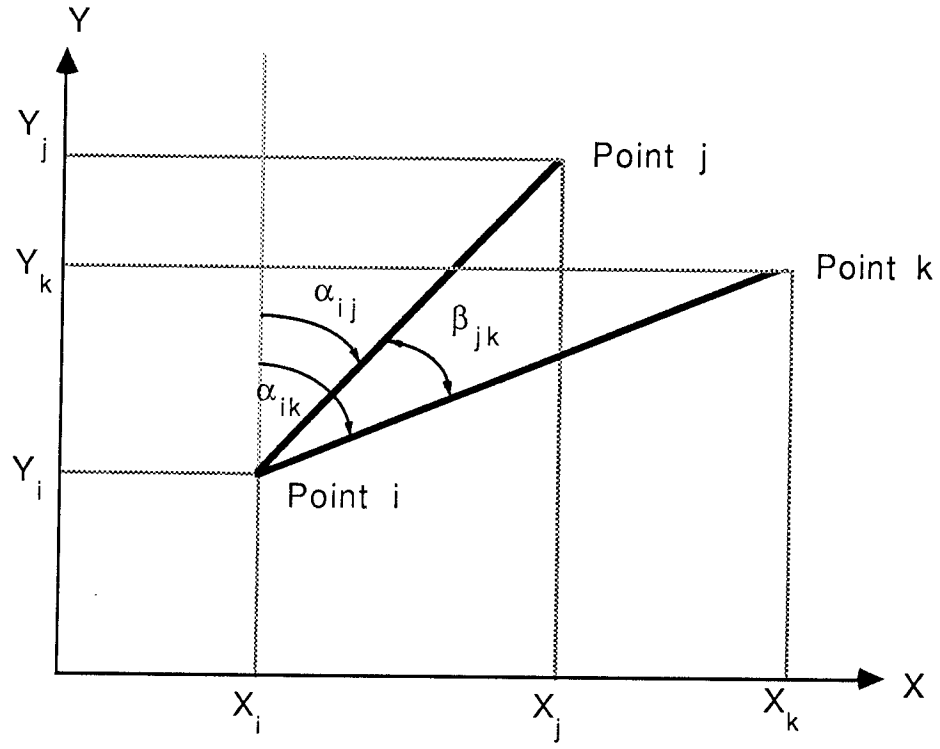

Figure A.2 Horizontal angle measurement between two object points, at an object point

Linearization of the equations for horizontal angles and azimuths can be found in Mikhail and Gracie (1981). An analogous solution, for aerial photogrammetry, is given in Wong and Elphingstone (1972).

A.8 Vertical Angle Observation

Observation equations to relate a vertical angle, measured between two object points in the object space coordinate system, to unknown parameters requires formulation.

A "true" vertical angle E_{jk}, between points j and k on the object, can be expressed in terms of a measured vertical angle E_{jk}^{oo} and a residual V_E.

$$E_{jk} = E_{jk}^{oo} + V_E \qquad ..(A.49)$$

The estimate of the vertical angle, $\hat{E}_{jk}$, can be expressed in terms of an approximate vertical angle E_{jk}^{o} and a correction term $\Delta\hat{E}_{jk}$.

$$\hat{E}_{jk} = E_{jk}^{o} + \Delta\hat{E}_{jk} \qquad ..(A.50)$$

For an unbiased estimate of the angle, equations A.49 and A.50 can be equated to give :

$$V_E - \Delta\hat{E}_{jk} = E_{jk}^{o} - E_{jk}^{oo} \qquad ..(A.51)$$

A problem with equations A.49 to A.51 is that they do not directly relate to the unknown parameters (ie X_j, Y_j, Z_j, X_k, Y_k, Z_k, which are the coordinates of the points between which the vertical angle was measured.) The general form of the equation for a vertical angle between two points in a rectangular coordinate system, with reference to figure A.3, is given by :

$$E_{ij} = \tan^{-1}\left(\frac{Z_j - Z_k}{SH_{jk}}\right) \qquad ..(A.52)$$

where $SH_{jk} = \sqrt{(X_j - X_k)^2 + (Y_j - Y_k)^2}$ = horizontal distance between points j and k.

Equation A.52 is non-linear and will be linearized by the Taylor series expansion of equation 3.7. Substitution of the linearized equation into equation A.51 gives the observation equation for a vertical angle measured between two object points.

$$V_E - \left(\frac{\partial E_{jk}}{\partial X_j}\right)^o \Delta\hat{X}_j - \left(\frac{\partial E_{jk}}{\partial Y_j}\right)^o \Delta\hat{Y}_j - \left(\frac{\partial E_{jk}}{\partial Z_j}\right)^o \Delta\hat{Z}_j - \left(\frac{\partial E_{jk}}{\partial X_k}\right)^o \Delta\hat{X}_k - \left(\frac{\partial E_{jk}}{\partial Y_k}\right)^o \Delta\hat{Y}_k - \left(\frac{\partial E_{jk}}{\partial Z_k}\right)^o \Delta\hat{Z}_k = E_{jk}^o - E_{jk}^{oo} \quad ..(A.53)$$

To simplify equation A.53 the following notation will be used :

$$e_1 = \left(\frac{\partial E_{jk}}{\partial X_j}\right)^o \qquad e_4 = \left(\frac{\partial E_{jk}}{\partial X_k}\right)^o$$
$$e_2 = \left(\frac{\partial E_{jk}}{\partial Y_j}\right)^o \qquad e_5 = \left(\frac{\partial E_{jk}}{\partial Y_k}\right)^o \quad ..(A.54)$$
$$e_3 = \left(\frac{\partial E_{jk}}{\partial Z_j}\right)^o \qquad e_6 = \left(\frac{\partial E_{jk}}{\partial Z_k}\right)^o$$

Equation A.53, in terms of the notation of equation A.54, takes the following form.

$$V_E - (e_1, e_2, e_3, e_4, e_5, e_6) \begin{pmatrix} \Delta\hat{X}_j \\ \Delta\hat{Y}_j \\ \Delta\hat{Z}_j \\ \Delta\hat{X}_k \\ \Delta\hat{Y}_k \\ \Delta\hat{Z}_k \end{pmatrix} = E_{jk}^o - E_{jk}^{oo} \quad ..(A.55)$$

The observation equation for **e** measured vertical angles can be expressed in matrix notation as :

$$\underset{(e,1)}{V_8} - \underset{(e,3n)}{A_8} . \underset{(3n,1)}{\hat{X}_2} = \underset{(e,1)}{c_8} \quad ..(A.56)$$

From equation A.54 it should be noted that each partial derivative is a function of the distance. Hence as the horizontal distance becomes small, ie $SH_{jk} \Rightarrow 0$, then the solution based on this observation equation will become unstable. Equation A.56 is a special case for a vertical angle measured between two points on the object. For a more general equation, where angles could be measured from camera stations to the object as well, then extension of equation A.56 to include the parameter set X_1 would be carried out. Such an observation equation would be of the following form.

$$V_8 - A_{81}.\hat{X}_1 - A_{82}.\hat{X}_2 = c_8 \qquad ..(A.57)$$

where the coefficient matrix A_{81} would be a null matrix if vertical angles were only measured on the object.

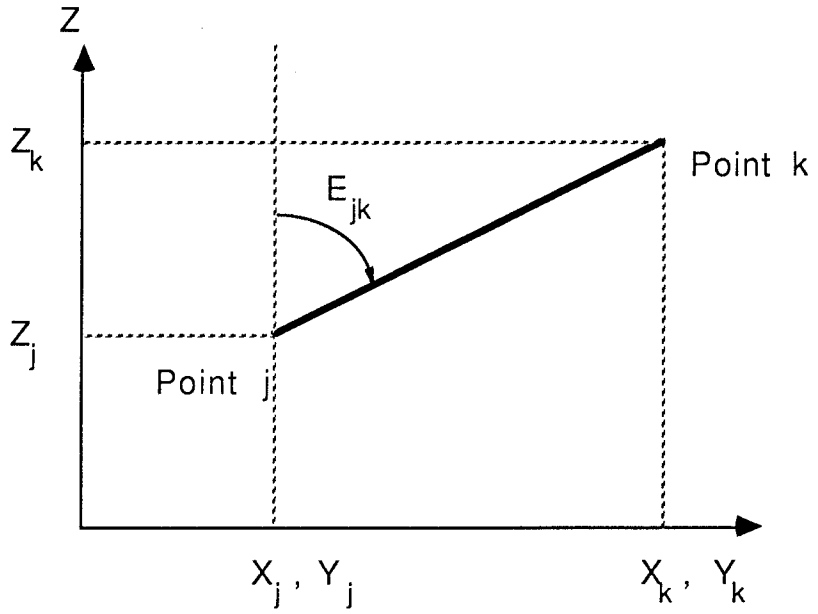

Figure A.3 Vertical angle observation between object points

BIBLIOGRAPHY

Abdel-Aziz, Y.I. and Karara, H.M. (1971) "Direct Linear Transformation from Comparator Coordinates into Object Space Coordinates in Close Range Photogrammetry", ASP Symposium on Close Range Photogrammetry, Illinois, January 1971

Amer, F. (1979) "Theoretical Reliability Studies for some Elementary Photogrammetric Procedures", Aerial Triangulation Symposium, Department of Surveying, University of Queensland, October 1979

American Society of Photogrammetry (1984) "Close-Range Photogrammetry and Surveying : State-Of-The-Art", Workshop Proceedings, American Society of Photogrammetry, Fall Convention, September 1984

Ashkenazi, V. (1975) "Network Analysis : Singularity, Rank and Invariant Criteria", Primer Congreso Venezolano de Geodesia, Maracaibo, December 1975

Ashkenazi, V. (1976) "Compendium of Formulae on Geodetic Position Networks", University of New South Wales, School of Surveying, August 1976

Bjermammar, A. (1973) "Theory of Errors and Generalized Matrix Inverses", Elsevier Scientific Publishing Company, Amsterdam

Blaha, G. (1971) "Inner Adjustment Constraints with an Emphasis on Range Observations", Department of Geodetic Science, Report No 148, Ohio State University, Columbus, Ohio

Brown, D.C. (1958) "Photogrammetric Flare Triangulation - A New Geodetic Tool", RCA Data Reduction Technical Report No 46, December 1958

Brown, D.C. (1964) "The Practical and Rigorous Adjustment of Large Photogrammetric Nets", Final Report, Contract No AF30(602)-3007, DBA, Florida

Brown, D.C. (1972) "Calibration of Close Range Cameras", International Society of Photogrammetry, Commission V, 12th Congress, Ottawa, July 1972

Brown, D.C. (1980) "Application of Close-Range Photogrammetry to Measurements of Structures in Orbit", Volume 1, GSI Technical Report No 80-012, Geodetic Services Inc., Melbourne, Florida, USA

Brown, D.C. (1982) "STARS, A Turnkey System for Close Range Photogrammetry", International Archives of Photogrammetry, Vol 24, Part V/1, pp 68 - 89

Brown, D.C. (1987) STARS Technical Bulletin, Geodetic Services Inc., Melbourne, Florida, USA

Burns, A.F. (1982) "Bundle Adjustment", M.Surv.Sc. Project Report, School of Surveying, University of New South Wales

Caspary, W.F. (1987) "Concepts of Network and Deformation Analysis", Monograph 11, School of Surveying, University of New South Wales

Cross, P.A. (1982) "Report of SSG 1.59 : Computer Aided Design of Geodetic Networks", Deutsche Geodätische Kommission, Series B, No 258/III, International Symposium on Geodetic Networks and Computations, Munich, September 1981, pp 13 - 21

Cross, P.A. and Whiting, M.B. (1982) "On the Design of Geodetic Networks using Iterative Methods", Deutsche Geodätische Kommission, Series B, No 258/III, International Symposium on Geodetic Networks and Computations, Munich, September 1981, pp 35 - 46

Draper, N.R. and Van Nostrand, R.C. (1979) "Ridge Regression and James-Stein Estimation : Review and Comments", Technometrics, Vol 21, No 4, November 1979

Faig, W. (1985) "Aerial Triangulation and Digital Mapping", Monograph 10, School of Surveying, University of New South Wales

Förstner, W. (1985) "The Reliability of Block Triangulation", Photogrammetric Engineering and Remote Sensing, Vol 51, pp 1137 - 1149

Fraser, C.S. (1980a) "Self-Calibration of a Non-Metric Camera at Multiple Focal Settings", Australian Journal of Geodesy, Photogrammetry and Surveying, No 32, pp 45 - 58

Fraser, C.S. (1980b) "On Variance Analysis of Minimally Constrained Photogrammetric Adjustments", Australian Journal of Geodesy, Photogrammetry and Surveying, No 33, pp 39 - 56

Fraser, C.S. (1982a) "Optimization of Precision in Close-Range Photogrammetry", Photogrammetric Engineering and Remote Sensing, Vol 48, pp 561-570

Fraser, C.S. (1982b) "On the use of Non-Metric cameras in Analytical Close-Range Photogrammetry", The Canadian Surveyor, Vol 36, No 3, September 1982, pp 259 - 279

Fraser, C.S. (1982c) "Film Unflatness Effects in Analytical Non-Metric Photogrammetry, International Archives of Photogrammetry, Vol 24, Part V/1, pp 156 - 166

Fraser, C.S. (1983) "Photogrammetric Monitoring of Turtle Mountain : A Feasibility Study", Photogrammetric Engineering and Remote Sensing, Vol 49, pp 1551 - 1559

Fraser, C.S. (1984) "Network Design Considerations for Non-Topographic Photogrammetry", Photogrammetric Engineering and Remote Sensing, Vol 50, pp 1115 - 1126

Fraser, C.S. (1985) "Photogrammetric Measurement of Thermal Deformation of a Large Process Compressor", Photogrammetric Engineering and Remote Sensing, Vol 51, pp 1569 - 1575

Fraser, C.S. (1987) "Limiting Error Propagation in Network Design", Photogrammetric Engineering and Remote Sensing, Vol 53, pp 487 - 493

Fraser, C.S. (1988a) "Precise Alignment and Verification by Photogrammetry", Presented Paper, 11th ESTEC Workshop on Antenna Measurements, Gothenburg, Sweden, June 1988

Fraser, C.S. (1988b) "State of the Art in Industrial Photogrammetry", International Society for Photogrammetry and Remote Sensing, Vol 27, No B5, Commission V, 16th Congress, Kyoto, July1988, pp 166 - 181

Fraser, C.S. (1988c) "Periodic Inspection of Industrial Tooling by Photogrammetry", Photogrammetric Engineering and Remote Sensing, Vol 54, pp 21 - 216

Fraser, C.S. (1989) Personal Communication

Fraser, C.S. and Brown, D.C. (1988) "Industrial Photogrammetry : New developments and Recent Applications", Photogrammetric Record, 12 (68), pp 197 - 217

Fraser, C.S. and Denham, R.L. (1988) "A Cine-Photogrammetric System for the Monitoring of a Dynamic Event Underwater", International Society for Photogrammetry and Remote Sensing, Vol 27,No B5, Commission V, 16th Congress, Kyoto, July1988, pp 182 - 193

Fryer, J.G. and Brown, D.C. (1986) "Lens Distortion for Close-Range Photogrammetry", Photogrammetric Engineering and Remote Sensing, Vol. 52, pp 51 - 58

Grafarend, E.W. (1974) "Optimization of Geodetic Networks", Bolletino di Geodesia a Science Affini, Vol 33, No 4, pp 351 - 406

Grafarend, E. and Schaffrin, B. (1974) "Unbiased Free Net Adjustment", Survey Review, Vol XXII, (171), pp 200-218

Granshaw, S.I. (1980) "Bundle Adjustment Methods in Engineering Photogrammetry", Photogrammetric Record, 10(56), pp 181 - 207, October 1980

Harvey, B.R. (1987) "Degrees of Freedom - Simplified", Australian Journal of Geodesy, Photogrammetry and Surveying, No 46 & 47, pp 57-68

Hearn, D. and Baker, M.P. (1986) "Computer Graphics", Prentice-Hall, New Jersey

Hottier, P. (1976) "Accuracy of Close-Range Analytical Restitutions : Practical Experiments and Prediction", Photogrammetric Engineering and Remote Sensing, Vol 42, pp 345 - 375

Jodoin, S.J. (1987) "The Calibration of a Parabolic Antenna with the Aid of Close-Range Photogrammetry and Surveying", Technical Report No 130, Department of Surveying Engineering, University of New Brunswick

Kilpelä, E. , Heikkilä, J. and Inkilä, K. (1981) "Compensation of Systematic Errors in Bundle Adjustment", Photogrammetria, 37 (1981), pp 1 - 13

Kilpelä, E. (1981) "Compensation of Systematic Errors of Image and Model Coordinates", Photogrammetria, 37 (1981), pp 15 - 44

Koch, K.R. (1982) Optimization of the Configuration of Geodetic Networks", Deutsche Geodätische Kommission, Series B, No 258/III, International Symposium on Geodetic Networks and Computations, Munich, September 1981, pp 82 - 89

Krakiwsky, E.J. (1982) "A Synthesis of Recent Advances in the Method of Least Squares", Publication 10003, Division of Surveying Engineering, The University of Calgary, Calgary, Canada

Leonard, T. (1975) "A Bayesian Approach to the Linear Model with Unequal Variances", Technometrics, Vol 17, No 1, February 1975

Marquardt, D.W. (1970) "Generalized Inverses, Ridge Regression, Biased Linear Estimation and Nonlinear Estimation", Technometrics, Vol 12, No 3, pp 591-612

Marzan, G.T. and Karara, H.M. (1976) "Rational Design for Close-Range Photogrammetry", Photogrammetry Series No 43, University of Illinois, Urbana, Illinois

Mepham, M.P. and Krakiwsky, E.J. (1982) "Interactive Network Design and Analysis", Deutsche Geodätische Kommission, Series B, No 258/III, International Symposium on Geodetic Networks and Computations, Munich, September 1981, pp 90 - 96

Mikhail, E.M. (1976) "Observations and Least Squares", IEP-A Dunn-Donnelley, New York

Mikhail, E.M. and Gracie, G. (1981) "Analysis and Adjustment of Surveying Measurements", Van Nostrand Reinhold Co, New York

Mittermayer, E. (1972) "A Generalization of the Least-Squares Method for the Adjustment of Free Networks", Bulletin Géodésique, No 104, pp 139 - 157

Moffitt, E.H. and Mikhail, E.M. (1980) "Photogrammetry", 3rd Edition, Harper & Row, New York

Niemeier, W. (1982) "Design, Diagnosis and Optimization of Monitoring Networks in Engineering Surveying", Presented Paper, Centennial Convention, Canadian Institute of Surveying, Ottawa, April 1982

Niemeier, W. (1987) Workshop on Engineering Networks and Deformation Analysis", Workshop Notes, School of Surveying, University of New South Wales, September 1987

Papo, H.B. and Shmutter, B. (1976) "Tank Calibration by Stereophotogrammetry", 13th Congress of the International Society of Photogrammetry, Commission V, Helsinki, July 1976

Papo, H.B. and Perelmuter, A. (1982) "Free Net Analysis in Close-Range Photogrammetry", Photogrammetric Engineering and Remote Sensing, Vol 48, pp 571-576

Pavlidis, T. (1982) "Algorithms for Graphics and Image Processing", Springer-Verlag, Berlin

Pelzer, H. (1979) "Some Criteria for the Accuracy and the Reliability of Networks", Presented Paper, XVII General Assembly of the International Union of Geodesy and Geophysics, Canberra, December 1979

Perelmuter, A. (1979) "Adjustment of Free Networks", Bulletin Géodésique, No 53/4, pp 291 - 296

Rüeger, J.M. (1989) Personal Communication

Schmitt, G. (1982) "Optimal Design of Geodetic Networks", Deutsche Geodätische Kommission, Series B, No 258/III, International Symposium on Geodetic Networks and Computations, Munich, September 1981, pp 7 - 12

Searl, S.R. (1971) "Linear Models", John Wiley & Sons, New York

Shortis, M.R. (1987) "Precise Monitoring of Large Engineering Structures Using Close Range Photogrammetry", Symposium on the Applications of Close Range Photogrammetry, Department of Surveying and Land Information, University of Melbourne, pp 58 - 75

Shortis, M.R. (1988) "Precision Evaluations of Digital Imagery for Close-Range Photogrammetric Applications", Photogrammetric Engineering and Remote Sensing, Vol 54, pp 1395 - 1401

Slama, C.C. (ed) (1980) "Manual of Photogrammetry", Fourth Edition, American Society of Photogrammetry, Falls Church, Virginia

Trinder, J.C. (1988) "Experiments on Target Location and Image Matching", International Society for Photogrammetry and Remote Sensing, Vol 27, No B3, Commission III, 16th Congress, Kyoto,1988, pp 785 - 792

Trinder, J.C. (1989) Personal Communication

Welsh, W. (1979) "A Review of the Adjustment of Free Networks", Survey Review, Vol XXV, (194), October 1979, pp 167-180

Wimmer, H. (1982) "Second Order Design of Geodetic Networks by an Iterative Approximation of a Given Criterion Matrix", Deutsche Geodätische Kommission, Series B, No 258/III, InternationalSymposium on Geodetic Networks and Computations, Munich, September 1981, pp 112 - 127

Wong, K.W. (1976) "Mathematical Formulation and Digital Analysis in Close-Range Photogrammetry", Photogrammetric Engineering and Remote Sensing, Vol 41, November 1975, pp 1355 - 1373

Wong, K.W. and Elphingstone, G. (1972) "Aerotriangulation by SAPGO", Photogrammetric Engineering, 1972, pp 779 - 790

Wong, K.W. and Ho W. (1986) "Close-Range Mapping with a Solid State Camera", Photogrammetric Engineering and Remote Sensing, Vol 52, pp 67-74

Publications from

THE SCHOOL OF SURVEYING, THE UNIVERSITY OF NEW SOUTH WALES.

All prices include postage by surface mail. Air mail rates on application. (Effective July 1989)

To order, write to Publications Officer, School of Surveying, The University of New South Wales, P.O. Box 1, Kensington N.S.W., 2033 AUSTRALIA

NOTE: ALL ORDERS MUST BE PREPAID

UNISURV REPORTS - G SERIES

Price (including postage): $3.50

G14. A. Stolz, "The computation of three dimensional Cartesian coordinates of terrestrial networks by the use of local astronomic vector systems", Unisurv Rep. 18, 47 pp.

G16. R.S. Mather et al, "Communications from Australia to Section V, International Association of Geodesy, XV General Assembly, International Union of Geodesy and Geophysics, Moscow 1971", Unisurv Rep. 22, 72 pp.

G17. Papers by R.S. Mather, H.L. Mitchell & A. Stolz on the following topics:- Four-dimensional geodesy, Network adjustment and Sea surface topography, Unisurv G17, 73 pp.

G18. Papers by L. Berlin, G.J.F. Holden, P.V. Angus-Leppan, H.L. Mitchell & A.H. Campbell on the following topics:- Photogrammetry co-ordinate systems for surveying integration, Geopotential networks and Linear measurement, Unisurv G18, 80 pp.

G19. R.S. Mather, P.V. Angus-Leppan, A. Stolz & I. Lloyd, "Aspects of four-dimensional geodesy", Unisurv G19, 100 pp.

G20. Papers by J.S. Allman, R.C. Lister, J.C. Trinder & R.S. Mather on the following topics:- Network adjustments, Photogrammetry, and 4-Dimensional geodesy, Unisurv G20, 133 pp.

G21. Papers by E. Grafarend, R.S. Mather & P.V. Angus-Leppan on the following topics:- Mathematical geodesy, Coastal geodesy and Refraction, Unisurv G21, 100 pp.

G22. Papers by R.S. Mather, J.R. Gilliland, F.K. Brunner, J.C. Trinder, K. Bretreger & G. Halsey on the following topics:- Gravity, Levelling, Refraction, ERTS imagery, Tidal effects on satellite orbits and Photogrammetry, Unisurv G22, 96 pp.

G23. Papers by R.S. Mather, E.G. Anderson, C. Rizos, K. Bretreger, K. Leppert, B.V. Hamon & P.V. Angus-Leppan on the following topics:- Earth tides, Sea surface topography, Atmospheric effects in physical geodesy, Mean sea level and Systematic errors in levelling, Unisurv G23, 96 pp.

G24. Papers by R.C. Patterson, R.S. Mather, R. Coleman, O.L. Colombo, J.C. Trinder, S.U. Nasca, T.L. Duyet & K. Bretreger on the following topics:- Adjustment theory, Sea surface topography determinations, Applications of LANDSAT imagery, Ocean loading of Earth tides, Physical geodesy, Photogrammetry and Oceanographic applications of satellites, Unisurv G24, 151 pp.

G25. Papers by S.M. Nakiboglu, B. Ducarme, P. Melchior, R.S. Mather, B.C. Barlow, C. Rizos, B. Hirsch, K. Bretreger, F.K. Brunner & P.V. Angus-Leppan on the following topics:- Hydrostatic equilibrium figures of the Earth, Earth tides, Gravity anomaly data banks for Australia, Recovery of tidal signals from satellite altimetry, Meteorological parameters for modelling terrestrial refraction and Crustal motion studies in Australia, Unisurv G25, 124 pp.

G26. Papers by R.S. Mather, E.G. Masters, R. Coleman, C. Rizos, B. Hirsch, C.S. Fraser, F.K. Brunner, P.V. Angus-Leppan, A.J. McCarthy & C. Wardrop on the following topics:- Four-dimensional geodesy, GEOS-3 altimetry data analysis, analysis of meteorological measurements for microwave EDM and Meteorological data logging system for geodetic refraction research, Unisurv G26, 113 pp.

G27. Papers by F.K. Brunner, C.S. Fraser, S.U. Nasca, J.C. Trinder, L. Berlin, R.S. Mather, O.L. Colombo & P.V. Angus-Leppan on the following topics:- Micrometeorology in geodetic refraction, LANDSAT imagery in topographic mapping, adjustment of large systems, GEOS-3 data analysis, Kernel functions and EDM reductions over sea, Unisurv G27, 101 pp.

G29. Papers by F.L. Clarke, R.S. Mather, D.R. Larden & J.R. Gilliland on the following topics:- Three dimensional network adjustment incorporating ξ , η and N, Geoid determinations with satellite altimetry, Geodynamic information from secular gravity changes and Height and free-air anomaly correlation, Unisurv G29, 87 pp.

From June 1979 Unisurv G's name was changed to Australian Journal of Geodesy, Photogrammetry and Surveying. These can be ordered from The Managing Editor, Australian Journal of Geodesy, Photogrammetry and Surveying, Institution of Surveyors - Australia , Box 4793 G.P.O., Sydney, N.S.W., 2001, AUSTRALIA.

UNISURV REPORTS - S SERIES

S8 - S19	Price (including postage):		$7.50
S20 onwards	Price (including postage):	Individuals	$18.00
		Institutions	$25.00

S8 A. Stolz, "Three-D Cartesian co-ordinates of part of the Australian geodetic network by the use of local astronomic vector systems", Unisurv Rep. S 8, 182 pp, 1972.

S9 H.L. Mitchell, "Relations between MSL & geodetic levelling in Australia", Unisurv Rep. S 9, 264 pp, 1973.

S10 A.J. Robinson, "Study of zero error & ground swing of the model MRA101 tellurometer", Unisurv Rep. S 10, 200 pp, 1973.

S12. G.J.F. Holden, "An evaluation of orthophotography in an integrated mapping system", Unisurv Rep. S 12, 232 pp, 1974.

S14. Edward G. Anderson, "The Effect of Topography on Solutions of Stokes` Problem", Unisurv Rep. S 14, 252 pp, 1976.

S15. A.H.W. Kearsley, "The Computation of Deflections of the Vertical from Gravity Anomalies", Unisurv Rep. S 15, 181 pp, 1976.

S16. K. Bretreger, "Earth Tide Effects on Geodetic Observations", Unisurv S 16, 173 pp, 1978.

S17. C. Rizos, "The role of the gravity field in sea surface topography studies", Unisurv S 17, 299 pp, 1980.

S18. B.C. Forster, "Some measures of urban residual quality from LANDSAT multi-spectral data", Unisurv S 18, 223 pp, 1981.

S19. Richard Coleman, "A Geodetic Basis for recovering Ocean Dynamic Information from Satellite Altimetry", Unisurv S 19,332 pp, 1981.

S20. Douglas R. Larden, "Monitoring the Earth's Rotation by Lunar Laser Ranging", Unisurv Report S 20, 280 pp, 1982.

S25. Ewan G. Masters, "Applications of Satellite Geodesy to Geodynamics", Unisurv Report S25, 208 pp, 1984.

S27. Bruce R. Harvey, "The Combination of VLBI and Ground Data for Geodesy and Geophysics", Unisurv Report S27, 239 pp, 1985.

S28. Rod Eckels, "Surveying with GPS in Australia", Unisurv S28, 220 pp, 1987.

S29. Gary S. Chisholm, "Integration of GPS into hydrographic survey operations", Unisurv S29, 190 pp, 1987.

S30. Gary Alan Jeffress, "An investigation of Doppler satellite positioning multi-station software", Unisurv S30, 118 pp, 1987.

S31. Jahja Soetandi, "A model for a cadastral land information system for Indonesia", Unisurv S31, 168 pp, 1988.

S33. R. D. Holloway, "The integration of GPS heights into the Australian Height Datum", Unisurv S33, 151 pp.,1988.

S34. Robin C. Mullin, "Data update in a Land Information Network", Unisurv S34, 168 pp. 1988.

S35. Bertrand Merminod, "The use of Kalman filters in GPS Navigation", Unisurv S35, 203 pp., 1989.

S36. Andrew R. Marshall, "Network design and optimisation in close range Photogrammetry", Unisurv S36, 249 pp., 1989.

S37. Wattana Jaroondhampinij, "A model of Computerised parcel-based Land Information System for the Department of Lands, Thailand," Unisurv S37, 281 pp., 1989.

PROCEEDINGS

Prices include postage by surface mail

P1. P.V. Angus-Leppan (Editor), "Proceedings of conference on refraction effects in geodesy & electronic distance measurement", 264 pp. Price: $6.50

P2. R.S. Mather & P.V. Angus-Leppan (Eds), "Australian Academy of Science/International Association of Geodesy Symposium on Earth`s Gravitational Field & Secular Variations in Position", 740 pp. Price $12.50

MONOGRAPHS

Prices include postage by surface mail

M1. R.S. Mather, "The theory and geodetic use of some common projections", (2nd edition), 125 pp. Price $9.00

M2. R.S. Mather, "The analysis of the earth's gravity field", 172 pp. Price $5.50

M3. G.G. Bennett, "Tables for prediction of daylight stars", 24 pp. Price $2.00

M4. G.G. Bennett, J.G. Freislich & M. Maughan, "Star prediction tables for the fixing of position", 200 pp. Price $5.00

M5. M. Maughan, "Survey computations", 98 pp. Price $8.00

M7. J.M. Rueger, "Introduction to Electronic Distance Measurement", (2nd Edition), 140 pp. Price $14.00

M8. A.H.W. Kearsley, "Geodetic Surveying". 77pp. Price $8.00

M10. W. Faig, "Aerial Triangulation and Digital Mapping", 102. pp. Price $13.00

M11. W.F. Caspary, "Concepts of Network and Deformation Analysis", 183 pp. Price $22.00

M12. F.K. Brunner, "Atmospheric Effects on Geodetic Space Measurements", 110 pp. Price $13.00